Introduction to Cellular Automata

J.L. Schiff

Contents

Preface

... synthetic universes defined by simple rules...

Tommaso Toffoli & Norman Margolus – *Cellular Automata Machines*

The history of cellular automata is only quite recent, coming to life at the hands of two fathers, John von Neumann and Stanislaw Ulam in the early 1950s, although it was re-invented several more times, as for example in the work of Konrad Zuse. Subsequent work in the early 1960s included that of Ulam and his coworkers at Los Alamos and by John Holland at the University of Michigan whose work on adapation continued for several decades. Early theoretical research was conducted by Hedlund (another example of re-invention), Moore, and Myhill, among many others, not always under the name of cellular automata, since the concept was still in its formative stages. A big boost to the popularization of the subject came from John Conway's highly addictive Game of Life presented in Martin Gardner's October 1970 column in *Scientific American*. Still the study of cellular automata lacked much depth, analysis, and applicability and could not really be called a scientific discipline.

All that changed in the early 1980s when physicist Stephen Wolfram in a seminal paper, "Statistical mechanics of cellular automata", initiated the first serious study of cellular automata. In this work and in a series of subsequent ones Wolfram began producing some of the images that have now become iconic in the field. Conferences were organized and people from various disciplines were being drawn into the field. It is now very much an established scientific discipline with applications found in a great many areas of science. Wolfram has counted more than 10,000 papers referencing his original works on the subject and the field of cellular automata has taken on a life of its own.

The cellular automaton paradigm is very appealing and its inherent simplicity belies its potential complexity. Simple local rules govern an array of cells that update the state they are in at each tick of a clock. It has been found that this is an excellent way to analyze a great many natural phenomena, the reason being that most physical processes are themselves local in nature – molecules interact locally with their neighbors, bacteria with their neighbors, ants with theirs and people likewise. Although natural phenomena are also continuous, examining the system at discrete time steps does not really diminish the power of the analysis. So in the artificial cellular automaton world we have an unfolding microcosm of the real world.

One of the things self-evident to everyone is the order that is found in Nature. From an ameoba to plants to animals to the universe itself, we find incredible order everywhere. This begs the obvious questions: Where did this order come from – how could it have originated? One of the fundamental lessons of cellular automata is that they are capable of self-organization. From simple local rules that say nothing whatsoever about global behavior, we find that global order is nonetheless preordained and manifest in so many of the systems that we will consider. In the words of theoretical biologist, Stuart Kauffman, it is, “order for free”. It is this order for free that allows us to emulate the order we find in Nature.

Related to the creation of order is the notion of complexity. How can a finite collection of chemicals make up a sentient human being? Clearly the whole is greater than the sum of its parts. How can termites build complex structures when no individual termite who starts a nest even lives to see its completion? The whole field of complexity has exploded over recent years and here too cellular automata play their part. One of the most endearing creatures that we shall encounter is Langton’s Ant in Chapter 6, and this little creature will teach us a lot about complexity.

Of course it is no longer possible in a single text to cover every aspect of the subject. The field, as Wolfram’s manuscript count shows, has simply grown too large. So this monograph is merely an introduction into the brave new world of cellular automata, hitting the highlights as the author sees them. A more advanced and mathematical account can be found in the excellent book by Ilachinski [2002].

One *caveat* concerning the applications of cellular automata. We are not making any claims that CA models are necessarily superior to other kinds of models or that they are even justified in every case. We are merely presenting them as one way of looking at the world which in some instances can be beneficial to the understanding of natural phenomena. At the very least, I think you will find them interesting. Even if the entire universe is not one monolithic cellular automaton, as at least one scientist believes, the journey to understanding that point of view is well worth the price of admission.

Finally, I wish to thank Auckland University students Michael Brough, Peter Lane, and Malcolm Walsh who produced many of the figures in the text from their cellular automata models and Samuel Dillon who produced the Rule 30 data encryption figures. Their assistance has been invaluable as their programming skills far exceed that of my own. I also wish to thank my daughter-in-law Yuka Schiff for many of the fine graphics and

my friend Michael Parish for introducing me to the facinating world of bees and Maeterlinck's classic monograph. A large debt of gratitude is owed to those who read the manuscript and provided many helpful suggestions: students Michael Brough and Dror Speiser, as well as professors Cristian Calude, David Griffeath, G. Bard Ermentrout, and Birgitt Schönfisch. Several of the CA images were produced with the specialized software of Stephen Wolfram's *New Kind of Science Explorer* which can be purchased from the website: http://www.wolframscience.com/, and Mirek Wojtowicz's *MCell* program which can be downloaded at his website: http://www.mirekw.com/ca/.

Chapter 1

Preliminaries

1.1 Self-Replicating Machines

The origins of cellular automata can be traced back to mathematician John von Neumann's attempt to create a self-replicating machine. In 1948, von Neumann read a paper at the Hixon Symposium in Pasadena, California ('The General and Logical Theory of Automata'), in which he outlined, among other things, a plan for a self-replicating machine (von Neumann actually refers to such a machine as an *automaton*). The question von Neumann addresses is this: "Can one build an aggregate out of such elements in such a manner that if it is put into a reservoir, in which float all these elements, each of which will at the end turn out to be another automaton exactly like the original one?" He then proceeds to outline the following argument to show that this is entirely feasible in principle.

One starts with a machine (universal constructor), A that has the ability to construct *any* other machine once it is furnished with a set of instructions denoted by I. Machine A is envisaged to float in the reservoir of liquid with all the necessary component parts that it requires for any particular construction. We now attach to our machine A, another component called B, that can make a copy of any instruction that is supplied to it. A final component, labeled C, von Neumann called the "control mechanism" which has the functions of initiating A to construct a machine as described by the instructions I, and then cause B to make a copy of the instructions I and supply the copy of the instructions to the machine newly formed by A. Then the entire apparatus can be denoted by $M = A + B + C$.

To get things rolling, we furnish a machine M with a set of instructions for constructing itself, I_M, and call the resulting system M'. It is this machine, M', that is capable of replicating itself. For, C initiates the construction of M by A, it then has B make a copy of the instructions I_M and these are furnished to M to form the system M' once again. And so on.

It is the multiple use of the instruction set I_M that is crucial here. Firstly, the instructions must be followed by A, secondly they must be copied by B, and lastly the copy must be attached to the machine constructed by A.

Overall, the copying mechanism is similar to the replication of living cells whereby the DNA (instructions) are first copied by cells preceding cell division. Interestingly, Christopher Langton [1986] comments: "Since he [von Neumann] was able to demonstrate that such a machine can exist, it becomes plausible that many, perhaps all, of the processes upon which life is based are algorithmically describable and that, therefore, life itself is achievable by machines". The study and implementation of these processes has become the domain of the newly emerging subject of *artificial life* and we shall encounter many instances of it throughout this book.

Von Neumann had now shown that a self-replicating machine was established in principle, but at the time of his lecture, did not suggest how one could be implemented. The technology of the day simply was not capable of such an implementation.

According to received wisdom, it was the Polish-American mathematician Stanislaw Ulam who suggested to von Neumann that he should try constructing his self-replicating automaton using the conceptual framework of what are now known as cellular automata. The resulting system outlined in the early 1950s and later completed after von Neumann's death by Arthur Burks was a universal Turing machine embedded in a 2-dimensional cellular lattice that had 29 states for each cell and a 5-cell neighborhood (now known as a von Neumann neighborhood) that required ∼200,000 cells. However, it was never actually implemented.

A simpler 8-state self-replicating cellular automaton was created by Codd [1968] with some computer assistance. Then in 1984, Christopher Langton demonstrated self-reproduction in an 86 cell looped pathway using 8 states with a 5-cell neighborhood, which did not exhibit the feature of universal construction as did the von Neumann and Codd machines, but simply reproduced itself. Langton's loop has a construction arm attached to it and consists of an outer sheath of cells that remain in a fixed state and an inner sequence of 'DNA' cells in various states that circulate around the loop (Figure 1.1). At the junction of the loop and arm, the 'DNA' cells are replicated: one copy goes back around the loop and the other copy travels down the construction arm where it is translated at the tip of the arm spawning new growth..

Once a side of the offspring loop is fully generated, the growth pattern makes a left turn and propagates another side and so on until the offspring loop is complete. Then the connection between parent and offspring is severed (cutting the umbilical cord so to speak) and both parent and offspring propagate separate construction arms to begin the process anew (Figure 1.2).

Construction continues in this fashion with each new loop generating at

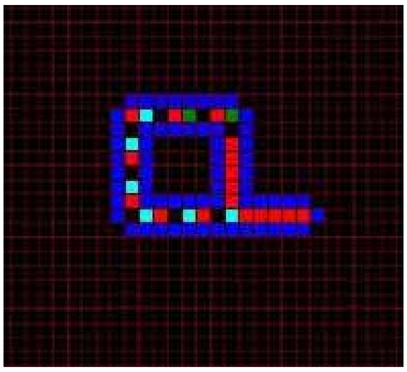

Figure 1.1: The Langton looped pathway in its initial configuration. The different colors represent the different cell states.

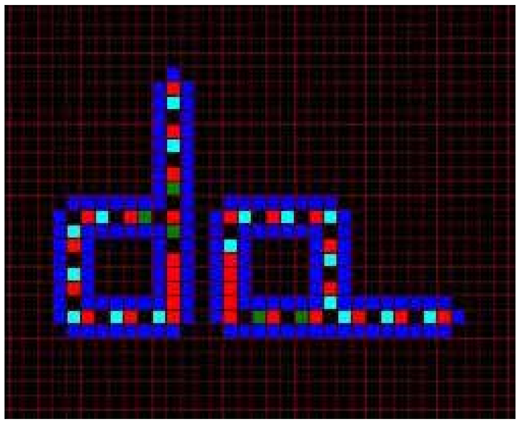

Figure 1.2: The parent (left) and offspring loops each propagating new construction arms after their connection has been severed.

least one new offspring. When a loop tries to extend an arm into a region already occupied, it will retract the arm and the 'DNA' of that loop is erased and the loop becomes inert. The Langton loops will continue this replication process indefinitely expanding outward with time and filling the plane.

Although each loop contains the same 'DNA' sequence, the number of times it can replicate itself will depend on the space available in its immediate environment.

A somewhat simpler self-replicating loop that dispenses with the outer sheath but also having 8 states was constructed by Reggia *et al.* [1993]. A simple and brief proof of the existence of a self-replicating CA machine capable of universal computation was given by A.R. Smith [1991]. Another approach was taken by Morita and Imai [1997] who devised cellular configu-

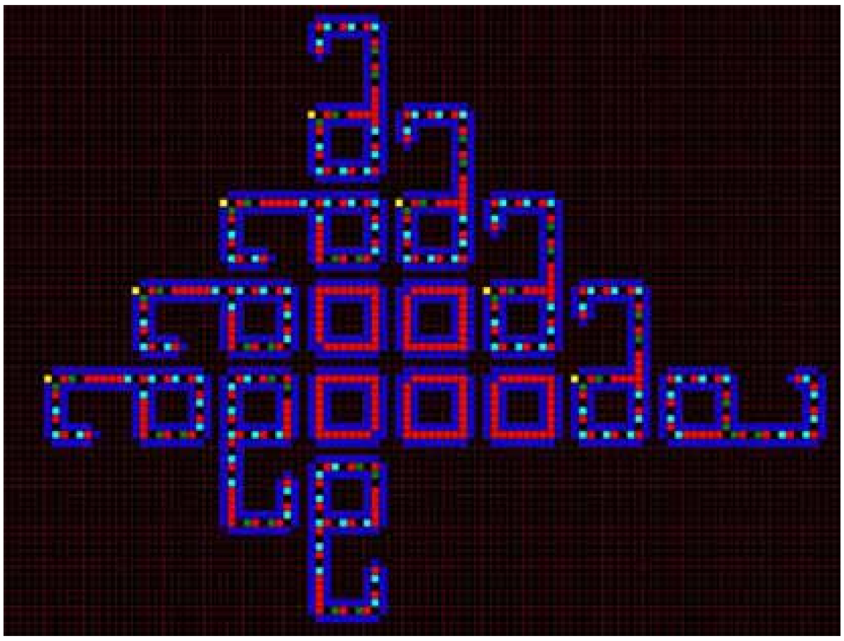

Figure 1.3: The replication continues indefinitely filling up the plane with loops.

rations that were able to reproduce by self-inspection rather than from any stored self-description.

In the realm of actual self-reproducing machines, a primitive form was demonstrated by Roger Penrose (the well-known physicist) and his father Lionel back in 1957 using a set of flat shaped wooden blocks that produced copies of a particular coupling when the blocks were shaken in a box enclosure. In 2001, Greg Chirikjian of Johns Hopkins University developed a LEGO robot that drove around a track and assembled modules to make a copy of itself. Recently, Hod Lipson and colleagues [Zykov *et al.* 2005] at Cornell University have created a self-replicating robot consisting of a tower of cubes that can swivel around and pick up other cubes and stack them to create another tower identical to itself. According to Lipson, this opens up the possibility of using robotic systems in future space travel that can repair themselves.

An overview of fifty years of research on self-replication can be found in the article by M. Sipper [1998] who also created an interactive self-replicator (Stauffer and Sipper [2002]). Certainly the notion of self-replication has proved enormously popular with the creators of computer viruses.

1.2 Grand Turing Machines

In his seminal 1936 paper on computable numbers ('On computable numbers, with an application to the Entscheidungsproblem'), English genius Alan Turing discussed a very general type of computer that has become know as a Turing machine. This machine is theoretical in nature and today still finds applications in computer science. In the words of computer scientist Edward Fredkin, "It was a way to formalize all the things that a mathematician could do with a pencil and paper". It can be thought of as a mechanical 'head' that has an infinite strip of tape in both directions that lies beneath it. The head can both read and write onto the tape. The head is allowed to exist in a finite number of internal states, say k. The state of the head changes by interacting with the input from the tape beneath it. The tape is divided into an endless succession of square cells in which either a number '1' is written or the cell is blank which we interpret as being the number '0'. While the tape is infinite in length, there can only be a finite number of cells containing the number '1'. The remaining cells must all be blank. The head reads just one such cell at a time – the one directly beneath it. Upon the head reading the value '0' or '1' of this cell, it either replaces this value with a '1' or '0' or with the same symbol. The head then moves either one square to the right or to the left (or not at all) and goes into one of its other allowable states. It then repeats the above sequence for each cycle of the machine. The new state of the head, the value the head gives to a particular cell, and the movement of the head left or right are all governed by some underlying set of instructions – the *state transition function*. There are also special starting and halting states. The output is written on a portion of the tape that can be read by an observer after a halt state has been reached.

As an example, let us assume that the head has just two allowable states 1 and 2, with a state transition function given by the format:

$$(\textbf{H}\text{ead }\textbf{S}\text{tate, }\textbf{C}\text{ell }\textbf{S}\text{tate}) \longrightarrow (\textbf{H}\text{ead }\textbf{S}\text{tate, }\textbf{C}\text{ell }\textbf{S}\text{tate, }\textbf{M}\text{ove})$$

specifically, say:

$$(1,1) \longrightarrow (2,0,1); (1,0) \longrightarrow (2,1,1); (2,1) \longrightarrow (1,0,-1); (2,0) \longrightarrow (1,1,-1).$$

These rules could also be depicted in graphical form of Figure 1.5, where the Head State 1 = H and Head State 2 = N.

So, this would mean that if the HS = 1 and is on a cell with CS = 1, then the HS becomes 2, the CS is changed to 0 and the head moves 1 cell to the right along the tape, and so forth. We can represent the evolution of this Turing machine by letting each step be depicted in a vertical downward

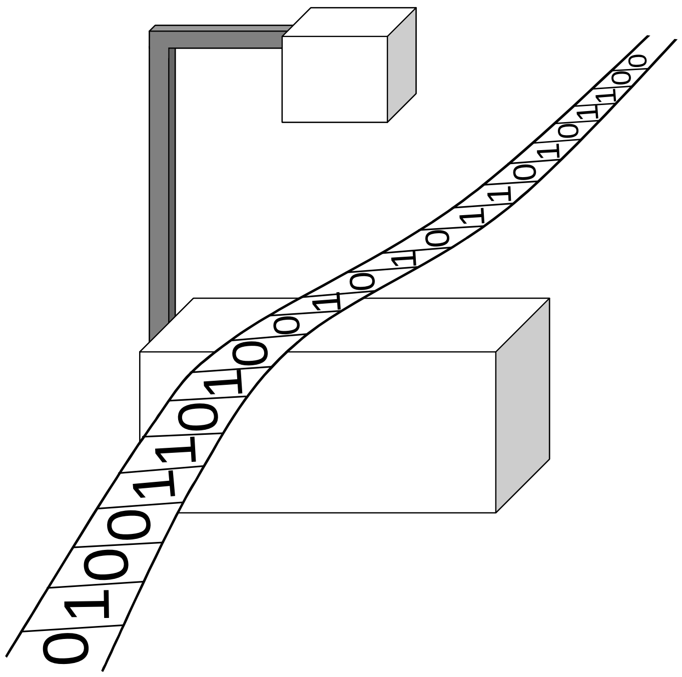

Figure 1.4: An idealized version of a Turing machine with the head reading the input of the tape below. The entire mechinism can move either one square to the right or left.

direction with moves of $+1$ being to the right and -1 being to the left. Thus the above Turing machine would evolve as in Figure 1.6 from an initial condition HS $= 1$, CS $= 0$.

Via the preceding rules, $(1,0) \longrightarrow (2,1,1)$, so that the HS is changed to 2, the initial cell state is changed to CS $= 1$, and the head moves one cell to the right. This state of affairs is denoted on the second line down, where we have the initial cell in state 1 (black), and the head (in HS $= 2$) has moved over one cell to the right, over a cell in state 0 (white). Next we find that: $(2,0) \longrightarrow (1,1,-1)$, meaning in that the HS now becomes $= 1$, the CS becomes 1, and the head moves one cell to the left, directly over the initial cell (which was black from before). Now the HS $= 1$ and CS $= 1$, so we use: $(1,1) \longrightarrow (2,0,1)$, which alters the head to HS $= 2$, the cell state changes to CS $= 0$, and the head moves one cell to the right again (which also was black from before). And merrily on the head goes, in this simple case never moving beyond the first two cells, and continually repeating its actions in a four step cycle.

One question that one may ask about any particular Turing machine is, given a particular input, will the machine stop? This general question

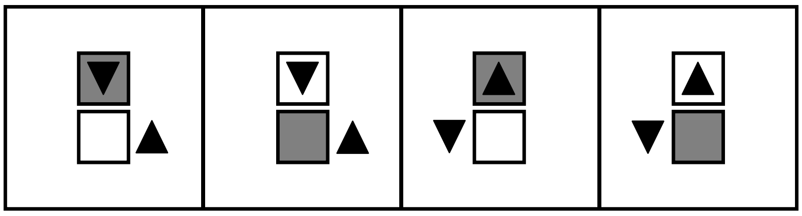

Figure 1.5: Graphical form of the Turing machine state transition function given in the text.

is known as the 'halting problem' and it was shown by Turing himself that there is no way in principle to decide whether any particular Turing machine will stop or not. It may be noted that this result has ramifications to the whole field of mathematics itself.

Many mathematical questions can be posed in the language of whether or not a specific Turing machine will halt or not. For example, Opperman's conjecture states that for any $n > 1$, between the numbers n^2 and $(n+1)^2$ one can always find a prime number. For example, between $3^2 = 9$ and $4^2 = 16$, lies a prime, in fact two in this case, 11 and 13. As the integers n start to get larger and larger, the number of primes starts to thin out so there is always a possibility that there will not be sufficient numbers of primes to fit between every n^2 and $(n+1)^2$. Fortunately, n^2 and $(n+1)^2$ spread out too. In spite of the elementary nature of this conjecture, no one has been able to prove or disprove it.

We could set up a Turing machine that would check to see if there was indeed a prime between every pair of numbers n^2 and $(n+1)^2$, and we could instruct the machine to stop if for some pair a prime was not found. If the Turing machine does stop, then we have produced a counterexample to the Opperman conjecture and it is false. If somehow we knew that this Turing machine never stopped, then we would know that the Opperman conjecture was indeed true. But being able to solve the halting problem for this particular Turing machine is equivalent to determining the truth or falsity of the Opperman conjecture.

This means that there can be no general algorithm for deciding the truth or falsity of mathematical problems, which was the 'Entscheidungsproblem' in the title of Turing's paper. This problem was first enunciated by the famous German mathematician, David Hilbert, at the 1900 International Congress of Mathematicians and was included in a list of 23 mathematical problems to be considered over the ensuing new century. This problem asked whether or not there was some general mechanical procedure that would be able to determine the truth or falsity of a large body of well-defined mathematical problems such as the Opperman conjecture. And as

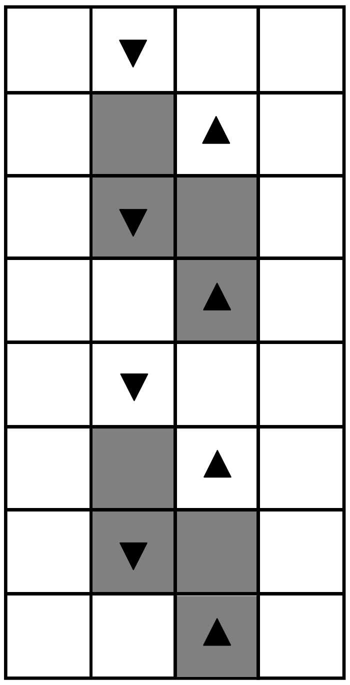

Figure 1.6: The evolution of the Turing machine example in the text starting with an initial condition HS = 1, CS = 0.

we have just seen, Turing showed this was not possible.

Turing machines with different sets of instructions are capable of doing different tasks, while there are some that are capable of emulating the performance of any other Turing machine. These are *universal Turing machines* and are said to be capable of performing *universal computation.* They can in fact do any calculation that is computable. Actually, the ubiquitous personal computer is effectively a universal Turing machine. Although a personal computer does not have an infinite storage capacity, it is essentially large enough to be considered so. Until recently, the simplest universal Turing machine was due to Marvin Minsky who in 1962 produced a universal Turing machine with 7 head states and 4 cell states. Based on the universality of Rule 110 (Section 3.5), Wolfram [2002] reduced this to just two head states and 5 cell states.

1.3 Register Machines

Computers basically perform operations on numbers that are stored in what are called *registers.* A (Minsky) register machine is just an idealization of the basic manipulations that are performed on the numbers contained within the registers of a real computer. In order for the computer to perform a simple calculation such as the addition of two numbers, it must take the numbers stored in one of the registers and combine it with the number stored in another register. A register machine has three types of instructions INC(rement), DEC(rement) and HALT. The INC instruction increments by 1 the number stored in a particular register and then the machine proceeds to process the next instruction. The DEC instruction has two components: it decrements by 1 the number stored in a particular register and then it will 'jump' to another specifically designated instruction. But there is one *caveat* here. The number in a register cannot be less than zero, so if the value of zero is stored in a register and that register is to be decremented, then the instruction is ignored and the machine proceeds to the next instruction. Finally, the HALT instruction does simply that – it halts the operation of the register machine.

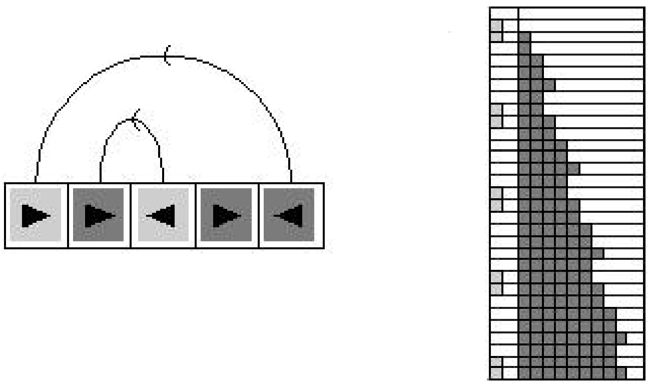

Figure 1.7: An example of a simple register machine with two registers and five instructions. Light gray indicates register 1 and dark gray register 2. An increment instruction is denoted by I and a decrement by J together with the path of the jump. The output after each step is at the right with the 1st column displaying the contents of register 1 and the 2nd column the contents of register 2.

Marvin Minsky [1967] showed that all one needs is just two registers to emulate a universal Turing machine.

1.4 Logic Gates

Logical statements are of the form: "April comes before May", "3 is less than 2", "All men are mortal" and are always considered to be either *true* or *false*, and as such, are given a truth value T (true) or F (false). This is a somewhat different philosophy from that normally assumed for statements in everyday conversation, but it is nevertheless the one adopted when discussing statements in a formal logical framework. We will denote declarative statements by capital letters such as:

P: All men are mortal.
Q: Socrates was a man.

Logical statements can be combined using connectives to form compound statements. The *conjunction* of statements P and Q is denoted by $P \wedge Q$. Consequently, if P and Q are as above, then $P \wedge Q$ is the statement: "All men are mortal and Socrates was a man". The *disjunction* of P and Q is denoted by $P \vee Q$ and for the above P and Q, then $P \vee Q$ represents: "All men are mortal or Socrates was a man", allowing for the possibility of both statements being true. The *negation* of a given statement P is denoted by $\neg P$. Thus if P represents the statement: "All men are mortal", then $\neg P$ represents the statement: "It is not the case that all men are mortal".

The truth value of the *Boolean relations* $\neg P$, $P \wedge Q$, and $P \vee Q$ is determined by the following principles and depends on the truth value of the statements P, Q according to the following Truth Table:

P	Q	$\neg P$	$P \wedge Q$	$P \vee Q$
T	T	F	T	T
T	F	F	F	T
F	T	T	F	T
F	F	T	F	F

Thus if the statement P: "All men are mortal" is true, then the statement $\neg P$: "It is not the case that all men are mortal" is false. Note that the conjunction $P \wedge Q$ is true only when both P and Q are true, whereas the disjunction $P \vee Q$ is true when either P or Q is true (or both are true).

At the heart of any computer system is the construction of the 'logic gates' NOT, AND, OR that are simply implementations of the input and output of the preceding Truth Table. These gates regulate the flow of a current through the system where T symbolizes the state 1 or 'current on' and F symbolizes 0 or 'current off' as below (actually, 'high' voltage and 'low' voltage, but that is of no consequence.

P	Q	$\neg P$	$P \wedge Q$	$P \vee Q$
1	1	0	1	1
1	0	0	0	1
0	1	1	0	1
0	0	1	0	0

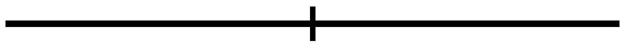

Figure 1.8: Line segment with two self-similar smaller segments and scale $r = \frac{1}{2}$.

1.5 Dimension

Most people probably realize that we live in a 3-dimensional space and that a plane is 2-dimensional, a line 1-dimensional and a point 0-dimensional. These are the *Euclidean dimensions* of our everyday world. Various other dimensions have arisen in mathematics and in the sequel we will discuss several of them. Of special relevance are the types of dimension that have non-integer values used to study fractals and chaotic attractors.

Let us consider a line segment of fixed length and divide it in half. Then each half is a replica of the original except they have been scaled down by a factor of $r = \frac{1}{2}$. We call r the *scale* and observe that the number of *self-similar segments* N, which is 2 in this case satisfies the relation $Nr^D = 1$, where $D = 1$ is the dimension of the line.

In dimension two, if we take a square and divide it up into $N = 4$ self-similar smaller sized squares, the scale r of a side of a square is again $\frac{1}{2}$ and we find again that $4(\frac{1}{2})^2 = 1$, that is, $Nr^D = 1$, where here the dimension D equals 2.

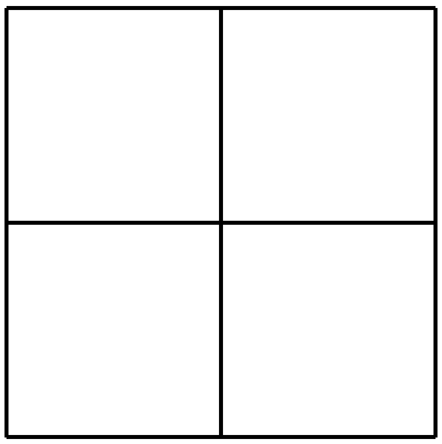

Figure 1.9: Square with four self-similar smaller sized squares and scale $r = \frac{1}{2}$.

Likewise for $D = 3$, a cube can be divided up into $N = 8$ self-similar but smaller sized cubes (Figure 1.10) with the scaling factor $r = \frac{1}{2}$ and again $8(\frac{1}{2})^3 = 1$, so that $Nr^D = 1$ holds in all three cases. Since $N = r^{-D}$, we say that N obeys a *power law.*

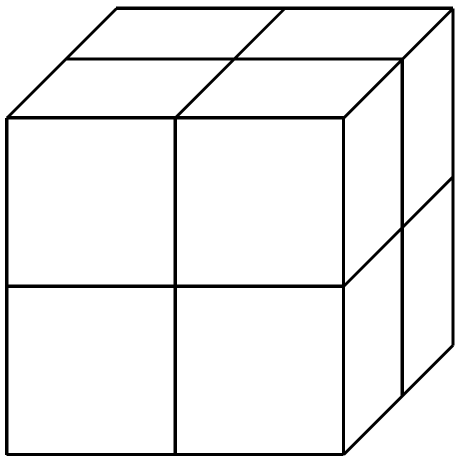

Figure 1.10: Cube with 8 self-similar smaller sized cubes with scale $r = \frac{1}{2}$.

Using the relation $Nr^D = 1$ and solving for D we find that

$$D = \frac{\log N}{\log(1/r)}. \tag{1.1}$$

This is taken to be the definition of the *similarity dimension* and it agrees with the Euclidean dimension of a line, square, and cube.

An example of a curve that does not have a proper integer dimension is the so-called *Koch curve.* It was given by Helge von Koch in 1904 as an example of a continuous curve that had no tangent at any point. It is constructed as follows. Starting with a line segment say of some unit length, replace the middle third of the line segment with a two-sided triangle having sides of length 1/3 as indicated in Figure 1.11.

We treat each resulting straight-line segment as above, replacing it with a two-sided triangle and continuing with this process ad infinitum. The limit of this process is the Koch curve that has no straight-line segments at all and no tangent at any point. Since the length of the curve grows by a factor of 4/3 at each step, the limiting length is infinite. Moreover, since each line segment is replaced by $N = 4$ self-similar segments and the scale for these segments is $r = 1/3$, the similarity dimension is $D = \log 4/\log 3 \simeq 1.262$. This dimension being greater than one gives some indication that the curve in some sense takes up more space than an ordinary line. Any figure that has a non-integer dimension, is called a *fractal*, and the similarity dimension is also referred to as the *fractal dimension.*

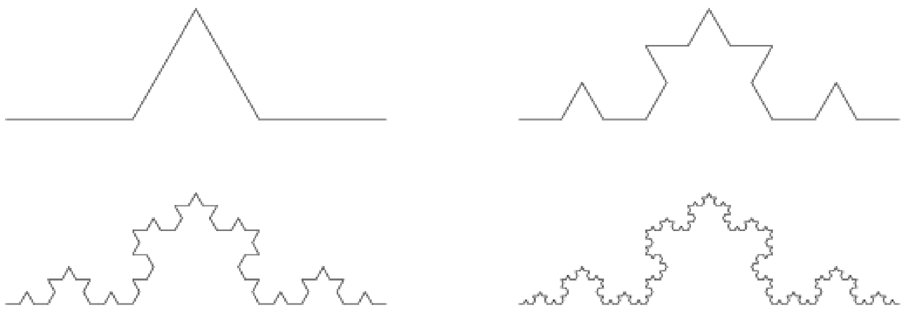

Figure 1.11: Starting from a straight line segment, here are the first four steps leading to the production of the Koch curve. Image courtesy G.W. Flake, *The Computational Beauty of Nature.*

Fractals have details at arbitrarily small scales and when that detail is in the repeated form of the whole, they are *self-similar.* This notion has been very useful in the computer generation of many artificial life forms (cf. eg. Mandelbrot [1982], Oppenheimer [1989]) as in the fern leaf (Figure 1.12)

Another mathematical construction that is rather fascinating and also has a non-integer similarity dimension is the famous *Cantor set*, due to the German mathematician Georg Cantor. We start with a line segment of length 1 and remove the middle third of it, $(1/3, 2/3)$, leaving the two closed intervals, $[0, 1/3]$and $[2/3, 1]$.

Next, remove the middle third of these two intervals, that is remove $(1/9, 2/9)$ and $(7/9, 8/9)$. This leaves four closed intervals similar to the original, and we again remove the middle third of each, and continue on indefinitely as indicated in the figure above. The limiting set, which consists of nothing but the endpoints of intervals, but no interval itself, is the Cantor set. Interestingly, if we total up the lengths of the line segments that were removed, we obtain:

$$\begin{aligned}\frac{1}{3}+\frac{2}{9}+\frac{4}{27}+... &= \left(\frac{1}{3}\right)\left(1+\frac{2}{3}+\left(\frac{2}{3}\right)^2+...\right)\\ &= \left(\frac{1}{3}\right)\left(\frac{1}{1-\frac{2}{3}}\right)=1,\end{aligned}$$

since the infinite sum is a geometric series. Thus we have removed from the unit interval an amount totaling 1 in length, but have in fact left behind an uncountable number of points in the process! As for the dimension of Cantor's barely noticable set of points, note that $r = 1/3$ and $N = 2$, so

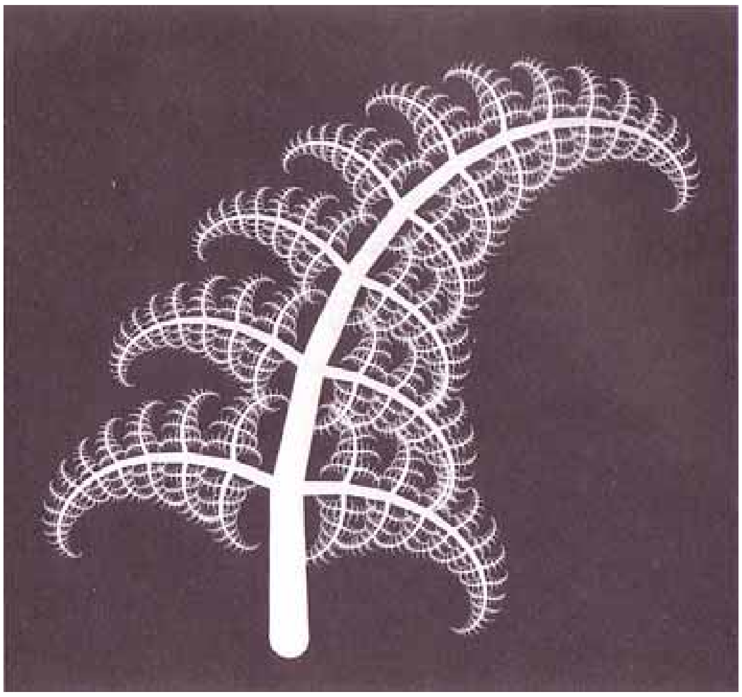

Figure 1.12: A fractal leaf form created using self-similarity. Courtesy Peter Oppenheimer, *The Artificial Menagerie*.

that the similarity dimension is $D = \log 2/\log 3 \simeq 0.631$. Even though the Cantor set has the same number of points as a solid line, its dimension is less than 1 because in some sense we have removed so much. On the other hand, a finite set of points, or even a countable set of points has similarity dimension zero. You can see why mathematicians just love the Cantor set.

Our final example will be encountered again when we talk about one-dimensional cellular automata and is the so-called Sierpiński triangle. We start with an equilateral triangle and remove an inverted version of a similar triangle having scale $r = \frac{1}{2}$ as in Figure 1.14. This results in $N = 3$ similar triangles from which we again remove an inverted version of a similar triangle having scale $r = \frac{1}{2}$. Continuing in this way results in the Sierpiński triangle having similarity dimension $D = \log 3/\log 2 \simeq 1.585$.

1.5.1 Capacity Dimension

In a similar vein to determining the length of a coastline, let us consider the *capacity dimension* of a fractal-like object given by

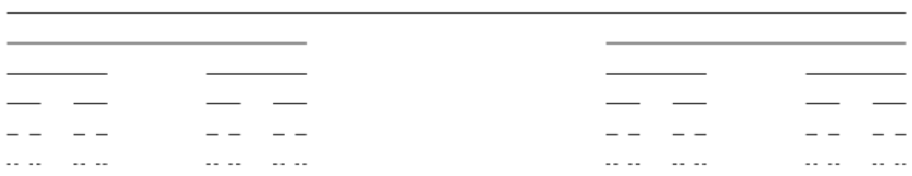

Figure 1.13: The construction of the Cantor set whereby the middle third of each remaining line segment is removed. Image courtesy G.W. Flake, *The Computational Beauty of Nature.*

$$D_C = \lim_{h \to 0} \frac{\log N(h)}{\log(1/h)}. \tag{1.2}$$

Here, h can be taken to be arbitrarily small and $N(h)$ is the number of steps of length h; to measure the capacity dimension one has to extrapolate the data. For fractal-like objects we should have a power law relation between $N(h)$ and h, say, $N(h) = ah^{-D_C}$ so that $\log N(h) = -D_C \log h + \log a$, and this relationship holds for all arbitrarily small h. Then solving for D_C yields

$$D_C = \frac{\log N(h)}{\log(1/h)} + \frac{\log a}{\log(1/h)},$$

and letting $h \longrightarrow 0$ kills off the last term in the preceding expression (since a is constant) and yields the desired equation. What this tells us is that the formulation in Equation 1.2 is just a means to get our hands on the exponential part of any power law relation between $N(h)$ and h. In this instance we will get the same value for D_C as we did for the similarity dimension of Equation 1.1

1.5.2 Kolmogorov Dimension

This is also known as the *box-counting dimension* and consists of a grid of boxes that covers the figure to be measured. The log of the number of boxes, $N(\beta)$, required to cover the figure, is plotted against the log of the length of the side of a box, β, for various box sizes. Again, a power law relation would yield a straight line representing the data points and the line's slope would give the more sophisticated sounding *Kolmogorov dimension,* D_K, of the figure.

Just as for the capacity dimension we define D_K in the analogous form,

$$D_K = \lim_{\beta \to 0} \frac{\log N(\beta)}{\log(1/\beta)}, \tag{1.3}$$

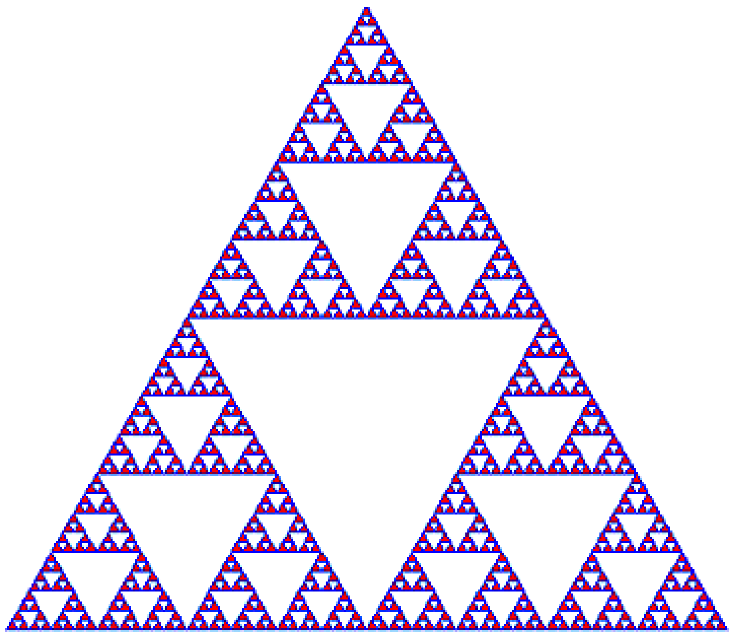

Figure 1.14: The Sierpiński triangle is the limiting case of the above figure.

where in this case $N(\beta)$ is the number of boxes intersected by the figure in question and β is the length of the side of each box.

If we consider the Cantor set and cover it with 3 bins, say [0,1/3], [1/3,2/3] and [2/3,1], then we see that only two of these contain points of the Cantor set since the 'middle third' is void by definition and we can count the endpoints 1/3 and 2/3 as belonging to the first and third bins with the other points of the set. As $\beta = 1/3$, we see that $\log N(\beta)/\log(1/\beta) = \log 2/\log 3$, and in general, taking the number of bins to be 3^n, we find that exactly 2^n boxes contain points of the Cantor set, so that

$$\frac{\log N(\beta)}{\log(1/\beta)} = \frac{\log 2^n}{\log 3^n} = \frac{\log 2}{\log 3} \simeq 0.631,$$

which is just the similarity dimension that was determined previously.

1.6 Information and Entropy

There is some kind of mystique about entropy.

Jean Bricmont

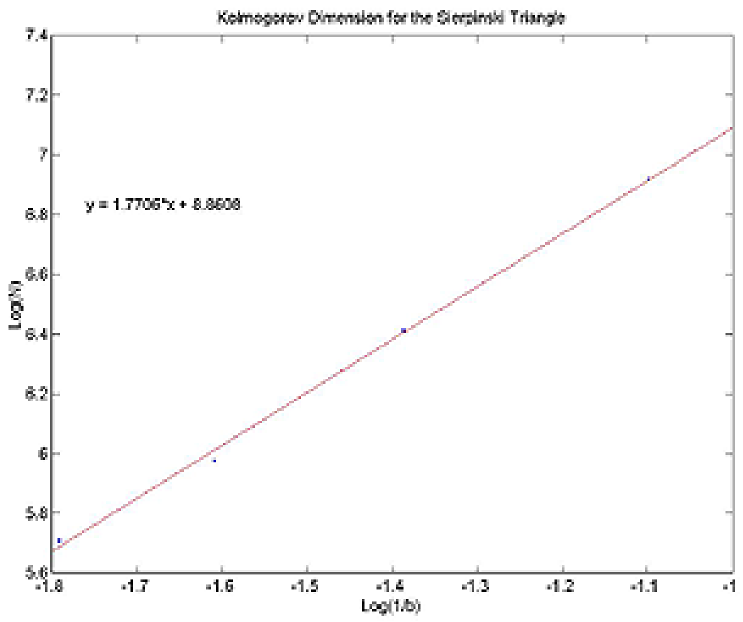

Figure 1.15: This is a plot of the log of the number of boxes needed to cover the Sierpiński triangle vs. the log of the box size in mm. The slope of the straight line gives the Kolmogorov dimension of 1.7706, in reasonably close agreement with the similarity dimension of 1.585 determined previously.

The mathematical treatment of information began with the work of Claude Shannon (1949) and is based on certain probabilities. If an event is unlikely to occur (i.e. has low probability) then the amount of information obtained about its occurrence is relatively high, whereas if the event has a high probability of occurring, then the amount of information regarding its occurrence is relatively low. If the probability of the event in question is denoted by P, then the information it conveyed by its occurrence is defined to be

$$I = \log_2 (1/P) \,.$$

Although we have taken base 2 here, it can vary depending on the context, but for our purposes we will use base 2. For example, information in a computer is stored as sequences of 0's and 1's, offering two possibilities for each digit. Each digit, which has a 1 in 2 chance of appearing thus holds $\log_2(2) = 1$ *bit* (binary digit) of information. Likewise, if you toss a coin and a heads turns up, then 1 bit of information is conveyed. Or, if you roll a six-sided die with each side having a probability of 1/6 of turning up and you roll a 5, then the information conveyed equals $\log_2(6) = 2.59$ *bits* (*binary digits*) of information. In fact, when any face turns up upon rolling the die, 2.59 bits of information are conveyed.

When we are dealing with events that have unequal probabilities, then the total amount of information is a weighted sum with the weight given to each contribution determined by the probability of its occurrence. For instance if P_1, P_2,..., P_N are the probabilities of N individual outcomes, subject to: $\sum_{i=1}^{n} P_i = 1$, then the *information* I of the entire system is given by

$$I = \sum_{i=1}^{N} P_i \log_2 (1/P_i)\,. \tag{1.4}$$

I is in general positive but can be zero if all but one of the probabilities are zero and the remaining one equals 1. I becomes a maximum when all the probabilities P_i are equal to $1/N$ and the maximum value of I is then the sum of N quantities of $\frac{1}{N}\log N$, giving $I_{\mathsf{max}} = \log N$.

This expression for information is formally related to another concept of entropy that originated from the work of Rudolf Clausius in 1865 as a measure of the amount of irreversible heat loss of a system and who formulated the Second Law of Thermodynamics as the notion that *the thermodynamic entropy of a closed system increases to a maximum.* This has led to the belief in the eventual so-called 'heat-death' of the universe, whereby the universe itself will reach a state of maximum entropy where all matter is cold and disordered. The second law was formalized by Bolzmann in 1872 who described entropy (H) by the mathematical formulation

$$H = -K \sum_{i=1}^{N} P_i \log_e P_i.$$

Boltzmann was interested in describing the dynamics of a gas and here the P_i represent the probabilities of gas molecules being in one of N particular states and K is the Boltzmann constant. With $K = 1$ we formally have the information I (except for a change of base) formulated by Shannon, and in fact, I is also referred to as *entropy* or *information entropy.* The concept of entropy has also been associated with 'disorder' and 'randomness' whereby high entropy is equivalent to a high degree of disorder (randomness) and low entropy is equivalent to a low level of disorder (non-randomness). In the sequel we will invoke the notion of entropy in this sense. It is sometimes claimed that biological systems violate the Second Law of Thermodynamics because they are ordered systems that arose from less ordered ones, but this is incorrect as biological systems are open to the environment and therefore cannot be considered closed. The Second Law describes *irreversible* processes (see Section 3.7) that increase in entropy along an arrow of time. Entropy is embraced by many other scientific disciplines, and has had a colorful and controversial history which continues to this day. According to Denbigh and Denbigh (1985), "A number of scientists and information theorists have maintained that entropy is a subjective concept and is a measure of human ignorance. Such a view, if it is valid, would create some profound philosophical problems and would tend to undermine the objectivity of the scientific enterprise as a whole." However, the authors conclude that, "... *thermodynamic* entropy is fully objective... and the same must apply to any other 'entropy' which is used as a surrogate."

There is also an *information dimension* associated with the information I. Let us consider the two dimensional case in which the figure to be measured is overlayed with a grid of n same-sized cells or bins as in the Kolomogorov dimension. To compute the information I, each probability P_i represents the number of figure elements in the ith box, divided by the total number of figure elements, say N. This is just the *relative frequency* of figure elements occuring in the *ith* box. Then I is computed according to equation

$$I = \sum_{i=1}^{N} P_i \log_2(1/P_i).$$

If a particular box has no figure elements in it then corresponding probability P_i is zero and there is no contribution to the information I in this case. Evidence suggests that I increases linearly as a function of $\log(1/\beta)$, where β is the length of the side of each bin over a suitable range of values. Of course if the bin size becomes too large and the entire figure fits into one bin, then $P = N/N = 1$ and hence $I = P\log_2(1/P) = 0$. On the other hand, if the bin size becomes too small, then at most one figure element lies in any given box and each nonzero P_i equals $1/N$. If we just take our sum over the bins that are non-empty, we see that there are now N of these and I is equal to $N \times \frac{1}{N}\log_2 N$ giving $I_{\mathrm{max}} = \log_2 N$, the maximum value for I. Any further decrease in bin size gives no further increase in information but only the same value for I.

The information dimension is given mathematically by

$$D_I = \lim_{\beta \longrightarrow 0} \frac{I}{\log_2(1/\beta)}. \tag{1.5}$$

To actually compute D_I, one can use the usual trick of graphing I against $\log_2(1/\beta)$ and the slope of the resulting straight line gives the required dimension (See Figure 1.16).

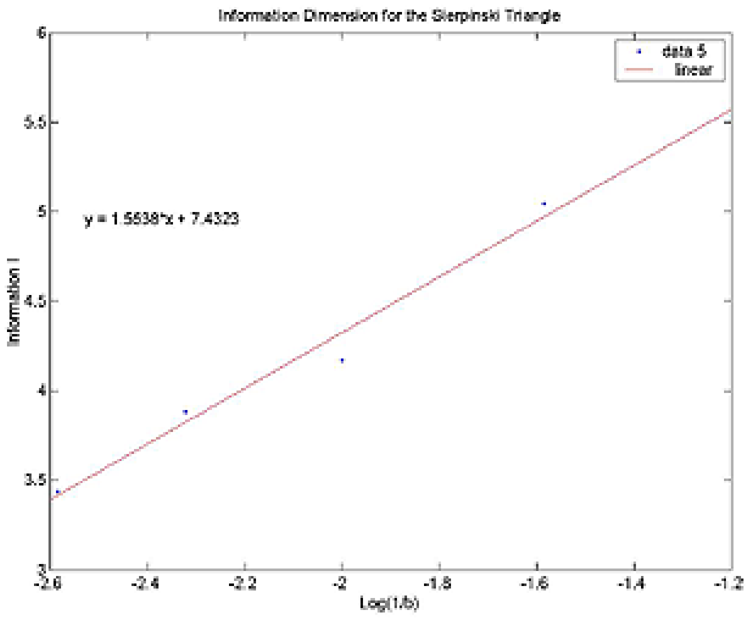

Figure 1.16: Here we have experimentally computed the information dimension for the Sierpiński triangle by the method explained in the text. The value of 1.5538 is in close agreement with the mathematically determined value of 1.585.

Note that that in the event when all the probabilities are equal, namely each $P_i = 1/N$, then we found that the information became a maximum and had the value $I = \log N$. Substituting this into D_I above gives

$$D_I = \lim_{\beta \longrightarrow 0} \frac{\log_2 N}{\log_2 (1/\beta)},$$

which already looks familiar and is of course the capacity dimension, D_C.

1.7 Randomness

In a general sense, we say that something is random if it has no regular pattern or that it is unpredictable. In a more technical sense, an infinitely long sequence is random if its Shannon information I is infinite. But for finite sequences which exist in the real world, many tests have had been developed that verify whether or not the sequence in question shares certain statistical properties with a hypothetical random sequence.

Some randomness like that displayed in coin-tossing, or dice throwing, are due to an exquisite sensitivity to the initial conditions that produced the outcome. Moreover, it has been known since the early 20th century that physics at the atomic level is governed by a degree of randomness such as in the radioactive decay of the atoms of some element. Using the random nature of quantum physics, a commercial quantum random number generator has been recently developed (called *Quantis*) that fires photons (light particles) at a semi-transparent mirror in which 50% are either reflected or transmitted with two detectors picking up the respective signals to generate a random sequence of 0's and 1's. To many scientists, the preceding examples are considered the only true form of randomness, because the outcome for any given event is not predictable or even repeatable. On the other hand, some 'deterministic' randomness like the values of the digits of $\pi = 3.141592653...$ or $e = 2.718281828...$ or $\sqrt{2} = 1.414213562$ and some of the one-dimensional cellular automata of Chapter 3, is computable from a simple algorithm. Or as we note in the next chapter, the random behavior in the evolution of the logistic equation when $a = 3$ is predictable on short time scales, but appears to be random in the long term. However, this sort of deterministic randomness is considered only *pseudorandom* by many because the output is always computable. Even the random numbers generated by computers are only pseudo-random since a computer is a deterministic system. According to my colleague, computer scientist Cristian Calude, given a sufficient amount of time and money, he would gladly compute the Nth digit of any of the above three numbers for any value of N. True random number generators like the Quantis are useful in cryptography and the scientific modelling of certain complex systems. However, for our purposes it will not be necessary to make any distinction between a truly random sequence and a pseudorandom one.

One topic that is intimately connected with cellular automata and shares many of its features is that of dynamical systems, which we take up in the next chapter.

Chapter 2

Dynamical Systems

... it may happen that small differences in the initial conditions produce very great ones in the final phenomena.
Henri Poincaré

One of the exciting new fields to arise out of 20th century mathematics is that of dynamical systems. Topics like 'chaos' and 'strange attractors' have become nearly household words even if most people do not know their precise meaning. Dynamical systems arise in the study of fluid flow, population genetics, ecology, and many other diverse fields where one seeks to model the change in behavior of a system over time. Several of the global features of dynamical systems such as attractors and periodicity over discrete time intervals, also occur in cellular automata, and thus it is worthwhile to have a working knowledge of the former. Indeed, cellular automata are dynamical systems in which space and time are discrete entities. We present here a brief summary of the salient features of dynamical systems and for the interested reader there are many fine texts on the subject (eg. Devaney [1989], Elaydi [2000], Sandefur [1990], Williams [1997]).

Let us suppose that we are interested in the size of some particular seasonally breeding insect population whose generations do not overlap. Denote the initial population size by x_0, and after the first year by x_1, after the second year by x_2 and so on with the population after the nth year denoted by x_n. Since the population size in any given year determines what it will be in the following year, we can write this deterministic feature of the population size in the form of a *dynamical system*:

$$x_{n+1} = f\left(x_n\right), \quad n = 0, 1, 2, 3, ...$$

where f signifies some mathematical function. The set of all the iterations x_n, $n = 0, 1, 2, 3, ...$ is known as the *orbit* or *trajectory* of the dynamical system. So for example, if the population size happens to triple from one generation to the next, we would have the relation

$$x_{n+1} = 3x_n, \quad n = 0, 1, 2, 3, ...$$

to describe the changing population size from one generation to the next. More generally, a linear growth model would be

$$x_{n+1} = ax_n, \quad n = 0, 1, 2, 3, ...$$

where if $a = 1$ the population remains static, and if $a > 1$ or $a < 1$ the population at each generation either grows or declines at a constant rate respectively.

More realistic equations taken from the biological literature are:

$$x_{n+1} = (1 + a)x_n - bx_n^2, \quad n = 0, 1, 2, 3, ... \tag{2.1}$$

and

$$x_{n+1} = x_n e^{[c(1-x_n)]},$$

where the parameters a, b and c are constants which have values restricted to a certain range that allow one to 'tune' the behavior of the dynamical system by varying these values appropriately. These parameters in some sense reflect the environmental conditions that the dynamical system is operating in. Equation 2.1 is referred to as the *logistic equation* and is used to model population growth, with the term b functioning as a "damping factor" because the term $-bx_n^2$ inhibits the growth of the population. These equations are *nonlinear* in the sense that the output is not proportional to the input as in the preceding system. We will consider a simplified form of the logistic equation for which $b = a$, namely:

$$x_{n+1} = (1 + a)x_n - ax_n^2, \quad n = 0, 1, 2, 3, ...$$

where a is a parameter in the range $0 < a < 3$. Analogous behavior arises in the parameter space $-3 < a < 0$. This dynamical system will serve to model all the characteristic features that we wish to exhibit.

First however, I cannot resist presenting an example of this model that features in James T. Sandefur's book [1990]. Suppose that x_n represents the fraction of those people on Earth who believe in alien beings at time period n, so that the quantity $(1 - x_n)$ is the fraction of non-believers. Furthermore, assume that in each time period the believers are able to win over a proportion of non-believers (or vice-versa) and that the proportion depends on the interaction (i.e. product) of the two groups: $x_n(1 - x_n)$. This now can be represented as the dynamical system

$$x_{n+1} = x_n + ax_n(1 - x_n),$$

which is just the logistic equation above. The parameter a can be positive, indicating that the belief in aliens is increasing, whereas $a < 0$ indicates belief is ebbing.

In order to get this system underway, let us take the value $a = 1$ and some initial value, say $x_0 = 0.25$ and compute the subsequent iterations x_n. So for example,

$$x_1 = 2x_0 - x_0^2 = 2(0.25) - (0.25)^2 = 0.4375,$$

and furthermore: $x_2 = 0.6836$, $x_3 = 0.8999$, $x_4 = 0.9900$, $x_5 = 0.9999$, $x_6 = 1.0000$, $x_7 = 1.0000$, $x_8 = 1.0000, ...$ with all subsequent iterations having the value x$_n$ = 1.0000. These values represent the orbit of the dynamical system and in this instance we refer to the value 1 as being an *attractor*. Taking some other initial value, say $x_0 = 0.5$, we find that the iterations: $x_1 = 0.7500$, $x_2 = 0.9375$, $x_3 = 0.9961$, $x_4 = 1.0000$, $x_5 = 1.0000$, $x_6 = 1.0000...$ are once again attracted to the value 1. In fact, over the entire permitted range of initial values where our dynamical system operates, the iterations will be attracted to the value 1. What's more, by allowing the parameter a to vary over the range $0 < a < 2$, we find that the value $x = 1$ is still an attractor for any sequence of iterations. The set of points that evolve to an attractor are said to lie in its *basin of attraction.*

To examine the nature of the attractor further, let us write our dynamical system as an ordinary function, namely

$$f(x) = (1 + a)x - ax^2,$$

so that

$$f(x_n) = (1 + a)x_n - ax_n^2 = x_{n+1}.$$

With $a = 1$ the preceding attractor $x = 1$ has the property that $f(1) = 1$. Any value x that has the property $f(x) = x$ is called a *fixed point* of the function f. Are there any other fixed points of our function? Setting

$$f(x) = (1 + a)x - ax^2 = x,$$

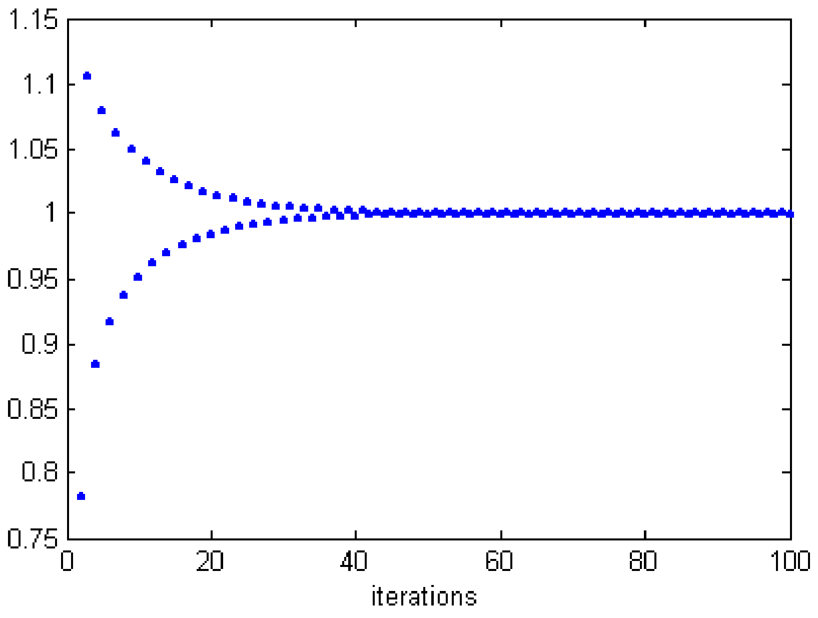

Figure 2.1: Here we have taken $a = 1.9$ and initial value $x_0 = 0.35$. The iterations are seen to converge to the value 1, the attractive fixed point.

and solving for x, we find that $x = 0, 1$ are the only fixed points. But these two fixed points are qualitatively different. While $x = 1$ is a fixed point attractor (also called a *stable* fixed point), the point $x = 0$ is a fixed point *repeller* (or *unstable* fixed point). This means that the iterates will always be repulsed from the vicinity of $x = 0$, no matter how close to it they may start (Figure 2.2).

There is a *derivative test* we can perform on the function f which can tell us *a priori* what type of fixed point we have. In particular, if $|f'(x)| < 1$ at a fixed point x, then it is an attractor and if $|f'(x)| > 1$, the fixed point is a repeller. Note that we have $f'(x) = 1+a-2ax$, so that whenever $0 < a < 2$, $|f'(0)| = 1 + a > 1$, indicating a repeller at $x = 0$, and $|f'(1)| = |1 - a| < 1$, indicating an attractor at $x = 1$.

For the region $2 < a < 2.449$, we obtain an *attractor of period two*, or *2-cycle* with the dynamical system oscillating between two fixed values as in Figure 2.3 .

In order to analyze the phenomenon of the 2-cycle, let us look at the function

$$f^2(x) = f(f(x)),$$

in other words,

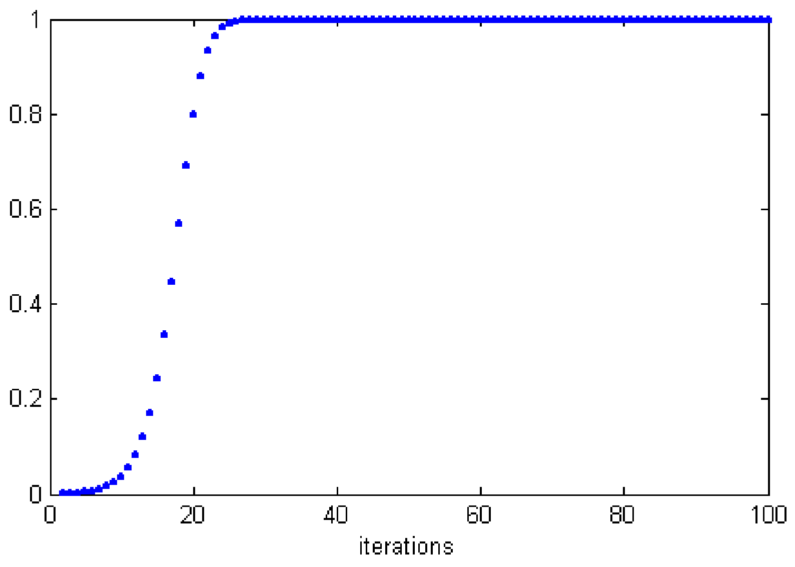

Figure 2.2: Here we have taken an initial value to be $x_0 = 0.001$ showing the repulsive nature of the value $x = 0$ and the attractive nature of $x = 1$ whenever $0 < a < 2$.

$$x_{n+2} = f^2(x_n).$$

Let the two values that the function f oscillates between be x_1^* and x_2^*, so that $f(x_1^*) = x_2^*$ and $f(x_2^*) = x_1^*$. Then

$$f(f(x_1^*) = f(x_2^*) = x_1^*,$$

and likewise

$$f(f(x_2^*) = f(x_1^*) = x_2^*,$$

which says that x_1^* and x_2^* are fixed points of the function f^2. In order to check the derivative condition at x_1^* and x_2^* we use a mathematical technique known as the chain-rule, which results in

$$\frac{d}{dx}f^2(x_1^*) = f'(x_1^*)f'(x_2^*) = \frac{d}{dx}f^2(x_2^*).$$

Checking the derivative condition on the example of the preceding two-cycle with $x_1^* = 0.7462...$, $x_2^* = 1.1628....$, and $a = 2.2$ we find that

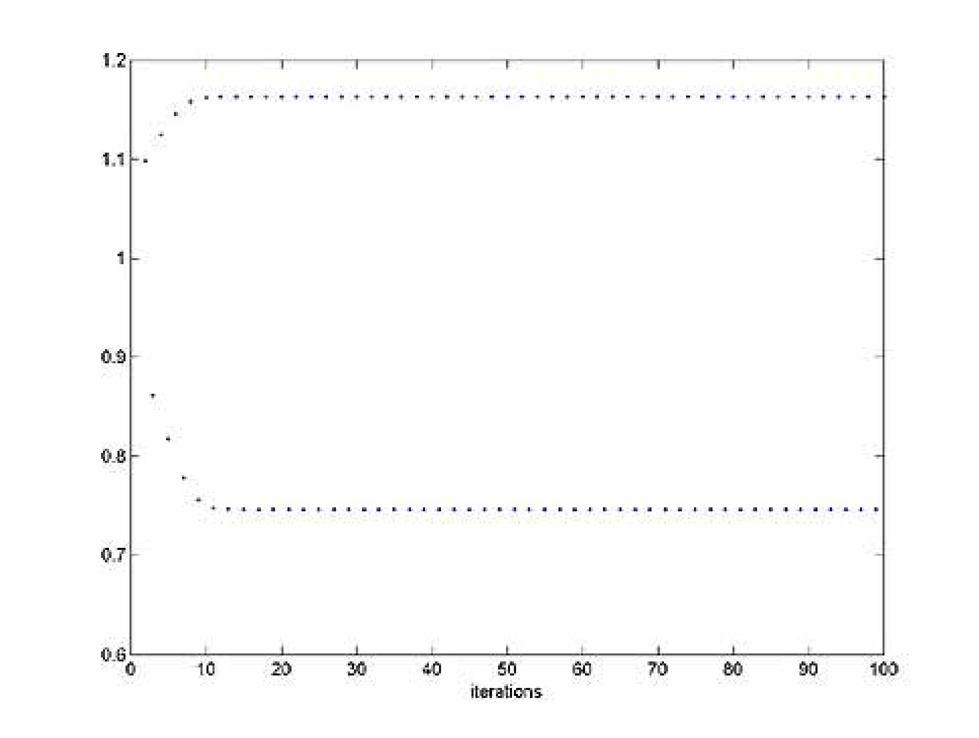

Figure 2.3: A 2-cycle for the parameter value $a = 2.2$ with the dynamical system oscillating between two fixed values, 0.7462... and 1.1628....

$$\left|\frac{d}{dx}f^2(x_1^*)\right| = \left|f'(x_1^*)f'(x_2^*)\right| = \left|\frac{d}{dx}f^2(x_2^*)\right| = 0.159... < 1.$$

Basically what this means is that if the initial point x_0 starts out near the fixed point x_1^* than the even indexed iterates of the orbit will converge to x_1^* and the odd indexed iterates will converge to the other fixed point, x_2^*. Clearly if x_0 starts out near x_2^* then the reverse happens. Periodic behavior is also found in certain cellular automata as will be pointed out in the sequel, although it is not such a significant feature as it is in dynamical systems.

Gradually increasing the parameter a, the 2-cycle is followed by a 4-cycle, 8-cycle, etc. Each of these cycles originate for a in some increasingly narrow band of values.

We can illustrate the behavior of our dynamical system by plotting the parameter value along one axis and plotting the values of the attractor along the other. At certain critical values of the parameter a, the dynamical system undergoes a bifurcation in the values generated and this produces a *bifurcation diagram* as depicted in Figure 2.5. One such value was $a = 2$,

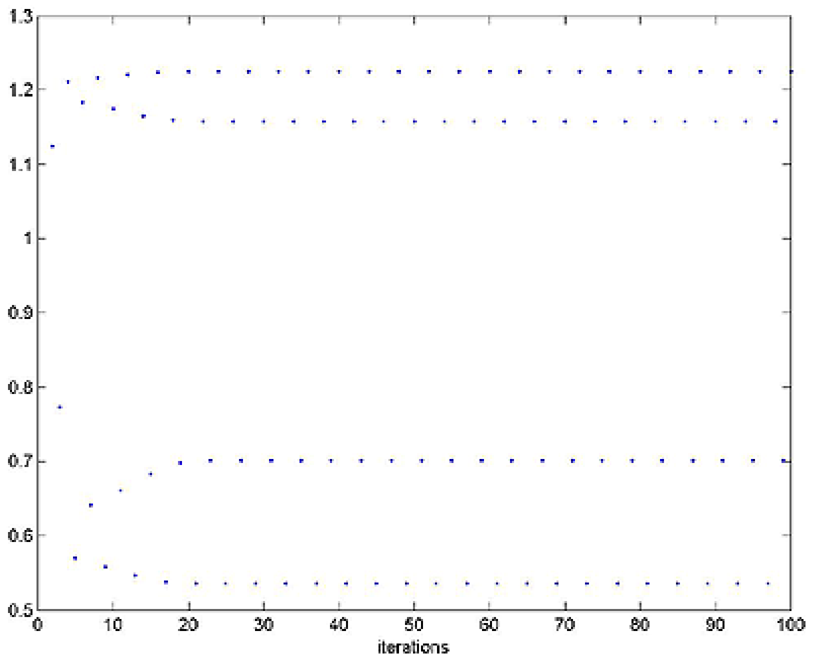

Figure 2.4: Here we have an attractor of period four or 4-cycle with $a = 2.5$ showing how the system oscillates between four distinct values.

whereby the dynamical system went from having a stable attractor (at $x = 1$) when $0 < a < 2$ to a 2-cycle for values of a slightly larger than 2.

When $2.57 < a \leq 3$, the period doubling behavior of our dynamical system breaks down and we enter the *chaotic regime*. Here there are infinitely many initial values x_0 that yield *aperiodic orbits*, that is, the iterates x_n wander erratically over a fixed interval. Of course, these can be difficult to distinguish from cycles with very long periods. For example, there is an odd period 3-cycle at $a = 2.8284$, which happens to exhibit its own period doubling (a 6-cycle at $a = 2.845$ and a 12-cycle at $a = 2.848$ were found). Even period cycles also turn up in this region, eg. at $a = 2.9605$ we have a return to a 4-cycle. All of these periodic cycles and infinitely more others exist within narrow windows of the parameter space.

At the end of our parameter interval when $a = 3$ (and at other values as well), our dynamical system effectively becomes a deterministic random number generator. At this point, we have what is commonly called *chaos*. One main feature of chaos is what is called *sensitivity to initial conditions*, that is, if we start off with two different initial values, say x_0 and y_0, no matter how close together, the resulting iterations x_n and y_n will eventu-

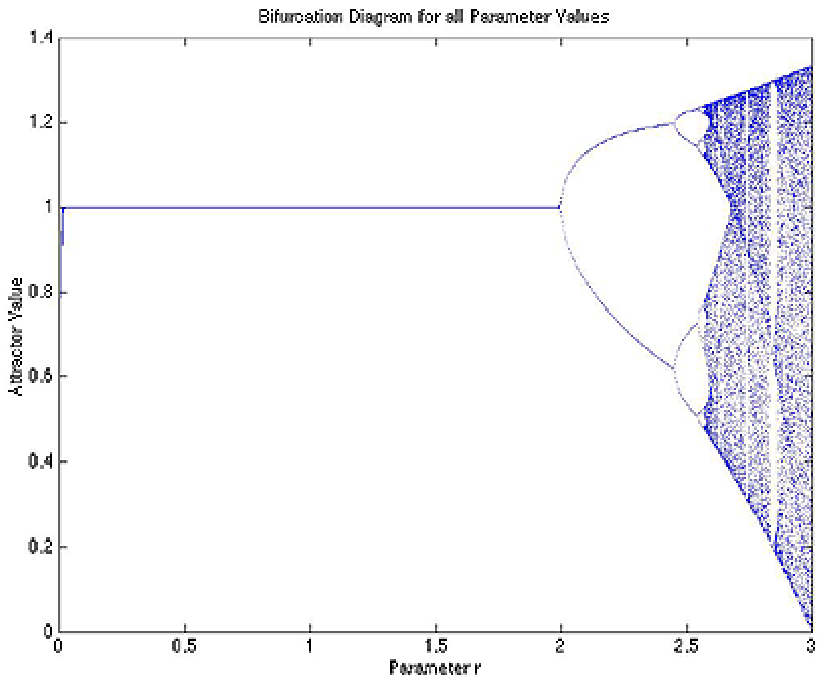

Figure 2.5: This diagram demonstrates how the values of the attractor of the dynamical system change as the parameter value a is varied and illustrates the common phenomenon of *bifurcation* and *period doubling* whereby a heirachy of 2^n-cycles are generated. The range of values of a over which the 2^n-cycle remains an attractor (i.e. stable), gradually diminishes.

ally diverge away from each other. This feature makes long term predictions about the dynamical system impossible, but does allow for short term predictions since initial values of the respective trajectories, $x_1, x_2, ...$ and $y_1, y_2, ...$ will remain close. This sensitivity is nicely illustrated with the following experiment, where the initial values x_0 and y_0 only differ in the 12th decimal place by one digit (one part in a trillion)! Yet within 40 iterations, the respective iterations x_n and y_n are already widely divergent.

$x_0 = 0.123456789012$	$x_0 = 0.123456789011$
$x_1 = 0.448102419788$	$x_1 = 0.448102419785$
$x_2 = 1.190022343293$	$x_2 = 1.190022343288$
.	.
.	.
.	.
$x_{40} = 0.508890113704$	$x_{40} = 1.006900670500.$

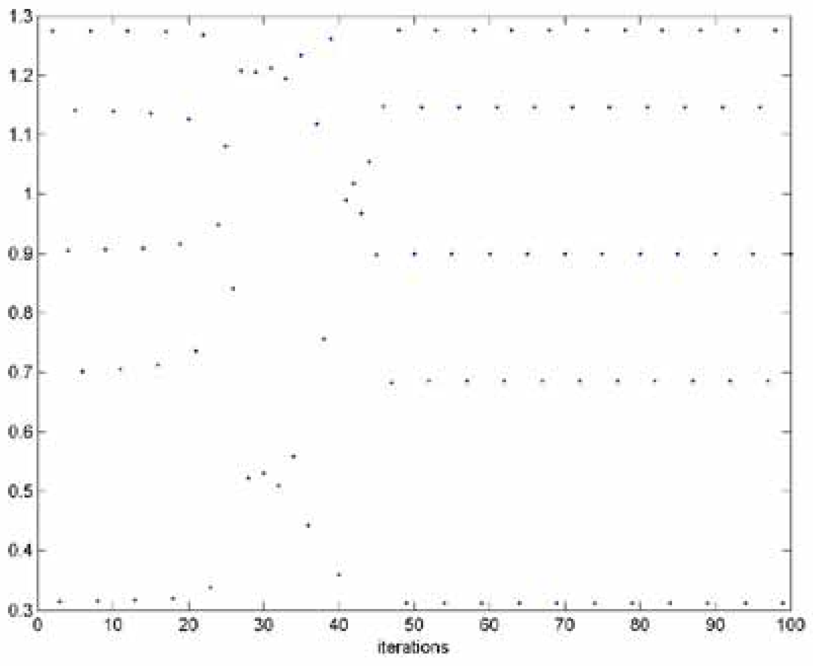

Figure 2.6: In the chaotic regime we can find even and odd period cycles amongst the aperiodic orbits. Here is a stable 5-cycle at $a = 2.7385$.

The corresponding iterations remain close at first, but gradually start to diverge, so that by the 40th iteration they are widely divergent and continue so thereafter. This extreme sensitivity to initial conditions is typical of a dynamical system in a chaotic state. An analagous situation arises in Class III cellular automata (see Section 3.8). It should be noted that when a dynamical system is not in a chaotic mode, say for a positive value of a that is less than 3 in the above system, then small differences in the input only result in small differences in the output.

A chaotic dynamical system has the feature that in practice long term predictions are impossible since one can never measure initial conditions with infinite precision. Therefore, as in the example above, the long term future of the iterations is in the hands of the Gods. However, it is still possible to make short term predictions since the values of a few iterations with slightly differing initial conditions will remain reasonably close in the short term. Most people experience this phenomenon daily when they watch the weather forecast on TV which is the forecaster's attempt to predict the behavior of a chaotic dynamical system for the next few days.

By taking two points initially very close together in this fashion, it is possible to measure the rate of convergence or divergence of the ensuing trajectories. As it turns out, the rate of convergence or divergence increases in an exponential fashion, and this rate has a value equal to ae^{bn}, where $a > 0$ and b are constants, and n is the number of the iteration. If b is negative, the trajectories of two neighboring points are converging at an exponential rate and if b is positive the values are diverging at an exponential rate. This divergence was illustrated in the preceding example, and an example of the case where the trajectories are converging exponentially is given by taking $a = 2.51$, and initial values $x_0 = 0.2$, $y_0 = 0.3$. Then after 100 iterations of each trajectory, we find that *both* are yielding the same cycle of four values to 12 decimal places:

0.528209070336
1.153711733697
0.708590766456
1.226880395750.

This is simply the period four attractor we saw above in Example 2.4 Note however, that by taking yet more decimal places there will be slight differences in the values of the iterates of the two trajectories but these will gradually diminish as we take more and more iterations and the two trajectories converge.

The value b is called a *local Lyapunov exponent* and when $b < 0$ neighboring trajectories converge as in the preceding case, and when $b > 0$ trajectories diverge as in the case of the chaotic attractor.

Although a glance at the data shows that the trajectory values of the chaos example initially are steadily growing apart, there will be times further on in the iterations when values will become closer, move apart, come closer again, etc. So what is needed is an average taken over the entire attractor and that is given by the *Lyapunov exponent.* It can be calculated by the formula

$$\lambda = \lim_{N\to\infty} \frac{1}{N} \sum_{n=1}^{N} \log_2 |dx_{n+1}/dx_n| \,,$$

where λ will be approximated by taking N reasonably large, so that in the case of our dynamical system we have

$$\lambda \approx \frac{1}{N} \sum_{n=1}^{N} \log_2 |1 + a - 2ax_n| \,, \qquad \left(x_{n+1} = (1+a)x_n - ax_n^2\right).$$

This gives an average global measure of the convergent or divergent nature of the dynamical system. A nice account of the mathematical de-

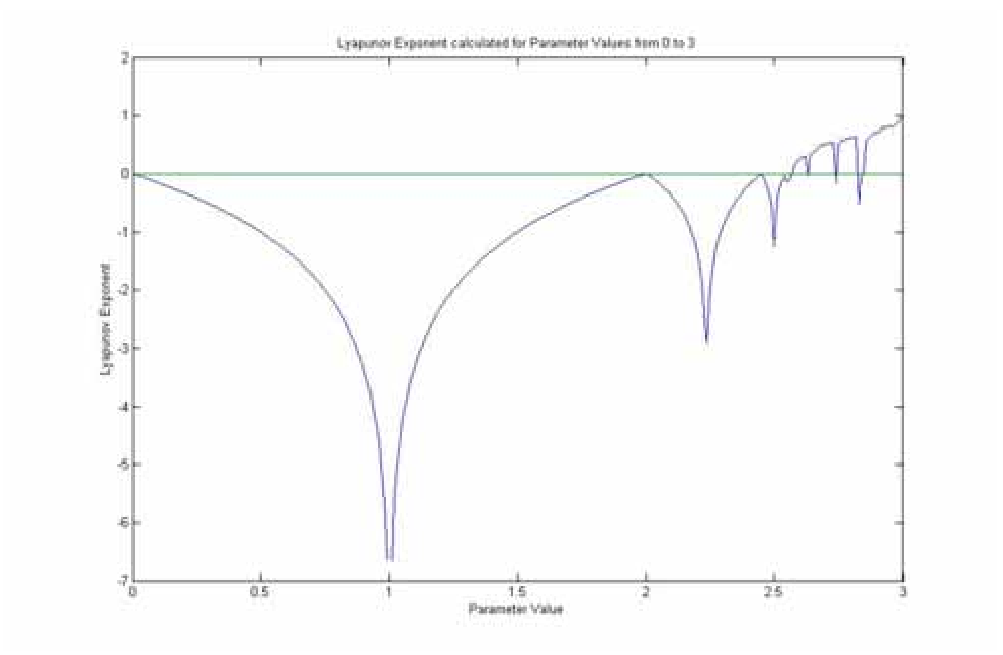

Figure 2.7: A graph of the value of the Lyapunov exponent λ for the range of parameter values $0 < a < 3$. When $\lambda < 0$ the dynamical system is stable, and for $\lambda > 0$ the system is chaotic. Note that there are intervals of stability in the chaotic regime beyond $a = 2.5699$.

velopment leading up to the formulation of this equation can be found in Williams [2001].

$\lambda < 0$: The iterations of the system approach a stable fixed point or a stable periodic orbit.

$\lambda = 0$: This occurs in our system when $a = 2$ at a bifurcation point.

$\lambda > 0$: The dynamical system is unstable and chaotic as we saw was the case in various regions of the parameter space after 2.5699 and when we took $a = 3$.

One important thing to note about chaos is that it is the result of a deterministic system. If you start with precisely the same initial value x_0 then the resulting orbit, even though it lacks periodicity, will be precisely the same. However, any slight deviation, no matter how small, will eventually lead to different values appearing in the orbit.

Another interesting phenomenon occurs at the starting point of the chaotic regime when $a = 2.5699...$ Here we obtain what is commonly known as a *strange attractor* in that the values of the orbit of the attractor form a Cantor set. Strangely enough, this attractor does not exhibit sensitivity to initial conditions and so would not be considered chaotic although

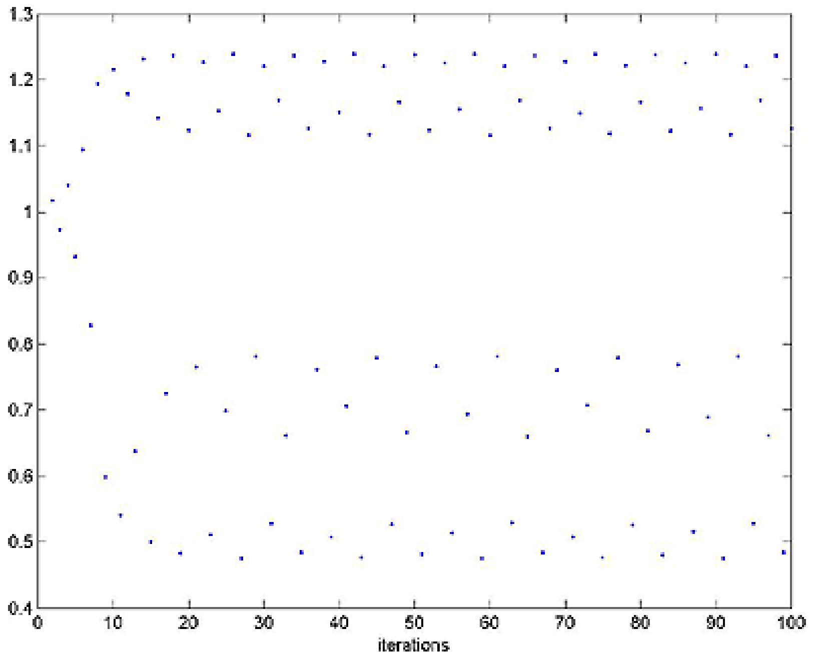

Figure 2.8: The strange attractor when the parameter value is set at $a = 2.5699$. The values of the orbit form a Cantor set.

some authors use the terms 'strange' and 'chaotic' synonymously (Williams [1997]).

Magnifying the scale depicted in Figure 2.8 a hundred-fold (and taking more iterations accordingly), we would see some of the 'arms' of the attractor resolving into more sets of 'arms', and even further magnification would resolve some the the resulting arms into yet further ones, and so forth. This type of infinite regression is typical of the Cantor set encountered in Section 1.5.

We are now ready to enter the remarkable world of cellular automata.

Chapter 3

One-Dimensional Cellular Automata

Cellular automata may be viewed as computers, in which data represented by initial configurations is processed by time evolution.

Stephen Wolfram

3.1 The Cellular Automaton

We will consider a lattice network of cells that are most commonly square in shape, but the cells can be hexagonal and other shapes as well. Each cell can exist in k different states, where k is a finite number equal to or greater than 2. One of these states has a special status and will be known as the ‘quiescent state’. The simplest case where each cell can exist in two possible states (not simultaneously), can be denoted by the symbols 0 and 1 and graphically by white and black, respectively. In more anthropomorphic terms, we can think of cells in the 0 (white/quiescent) state as ‘dead’ and those in the 1 (black) state as ‘alive’.

The lattice of cells can be $n(\geq 1)$ dimensional, but most of the work on cellular automata has been for one and two dimensions, particularly the former. In the sequel, we shall generally consider square cells as the basic unit of our automata. In the one-dimensional case, these form a row of adjacent boxes. In principle, the number of boxes in any array is infinite, but for practical purposes it will simply be taken sufficiently large to illustrate the behavior in question, often with certain conditions imposed on the cells along the boundaries. In some cases, intentional restrictions will be made on the size of the lattice as well.

In order for the cells of our lattice to evolve we need time to change, and this is done in an unusual manner by considering changes to the states of cells in the lattice only at discrete moments in time, that is, at time steps $t = 0, 1, 2, 3....$ as in the ticking of a clock. The time $t = 0$ usually denotes the initial time period before any change of the cells' states has taken place. One further ingredient that is needed for our cellular lattice to evolve with discrete time steps is a local rule or *local transition function* governing how each cell alters its state from the present instant of time to the next based on a set of rules that take into account the cell's current state and the current state of its neighbors. Of course, which cells are considered to be neighbors, needs to be precisely defined. This alteration of cell states takes place *synchronously* for all cells in the lattice. The transition function can be deterministic or probabilistic, but in most cases (some exceptions are models discussed in the chapter on Applications) we will consider only the former. The lattice of cells, the set of allowable states, together with the transition function is called a *cellular automaton.* Any assignment of state values to the entire lattice of cells by the transition function results in a *configuration* at a any particular time step.

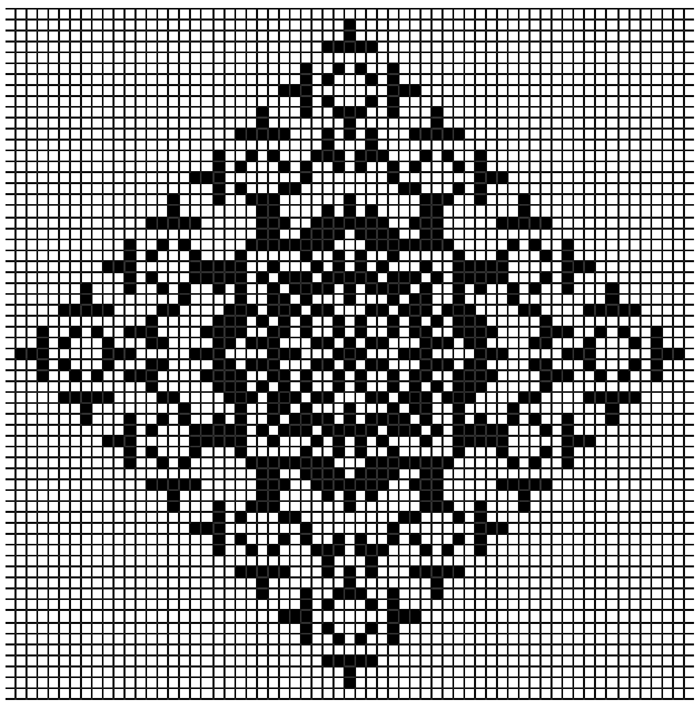

Figure 3.1: A two-dimensional configuration with each cell taking one of two state values, black or white according to a particular local transition function. The first printed reference to a system such as the above, even using the word 'automata', is to be found in the paper by Ulam [1950].

Therefore the three fundamental features of a cellular automaton are:

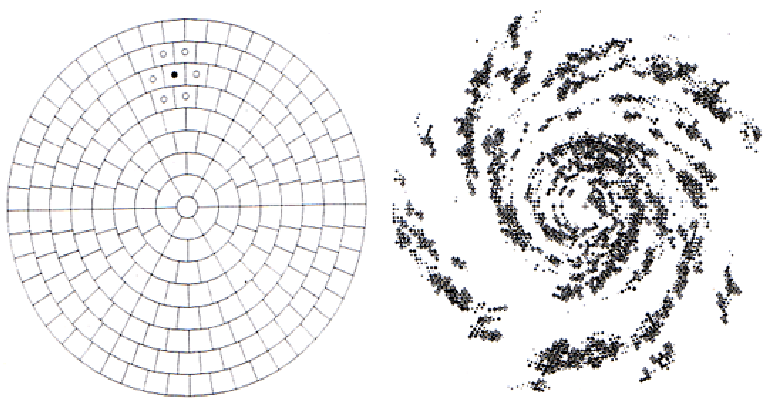

Figure 3.2: In this setting the neighbors of each cell change due to the differential rotation of the rings of the polar grid that is used to emulate galaxy formation. The black circle is an active region of star formation which induces star formation in its neighbors with a certain probability at the next time step. At right is a typical galaxy simulation.

- *homogeneity*: all cell states are updated by the same set of rules;
- *parallelism*: all cell states are updated simultaneously;
- *locality*: the rules are local in nature.

There has been some recent work on the *asynchronous* updating of cell states (cf. eg. Bersini and Detour [1994], Ingerson and Buvel [1984], Schönfisch & de Roos [1999]). This can be achieved in a number of different ways and is discussed in Section 4.4.

Other liberties with the rules of a cellular automaton can be taken. In one interesting example, galaxy formation has been simulated by Shulman & Seiden [1986] using a CA approach on a polar grid whose rings rotate at different rates (see Figure 3.2). Theirs was a simple percolation model and achieves the basic structure of a spiral galaxy without a detailed analysis of the astrophysical dynamics involved.

In another digression from the conventional CA definition, Moshe Sipper [1994] considered different rules for different cells as well as the evolution of rules over time. There will be other instances in the sequel when we will stray slightly from strict adherence to the classical cellular automaton definition.

A fundamental precept of cellular automata is that the local transition function determining the state of each individual cell at a particular time step should be based upon the state of those cells in its immediate neighborhood at the previous time step or even previous time steps. Thus the rules are strictly local in nature and each cell becomes an information processing unit integrating the state of the cells around it and altering its own state in unison with all the others at the next time step in accordance with the stipulated rule. Thus, any global patterns of the system are an *emergent* feature of the effect of the locally defined transition function. That is, global features emerge from the strictly local interaction of individual cells each of which is only aware of its immediate environment. This emergent behavior will be discussed more comprehensively in Chapter 5, but it is a salient feature that one should always be aware of in our development of cellular automata theory.

3.2 Transition functions

Most of the dynamical features of cellular automata can be found in the study of the one-dimensional case. Here we define a neighborhood of a cell c having radius (range) r as the r cells to the left of c and the same number of cells to the right of c. Counting c itself, this neighborhood contains $2r+1$ cells. In the simplest case $r = 1$ and $k = 2$ for the allowable states. In this instance, a three-cell neighborhood with two different states 0 and 1 for each cell can be expressed in $2^3 = 8$ different ways. All eight neighborhood-states with $r = 1$ and $k = 2$ are illustrated below (Figure 3.3), and in general there are k^{2r+1} one-dimensional neighborhood-states..

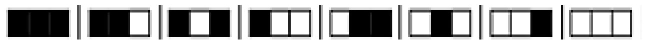

Figure 3.3: The eight possible neighborhood-states with $r = 1$ and $k = 2$.

Let us adopt this notation: $c_i(t)$ denotes the state of the ith cell at time t (Figure 3.4).

At the next time step, $t+1$, the cell state will be $c_i(t+1)$. Mathematically we can express the dependence of a cell's state at time step $t+1$ on the state of its left-hand and right-hand nearest neighbors $c_{i-1}(t)$ and $c_{i+1}(t)$ at time step t, by the relation:

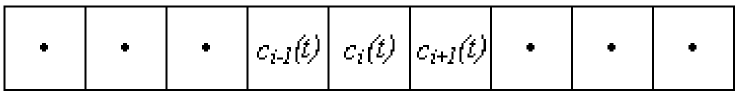

Figure 3.4: The cell states of the central cell $c_i$and its two nearest neighbors c_{i-1} and c_{i+1} at the time step t.

$$c_i(t+1) = \varphi\left[c_{i-1}(t), c_i(t), c_{i+1}(t)\right],$$

where φ is the local transition function. For example, consider the simple transition rule

$$c_i(t+1) = c_{i-1}(t) + c_i(t) + c_{i+1}(t) \mod 2, \tag{3.1}$$

where mod 2 means taking the remainder after division of the indicated sum by 2, resulting in either 0 or 1. We can put this rule into a (transition) table format by adding $c_{i-1}(t) + c_i(t) + c_{i+1}(t) \mod 2$ for the eight possible different input values:

$c_{i-1}(t)$	$c_i(t)$	$c_{i+1}(t)$	$c_i(t+1)$
1	1	1	1
1	1	0	0
1	0	1	0
1	0	0	1
0	1	1	0
0	1	0	1
0	0	1	1
0	0	0	0

(3.2a)

A very convenient way to illustrate the allowable rules for one-dimensional cellular automata with $r = 1$ and $k = 2$ is to indicate the state (color) of the middle cell at the next time step, given the state (color) of itself and its two nearest neighbors:

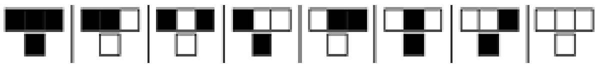

(3.3)

Here the middle cell at time t (in the top row) has its state altered according to the state of its two nearest neighbors and its own state to yield the cell's new state at time $t + 1$ (bottom row). This also represents the preceding rule 3.1 above. Observe that in four of the eight cases a black cell appears. One consequence of this is that if we took a disordered array of an infinite number of cell sites, then the average fraction (or *density*) of black cell sites that evolve after one iteration will be 0.5.

The cellular automaton defined by this rule has the graphical representation depicted in Figure 3.5 starting with a single black cell with each subsequent generation of the automaton appearing on the next line down.

So how many possible rules are there for $r = 1$ and $k = 2$? Since there are 8 possible neighborhood-states of 3 cells and each of these results in

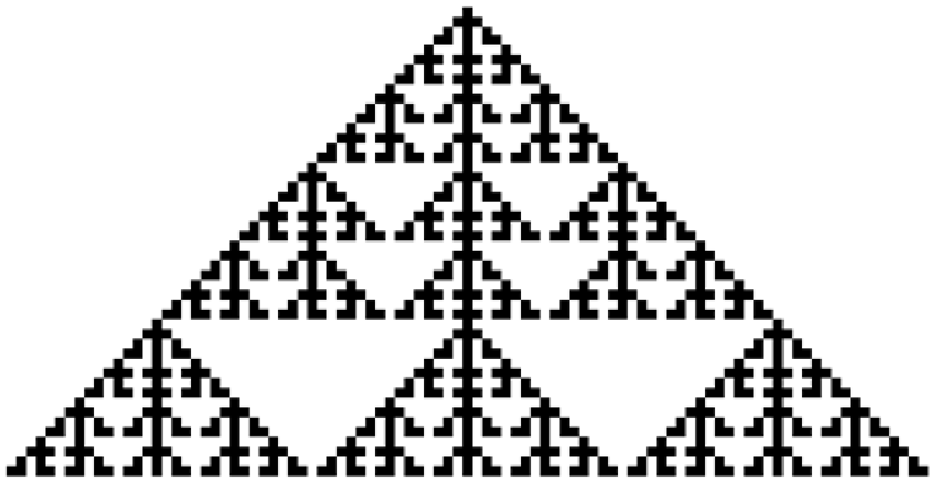

Figure 3.5: The evolution of the rule in the text starting with a single black cell. Each new line downward represents the evolution of the automaton at the next time step.

two possible state outcomes for the middle cell, there are $2^8 = 256$ possible transition rules by which this can be achieved. Wolfram described these as *elementary* cellular automata. By considering a white cell as being in state 0 and a black cell in state 1 we can identify the rule given in the form of 3.2a or 3.3 by its 8 output states (or *rulestring*): 10010110, which in base 2 happens to be the number 150. So this rule is referred to as Rule 150 and is the rule above depicted in four different formats.

In a similar fashion, all 256 elementary cellular automata can be numbered starting from:

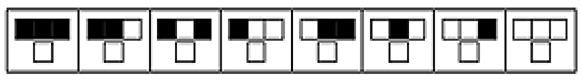

= Rule 0

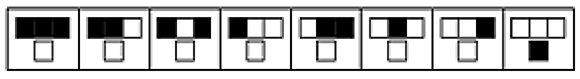

= Rule 1

.

.

.

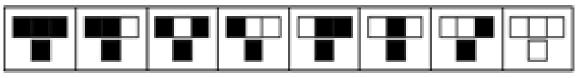
= Rule 254

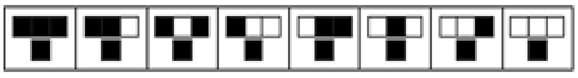
= Rule 255

A complete illustration of all 256 elementary cellular automata starting with a standard initial condition of one black cell is given in the Appendix. Many of the salient features found in cellular automata theory can be observed in these elementary ones and we shall refer to them often. These elementary cellular automata are examples of *first order automata* in the sense that the state of a cell at time step $t+1$ only depends on the state of its neighbors at the previous time step t. Whereas in a *second order automaton* a cell's state at time step $t+1$ is rather more demanding and depends on the state of its neighbors at time steps t as well as $t-1$. Unless otherwise specified, we will mainly be considering first order automata although second order automata will come into play in our discussion of reversibility.

Perhaps you are thinking that this is not so much to work with, so if we merely increase the radius to $r = 2$ then there are $2^5 = 32$ possible neighborhood-states and $2^{32} = 4,294,967,296$ possible rules. On the other hand, if we keep $r = 1$ and merely increase the allowable states per cell to 3, then there are $3^3 = 27$ possible neighborhood-states and an astronomical $3^{27} = 7,625,597,484,987$ possible rules! That should be plenty.

3.3 Totalistic rules

This class of rules is defined by taking the local transition function as some function of the *sum* of the values of the neighborhood cell sites. So for example, if $r = 1$, $k = 2$, we have

$$c_i(t+1) = \varphi\left[c_{i-1}(t) + c_i(t) + c_{i+1}(t)\right].$$

An example is the Rule 150 above given by

$$c_i(t+1) = c_{i-1}(t) + c_i(t) + c_{i+1}(t) \mod 2.$$

So how many such totalistic rules are there with $r = 1$, $k = 2$? With the two states 0 and 1 for each of the three cells, there are just the four possible totals of the cell states: $0, 1, 2$, and 3. For example, our Rule 150 can also be depicted by the following transition table:

sum (t)	3	2	1	0
$c_i(t+1)$	1	0	1	0

.

So we can see that in general each of the four sums accruing at time step t can yield at the next time step either a 0 or 1, thus giving $2^4 = 16$ possible totalistic rules, of which the preceding Rule 150 is one.

Breaking away from the elementary cellular automata and allowing three states per cell ($k = 3$) but maintaining nearest neighbors ($r = 1$), let us take cell states: $0 =$ white, $1 =$ gray, and $2 =$ black. Thus there are seven possible sums: $0, 1, 2, 3, 4, 5$, and 6, each of which can yield a $0, 1$ or 2 at the next time step. An example is:

sum (t)	6	5	4	3	2	1	0
$c_i(t+1)$	1	1	0	1	2	1	0

and in fact, there are $3^7 = 2187$ such totalistic rules. In order to systematically enumerate them, the cellular automaton number is the base 3 value of $c_i(t + 1)$ in the second row as in the preceding table. The number given above, 1101210, is the value 1020 in base 3 and so this automaton is labeled Code 1020 and has the appearance in Figure 3.6 starting with a single gray cell.

3.4 Boundary conditions

There is the small matter of what should be the neighborhood of the cells at the extreme left and right of the lattice. In many cases we will take the lattice to be sufficiently large in extent so that these cells do not come into our considerations and the lattice can be considered to be effectively infinite. However, in some cases the lattice will be finite in extent and there are three main types of boundary conditions:

(i) Periodic (also known as 'wrap'): Here we consider the two cells at the extreme left and right ends to be neighbors of each other, thus making the lattice into a continuous loop in the one-dimensional case. As well, it is also possible to prescribe the array in the vertical direction (in the two-dimensional case) so that the top and bottom cells are also neighbors, thus making the cellular array into the shape of a torus, or donut. Periodic

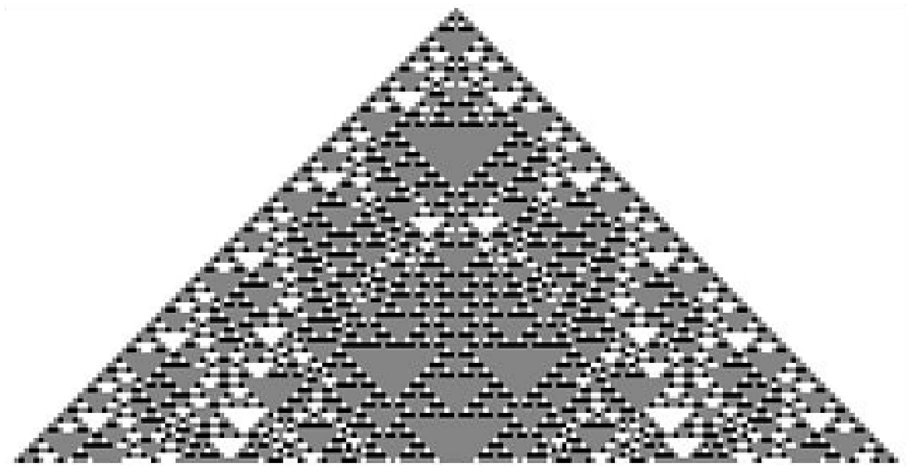

Figure 3.6: Totalistic Code 1020 = 1101210 in base 3, generated from a single gray cell (cell state = 1) with 3 states per cell and nearest neighbors.

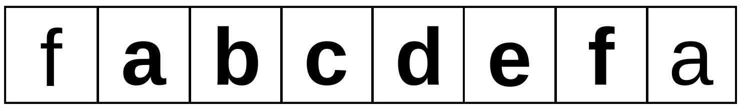

Figure 3.7: For the finite 1-dimensional array of cells labeled: a, b, c, d, e, f, periodic boundary conditions ensure that cell a has the left-hand neighbor f and cell f has the right-hand neighbor a as if the array were joined into a loop.

boundary conditions are the best at simulating an infinite array since no boundary is apparent to any cell.

(ii) Reflective: In this case the cells states at the extremities are repeated in order to provide neighboring cell values for them.

(iii) Fixed: In some instances, we want the boundary values to take on some fixed value such as when modelling a problem in heat conduction (see Section 5.5.5). Thus the values along the boundary remain constant throughout the simulation.

3.5 Some Elementary Cellular Automata

In the sequel we will consider various elementary cellular automata that have an initial condition of a single black (i.e. state 1) cell, all the others being white (state 0). Of course we will not discuss all 256 cases and nor is this necessary, as for example, Rule 0 only produces cells that are in state 0

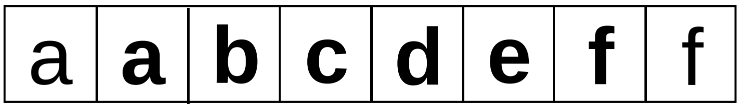

Figure 3.8: With reflective boundary conditions, the same array of cells will have the first and last cells repeated in order to provide neighbors for them.

and is therefore of zero interest.

Rule 1 has the distinguishing feature (noted above) that a neighborhood of cells entirely in state 0 (quiescent) spawns a live cell at the next time step. In some theoretical considerations (see Section 4.1.6) this condition will not be permitted. This yields the following automaton starting from a single black cell:

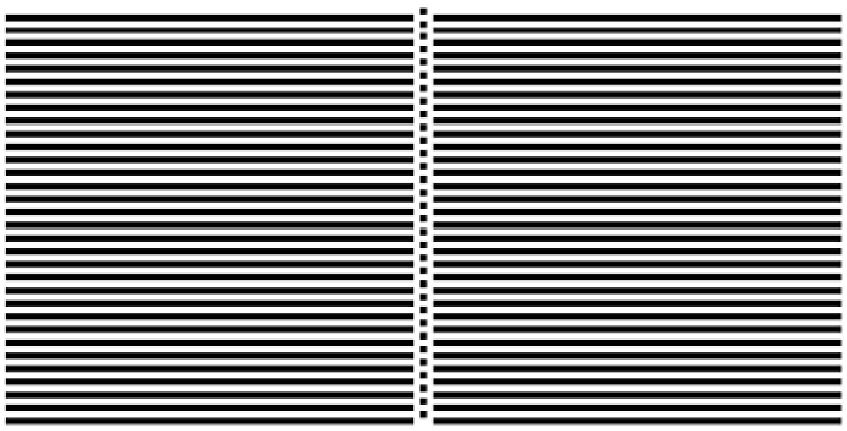

Figure 3.9: Rule 1 starting with a single black cell illustrating its repetitive nature.

In principle, this array must be infinite in extent to the left and right of the starting cell.

Let us skip now to look at Rule 30:

$$c_i(t+1) = [c_{i-1}(t) + c_i(t) + c_{i+1}(t) + c_i(t)c_{i+1}(t)] \mod 2$$

where we are immediately struck by its quite random appearance (Figure 3.10).

Considering the central column of cells, which have states: 1101110011..., Wolfram [1986] applied various statistical tests and found the sequence of 1's and 0's to be completely random. Of course this is the intrinsic randomness as discussed earlier and every time Rule 30 is executed it will produce the

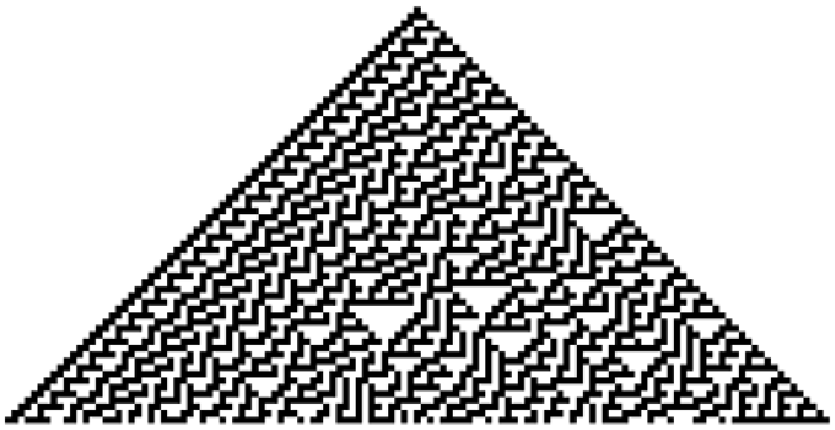

Figure 3.10: Rule 30 depicting a rather random appearance containing triangles of various sizes.

same sequence of digits along the central column. Nevertheless, no pattern whatsoever can be discerned in these digits in the sense mentioned, and so they are considered random.

To consider the randomness of the central column of (in this example taking a sample of 960) cells a bit further, if it is truly random, then one would expect that the number of 0's and 1's in any long sequence to be roughly equal, so that each digit occurs roughly half the time. Likewise, we should find approximately equal numbers of the four pairs of digits: 00, 01, 10, 11, (among the 480 possible pairs of digits) so that the frequency of occurance (called the *block frequency*) of each pair is 1/4, and for the eight triples of digits: 000, 001, ... 111, (among the 320 triples) each should have a block frequency approximately of 1/8, and similarly for the sixteen quadruples: 0000, 0001, ... 1111, (among the 240 quadruples) each should have a block frequency of 1/16. To test this, a sequence of 960 cells in length from the central column was sampled and the block frequency of each block length up to length four was calculated. Here is a table of the counts for each block size:

Block size	**Observed count**							
1	498	462						
2	134	116	114	116				
3	55	38	34	41	41	38	28	45
4	22	16	16	19	9	16	16	15
	19	11	11	13	17	19		

The expected counts E_i for each block size respectively are based on their probability of occurance p_i, with $E_i = p_iN$, and $N = 960$:

Block size	**Expected count**
1	$E_1 = E_2 = 1/2 \times 960 = 480;$
2	$E_1 = E_2 = E_3 = E_4 = 1/4 \times 480 = 120;$
3	$E_1 = E_2 = ... = E_8 = 1/8 \times 320 = 40;$
4	$E_1 = E_2 = ... = E_{16} = 1/16 \times 240 = 15.$

In order to compare the observed counts for each particular block size with the expected counts in each case, we use a statistical tool known as the *chi-squared test.* This is just a general measure of how much the observed values deviate from the expected ones determined by their probabilities, and is given by:

$$\chi^2 = \sum_{i=1}^{k} \frac{(O_i - E_i)^2}{E_i},$$

where O_i represents the *observed* counts for a particular block size, E_i are the *expected* counts and k is the number of different blocks considered in each case. The formula gives the value denoted by χ^2, called *chi-squared.* So for example, if we consider blocks of size 3, then $k = 8$ and each E_i equals 40. Based on the data above we find:

Block size 1: $\chi^2 = 1.35$
Block size 2: $\chi^2 = 2.2$
Block size 3: $\chi^2 = 11$
Block size 4: $\chi^2 = 16$

Next we need to interpret these numbers to see if they mean that our data is actually random. In order to do this, there are standard tables for comparing your chi-squared values with truly random ones. So for example, if we look up the value of $\chi^2 = 1.35$ for our block size $= 1$, we find that between 20 - 30% of the time a truly random sequence will have an even larger chi-squared value. Since the χ^2 value is a measure of the deviation from the theoretical expected values, this is indeed a good indication of randomness for Rule 30. Taking say, block size 4 and our value of $\chi^2 = 16$, we find from the tables that between 30 - 50% of the time a random sequence will have a larger chi-squared value, again a strong indication of randomness for Rule 30. The other χ^2 values give similar results and we may confidently conclude that the pattern of black and white cells along the central column of Rule 30 is indeed random.

Various other tests for randomness are discussed in the book by Donald Knuth [1981], and again Rule 30 passes all of these tests as well (Wolfram [1986]).

Rule 30 has also been proposed by Wolfram in 1986 as the basis for an encryption system. To implement such a system the first step is to transcribe all of the plaintext message into 8 bit ASCII characters. So for example, the letter 'a' is denoted by 01100001 (=97), 'b' is 01100010 (=98) and 'space' is 00100000 (=32) and so forth. For ease of handling purposes we put this into an $8 \times n$ array where n is the length of the message (including spaces and punctuation). Thus the plaintext message:

Once upon a time...

is put into an array where each row represents a letter with white = 0, black = 1; see Figure 3.11.

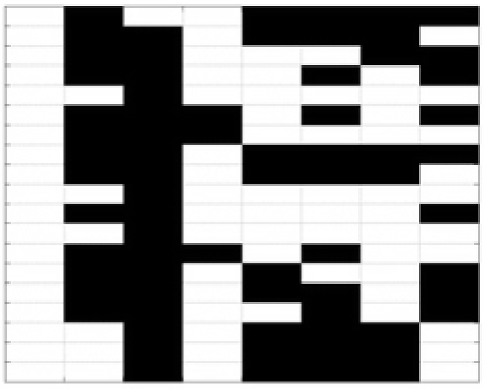

Figure 3.11: The plaintext message, "Once upon a time..." transcribed into 8-bit ASCII with 0 = white and 1 = black.

So the first letter 'O' is 79 = 01001111 appears on the first row and on the fifth row we have a 'space' which is 32 = 00100000 and so forth. Let us denote an abitrary member of this array by a_i. To encrypt this message we take some specific set of random initial values and evolve Rule 30 from them. Now take the cell values of 1's and 0's of the central (or any other) column and denote these values by b_i. (Actually taking every other value from a particular column provides a higher level of security). In Figure 3.12 are the values b_i of Rule 30 derived from the initial condition 1772712395 expressed as a 31-digit binary number taking every second cell value of the 16th column that we will use to encrypt our message.

Then we simply apply the 'EXCLUSIVE OR' (XOR) operation

$$a_i \vee^* b_i = c_i$$

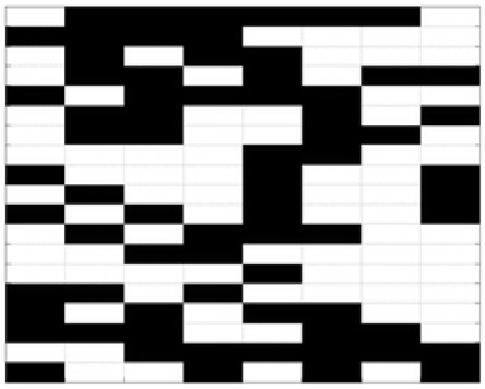

Figure 3.12: The values given by Rule 30 derived from the initial condition 1772712395 expressed as a binary digit number and taking every second number of the 16 column.

taking elements from the plaintext array and Rule 30 array consecutively, with 1 = True, 0 = False. This results in the ciphertext c_i, which we also put into an array format (Figure 3.13).

For example, starting with the top row and taking consecutively the elements of the message and Rule 30, forming $a_i \vee^* b_i = c_i$ we have, $0 \vee^* 0 = 0$, $1 \vee^* 1 = 0$, $0 \vee^* 1 = 1$, etc. The 'exclusive or' is slightly more restrictive than the usual $\vee$ operation and differs from it only in so far as if P and Q both true, then $P \vee^* Q$ is now false. If either just one of P or Q is true, then as for the usual disjunction, $P \vee^* Q$ is likewise true.

The ciphertext message can now be transmitted. In order to decode the message, one simply has to run Rule 30 taking the *same set* of random initial conditions and applying the 'exclusive or' operation consecutively to the ciphertext and the same elements b_i of Rule 30 that were used for the encryption:

$$c_i \vee^* b_i = a_i.$$

The result of this second application of the 'exclusive or' operation returns the original values a_i which is this case translates into: *Once upon a time...*

The reason this works is that two consecutive applications of the 'exclusive or' operation returns the original value. For example, for a value of 1 in the text and a value of 1 from Rule 30, we have $1 \vee^* 1 = 0$ and taking this result again with 1 from Rule 30, we have: $0 \vee^* 1 = 1$, which is the original text value. The other three possibilities are verified similarly.

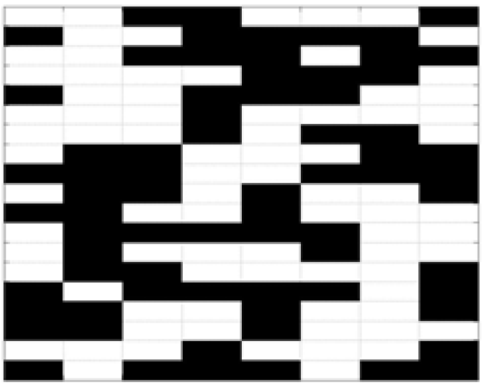

Figure 3.13: The ciphertext of the original message encoded using Rule 30 according to the algorithm explained in the text.

One disadvantage to this method of encipherment is that the random initial conditions for Rule 30 must be communicated to the message recipient in advance. This has been a weakness of secret codes over the centuries that have relied on the 'key' having to be known to both parties to encipher and decipher a message. There is always the danger that the key will be discovered by those for whom the message is not intended. Sometimes this key would change daily and so-called *one time pads* would be used for this purpose. New developments in quantum cryptography are making the distribution of the key absolutely secure (see Bennett, Brassard and Ekert [1992]). Individual photons are sent by fiber optic cable between the two parties and any attempt to eavesdrop on these photons will perturb them in such a way that can be detected by the intended recipients.

Another form of encryption, *public key encryption*, based on the extreme difficulty of factoring the product of two large prime numbers into its constituent parts, is considered uncrackable at the present time. This method was discovered by Clifford Cocks of the British Government Communication Headquarters in 1973 and independently in 1977 by Ron **R**ivest, Adi **S**hamir, and Leonard **A**dleman of MIT and has become known as RSA. In the quaint jargon of cryptography, Alice creates a public encryption key which is just the product of two prime numbers, say $N = p \times q = 10151 \times 14533 = 147524483$, but keeping the values of p and q secret. This allows anyone who knows the key to send Alice a message. For example, if Bob wants to send Alice a message he simply uses a particular mathematical algorithm (called a 'one-way function' – also publically known) that invokes Alice's key $N = 147524483$ to encrypt the plaintext and send it to her. To decipher the message requires knowing the values of p and q so that

Alice is the only one who can do this. The ciphertext message is secure because in practice, the prime numbers that Alice has chosen, p and q, are very large (say 100 digits long!) and once multiplied together, the number N cannot be factored into its constituent parts by even the most powerful computers. It is conceivable that someday there will be found some mathematical algorithm for achieving the factorization of extremely large numbers in a reasonable period of time, but until then the RSA encryption method is totally secure although encrypting large amounts of data with it is cumbersome. It is the de-facto standard for secure transactions on the Internet. A CA scheme for the authentication of digital messages and images has been developed by Mukherjee *et al.* [2002]. A fascinating account of the history of cryptography is Simon Singh's, *The Code Book* [1999].

Several elementary cellular automata (Rules 18, 22, 26,82,146,154, 210, and 218 among others – see Appendix) have the nested triangle appearance of Rule 90 which is given by the formula: $c_i(t+1) = c_{i-1}(t) + c_{i+1}(t) \mod 2$.

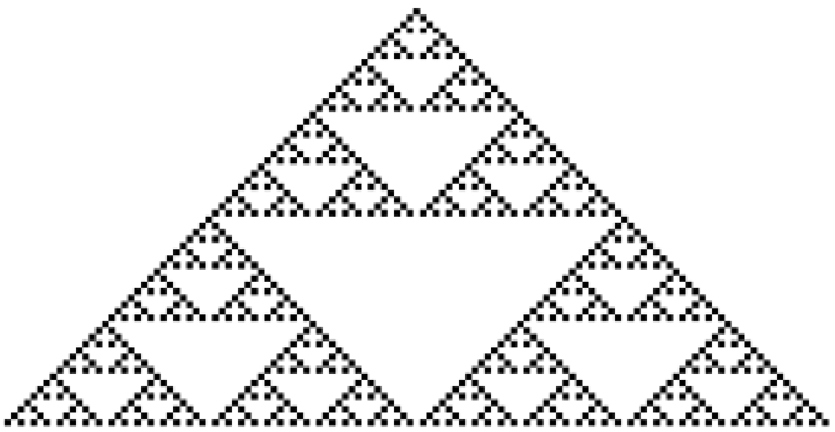

Figure 3.14: Rule 90 after 66 steps of its evolution.

In the limiting case, this automaton depicts the Sierpiński triangle and has fractal dimension 1.585. It has been shown by D.A. Lind [1984] that starting from any initial configuration, the limiting frequency of 1's and 0's is always 1/2 for each. This is an exceptional result because in general it is impossible to say much of anything about the long term evolution of a particular cellular automaton.

Rule 90 also has a connection with Pascal's triangle, a familiar object in elementary mathematics. A consequence of the well-known Binomial Theorem is the expansion:

$$(1+x)^n = 1 + nx + \frac{n(n-1)}{1\cdot 2}x^2 + \frac{n(n-1)(n-2)}{1\cdot 2\cdot 3}x^3 + ... + nx^{n-1} + x^n,$$

for positive integer values of n. So for example:

$$(1+x)^5 = 1 + 5x + 10x^2 + 10x^3 + 5x^4 + x^5.$$

Pascal's triangle derives the coefficients of the expansion by starting with a 1 at the apex of the triangle, then the first binomial expansion of $(1+x)^1$ has coefficients $(1,1)$ which form the next row of the triangle, and the coefficients of $(1+x)^2$ which are $(1,2,1)$ are on next row, where the 2 is the sum of the previous two 1's. The next row will have a 1 at either end and between them we add the first 1 and 2 from the previous row to get 3 as the next digit, then add the 2 and 1 from the previous row to get another 3 so that the 3rd row is: $(1,3,3,1)$. In general, we always start and finish a row with a 1 and the digits in between are obtained by adding the consecutive digits of the previous row. This generates a triangle of digits known as Pascal's triangle that gives the binomial coefficients of $(1+x)^n$. If we overlay this triangle of digits with a grid of square cells and color the cells black that have odd numbers in them, then we obtain the pattern of Rule 90.

Rule 110 is quite unremarkable in appearance starting from a single black cell (Figure 3.15).

Its rule structure: 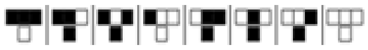 gives nothing away regarding its sophisticated potential, which Wolfram suspected would be nothing less than universal computation. And indeed, during the 1990s his research assistant, Matthew Cook, demonstrated that Rule 110 was capable of universal computation! This was demonstrated by showing that Rule 110 could in fact emulate any of what are called *cyclic tag systems.* Since some of these can emulate any Turing machine and since some Turing machines are capable of universal computation, it logically follows that Rule 110 is likewise capable of universal computation.

Rule 150 has been introduced in Section 3.2 and starting from a single black cell has the appearance depicted in Figure 3.5. Remarkably, in the same way that Rule 90 is related to the coefficients of the binomial expansion, with odd numbered cell entries being black, Rule 150 is related to the coefficients of the trinomial expansion

$$(1+x+x^2)^n.$$

So for example, taking $n=8$ gives the coefficients: **1**, 8, 36, 112, 266, 504, 784, 1016, **1107**, 1016, 784, 504, 266, 112, 36, 8, **1** with the first, middle

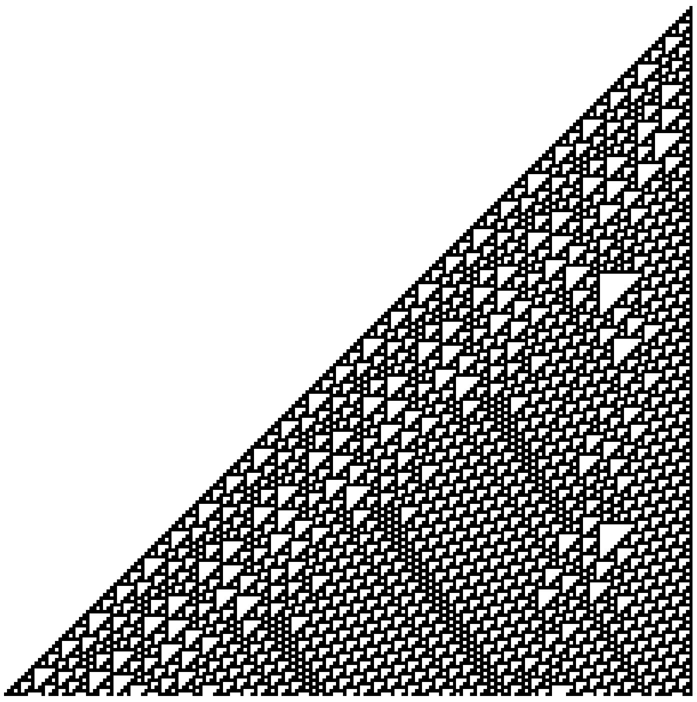

Figure 3.15: The evolution of Rule 110 starting with one black cell.

and last coefficients being the only odd ones. These determine which cells are black in the *9th* row of Rule 150 and all other black cells are obtained in a similar fashion.

3.6 Additivity

Some rules like Rule 90 or Rule 150 have a special property of being what is called 'additive'. Taking another look at Rule 90: $c_i(t{+}1) = c_{i-1}(t){+}c_{i+1}(t) \mod 2$, we find that the value of the central cell at the next time step depends on a sum of the neighboring cells' states. We can extend the sum notion slightly to what mathematicians call a 'linear combination' which for $k = 2$ and $r = 1$ is a sum of integer multiples of the neighborhood states:

$$c_i(t+1) = \alpha c_{i-1}(t) + \beta c_i(t) + \gamma c_{i+1}(t) \mod 2,$$

and the α, β, γ are integer constants 0 or 1. In general, for k states per cell there are 0 to $k-1$ values for the constants and all the arithmetic is taken $\mod k$. For k states and range r there are k^{2r+1} additive rules or $2^{2\cdot 1+1} = 8$ additive rules among the 256 elementary cellular automata.

These are found by taking all possible choices of 0 and 1 for α, β, γ giving: Rule 0 ($\alpha = \beta = \gamma = 0$), Rule 60 ($c_{i-1} + c_i$), Rule 90 ($c_{i-1} + c_{i+1}$), Rule 102 ($c_i + c_{i+1}$), Rule 150 ($c_{i-1} + c_i + c_{i+1}$), Rule 170 ($c_{i+1}$), Rule 204 ($c_i$), Rule 240 ($c_{i-1}$).

The above notion of additivity can easily be seen by taking Rule 150 for example and looking at its transition function (Figure 3.16) :

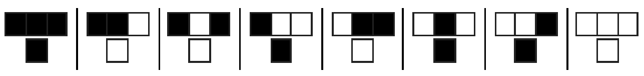

Figure 3.16:

It is clear from the rule that the right-hand neighbor, central cell, and left-hand neighbor state values can be added (mod 2) to give the state value of the central cell at the next time step.

The additive CA also have the advantage that an algebraic analysis can be used to determine certain of their global properties (Martin, Odlyzko & Wolfram [1984]).

3.7 Reversibility

It is thought that the laws of physics are time-reversible, in other words, if the state of a system is known at a given instant of time, it is possible to completely describe not only the future evolution of the system, but its past as well. This is due to the fact that in the equations describing these systems, the time variable t can be replaced by $-t$ and the equations still remain valid. According to Einstein, "... the distinction between past, present, and future is only an illusion, however persistent" (excerpt from a letter to the widow of his friend Michele Besso). This is seemingly at odds with the Second Law of Thermodynamics which describes irreversible processes that proceed with increasing entropy along an arrow of time. This dichotomy – the microscopic laws of physics are reversible, yet the macroscopic world is filled with irreversible phenomena, has exercised the minds of physicists and philosophers at least since the 1860s amid much controversy and confusion. To demonstrate the flavor of the controversy, let me just quote Jean Bricmont [1997], professor of theoretical physics at the University of Louvain, Belgium: "It is perfectly possible to give a natural account of irreversible phenomena on the basis of reversible fundamental laws, and of suitable assumptions about initial conditions. This was essentially done a century ago by Boltzmann, and despite numerous misunderstandings and misguided objections (some of them coming from famous scientists, such as Zermelo or Poincaré), his explanation still holds today. Yet [Ilya] Prigogine writes...

'He (Boltzmann) was forced to conclude that the irreversibility postulated by thermodynamics was incompatible with the reversible laws of dynamics'. This is in rather sharp contrast with Boltzmann's own words: 'From the fact that the differential equations of mechanics are left unchanged by reversing the sign of time without anything else, Herr Ostwald concludes that the mechanical view of the world cannot explain why natural processes run preferentially in a definite direction. But such a view appears to me to overlook that mechanical events are determined not only by differential equations, but also by initial conditions...'

As Bricmont further elaborates, "...irreversibility does not lead to a *contradiction* with the basic physical laws. Indeed, the laws of physics are always of the form given some initial conditions, here is the result after some time. But they never tell us how the world *is* or *evolves*. In order to account for that, one always needs to assume something about the initial conditions." (Incidently, Jean Bricmont is also co-author of *Intellectual Impostures* (published in the USA as *Fashionable Nonsense*), an exposé of pseudo-intellectual, pseudo-scientific discourse that passes for profound philosophical thought).

In fact, there are some reversible cellular automata that do proceed from a disordered state to an ordered one, i.e. from a state of high entropy to a state of low entropy. And of course the key here is to precisely know the correct initial conditions. In Figure 3.17, the automaton proceeds in the first column from a state of randomness to a highly ordered state. How was this highly unusual state of affairs achieved? Namely, by running the inverse of the automaton (starting at the top of column 5) until a final state is reached and capturing the values of this final state for the initial conditions we started with in column 1.

Thus in order to attain reversibility, it all depends on knowledge of the initial conditions of the system. But therein lies the rub when it comes to actual physical systems. As Stephen Wolfram states [2002], "... no reasonable experiment can ever involve setting up the kind of initial conditions that will lead to decreases in randomness, and that therefore all practical experiments will tend to show only increases in randomness.... It is this basic argument that I believe explains the observed validity of the Second Law of Thermodynamics."

By way of contrast, *irreversible* cellular automata may exhibit a decrease in the number of possible configurations over time ("compression of states") and hence a decrease in entropy. This means that the number of reachable configurations diminishes over time and the system tends towards a more ordered state.

For example, let us consider a finite cellular automaton with N cells and two possible states per cell, so that there are 2^N possible configurations. If we consider our automaton to be initially completely disordered then any configuration is equally likely, having a probability of occurence of $1/2^N$.

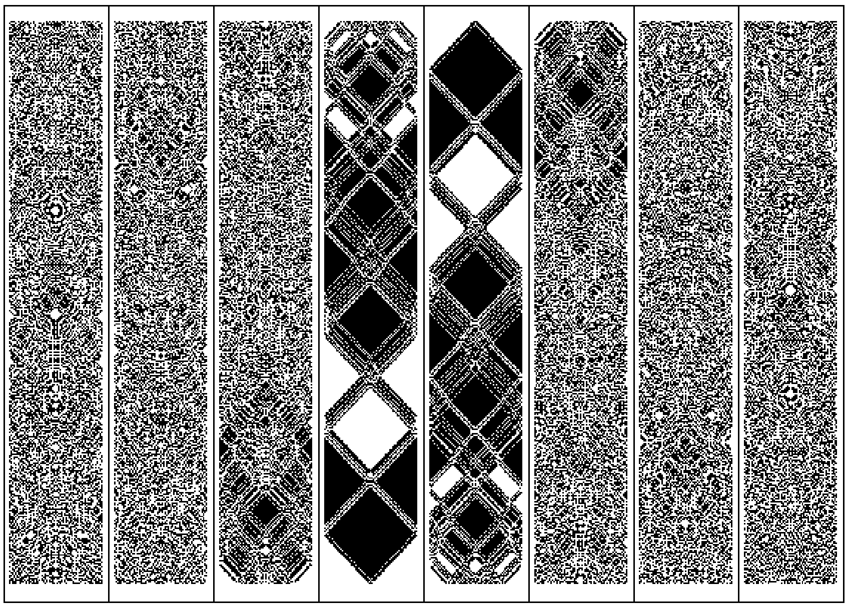

Figure 3.17: This reversible automaton proceeds from a completely disordered state to a highly ordered one, contrary to the Second Law of Thermodynamics. This was achievable by knowing precisely the initial conditions to start with. So the trick is to run the inverse of the rule until the automaton becomes completely disordered and the final state of the system is used for the initial state of the original rule.

Thus the automation is in a state of maximum entropy. Now at the first time step let each one of the 2^N possible initial configurations evolve according to the transition rule and let us record each of the configurations thusly reached. Some of these configurations may now be the same, say one configuration appears m times among these 2^N configurations. Then its probability of occurence at this time step becomes $m/2^N$. At each subsequent time step, we will compute the probability of occurrence in this fashion for each of the descendent configurations generated by the time evolution of the initial ensemble of configurations. Whenever some configurations appear multiple times, others will not appear at all and the probability of occurence of these latter will be zero. We have illustrated a simplified version of this situation in the table below with the label of *all* the possible initial configurations of an automaton along the top row and time being vertical. So 'a' is just the name for a configuration of black and white cells, likewise 'b' etc. If our automaton was just 10 cells wide, there would indeed be $2^{10} = 1024$ such configurations, but the eight listed here will suffice to illustrate our point. Now the local transition function will give rise to the transformation of one configuration into another, say: $a \longrightarrow b$, $b \longrightarrow c$, $c \longrightarrow d$, $d \longrightarrow e$, $e \longrightarrow f$, $f \longrightarrow g$, $g \longrightarrow h$, $h \longrightarrow g$. This automaton is irreversible as configuration g has two predecessors, namely f and h.

	a	b	c	d	e	f	g	h
1	b	c	d	e	f	g	h	g
2	c	d	e	f	g	h	g	h
3	d	e	f	g	h	g	h	g
4	e	f	g	h	g	h	g	h
5	f	g	h	g	h	g	h	g
6	g	h	g	h	g	h	g	h

All the possible initial configurations of a cellular automaton are on the top row and their subsequent evolution after 6 time steps runs vertically. Note that the number of configurations diminishes so that only g and h are final states. At the 1st time step, the probability of occurence of configuration g is 1/4 and that of h is 1/8, whereas at the 6th time step, the probability of occurence of configurations g and h is 1/2.

In this simplified example, we find that as the system evolves a, b, c, d, e, and f, are unreachable configurations. A configuration that is unreachable by any initial configuration of a particular cellular automaton is called a *Garden of Eden* configuration and this topic will be pursued more rigorously in Section 4.1.6

Taking a real example that nicely illustrates this compression of states as the automaton evolves is the graph of the evolution of Rule 126 (Figure 3.18). Considering all the $2^{10} = 1024$ initial configurations that are 10 cells

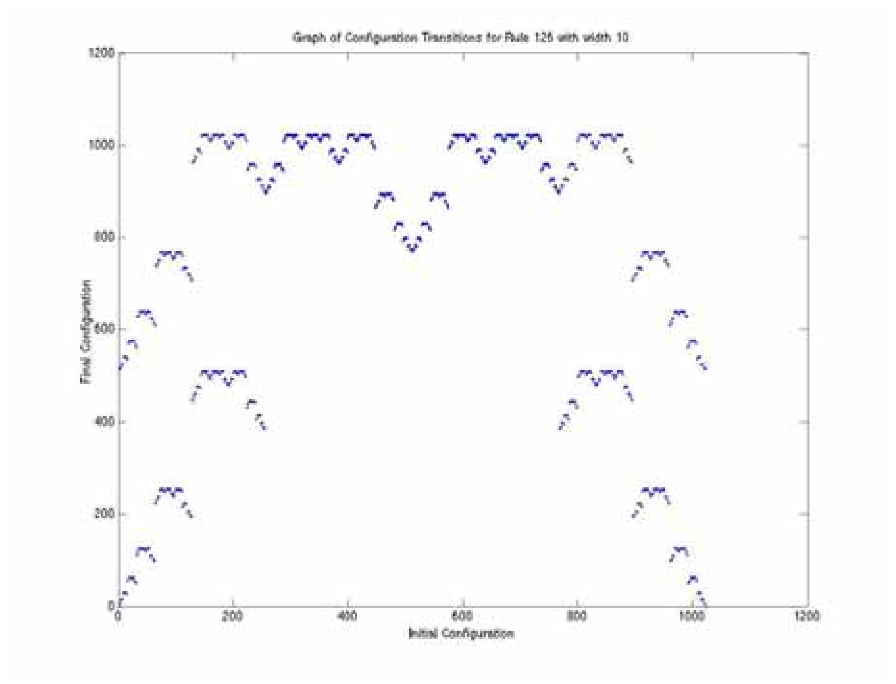

Figure 3.18: The time evolution of Rule 126 for each of the 1024 initial configurations of 10 cells wide. A dot indicates the final configuration and the various plateaus show the favored final states. The graph is also symmetric about the centerline owing to the fact that it has a symmetric rulestring: 126 = 01111110.

wide and letting each evolve until it reaches a final configuration, we find various final states (indicated by a dot) are reached multiple times.

In order to compute the entropy of a finite automaton as above, we use the formulation: $S = \sum_{i=1}^{2^N} P_i \log_2 (1/P_i)$, where P_i is the probability of occurence of the ith configuration at a given time step as described above. If we compute S at each of various time steps, we typically obtain the result illustrated in Figure 3.19) showing a decrease over time from maximum entropy that is indicative of the increasing self-organization of the automaton.

If we apply the same procedure in computing the entropy for Rule 30, which in Section 3.5 indicated complete randomness along its central column, we find something rather interesting. Starting from a random initial configuration, the entropy over time still decreases somewhat, although to a lesser extent than for Rule 126, indicating some degree of overall self-organization (Figure 3.20). This is in spite of the fact that the black and white pattern in any individual column is completely random!

On the other hand, reversibility in cellular automata is very uncommon but is prevalent in a few elementary cellular automata, namely Rules 15, 51,

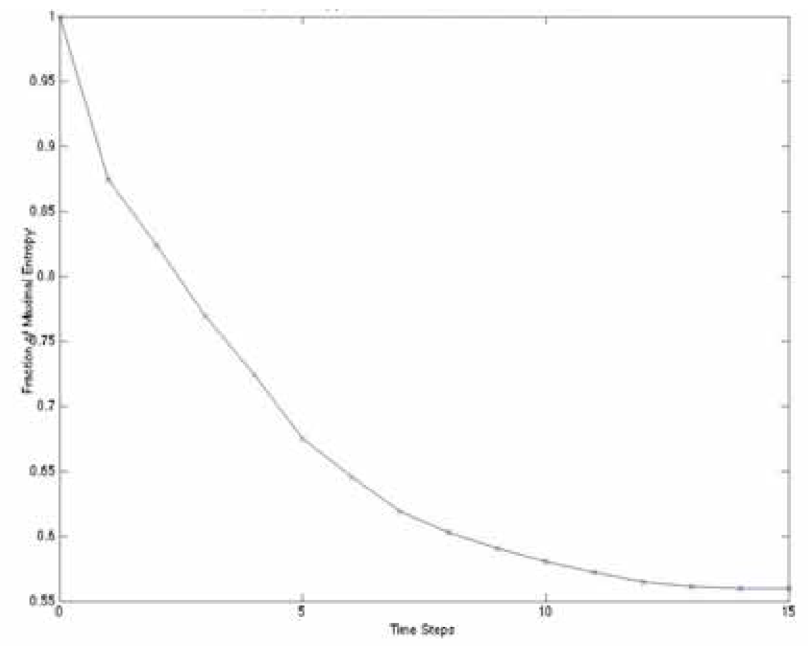

Figure 3.19: Graph showing the entropy as a function of time for the ensemble of 2^{15} initial configurations (cell width = 15) evolving according to (irreversible) Rule 94. The entropy decreases from a maximum at its initial state to a minimum after 14 time steps indicative of irreversibility.

85, 170, 204 and 240. As in the case with Rule 15 with random initial conditions (Figure 3.21)whose transition rule is given by: 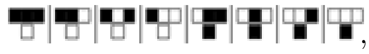, one can start on any line and go backwards in time steps using the rule rotated by 180 degrees, that is: 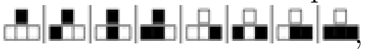, which turns out to be Rule 85 (and hence also reversible). Next, considering Rule 204: 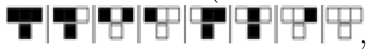, its rotated rule: 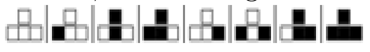 is actually itself and the same is true for Rule 51. That just leaves Rule 170 whose inverse is Rule 240.

A mathematical framework for the notion of reversibility is considered later in the sequel concerning the Garden of Eden.

We found that in irreversible automata, the number of configurations could diminish with time ("compression of states"), however, it is a theorem of the great French mathematician, Joseph Liouville, that the total number of configurations in a reversible system remains constant.

There is an interesting way in which to create *reversible* rules due to Edward Fredkin.What one does is to consider the transition function for the particular rule, say it is given by $\varphi\left[c_{i-1}(t), c_i(t), c_{i+1}(t)\right]$, and then add the state of the central cell at the previous time step: $c_i\,(t-1)$. This gives the

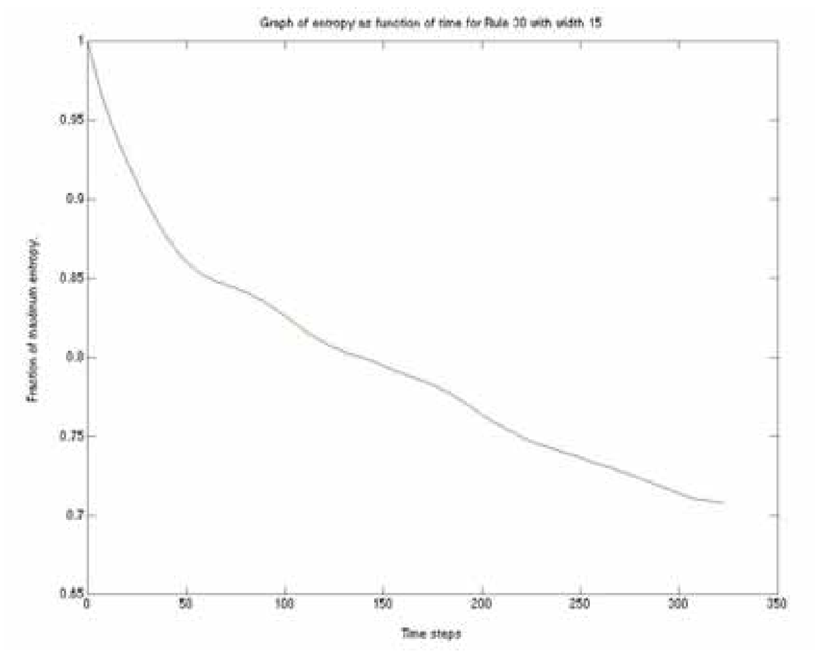

Figure 3.20: Computing the entropy of Rule 30 as it evolves with time we find that it decreases somewhat, indicating a certain degree of overall self-organization even though any individual column is random.

new rule

$$c_i(t+1) = \varphi\left[c_{i-1}(t), c_i(t), c_{i+1}(t)\right] + c_i\left(t-1\right) \mod 2,$$

which has a unique inverse given by

$$c_i(t-1) = \varphi\left[c_{i-1}(t), c_i(t), c_{i+1}(t)\right] + c_i\left(t+1\right) \mod 2.$$

For example, Rule 90 can be described by

$$c_i(t+1) = c_{i-1}(t) + c_{i+1}(t) \mod 2,$$

which normally is not reversible, but it does have a reversible counterpart, Rule 90R, which can be expressed as:

$$c_i(t+1) = c_{i-1}(t) + c_{i+1}(t) + c_i\left(t-1\right) \mod 2.$$

In other words, to determine the value of a cell at the next time step, look to the immediate left of the cell, look to the right, look behind the cell

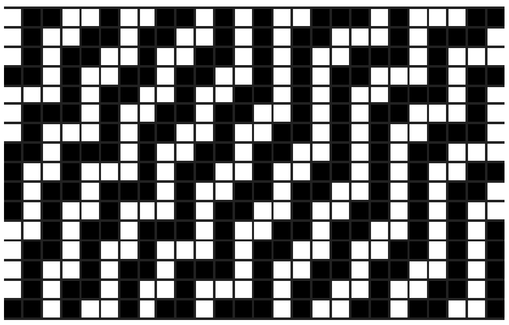

Figure 3.21: The reversible CA evolved using Rule 15 and random initial conditions.

and take the sum of these three cell states and divide by 2. The remainder, either 0 or 1, is the cell's state at the next time step.

The inverse then will have the form:

$$c_i(t-1) = c_{i-1}(t) + c_{i+1}(t) + c_i\,(t+1) \mod 2.$$

The evolution of Rule 90R depicted in Figure 3.22 with periodic boundary conditions can be visually checked and seen to be fully reversible according to the above rules.

The above reversible rules are examples of *second order* cellular automata because a cell's state not only depends on the value of the neighboring cell states at the previous time step, but also at the time step before that. The reversible rule in Figure 3.17 is Rule 94R.

Cellular automata with more states per cell also have some that are reversible, but as in the case of the elementary ones, it is only a small percentage of the total that actually are.

3.8 Classification of Cellular Automata

In the early 80s, Wolfram began to classify cellular automata by the complexity of their evolutionary behavior. Four basic classes were distinguished, although some automata have a mixture of different classes and some fall between two classes. Nevertheless, the vast majority of automata can be classified in this fashion, from elementary automata, to more complex systems. In some respects, this classification parallels the types of behavior exhibited by dynamical systems discussed in the Preliminaries. The same four fundamental classes of behavior are to be found over a broad range of cell state values (k), neighborhood radius (r) and dimension of the cellular automaton.

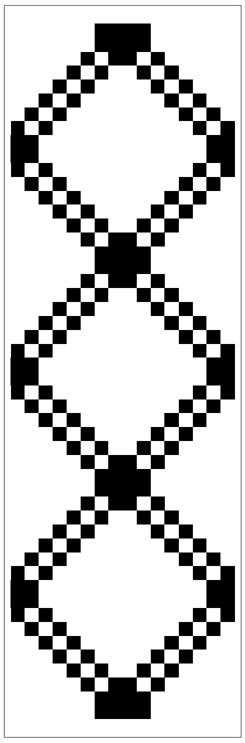

Figure 3.22: This is the reversible Rule 90R with periodic boundary conditions.

Class I: This behavior is the simplest and evolves to a uniformly constant state for all new cells (Figure 3.23).

This class of automaton resembles dynamical systems that tend to a fixed point attractor. In fact, the configuration of all black cells is a fixed point (stable, stationary) attractor in the space of all space of all possible configurations, in that for all initial configurations of the cells, the automaton evolves to this one fixed state. Automata in this class cannot be reversible because the initial information is completely lost.

Class II: In this case, the evolution is towards continually repeating structures or periodic structures (Figure 3.24). Class II automata resemble the periodic (cyclic) behavior exhibited by dynamical systems. They can also act as a kind of filter in that certain sequences of data can be preserved while others are made void. For example, the cellular automaton in Figure 3.25 preferentially selects the sequence 010 (white-black-white) while all other sequences of 1's and 0's are lost, becoming 0. This sort of selection

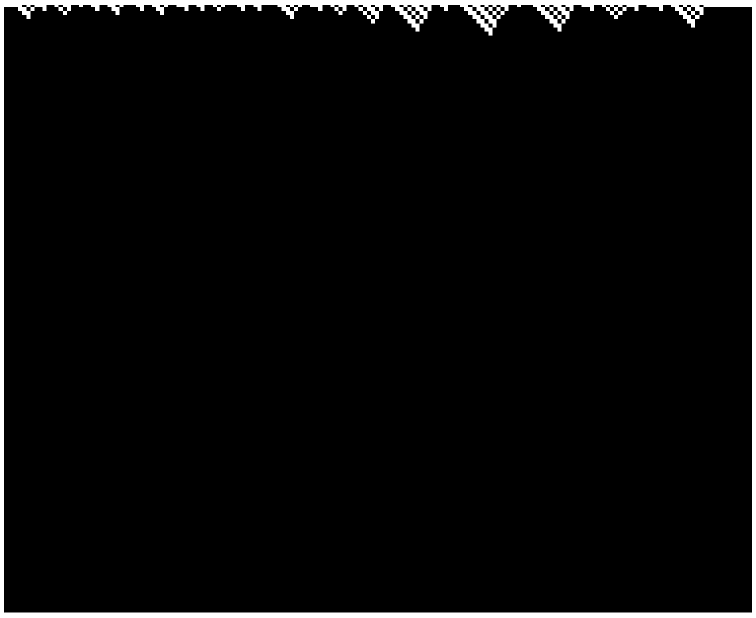

Figure 3.23: This is Rule 249 depicting the evolution to a uniformly constant state from random initial conditions. Any other set of initial conditions would evolve to the same fixed state.

process is useful in digital image processing.

Related to Class II systems are systems of *finite size*. In these systems, the domain of cells is finite in extent which is what we have in all practical cases, and this inevitably leads to periodic behavior. In the example below of Figure 3.26, Rule 150 shows differing periodicities depending on the size of the domain. Periodic boundary conditions are to be used. Because of the finiteness of the domain, the system eventually finds itself in a previous state and thus is forced to repeat itself. The maximum possible period is of course affected by the maximum possible number of states, which in the case of two states per cell, is 2^n for a domain of n cells. Thus the period can in principle be extremely large even for a modest sized domain. Often however, the period is much less than the maximum and its actual value is greatly effected by the domain size.

In a Class II system, as in the preceding example, various parts evolve independently of one another without any long-range communication, thus producing the periodic behavior typical of a system of finite size.

Class III: These automata exhibit random behavior typically with triangular features present (Figure 3.27).

Class III automata are analogous to chaotic dynamical systems. Like the

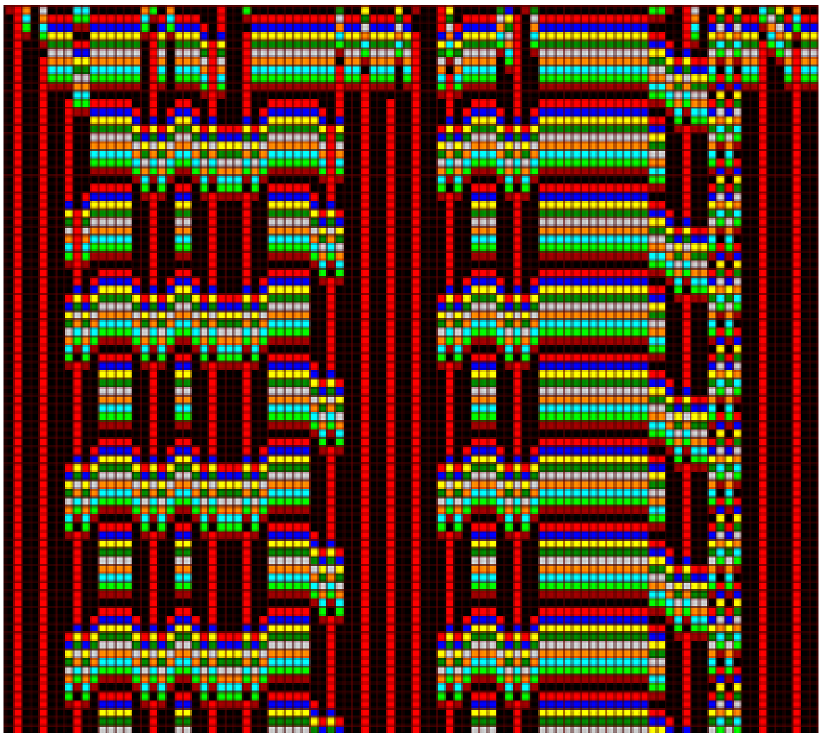

Figure 3.24: This automaton exemplifies the typical behavior of repeating structures found in Class II systems.

latter, they are very sensitive to initial conditions and play an important role in the study of randomness. For example, Figure 3.28 shows the Class III Rule 126 with the value of just one cell changed in the initial conditions.

Class IV: In this, the most interesting of all the Wolfram classes, but not as rigorously defined as the others, localized structures are produced that move about and interact with each other as the automaton evolves (See Figure 3.29).

Although the classes I, II, and III are similar in nature to corresponding types of behavior found in dynamical systems, Class IV behavior has no dynamical system equivalent and in fact fits between Class II and Class III in the sense that it is poised between periodicity and randomness. According to Wolfram [1984], this is where universal computation could be possible – in the netherworld between order and chaos. This region is the so-called "edge of chaos", a term coined by Norman Packard although the idea probably originates with Christopher Langton [1986]. The salient feature of Class IV behavior is that information can be transmitted through time and space opening up the possibility for complex computations to be made.

Of the elementary one-dimensional cellular automata, we have already

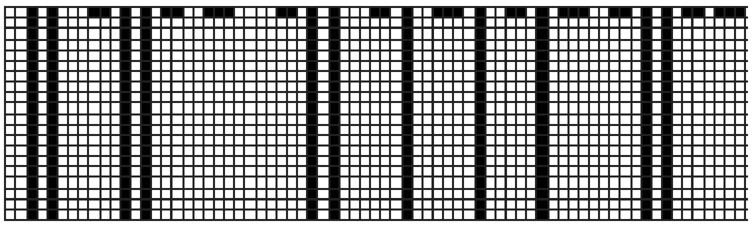

Figure 3.25: This is an example of a the preservation of the data string 010 by elementary Rule 4.

mentioned that Rule 110 is capable of universal computation and is of Class IV. By trivially reversing left and right we obtain Rule 124 which of course is also of Class IV as are the black and white reversals in Rules 137 and 193. But these all effectively have the same dynamics. Among all the other elementary cellular automata, it is possible that Rule 54 is also of Class IV but according to Wolfram this is not entirely conclusive.

3.8.1 Langton's Parameter

Because there is at least a formal similarity between the types of behavior exhibited by dynamical systems and cellular automata, Christopher Langton sought a 'tunable' parameter as we have seen in the analysis of the one-dimensional dynamical system that could be used in some sense to classify automata. However, it must of necessity only be an approximate classification scheme for most questions about the long term evolution of cellular automata are undecidable. For example, the automaton (Code 357, $r = 1$, $k = 3$) of Figure 3.30 evolves to the quiescent state only after 88 steps so that this is a Class I automaton.

However, another automaton that starts out looking similar to this one, goes on indefinitely (Figure 3.31).

If the behavior dies out quickly, then the automaton is clearly seen to be of Class I, but if it does not, it could still be of Class I, simply reaching a constant state after a very long number of time steps. Or it could be of Class II with a repeating pattern of possibly a very high period, or even some other class. There is simply no way to determine *a priori* whether the automaton dies out or not other than letting the system evolve for as long as practicable. This question is essentially the same as the 'halting problem' for Turing machines.

Figure 3.32 is another example where first appearances are deceiving. There are 10 states per cell and there appears to be the kind of complex interactions that one would expect from a Class IV automaton. However, letting the automaton evolve for some considerable period of time, we find that it settles into typical Class II behavior (Figure 3.33).

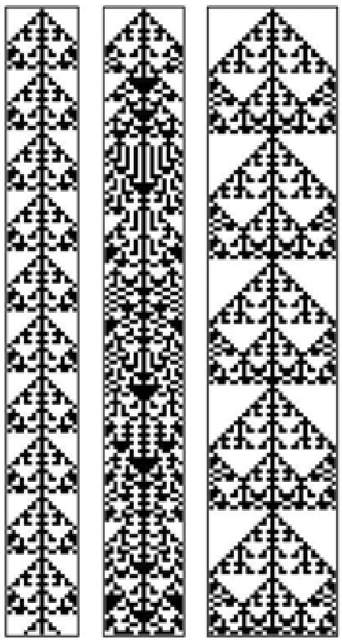

Figure 3.26: Rule 150 in finite domains (with periodic boundaries) of widths 17, 19, and 31 with periods 15, 510, and 31 respectively.

Related to this are cellular automata that Wolfram refers to as 'computationally irreducible'. There are some physical systems for which it is possible to find a formula or algorithm that will give the state of the system at some time t so that it is not actually necessary to let the system evolve until time t in order to see this. Certainly Rule 255:

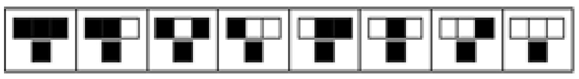

is an obvious case in point. If there is to be a formula or algorithm defining the state of a system at a given time t, then it will have to involve less computation than the explicit time evolution of the system itself, and hence must be 'more sophisticated'. But as we will see below, there are some cellular automata (even one-dimensional) that are capable of universal computation and thus able to perform the most sophisticated computations that can be done. The upshot is that there will be some automata for which a description of their long term behavior is not possible and the only way to find out is to let them evolve. This can even be the case for Class III automata that are not capable of universal computation such as Rule 30 but whose output is nevertheless random (in the sense we discussed). Thus questions about such automata as to whether or not they evolve to a quiescent state

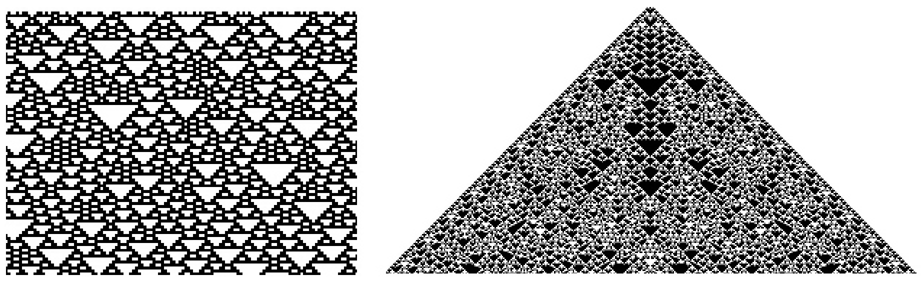

Figure 3.27: This is Rule 126 (left) and Code 2013 showing the typical random behavior found in Class III cellular automata.

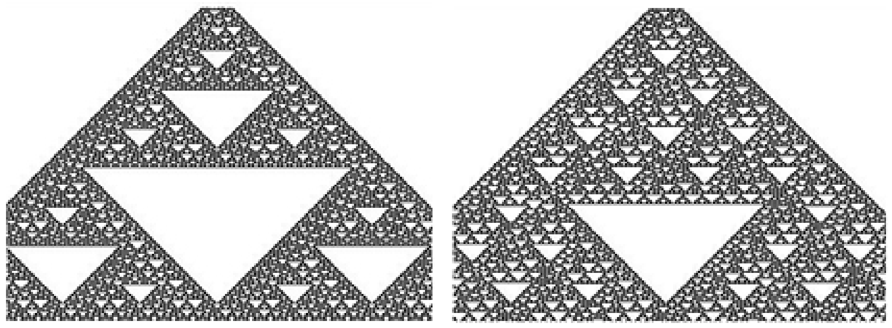

Figure 3.28: The evolution of Rule 126 from initial conditions differing by only one cell's state. This is typical of Class III behavior and chaotic dynamical systems.

are formally undecidable.

In spite of the foregoing difficulties with classification of cellular automata there is still some quantitative measure that we can associate with the four different Wolfram classes. Note that for one particular cellular automaton with k states per cell and a neighborhood radius of r, we found (Section 3.2) there are $n = k^{2r+1}$ different neighborhood-states. For instance, when $k = 2$ and $r = 1$, we have $n = 8$ neighborhood-states making up the transition function. In general, the number of neighborhood-states is given by $n = k^{\rho}$, where ρ is the number of neighbors. If we denote the number of quiescent states of the central cell resulting from these neighborhood-states by n_q, then the Langton parameter is given by:

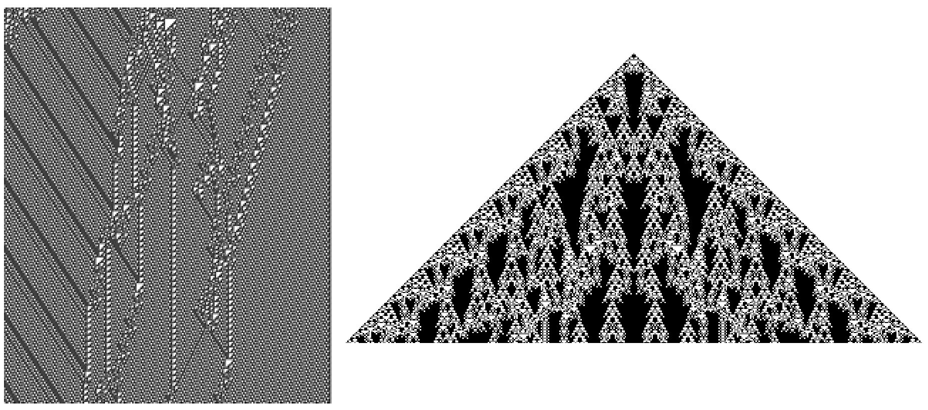

Figure 3.29: Complex interactions between localized structures in Rule 110 and Code 1635, typical of Class IV behavior.

$$\lambda = \frac{k^\rho - n_q}{k^\rho},$$

which simply represents the fraction of output states that are active (non-quiescent) in the particular transition function defining the automaton. When $n_q = k^\rho$, then all the output states are quiescent and $\lambda = 0$. When $n_q = 0$, there are no quiescent output states and $\lambda = 1$. When all the states are equally represented in the output, we have $\lambda = 1 - \frac{1}{k}$ so that the domain of interest is $0 \leq \lambda \leq 1 - \frac{1}{k}$. When $k = 2$, the roles of the quiescent and non-quiescent cells tend to reverse themselves for high values of λ.

As an example, Rule 12: 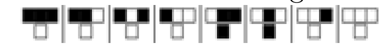 has $\lambda = \frac{8-6}{8} = 0.25$, which is just the fraction of 1's in the output, and indeed it exhibits the simple periodic behavior of Class II (Figure 3.34).

In Langton's words, the λ value of a transition function "... is an aggregrate statistic that is *correlated* with, but not a certain predictor of a certain level of behavioral complexity." It reflects average behavior of a class of rules. Bearing this in mind, we find a correlation with the four classes of cellular automata as indicated in Figure 3.35.

Here again we observe that Class IV is associated with Class II behavior and precedes Class III. In Class IV, there are periodic structures as in Class II, but unlike Class II where these structures do not interact, in Class IV automata some of these structures interact in complex ways. Because of these complex interactions, Class IV behavior is also on the verge of the random behavior exhibited in Class III automata. This suggests (on average) the following transition of class behavorial regimes with increasing λ from 0 to $1 - 1/k$:

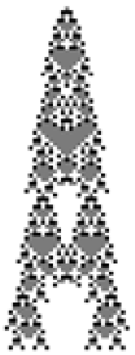

Figure 3.30: Code 357, $r = 1$, $k = 3$, evolves to a quiescent state after 88 time steps and is thus a Class I automaton.

$$\text{Fixed Point} \Longrightarrow \text{Periodic} \Longrightarrow \text{Complex} \Longrightarrow \text{Chaotic}$$

This dynamical discrimination works reasonably well for 'large' values of k and ρ, say $k \geq 4$, $\rho \geq 5$ but less so for the simplest 1-dimensional case of $k = 2$. For example, taking $\rho = 3$, the dynamics are "only roughly correlated" with the Langton parameter. Rule 18: 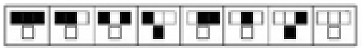 as well as Rule 40: 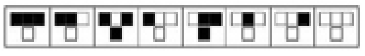 both have $\lambda = 0.25$, yet Rule 18 is Class III (Figure 3.36 left) and Rule 40 (Figure 3.36 right) is Class I and we have already seen that Rule 12 ($\lambda = 0.25$) exhibits Class II behavior. Another approach to distinguish the four Wolfram classes, based on what are called *mean field theory curves*, has been taken by H.V. McIntosh [1990].

3.9 Universal Computation

It is a remarkable fact that one-dimensional cellular automata are capable of universal computation. As mentioned in the Preliminaries, this is essentially a consequence of the fact that the logic gates, NOT, AND, and OR can be emulated coupled with memory storage and retrieval. These computer functions were demonstrated by Wolfram [*2002,* p.662] with the composition of each logic gate given in Figures 3.37, 3.38, and 3.39. There are five cell states (denoted by five colors – white, light gray, medium gray, dark gray = 0, black = 1) and the transition rule, without going into the precise details is the same for each of the logic gates.

In addition to the logic gates themselves, Wolfram demonstrated how information could be stored and retrieved in random-access memory (Figure 3.40).

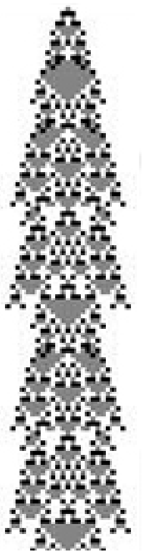

Figure 3.31: Code 600 ($r = 1$, $k = 3$) that does continue indefinitely as it has a repeating pattern.

It is Chris Langton's contention ([1990]), based on empirical experiments, that rules capable of complex computations and indeed universal computation are likely to be found for λ values near the transition between order and chaos. This is analogous to Wolfram's contention that Class IV automata are capable of universal computation. The idea being that complex computations require information transmission and storage coupled with interaction between them. The likely place to find such capabilities, according to Langton, is not in the ordered or chaotic regimes but rather in the "phase transition" between them where there are long transients and complex, unpredictable behavior.

3.10 Density Problem

A prototype of many problems in the CA field is that of the so-called density classification problem. In the one-dimensional two-state version it is desired that the evolved cellular automaton becomes either all 1's or all 0's depending on whether the initial configuration was more than half 1's or more than half 0's respectively. The evolution of such a CA algorithm is thus a means to 'classify' the binary string of 0's and 1's according to their frequency (density). The problem is actually difficult for a cellular automaton because the global property of discerning the higher frequency of either the 0's or 1's must be carried out by local interactions only. In fact, it was shown by Land & Belew [1995] that the density problem cannot be solved

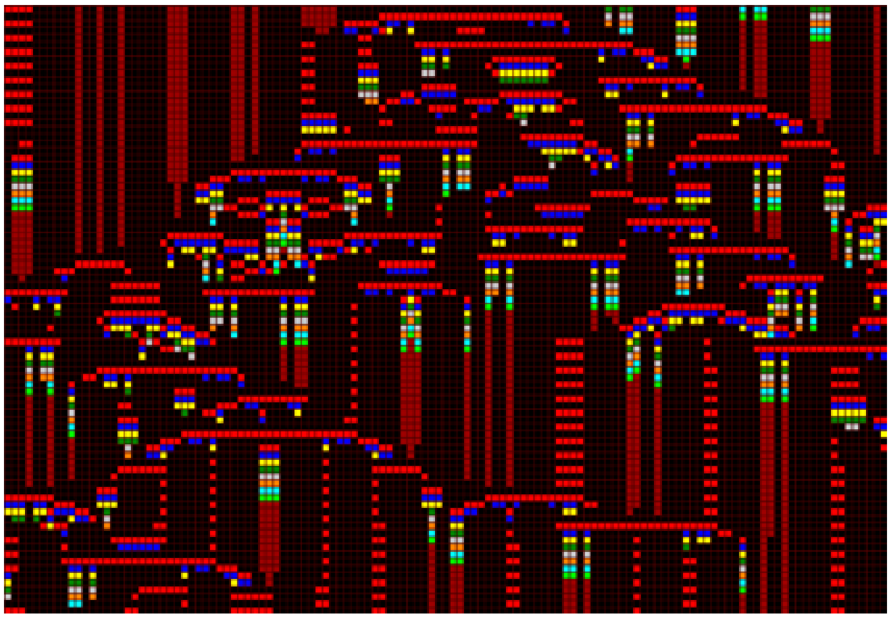

Figure 3.32: This cellular automaton apparently looks like Class IV but subsequently evolves into Class II.

perfectly by any two-state CA having radius $r \geq 1$.

However, all is not lost. If the output conditions of the problem are relaxed slightly then in fact there is a perfect solution proved by Capcarrere, Sipper, & Tomassini [1996]. The humble elementary Rule 184 given by:

$$c_i(t+1) = \begin{cases} c_{i-1}(t) \text{ if } c_i(t) = 0 \\ c_{i+1}(t) \text{ if } c_i(t) = 1, \end{cases}$$

is able to classify any binary string of length N in the following sense. If the density of 1's (resp. 0's) is > 0.5, then the automaton evolves to a fixed state with a block (or blocks) of at least two cells in state 1 (resp. state 0) within $[N/2]$ time steps with the rest of the output being alternating 0's and 1's. (Here the brackets mean to round down to the nearest integer). Even in the case when the density of 1's and 0's is exactly 0.5, the automaton evolves towards a state of solely alternating 1's and 0's, thus perfectly classifiying the density of the initial binary string. The same holds true for Rule 226 which is just the reflected version of Rule 184.

Since the density problem is not perfectly solvable in its initial formulation, attempts have been made to classify the density of a binary string 'most' of the time. One of the best algorithms is the Gaks-Kurdyumov-Levin (GKL) rule which is nearly always successful with binary strings having high

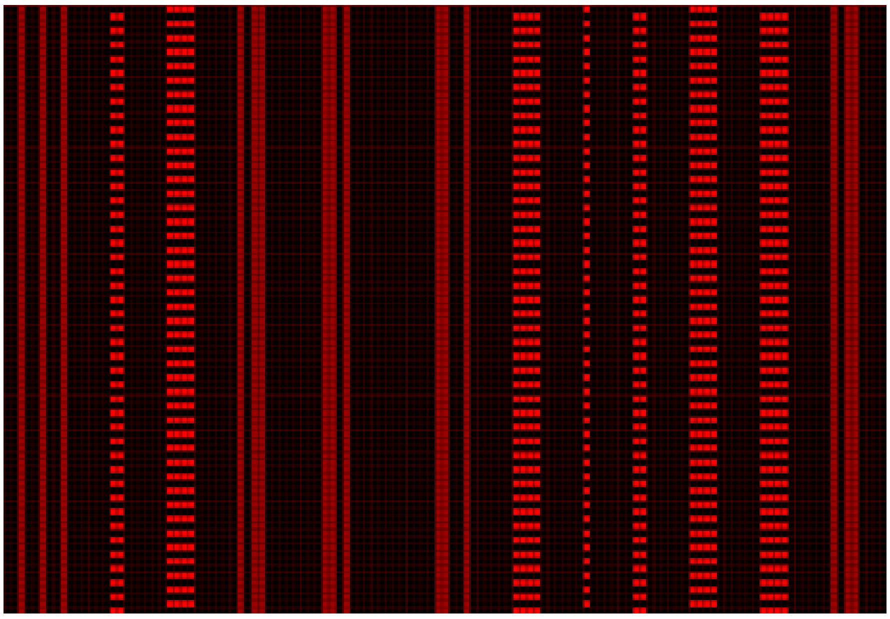

Figure 3.33: The evolution of the cellular automaton in the preceding figure.

or low initial densities. The GKL rule is a wonderful piece of ingenuity that is a two-state, $r = 3$ rule defined by:

$$\begin{aligned} c_i(t+1) &= majority\{c_i(t), c_{i-1}(t), c_{i-3}(t)\} \qquad \text{if } c_i(t) = 0 \\ c_i(t+1) &= majority\{c_i(t), c_{i+1}(t), c_{i+3}(t)\} \qquad \text{if } c_i(t) = 1, \end{aligned}$$

where the term 'majority' means that if two out of the three cells are in state 0 (resp. 1), then that value is taken for the central cell update at the next time step.

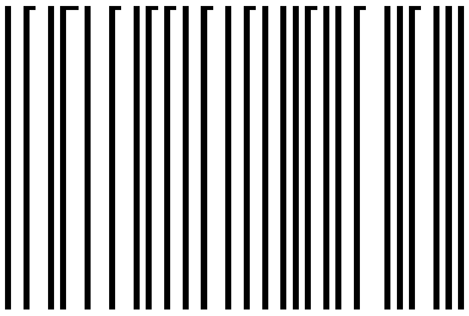

Figure 3.34: Rule 12 displaying Class II behavior with $\lambda = 0.25$.

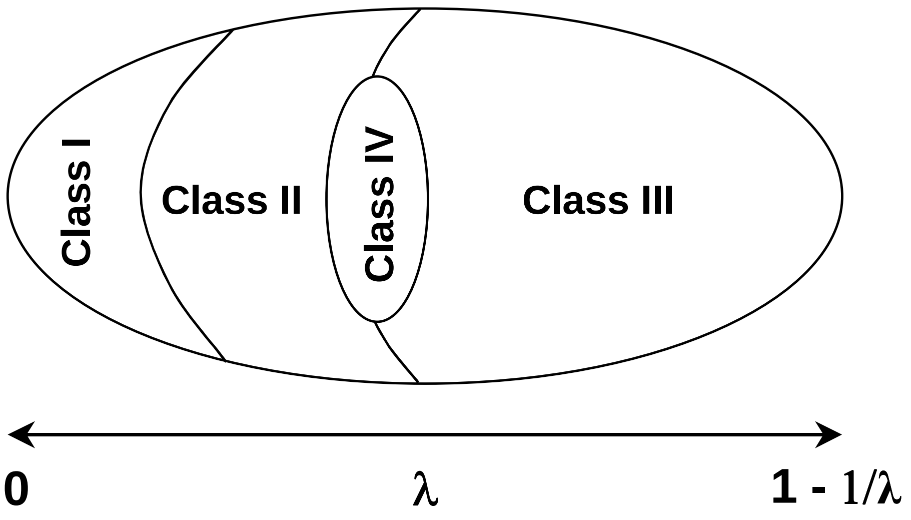

Figure 3.35: The association of the Langton parameter λ with the different Wolfram classes. Note that a specific value of λ can be associated with more than one class. Adapted from W. Flake, *The Computational Beauty of Nature*.

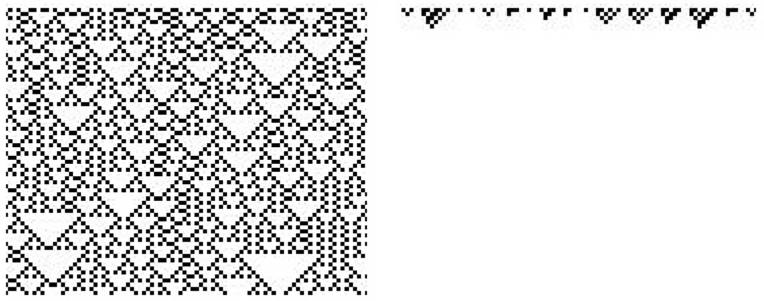

Figure 3.36: The evolution of Class III Rule 18 (left) and Class I Rule 40 (right). Both rules have Langton parameter $\lambda = 0.25$.

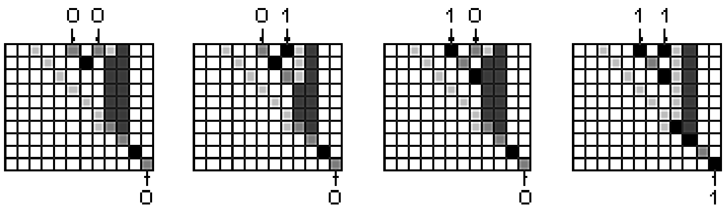

Figure 3.37: The logic AND gate where the input is fed into the first row of the automaton with specific initial conditions and the desired output of 1 at the bottom right only in the case when both inputs P and Q are 1.

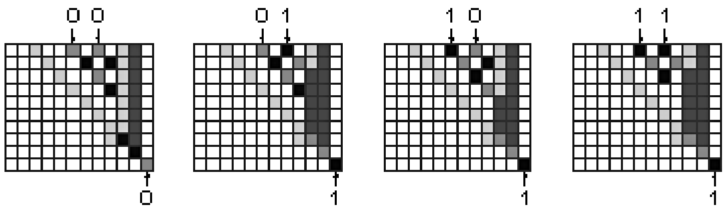

Figure 3.38: The logic OR gate which is a slight variation of the AND gate above giving the output 1 in all but the first case when inputs P and Q are both 0.

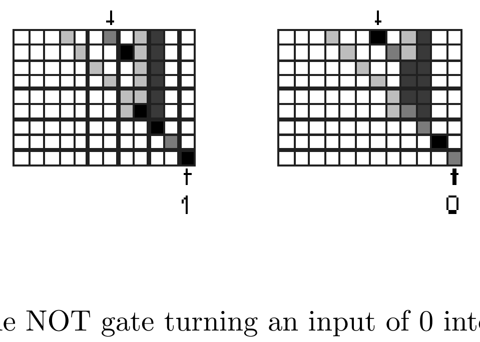

Figure 3.39: The NOT gate turning an input of 0 into 1 and 1 into 0.

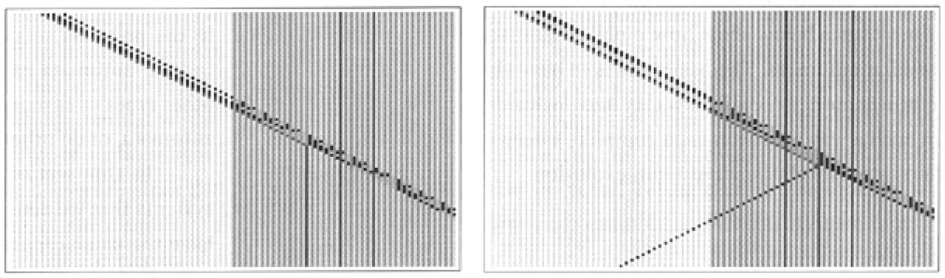

Figure 3.40: A one-dimensional cellular automaton model to illustrate the storage and retrieval of information. The memory is on the right in each figure and in the first figure a 1 is stored in the memory position 13. In the second figure a 1 is retrieved from the memory position 19. From Wolfram [2002], p. 663.

Roughly speaking, densities of local regions are classified and these regions expand with time. Where there are regions of equal density of 0's and 1's, a checkerboard or white/black boundary signal is propagated indicating that the classification be carried out on a wider scale. As effective as the GKL rule is with initial conditions away from the critical density of 0.5, it was found that for densities very near the critical value, the GKL rule failed up to 30% of the time (Mitchell, Hraber, and Crutchfield [1993]).

Norman Packard [1988] experimented with genetic algorithms (see Section 5.4.1) to solve the density classification problem and came to the seemingly reasonable conclusion that when CA are evolved (as in GAs) to perform complex computations, the evolution is driven to rules near the transition to chaos. Similar experiments conducted by Mitchell *et al.* also applied genetic algorithms to the density problem to produce very successful evolved CAs, although as it happens, none quite as successful as GKL. The authors results however were "strikingly different" from those reported by Packard. They found that the most successful evolved rules for solving the density problem were found close to $\lambda = 0.5$ which is the theoretical value they also deduced, and not near the transition to chaos. Packard's results were seen as possible "artifacts of mechanisms in the particular GA that was used rather than a result of any computational advantage conferred" by the transitional regions. Interestingly, Rule 184 also has $\lambda = 0.5$.

Again using GAs, an asynchronous approach to the problem was studied by Tomassini & Venzi [2002], although their results showed that the performance of asynchronous algorithms were inferior to the best evolved synchronous CAs or the GKL rule although they were more robust in the presence of noise.

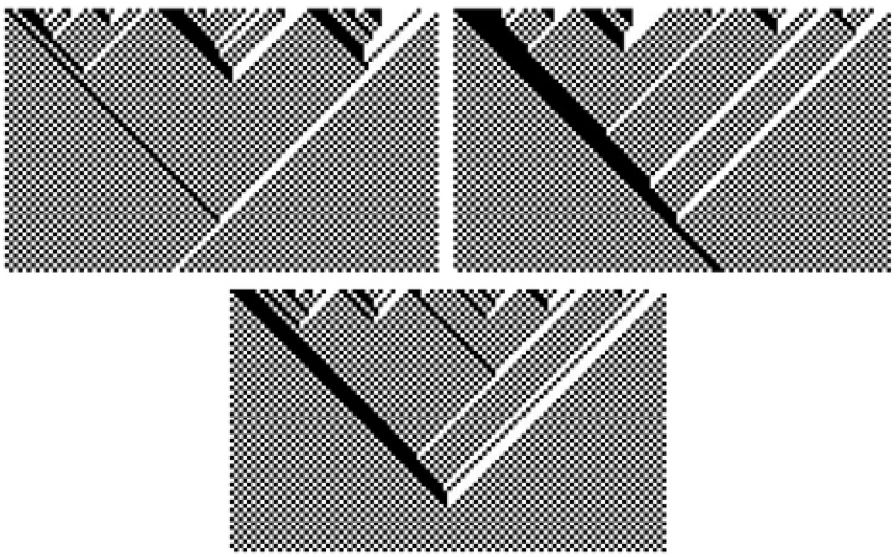

Figure 3.41: Rule 184 classifying densities in the sense mentioned in the text of 51 white/49 black (left), 51 black/49 white (right) and 50 white/50 black (bottom).

3.11 Synchronization

An interesting problem, of which there are now many variations, and first posed by John Myhill in 1957, has to do with the synchronization of the output of an arbitrarily long but finite row of CA. At some time step, all the cells should, for the first time, attain the same state value. Like the density problem, this is difficult for CA since a particular global state must be reached solely by local interactions. This has become known as the 'firing squad problem' or 'firing squad synchronization problem' (FSSP). A cell at one end of the row (a 'general') is distinguished from the others (the 'soldiers'). Taking a 3-cell neighborhood, the problem is to choose the states for each cell and suitable transition functions such that the soldier cells will all be in the same (firing) state for the first time at the same time step. McCarthy and Minsky (see Minsky [1967]) showed that there exist solutions for n cells in $3n-1$, $\frac{5}{2}n-1$,... time steps. A 'minimal time solution' is one achieved in $2n-1$ time steps, which is the number of time steps it takes for a general to send a signal to the far-end member and receive a reply. Waksman [1966] gave a minimal time solution involving 16 states per cell, while Balzer [1967] gave one with 8 states per cell and showed that there was no minimal time solution with only 4 states per cell.

The best minimal time solution to date has been demonstrated by Jacques

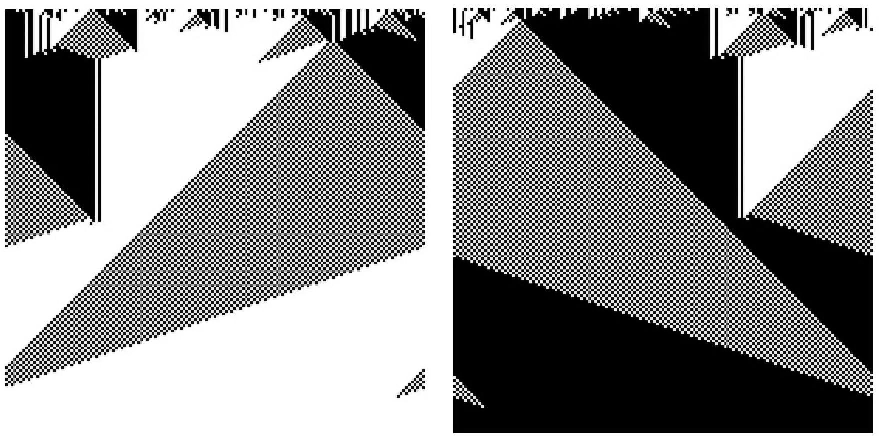

Figure 3.42: The GKL rule classifying initial densities of 77 white/72 black cells (left) and 72 black/77 white (right).

Mazoyer [1987] in a *tour de force* of technical analysis using 6 states. The question is still open whether 6 or 5 states per cell is the least number required. Two generals can also be taken, one at each end who do not reach the firing state (see examples in Wolfram [2002], p.1035).

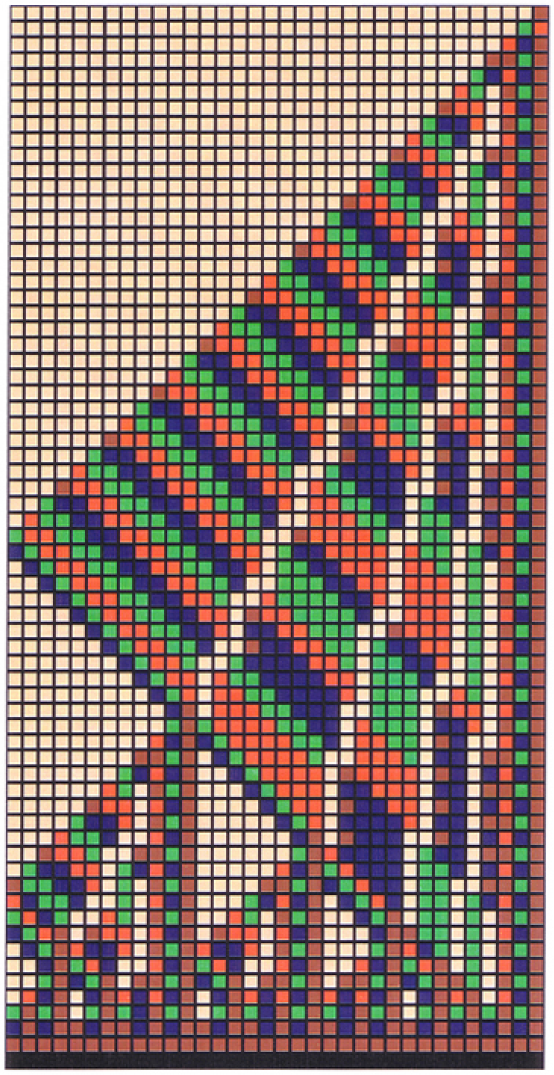

Figure 3.43: The minimal time solution of Jacques Mazoyer of the firing squad synchronization problem using 6 states. Here $n = 34$ and time increases from top to bottom. The general is on the right-hand side and also reaches the firing state (black) together with all the soldiers in 67 time steps. Courtesy Jacques Mazoyer.

Chapter 4

Two-Dimensional Automata

The chessboard is the world, the pieces are the phenomena of the universe, the rules of the game are what we call the laws of Nature.

Thomas Henry Huxley

Two-dimensional cellular automata exhibit some of the same characteristics as do one-dimensional automata. There are two fundamental types of neighborhood that are mainly considered. First there is the *von Neumann* neighborhood (the 5-cell version of which was used in the construction of his self-replicating machine), consisting of the 4 or 5 cell array depending on whether or not the central cell is counted:

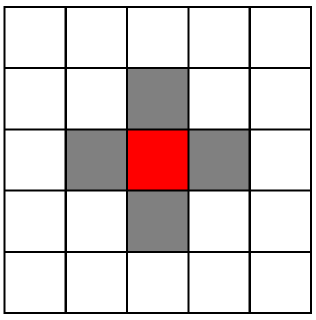

Figure 4.1: The von Neumann neighborhood surrounding a central cell.

The *Moore* neighborhood consists of the 8 or 9 cell array depending on whether or not the central cell is counted (Figure 4.2).

In both cases $r = 1$ and each is useful depending on the context. The extended Moore neighborhood has the same form as the preceding but with $r > 1$.

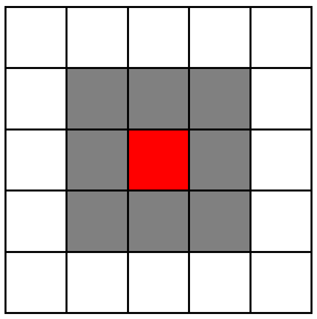

Figure 4.2: The Moore neighborhood with $r = 1$.

Typically, in a rectangular array, a neighborhood is enumerated as in the von Neumann neighborhood illustrated below (Figure 4.3) and analogously for the Moore neighborhood. The state of the $(i, j)th$ cell is denoted by $c_{i,j}$.

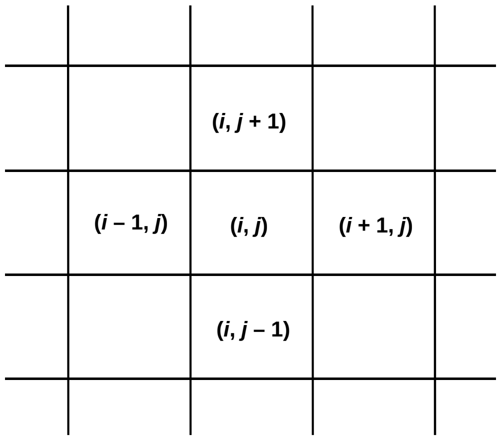

Figure 4.3: The enumeration of the cells of the von Neumann neighborhood.

In the 1-dimensional case with $k = 2$, $r = 1$, there were just $2^3 = 8$ possible neighborhood-states. Now however, with just two states 0 and 1 and a 9-cell Moore neighborhood (again, $k = 2$, $r = 1$), there are $2^9 = 512$ possible neighborhood-states ranging from all white to all black with all the various 510 other combinations of white and black cells in between. A given transition function would tell us how the central cell of each of the 512 neighborhood-states should change at the next time step. How many such transition functions are there? A staggering $2^{512} \approx 10^{154}$, more than the number of all the atoms in the universe! Even with a 5-cell neighborhood,

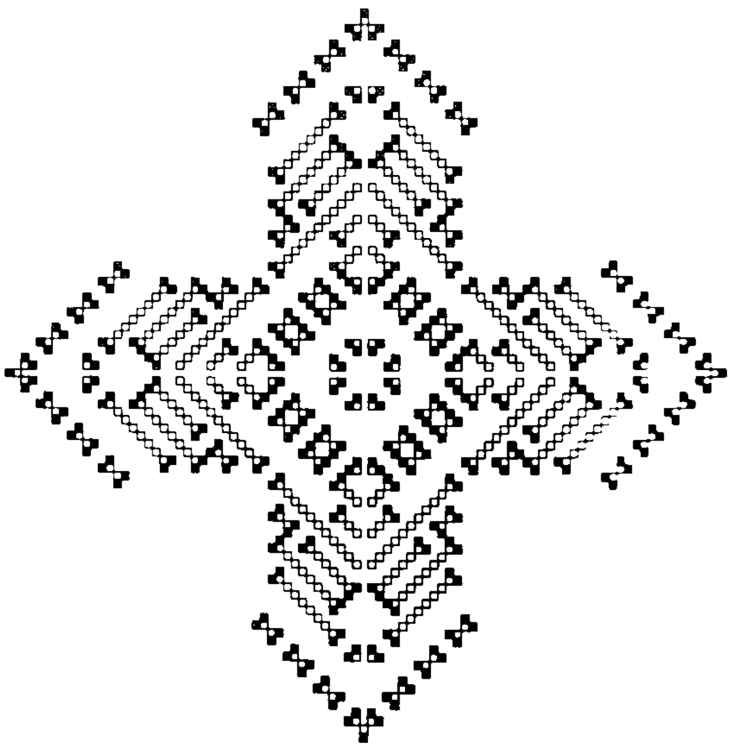

Figure 4.4: The 'dog bone' configuration as referred to by Schrandt and Ulam in which a cell becomes alive in the next generation if it it has exactly one alive (black) neighbor in the current generation and any cell of the previous generation dies.

there are still $2^{32} \approx$ ten billion possible transition functions to choose from.

Beginning in the early 1960s, Stanislaw Ulam and co-workers J. Holladay and Robert Schrandt at Los Alamos Scientific Laboratory began using computing machines to investigate various two-dimensional cellular automata. An infinite plane was considered and divided up into identical squares. The transition rules were eclectic and the results were mostly empirical. One particular automaton was as follows: A cell became alive at the next generation if it was a neighbor (in the von Neumann sense) of exactly one live cell of the current generation. This rule was later coupled with a 'death rule' that required all cells that were a fixed number (m) of generations old to die. Say if $m = 2$, then the $(n + 1)st$ generation is derived from the nth generation and the $(n - 1)st$ generation is erased. Thus only the last two generations survive in any configuration (See Figure 4.4).

We can use the same transition rule together with the death rule, and two different initial configurations on the same array, say in different colors

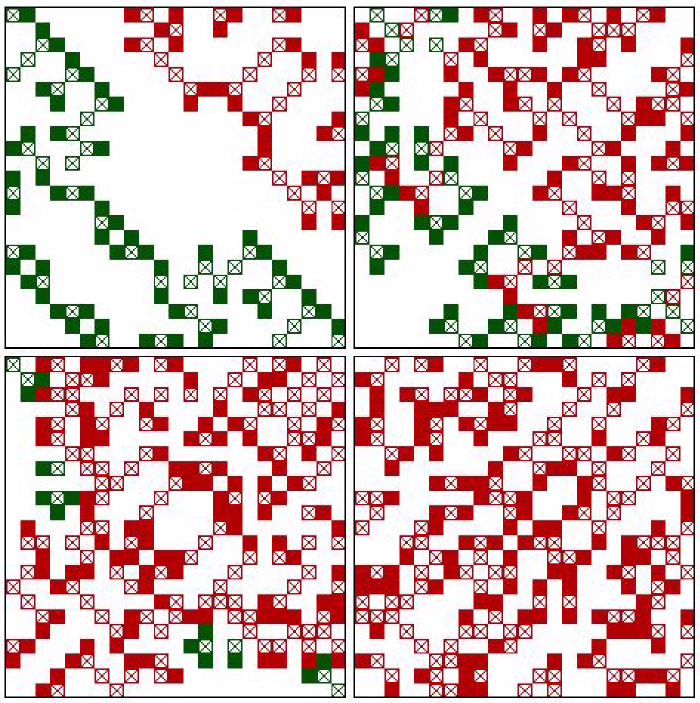

Figure 4.5: A contest on a finite array in which one system (red) on the top right of (a) gradually eliminates the system on the bottom left (green) of (a). Solid cells represent the current generation, crosses the previous generation. The figures represent the situation at generations: 11, 32, 49, and 77 respectively.

to distinguish their respective live cells. The growth rule prohibits the appearance of a live cell at the next generation that has two live neighbors at the present generation, and this condition now includes neighbors of either color. This leads to contests between the two opposing systems with the result that one or both may end up eliminated (Figure 4.5).

4.1 The Game of Life

It is probable, given a large enough "Life" space, initially in a random state, that after a long time, intelligent self-reproducing animals will emerge and populate some parts of the space.

John Conway

The Game of Life first entered the world stage from the pages of Martin Gardner's *Mathematical Games* column in the October 1970 issue of *Scientific American.* The creator of the Game of Life was the English mathematician, John Horton Conway. Originally, Life was to be played out using counters on a chess or Go board, but soon computer screens became Life's natural domain. The Game of Life caused an international sensation following its rather dramatic creation (R.K. Guy [1985]):

... only after the rejection of many patterns, triangular and hexagonal lattices as well as square ones, and of many other laws of birth and death, including the introduction of two and even three sexes. Acres of squared paper were covered, and he and his admiring entourage of graduate students shuffled poker chips, foreign coins, cowrie shells, Go stones or whatever came to hand, until there was a viable balance between life and death.

The rules for the Game of Life are quite simple as each cell has exactly two states (1 - alive, or 0 - dead) and the 8-cell Moore neighborhood is the one considered to determine the state of the central cell:

• A dead cell becomes alive at the next generation if exactly 3 of its 8 neighbors are alive;

• A live cell at the next generation remains alive if either 2 or 3 of its 8 neighbors is alive but otherwise it dies.

In anthropomorphic terms, the second rule says that if a cell is alive but only one if its neighbors is also alive, then the first cell will die of loneliness. On the other hand, if more than three of a cell's neighbors are also alive, then the cell will die of overcrowding. By the first rule, live cells are born from a *ménage á trois.* Of course this is not really a game that you play in the conventional sense but rather a microcosm of another universe that one can explore since we know its physics entirely. An excellent exposition of the Game of Life can be found in the monograph *The Recursive Universe* by William Poundstone [1985].

There are many variants of Conway's original set of rules, as well as using other lattices such as triangular or hexagonal ones or considering Life in other dimensions, but none seem to offer the richness and diversity of the original game. It is common to let the Game of Life evolve on a lattice with periodic boundary conditions ('wrap'), that is to say, cells on the extreme left and right are considered neighbors, and cells at the extreme top and bottom of the lattice are also to be considered neighbors. Whereas, using periodic boundary conditions in the one-dimensional case resulted in a continuous loop, in the two-dimensional case our lattice becomes a torus (donut shaped).

The Game of Life is an example of a Class IV automaton. We note that Packard and Wolfram [1985] found no two-dimensional Class IV cellular automata other than "trivial variants of Life". When the updating of cells is asynchronous, the Game of Life no longer exhibits Class IV behavior but instead converges to a stationary state (Bersini & Detour [1994]).

Life is also an example of an ‘outer totalistic’ rule in that the state of the central cell at the next time step depends on the prior state of the central cell as well as the sum of the values of the 8 neighboring cells. The preceding rules for the Game of Life can be represented in the following transition table:

				s	u	m			
$c_i(t)$	8	7	6	5	4	3	2	1	0
0	0	0	0	0	0	1	0	0	0
1	0	0	0	0	0	1	1	0	0

where the row that one considers for the value of $c_{i+1}(t)$ is given by the value of the central cell state $c_i(t)$.

Conway had considered the rules very carefully so that Life is carefully poised between having patterns that die out quickly and those that continue to grow. In fact, when Life was first proposed, Conway conjectured that no initial collection of live cells could grow without bound and offered a \$50 prize to the first person who could prove or disprove this before the end of 1970. The conjecture was short lived as we will see below.

4.1.1 Lifeforms

There is an entire pantheon of Lifeforms and the interested reader can refer to the website: http://pentadecathlon.com/index.shtml. We will discuss the evolution of just some of the more common ones. Clearly any fewer than three cells will die in one generation. For a triplet of live cells (that do not vanish after the first generation), they either rapidly evolve to extinction (top three rows of Figure 4.6), become a block of static cells that remains unchanged with all subsequent generations (4th row), or become an oscillating 2-cycle triplet (bottom row):

Four-cell configurations evolve to stable forms (top four rows of Figure 4.7) as well as a long sequence of various forms.

The 5-cell ’R-pentomino’ (see Figure 4.12 right) is one of the most fascinating elementary Lifeforms in that its evolutionary history does not stabilize until 1103 generations. In the process it generates what are known as ‘gliders’, (discussed below) among other Lifeforms.

4.1.2 Invariant Forms

Some configurations in the Game of Life remain unchanged at every time step (Figure 4.8). We have already seen the block of four cells and what is known as the ‘beehive’ (the terminal figure of rows 2,3, and 4 of Figure 4.7).

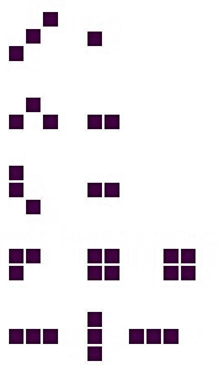

Figure 4.6: The possible evolutionary histories of three cells in the Game of Life. The orientation of the initial cells is not relevant.

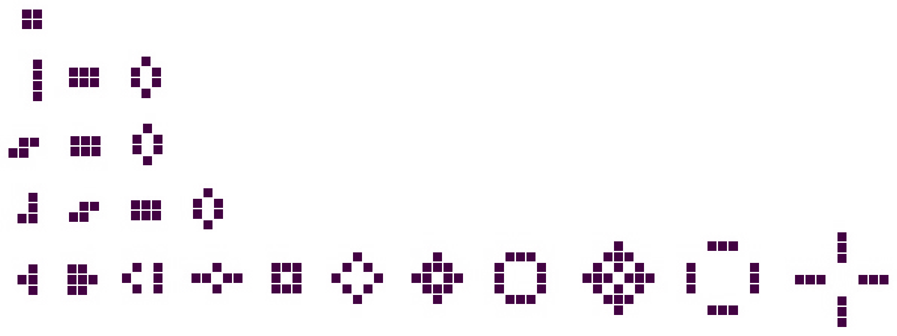

Figure 4.7: The evolution of 4 live cells with time increasing to the right. The last two configurations of the last row alternate in a two-cycle.

The ‘block’ is the most common and it turns up frequently in Life. As each cell of the block has exactly three live neighbors, they all persist in time yet surrounding dead cells have only two live neighbors which is insufficient for them to spring into life.

4.1.3 Oscillators

There are some Lifeforms that exhibit periodic behavior oscillating indefinitely between a fixed number of configurations. Period-2 oscillators alternate between two distinct states; they arise spontaneously and are very common; see Figure 4.9.

Many other cyclic oscillators have been created artificially, including periods 3,4,5,... 18, plus a variety of others, including one of period 144 by

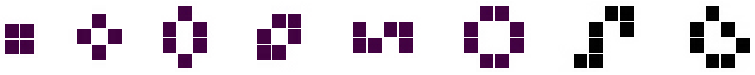

Figure 4.8: Some common invariant forms (l to r): block, tub, beehive, ship, snake, pond, fishhook or eater, loaf.

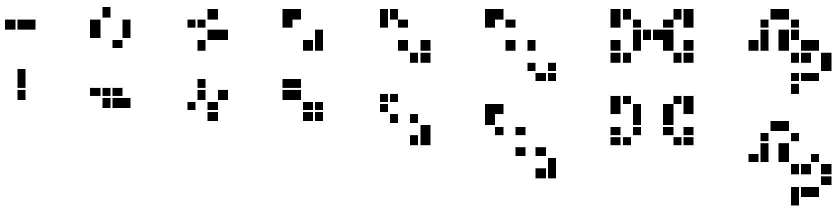

Figure 4.9: Period-2 oscillators. The two rows indicate the two different forms of each oscillator.

Achim Flammenkamp.

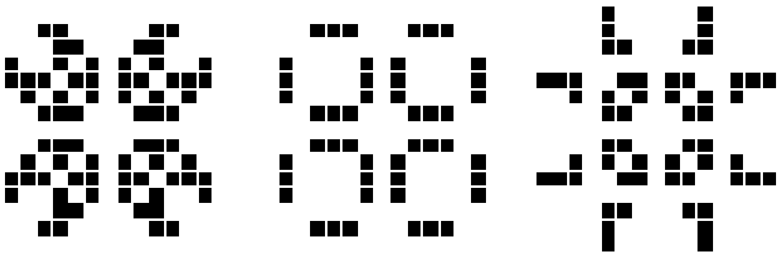

Figure 4.10: An elaborate period 3 oscillator known as the CP-pulsar displaying its three different states. The final state returns to the first at the next time step.

4.1.4 Methuselah Configuations

Such initial patterns have less than 10 live starting cells but they continue to evolve to considerable old age before stabilizing and necessarily exclude configurations that grow forever in the sense of an ever increasing number of alive cells. An R-pentomino (Figure 4.12 right) remains alive for 1103 generations having produced six gliders that march off to infinity. The acorn (center) was discovered by Charles Corderman and remains alive for 5,206

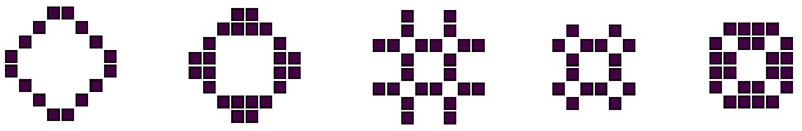

Figure 4.11: A period 5 oscillator displaying its five different Lifeforms.

generations. Rabbits were discovered by Andrew Trevorrow in 1986 and stabilize after 17,331 into an oscillating 2-cycle having produced 39 gliders.

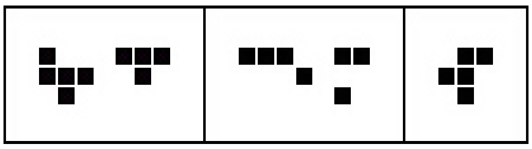

Figure 4.12: Methuselah configurations (l to r): rabbits, acorn, and R-pentomino.

4.1.5 Gliders

Gliders are another 5-cell configuration and they actually move one cell diagonally at the fourth time step (Figure 4.13). They are known as gliders as at time step $t+2$, they are reflected in a diagonal line, mathematically, a "glide reflection". By time step $t+4$ the glider is reflected once again back to its original orientation, but one cell (diagonally) displaced. This 4-cycle is then endlessly repeated. The glider is a marvelous creature to watch as it marches in its ungainly fashion across the computer screen. In the words of computer scientist Steve Grand, "The glider is a thing – a coherent persistent phenomenon that moves across 'space' – and yet is not separate from or superimposed on that space. It is simply a self-propagating disturbance in the space created by these little rule-following [cells]" (*Creation*, p. 40).

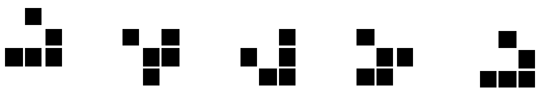

Figure 4.13: A glider moves one cell diagonally to the right after four generations.

The maximum speed that information can propagate from one cell to

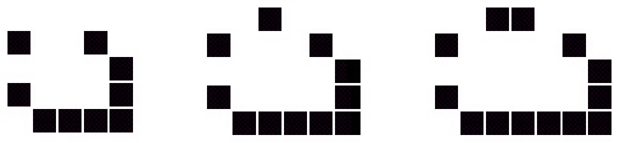

Figure 4.14: From left to right: light-weight, medium-weight, and heavy-weight spaceships. These move horizontally at the speed $c/2$.

another (either horizontally, vertically, or diagonally) is one cell per generation. In Life, this is known as the *speed of light* (c). Since the glider moves exactly one diagonal cell after four generations, it is said to move at one-fourth the speed of light ($c/4$).

Conway has proved that the maximum speed of any configuration moving horizontally or vertically is $c/2$. Configurations that actually do move at this speed are what Conway called 'spaceships', depicted in Figure 4.14.

One of the most remarkable configurations to arise in the early days of Life, was the 'glider gun'. This arose out of work done by Robert April, Michael Beeler, R. William Gosper Jr., Richard Howell, Richard Schroeppel and Michael Speciner who were in the Artificial Intelligence Project at M.I.T. In November, 1970 they claimed the $50 prize offered by Conway by demonstrating the glider gun (Figure 4.15) found by Gosper that would indefinitely generate gliders every 30 generations, thus disproving Conway's conjecture that the number of live cells cannot grow without bound. Somewhat remarkably, Gosper's group found that the collision of 13 specially arranged gliders can create their glider gun. Since then glider guns have been found with other periods of generation, even one having period 256.

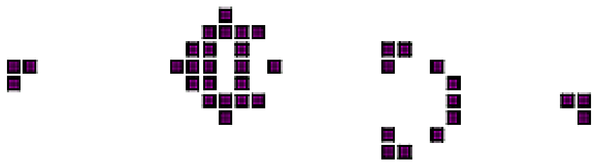

Figure 4.15: The initial configuration of the original glider gun discovered by Bill Gosper that generates a new glider every 30 generations.

Another way to produce unbounded growth in Life is via a 'puffer train'. These objects travel in a vertical direction and leave behind 'smoke' or 'debris' that becomes stable. The first puffer train was also found by Bill

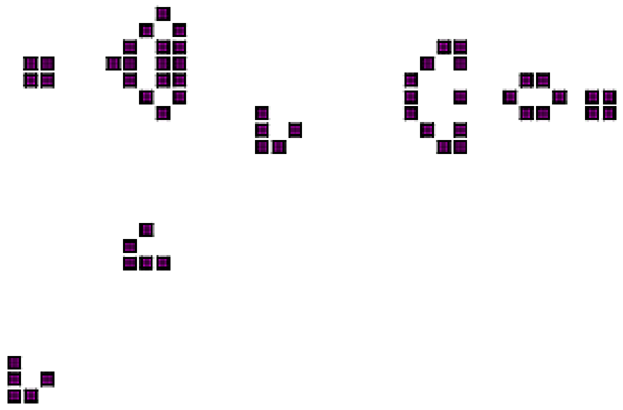

Figure 4.16: The glider gun after it has fired off three gliders toward the lower left.

Gosper and consisted of an engine escorted by two lightweight spaceships. Since then numerous other ones have been discovered (Figure 4.17).

There are also 'glider eaters' that devour gliders and are useful in the creation of logic gates (Figure 4.18).

Another type of unbounded growth was discovered by David Bell in 1993. Starting with a finite configuration of live cells, it produces a 'spacefiller' which is a feature that can appear in other cellular automata (Figure 4.19).

4.1.6 Garden of Eden

The evolution of a cellular automaton is governed by the local transition function which alters the states of all cells in the array synchronously at discrete time steps. Thus, patterns of cells are changed into other patterns of cells as the system evolves. It is natural to ask if there are some patterns of cells that do not arise at all in the evolution of the system?

A cellular automaton configuration that can have no prior configuration generating it (via the underlying local transition function) is called a *Garden of Eden* pattern, a term due to John W. Tukey of Princeton University. In a paper in 1962, Edward F. Moore found that in the evolution of a cellular automaton, if a particular configuration had more than one distinct predecessor, then there would have to exist some configuration that would have no predecessor (the Garden of Eden pattern). This was only an 'existence theorem' and no method was given for actually finding the Garden of Eden configuration. The converse to this result was established by John Myhill in 1963, namely, if there is a Garden of Eden configuration with no predecessor, then some configuration must have two distinct predecessors. Both results

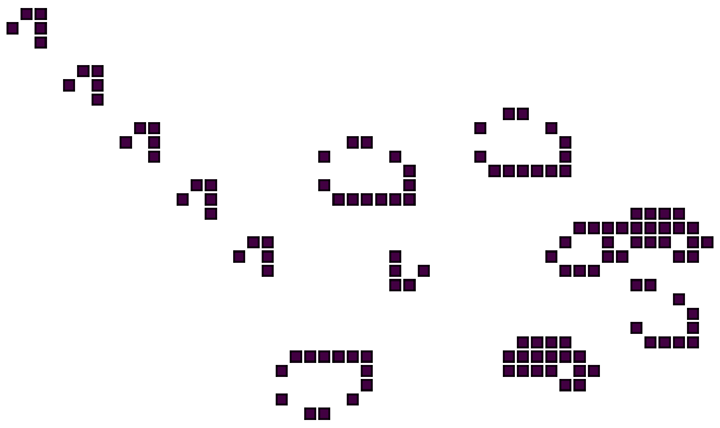

Figure 4.17: A period 16 puffer train (at right) that produces a smoke trail. Based on a design of Tim Coe.

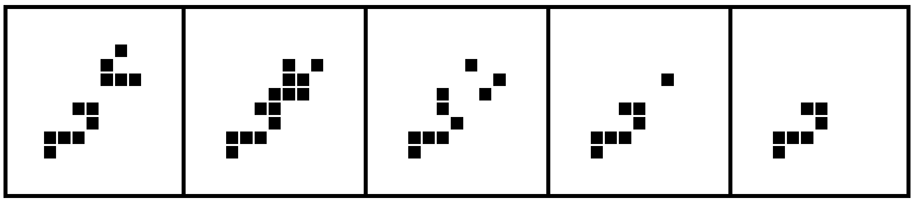

Figure 4.18: In this sequence, a glider-eater in bottom left of the first frame is confronted by a glider approaching at 45 degrees. The glider is gradually eaten until it has disappeared in the last frame. The glider-eater is an essential component of certain logic gates.

are quite general, applying to any cellular automata of finite configurations (i.e. those configurations with only a finite number of non-quiescent cells – although the configurations are infinite in number) and in any dimension. It is clear that if the array consists of a *finite number* of cells, say N, then the total number of possible configurations allowing for two possible states per cell is just 2^N, with at most 2^N possible outcomes resulting from the transition function acting on each of these. If it so happens that two different configurations are transformed by the action of the transition function onto the same configuration, then only $2^N - 1$ configurations have been generated by the transition function, leaving one configuration without a precedessor. But the Moore and Myhill theorems are about the infinitely many finite configurations of cellular automata within infinite arrays.

Because the Game of Life does have configurations that have more than

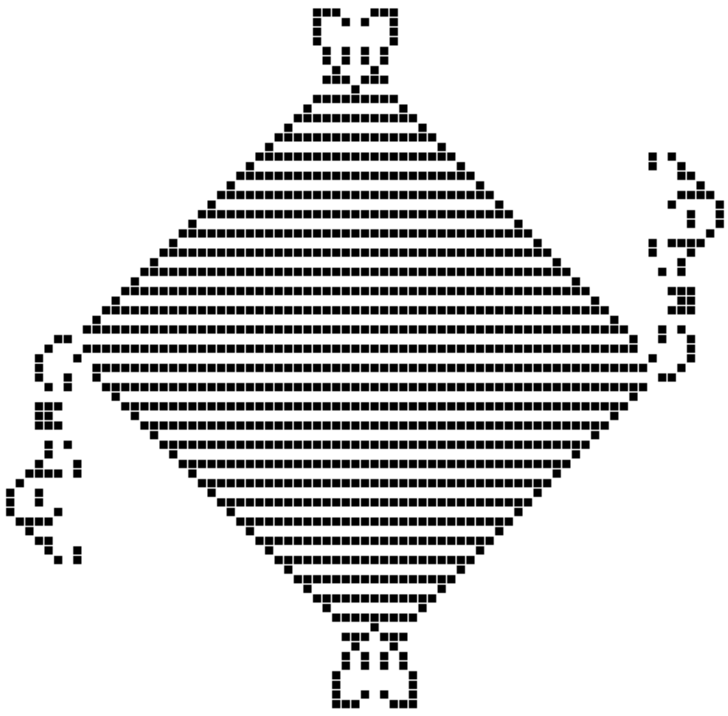

Figure 4.19: The spacefiller Lifeform of David Bell after 46 time steps.

one predecessor (for example, a block has numerous precedessors), and the fact that finite configurations are transformed to finite configurations, Garden of Eden patterns must exist and indeed have been found over the years. Roger Banks found the first one in 1971 with 226 live cells. The one with the smallest number of live cells (at the time of this writing) is 143 due to Achim Flammenkamp (Figure 4.20 right).

The preceding considerations can be discussed in a more mathematical framework. In general, a function f is called *injective* (or *one-to-one*) if whenever $x \neq y$ then $f(x) \neq f(y)$. In other words, distinct points x and y must have distinct *images* $f(x)$ and $f(y)$. This also means that if $f(x) = z$, then no other point can be mapped by f to z, since if some other point y did satisfy $f(y) = z$, then we would have $x \neq y$ and $f(x) = f(y)$, a clear violation of the injective property of f.

We now consider the collection of all *finite* configurations C of a cellular automaton, such as the Game of Life. By finite, we mean that all but a finite number of cells in the lattice are in the quiescent state. Then any configuration belonging to C is transformed by the local transition function acting on each cell into another configuration and moreover, that configu-

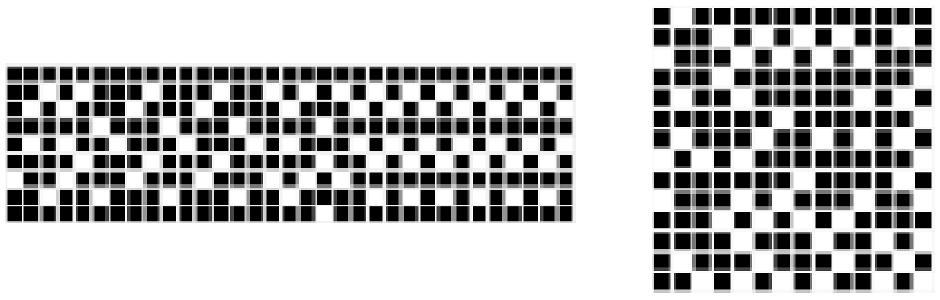

Figure 4.20: The Garden of Eden configurations for the Game of Life of Roger Banks (left) and Achim Flammenkamp, having 226 and 143 live cells respectively .

ration will also belong to C if we make the supposition that if a cell and all its neighbors are in a quiescent state, then the cell remains quiescent at the next time step. Therefore, although the array is infinite in extent, only finitely many cells at any time step ever leave the non-quiescent state and no infinite configuration ever becomes the successor of any finite configuration. We have already encountered an example in Rule 1 where this is not the case since its rule string is given by:

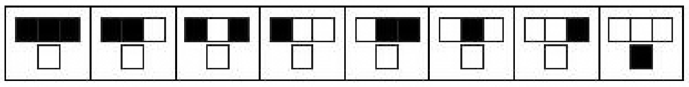

Figure 4.21: Rule 1 allows something to be created from nothing which is not allowed in the present context.

Hence a quiescent neighborhood generates a live central cell at the next time step. This results in an initial finite configuration of one black cell generating an infinite configuration at the next time step and it is exactly this sort of behavior we wish to exclude. We are in a sense getting something from nothing and that is not allowed here.

The transformation from one configuration into another induced by the local action of the transition function can be considered as another function, the *global transition function* F that maps configurations c belonging to C to other configurations c' in C. So for example, in the one-dimensional case taking nearest neighbors, if ϕ is the local transition function, we define the global transition function by

$$[F(c)]_i = \phi[c_{i-1}, c_i, c_{i+1}],$$

where we have suppressed the time step t in the notation.

If the global transition function F is *not* injective, then this would mean that two distinct configurations, say c and c' in C would be mapped to the same configuration (remembering that F is induced by the local transition function), so that there would be a configuration with two predecessors (c and c') as was discussed above. Therefore, having more than one predecessor configuration is equivalent to the global function F not being injective.

Since F is a mapping from C to C, symbolically, $F : C \longrightarrow C$, we can ask if *every* configuration c in C arises as the image of the global transition function acting on some other c belonging to C? If the answer is yes, then we say that the function F is *surjective* (or *onto*). In other words, for every c' in C, there is some other c in C such that $F(c) = c'$. Then, if it so happens that F is *not* surjective, we find that there is some c' belonging to C with no other configuration in C that is transformed into it. Such a configuration c' is then a Garden of Eden configuration since it would have no precedessor arising from the global transition function F, and thus from the local transition function. Therefore, the existence of a Garden of Eden configuration is equivalent to the global transition function being not surjective.

We can now state the:

Moore-Myhill Theorem. *If C is the collection of all finite configurations and $F : C \longrightarrow C$ is the global transition function, then F is not injective if and only if it is not surjective.*

In other words, if some configuration has more than one precedessor (F is not injective), then there is some configuration with no precedessor (F is not surjective), and conversely. Moore's theorem is the first result and Myhill's the converse. In most contexts injective and surjective are two mathematical properties that normally have nothing to do with one another.

The global transition function (in the preceding context) being surjective is now also injective and this latter is equivalent to the cellular automaton being *reversible* (also called *invertible*), that is, at every time step it is possible to go back to a unique predecessor configuration, as was discussed in the section on reversibility in Chapter 3. Since we know that the Game of Life has Garden of Eden configurations, then by the Moore-Myhill theorem it cannot be reversible. But of course we already know this as the 'beehive' configuration has multiple predecessors as is seen in Figure 4.7. In general, given the local transition function for a two-dimensional cellular automaton, the question of reversibility is undecidable (Kari [1990]), although for one-dimensional cellular automata, the question of reversibility is decidable (Amoroso and Patt [1972]).

When Moore proved his theorem, he was interested in the question of when a machine was unable to replicate itself. About the Garden of Eden configuration, Moore had this to say. "Since it is a machine that cannot arise by reproduction, it must be a machine that cannot reproduce itself."

Another result of Moore's about the rate at which a cellular automaton configuration can replicate itself is found later in Section 4.3.

Interestingly, if we drop the restriction of finite configurations then in the general case we have the following result of Hedlund [1969] who was one of the earliest pioneers in the subject of cellular automata:

Hedlund Theorem. *If the global transition function on the set of all configurations is injective then it is also surjective.*

The situation is more straightforward with respect to additive CA. If φ is the local transition function acting on cell states $c_1, c_2, ...c_n$ in some neighborhood given by

$$\varphi(c_1, c_2, ...c_n) = \sum_{i=1}^{n} \lambda_i c_i \mod m,$$

then the global transition F is surjective if the greatest common divisor of all the numbers λ_1, λ_2, ... λ_n, m, is 1.

4.1.7 Universal Computation in Life

An outline of a proof that the Game of Life was capable of universal computation was presented by John Conway in 1982 (in the book in *Winning Ways for your Mathematical Plays,* vol.2) and independently by William Gosper. The key here is to use a glider gun to emit gliders at regular intervals. This permits the transmission of information from one region to another and simulates the electrical pulses of a regular computer. As the Game of Life is a Class IV cellular automaton (whose Langton parameter is $\lambda = 0.273$ which lies in the phase transition region), it is not surprising that it could be capable of universal computation, in view of Wolfram's conjecture that all Class IV automata should have this capability.

As was mentioned in the Preliminaries, at the heart of any computer system is the construction of the 'logic gates' NOT, AND, OR. What Conway and Gosper demonstrated was that each of these logic gates could be constructed within the Game of Life, together with a form of infinite memory storage.

In order to construct the NOT gate we consider that P is either a 0 or 1 and a data source gun that emits a glider whenever P is 1 and nothing whenever P is 0. An emitter glider gun at E is positioned as in Figure 4.22 and is synchronized to fire gliders simultaneously. Whenever two gliders collide they will annihilate one another. Hence, P being 0 permits the unfettered passage of a glider from the gun E, thus turning a 0 into a 1, whereas if P is 1 it emits a glider that collides and annihilates the glider from the gun E resulting in a void that turns the 1 into a 0. The result at receptor R is *not* P.

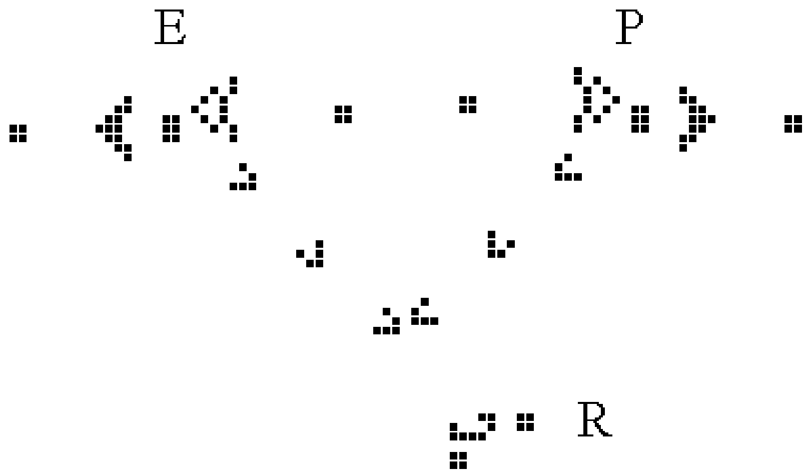

Figure 4.22: The implementation of the NOT gate in the Game of Life. If P is 0 the result at the receptor R is 1 and if P is 1 the receptor receives no input, or 0 since the colliding gliders annihilate one another.

We can construct the AND logic gate $P \wedge Q$ by adjoining a bit more structure to the NOT gave as indicated in Figure 4.23. According to the Truth Table the conjunction $P \wedge Q$ is to be the value 1 only when P is 1 and Q is 1. In all other cases, $P \wedge Q$ is to be 0. Taking P and Q both to have truth value 1 as in the figure, results in a glider emanating from the glider gun Q being annihilated by the glider emanating from the emitter E, whereas the glider from P passes unhindered to produce a 1 at the receptor R. However, if P is 1 and a glider emanates from P, and Q is 0 so that nothing emanates from Q, then the glider from P this time is annihilated by the one from E and the receptor R receives no data, hence is 0. On the other hand, if P is 0 and Q is 1, then the glider from Q is annihilated by the glider from E so that again R becomes 0. Finally, if both P and Q are 0 then the glider from the emitter E is eaten by the glider eater and R is once again 0.

The OR gate incorporates a portion of the AND gate as depicted in Figure 4.24 but now we are provided with two emitter glider guns, both designated E. Note that $P \vee Q$ has truth value 1 if P or Q is 1 (or both) and is 0 in all other cases. Suppose firstly that P is 0 and Q is 1 as in the figure. Then the gliders from Q are annihilated by the emitter on the right, but the emitter on the left produces a signal at the receptor R. Similarly, if P is 1 and Q is 0, P's gliders are annihilated this time, but the receptor R still receives an input. If both P and Q are on, then again R receives a signal. Only when both P and Q are off do the gliders from each emitter

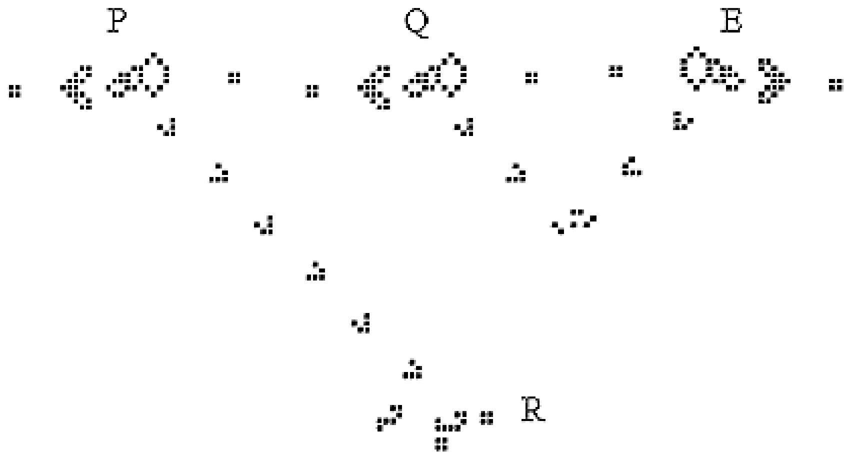

Figure 4.23: The AND gate in the Game of Life. Only when both P and Q are on does the receptor R receive any data. If only P or Q is on (i.e. emitting gliders), then the gliders from E annihilate them and the receptor R receives nothing. Note the glider-eater at the bottom left which mops up gliders emitted by E when both P and Q are off.

annihilate each other and there is no signal at the receptor.

Memory storage for the universal computer is accomplished by simulating a Minsky register by sliding a Life block utilizing a salvo of gliders to either push it or pull it along a diagonal. In the Conway model, the block (whose location gives its numerical value which can be arbitrarily large) could be pulled 3 units along a diagonal by a 2-glider salvo, whereas a 30-glider salvo was required to push the block 3 units along the diagonal. A test for zero was also implemented. This 'sliding block memory' was later improved by Dean Hickerson in a much more practical construction that allowed a block to be pulled just one unit by a 2-glider salvo and pushed one unit by a 3-glider salvo. This latter became the basis for the construction of a universal register machine implemented in Life by Paul Chapman (http://www.igblan.com/ca/) in November 2002. This machine is capable of universal computation with communication between the various components carried out by lightweight spaceships. Therefore the Game of Life has all the computational ability of any modern electronic computer.

In this context it should also be mentioned that Paul Rendell in 2000 constructed a Turing machine, however, with a finite tape which could in principle be extended to a universal Turing machine and thus capable of universal computation.

In the spirit of von Neumann, Conway in *Winning Ways* demonstrated that there are configurations in Life capable of self-replication.

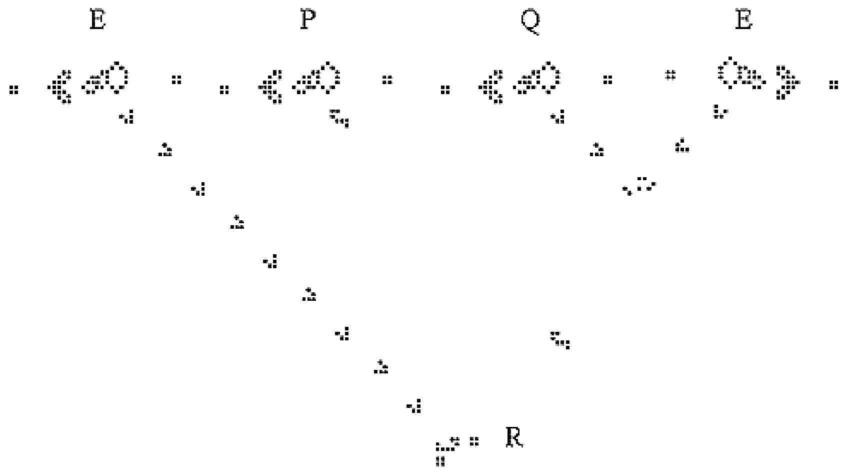

Figure 4.24: The OR gate in the Game of Life. If both P and Q are off then the gliders from each emitter E annihilate each other and there is no signal at the receptor R. In the other cases when either P or Q are on or both are on, a signal is received by the receptor R from the emitter on the left.

There are many websites devoted to the Game of Life. Actually seeing the mélange of Lifeforms develop and evolve is a wonderful experience to behold. One of the best implementations is *Life 32* by John Bontes which can be downloaded at: http://psoup.math.wisc.edu/Life32.html. An excellent resource website is Paul Callahan's:

http://www.radicaleye.com/lifepage/lifepage.html#glossback.

4.2 Other Automata

There is actually a myriad of two-dimensional cellular automata that have been created over the past thirty years. One of the classical models is called *Brian's Brain* and is due to Brian Silverman. The automaton has three cell states denoted as 'ready'(0), 'firing'(1), and 'refractory'(2) respectively. The rules bear some resemblance with how neurons in the brain behave (a more sophisticated model of neural activity will be presented in Chapter 5):

• A cell fires only if it is in the 'ready'(0) state and exactly two of its (eight) neighbors are 'firing'(1);

• Upon firing, a cell changes to the 'refractory' state (2) for one time step and then reverts to the 'ready' state (0).

As in the Game of Life, there are various Brainforms such as 'haulers', 'butterflies' and 'twizzlers'. The butterflies are the analogue to the gliders

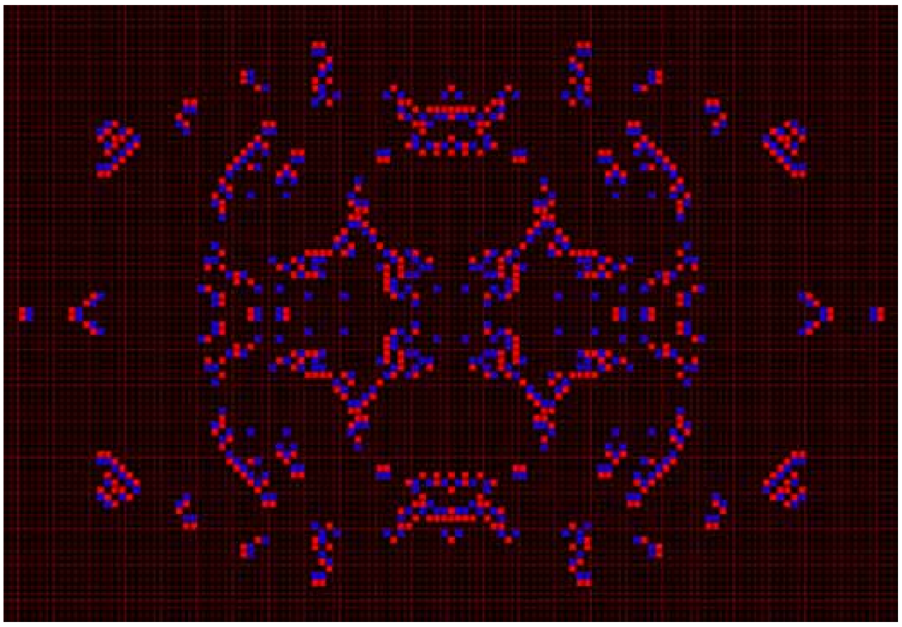

Figure 4.25: The three state cellular automaton Brian's Brain created by Brian Silverman. Waves of live cells tend to sweep across the array. Here the colors are: black = ready, red = firing, blue = refractory.

in Life and move diagonally at the rate of one cell every four time steps. A 'butterfly gun' has been implemented by Rudy Rucker in his CelLab environment.

Another ingenious creation by Silverman is called *Wireworld* and allows for the creation of sophisticated electronic circuits. This automaton has four states: 'background'(0), 'electron head'(1), 'electron tail'(2), and 'wire'(3) and the following set of rules for each time step:

- 'Background' cells never change their state;
- 'Electron head'(1) cells change their state to 'electron tail'(2);
- 'Electron tail'(2) cells change their state to 'wire'(3);
- 'Wire'(3) cells change their state to 'electron head'(1) if one or two of its eight neighbors are 'electron heads'(1).

An adjacent pair of an 'electron tail' (T) and 'electron head' (H) comprise an 'electron' which can be sent along a strand of 'wire' (W) cells in accordance with the preceding rules (THWWW...$\longrightarrow$WTHWW...). With this set-up it is possible to build AND, OR, and NOT gates, memory storage and hence a computer. An AND gate is depicted in Figure 4.26.

A simple adder has been constructed by student Peter Lane that computes the sum in base 2 of two inputs as in Figure 4.27.

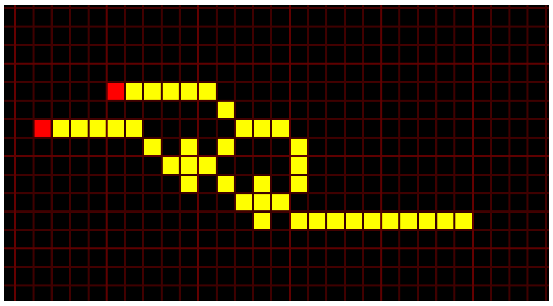

Figure 4.26: The arrangement of the AND gate in *Wireworld*. Two electron head cells are the inputs at the left along paths of wire cells. Only when there are two electrons entering this configuration will the output be an electron. Other cases result in no output.

Here the two inputs are given on the left and fed into the circuit so that the following binary output is computed:

input A	input B	top output (2^1)	bottom ouput (2^0)
0	0	0	0
0	1	0	1
1	0	0	1
1	1	1	0

A binary adder has also been demonstrated in the Game of Life by D.J. Buckingham [1978].

Another interesting two-state, two-dimensional cellular automaton is called Vote (also called Majority) created by Gérard Vichniac and is a totalistic rule given by the rule table:

sum	9	8	7	6	5	4	3	2	1	0
$c(t+1)$	1	1	1	1	1	0	0	0	0	0

.

where $c(t+1)$ is the value taken by the central cell of the 9-cell Moore neighborhood at the next time step. Here one can easily see where the automaton gets its name. If 5 or more of the cells (i.e. a majority) are '1', then the central cell's state also takes the value '1' at the next time step. But if less than 5 cells (i.e. a minority) take the value '1', then the central cell becomes '0'. The time evolution from a random initial state depends critically on the initial concentration of 1's and 0's and yields large shifting regions made up respectively of the two states and dominance at the initial stage leads to even greater dominance at the equilibrium stage (Figure 4.28). The totalistic code number is 992 which is 1111100000 in

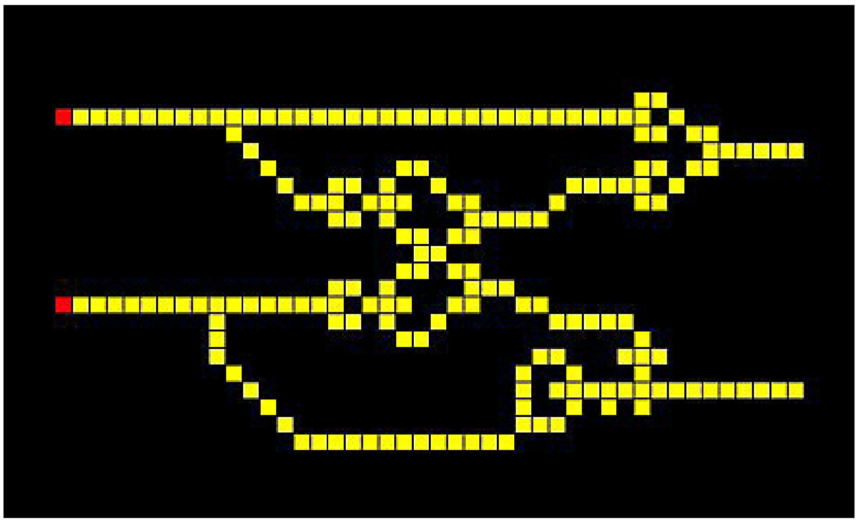

Figure 4.27: A simple adder in *Wireworld* that computes the sum of two inputs in base 2 with the result outputed at the bottom.

base 2. Von Neumann neighborhoods can also be considered so that $c(t+1)$ becomes 1 whenever the neighborhood sum is 3 or more. These automata are related to models of percolation and pattern formation on animal coats.

There is another more scientific way to depict the Vote rule by using the so-called *Heaviside step-function* H, also referred to as a *threshold* function.. This is defined as follows:

$$H(x) = \begin{cases} 1 \text{ if } x \geq 0 \\ 0 \text{ if } x < 0 \end{cases} .$$

Thus you obtain an output of 1 if the quantity x, whatever it happens to be, is nonnegative, and otherwise the output is 0. If we denote the nine cells of the Moore neighborhood (with a slight abuse of our usual notation) by $c_1(t)$, $c_2(t)$, ... $c_9(t)$, then according to the Vote rule, the value of the central cell at the next time step is given by:

$$H\left(\sum_{i=1}^{9} c_i(t) - 5\right),$$

whereby if five or more of the cells have state value '1', then the function H returns the value '1', otherwise it is '0'. The value of 5 is just a threshold value that turns 'on' the central cell at the next time step once the threshold is reached. This notion is an underlying feature of various cellular automata models in biology (see Section 5.4).

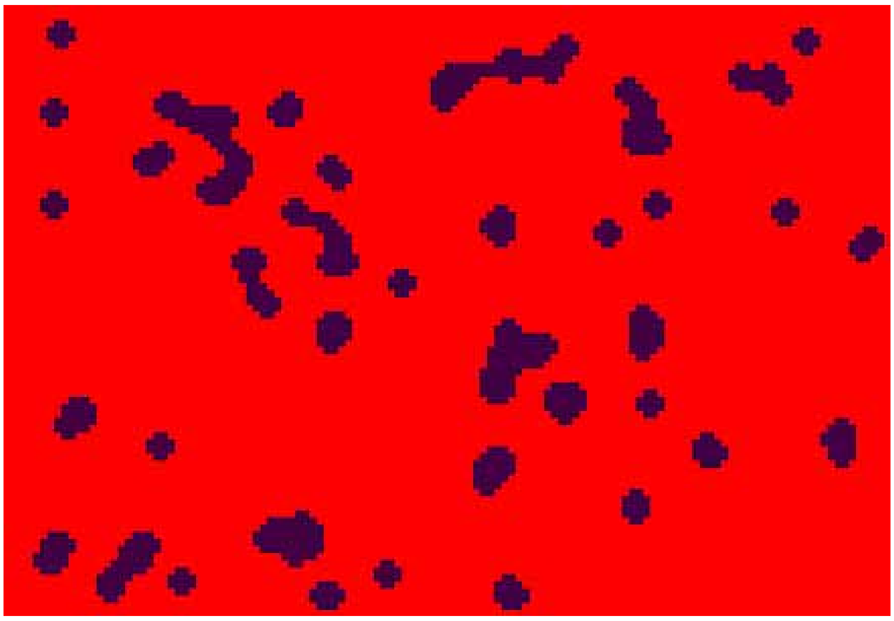

Figure 4.28: The cellular automaton Vote which decides the value of the central cell of a Moore neighborhood by what a majority of the values of its neighbors are. The initial configuration had 60% red (zero state) cells and the above is the equilibrium state.

Another variant of Vote due to Vishniac reverses the states of the sum 4 and 5 values.

sum	9	8	7	6	5	4	3	2	1	0
$c(t+1)$	1	1	1	1	0	1	0	0	0	0

This has the effect of permitting interchange at the boundary between regions of opposing colors where the majority is not very strong for either. This CA has served as a model of annealing.

4.2.1 Partitioning Cellular Automata

A new type of neighborhood was devised by Margolus that is fundamentally different from either the von Neumann or Moore neighborhoods. It consists of a partitioning of the usual lattice into blocks of cells, which is 2x2 in size in the simplest case and which we only consider here. The transition rule, or rather *block rule*, updates the entire block as a distinct entity rather than any individual cell as in the usual cellular automaton. Another unique feature is that two overlapping partitionings into 2x2 are employed, one say

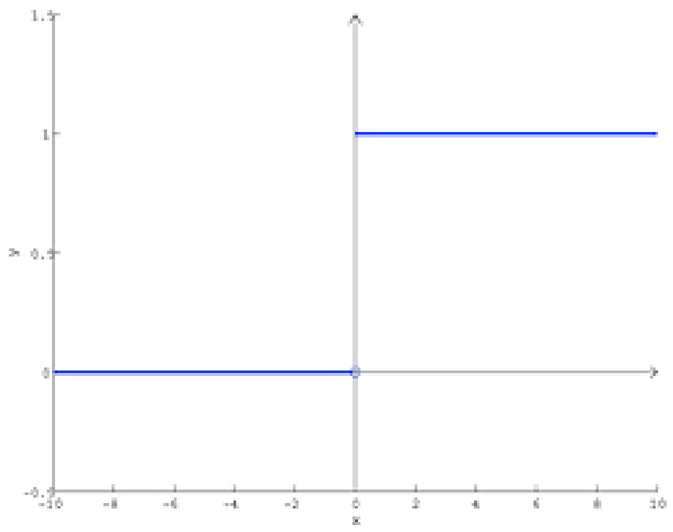

Figure 4.29: The Heaviside step function which only has an output when a nonnegative threshold has been reached.

given by dark lines, and one by light lines as in Figure 4.30 below. At each time step, one switches from one type of neighborhood to the other.

The block rule is applied to all 2x2 blocks alternating between utilizing the dark neighborhoods and light neighborhoods. At first glance this system appears to be very unlike an ordinary cellular automaton, but with more states and neighbors, it can indeed be expressed as an ordinary cellular automaton. The Margolus neighborhood comes into its own in the section on lattice gas automata in Chapter 5..

4.3 Replication

It is possible to demonstrate a trivial form of self-replication in a two-dimensional cellular automaton model of Edward Fredkin. In our first example, known as the 'parity rule', given a 4-cell von Neumann neighborhood:

• a central cell state becomes 1 (alive/black) if it had an odd number of black (0) neighbors at the previous time step;

• a central cell becomes 0 (dead/white) if it had an even number of black (0) neighbors at the previous time step.

This is also the transition function of the one-dimensional Rule 90 and is outer totalistic in that we are only considering the sum of the four cell states other than the central one. The effect is a quadrupling of any initial cell pattern (Figure 4.31, top left) each 2^n generations, with n depending on the original configuration.

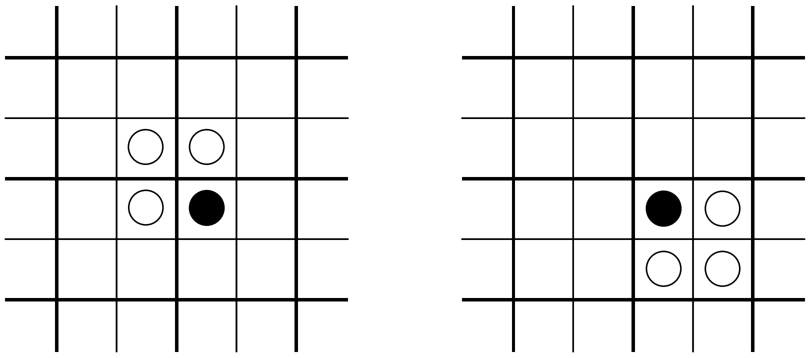

Figure 4.30: A Margolus neighborhood consists of two distinct overlapping 2x2 blocks of cells and a particular cell has successively two overlapping neighborhoods. The neighbors of a black cell (indicated by the black dot) in a 'light' neighborhood are indicated at the left, and the neighbors of a 'dark' neighborhood are as on the right.

Here the outer totalistic rule we have used is given by the transition table:

sum	4	3	2	1	0
$c(t+1)$	0	1	0	1	0

.

where $c(t + 1)$ is the value of the central cell and the initial pattern has replicated after $32 = 2^5$ time steps (as do all the others below). However, if we take into account the state of the inner cell as well as the 4-cell von Neumann neighborhood, we have the totalistic rule:

sum	5	4	3	2	1	0
$c(t+1)$	1	0	1	0	1	0

with a 5-fold replication of the initial pattern (Figure 4.31, top right).

We can also consider the analogous replication with respect to an 8-cell Moore neighborhood and here we implement the Fredkin (outer totalistic) rule given by the transition table:

sum	8	7	6	5	4	3	2	1	0
$c(t+1)$	0	1	0	1	0	1	0	1	0

that results in an 8-fold replication (Figure 4.31, bottom left).

And lastly, we have a 9-cell Moore neighborhood counterpart with the totalistic rule:

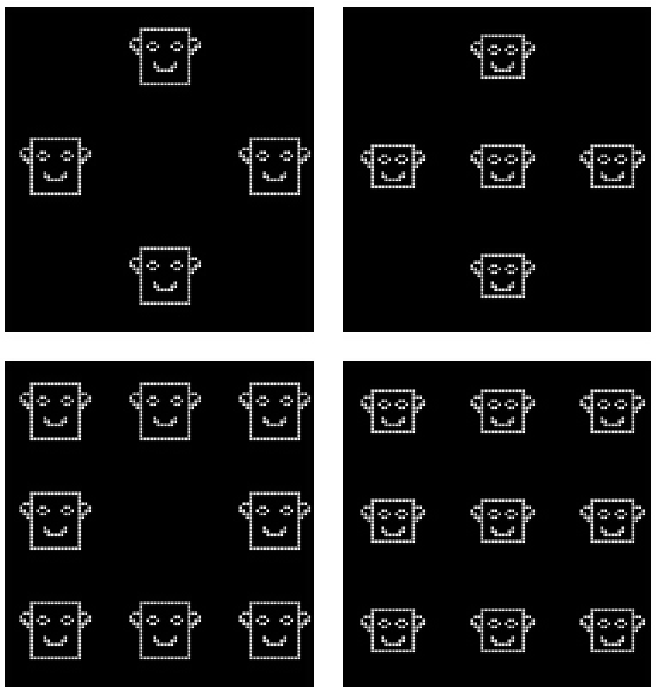

Figure 4.31:

sum	9	8	7	6	5	4	3	2	1	0
$c(t+1)$	1	0	1	0	1	0	1	0	1	0

.

which replicates a two-dimensional configuration 9-fold (Figure 4.31, bottom right). This so-called 'parity rule' can be designated Code 692 which is the value in base 2 of the binary digits.

It must be noted however, that none of the foregoing examples represents the same sort of replication in the von Neumann sense we saw in the Introduction as it is purely a consequence of the transition function and not accomplished by the automaton itself.

Edward F. Moore, whom we encountered previously regarding Garden of Eden configurations also made an interesting observation concerning the rate at which a configuration can replicate. Here again, as in the discussion of Moore's Garden of Eden theorem, we are only considering finite configurations. Again, we also require the further condition that if a cell is in a quiescent state and all its neighbors upon which the transition function acts are in the same state, then the cell remains in the quiescent state at the next time step. If we denote a finite configuration by c and the number of copies of c at any time step t by $\#c$, Moore showed that

$$\#c \leq kt^2,$$

where k is some positive constant. One consequence of this is that a self-reproducing configuration cannot keep doubling with each time step, since the values of t^2 are $1, 4, 9, 16, 25, 36, 49...$ and doubling yields $\#c$ values of $2, 4, 8, 16, 32, 64, 128, ...$

To see how Moore established this result, suppose that the smallest *square* array that contains the initial configuration c has s cells on a side, and hence an area of s^2. At the next time step, $t = 1$, the square array can only grow (via the action of the transition function) by one cell on each of its four sides, so that the square array now has area $(s+2)^2$. At time step $t = 2$, the square array will have an area equal to $(s+4)^2$, and in general, the array will have area $(s + 2t)^2$ at each time step t. This value also represents the maximum number of alive (non-quiescent) cells at each time step t. Letting a denote the number of alive cells of the configuration c, then the number of copies of c at each time step is at most

$$\frac{(s + 2t)^2}{a}.$$

By expanding and simplifying this expression, we arrive at Moore's inequality above.

4.4 Asynchronous Updating

In general, it has been found that the asynchronous cellular automata evolve much differently from their synchronous counterparts. For example, cyclic dynamics can only occur with synchronous updating although the set of stable attractors of a CA are the same for both update regimes (Schönfisch & de Roos [1999]). Indeed, any configuration that is stable under one updating regime is stable under any other since it is of no consequence in what order the cells are updated. In addition, various patterns formed in synchronous updating are absent with asynchronous updating. For example, in the two-dimensional version of the Iterated Prisoner's Dilemma (see Section 5.3), Huberman & Glance [1993] found that the complex mosaics of defecting and cooperating cells attained with synchronous updating completely disappeared with asynchronous updating and the CA reached a fixed state of entirely defecting cells. Similarly, we have already mentioned that the Game of Life also converges to a stable state with asynchronous updating.

So, the question arises as to which updating regime is the most appropriate for modelling physical phenomena. Some argue that asynchronous updating is more natural since there is no universal clock in Nature. The highly geometric patterns produced in synchronous updating dissolve away with asynchronous regimes and hence are really artifacts of the updating regime. However, weighing in on the side of synchrony we have M. Sipper [1995] who states that, "It may be argued that from a physical point of view synchrony is justified: since we model a continuous spatial and temporal world we must examine each spatial location at every time step, no matter how small we choose these (discrete) steps to be." However, as pointed out by Schönfisch & de Roos [1994], "... the difference between synchronous and asynchronous update is a question of how we look at the (real) process. If we observe only in large time intervals we will see that all cells have been updated (at least) once in one time step, implying synchrony. If we refine the time scale such that in every time interval at the most one event will happen, then we find asynchrony... In summary, it will depend on the actual cellular automata how strong the influence of different updating methods will be."

There are various methods to update cells asynchronously and these fall into two distinct categories, *step-driven* and *time-driven.* In step-driven updating, each cell of the array is updated by some algorithm one cell at a time. For example, in the simplest case, a fixed directional line-by-line sweep of each row can be made to update each of the cells sequentially. Or, the cells can be randomly ordered and each pass is made through this ordering or one can even take a different ordering for each pass. In time-driven updating, each cell has an internal clock that 'wakes up' the cell at some specific point in time so that its state can be updated. This waking up can also be done in a stochastic manner so that each cell will be updated with a certain probability, p.

In the sequel, we consider an example found in Roli & Zambonelli [2002] of the local rule:

- A dead (black) cell becomes alive (white) if it has 2 alive neighbors;
- A living cell remains alive if it has 1 or 2 neighbors alive, otherwise it dies..

These criteria are a watered-down version of the Game of Life but it has some star-studded dynamics of its own in the synchronous case (Figure 4.32).

However, starting with the same block of 4 black cells in the asynchronous case is much less dramatic and leads to a stationary state as in Figure 4.33.

Roli & Zambonelli considered a third type of updating regime in addition to synchronous and asynchronous that they termed *dissipative.* These CA (called dissipative cellular automata – DCA) have asynchronous time-driven updating, but also allow an external perturbation to change the state of any of the cells of the array concurrently with the transition function. This can be thought of in terms of the environment interacting with the automaton by providing 'energy'. The notion of a DCA was inspired by the dissipative

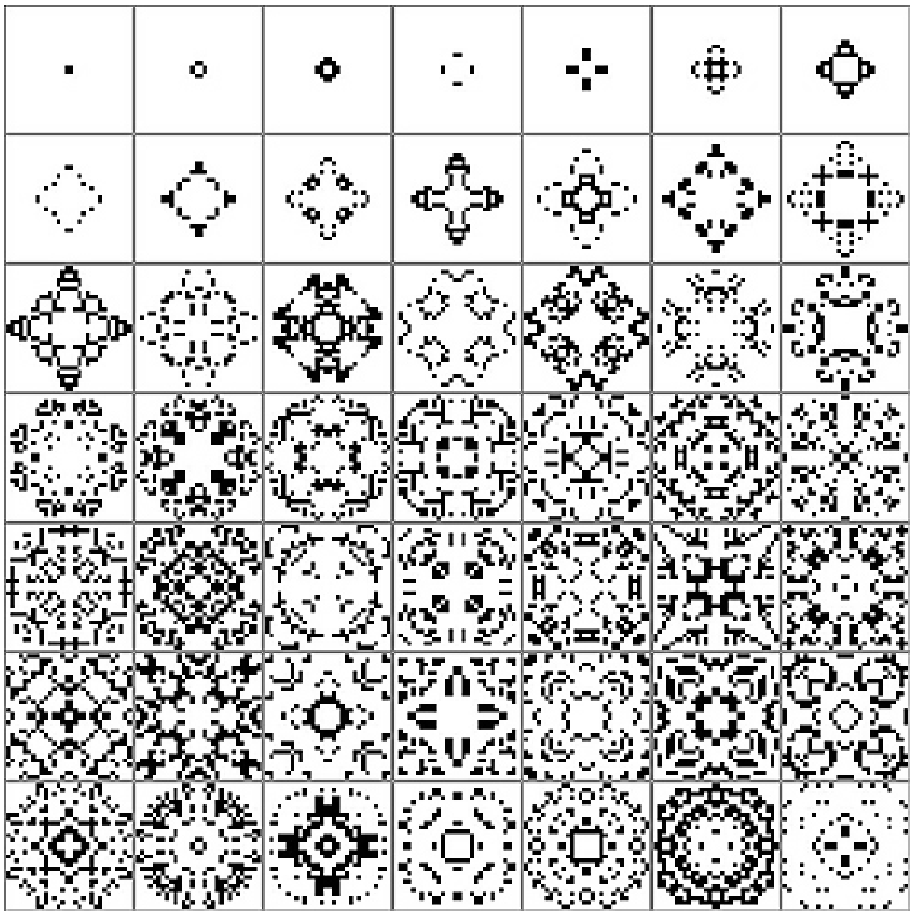

Figure 4.32: Starting with four black cells and the CA in the text under synchronous updating. These are the first 49 configurations with many similar that follow.

systems much studied by Ilya Prigogine and his school (cf. eg. Nicolis & Prigogine [1989]).

One way to achieve interaction with the environment is for the perturbation to take the form of forcing cells at random to become alive with a certain probability, p_d. The degree of perturbation must be sufficiently high to affect the dynamics of the CA, but not too high so as to make the behavior essentially random. The ratio p_d/p_c is the crucial factor here and although stationary configurations are not reached, nevertheless large-scale patterns do persist.

Because of the open nature of DCA to their environment, the authors assert that, “the dynamic behavior of DCA is likely to provide useful insight into the behavior of real-world open agent systems.”

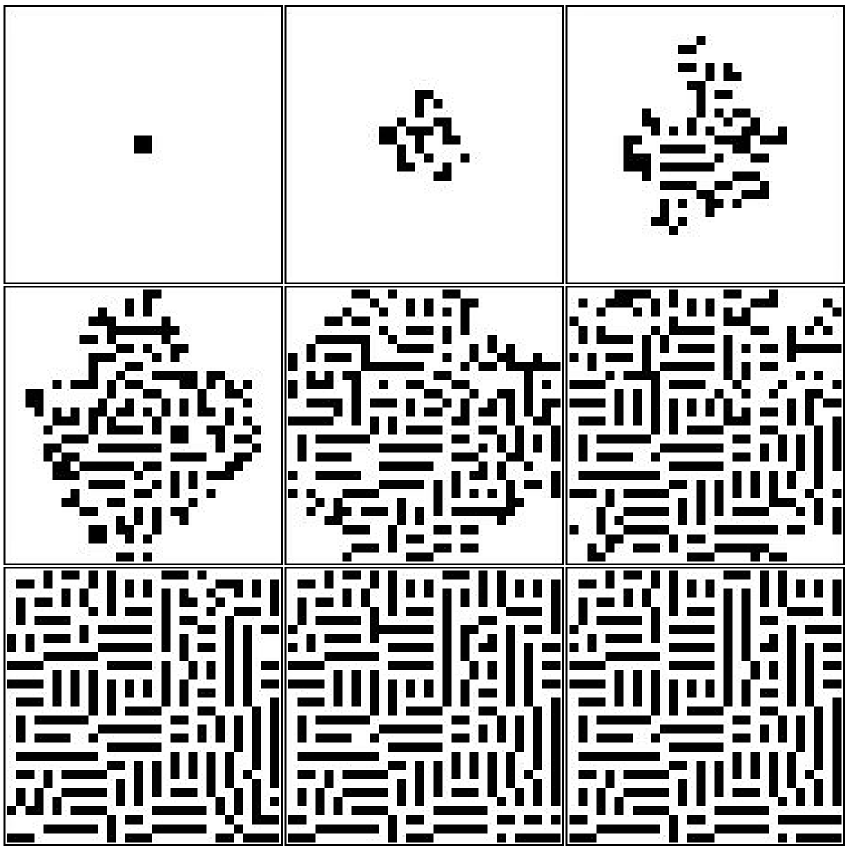

Figure 4.33: What a difference a delay makes! The asynchronous updating of the same CA with each cell being updated or not with a probability of $p_c = 0.5$. The configurations are a sampling every 10 steps and the final configuration is stable.

A certain class of CA was shown by Goles and Martinez [1990] to have both stationary and cyclic states with synchronous updating but only stationary states were attainable with asynchronous updating.

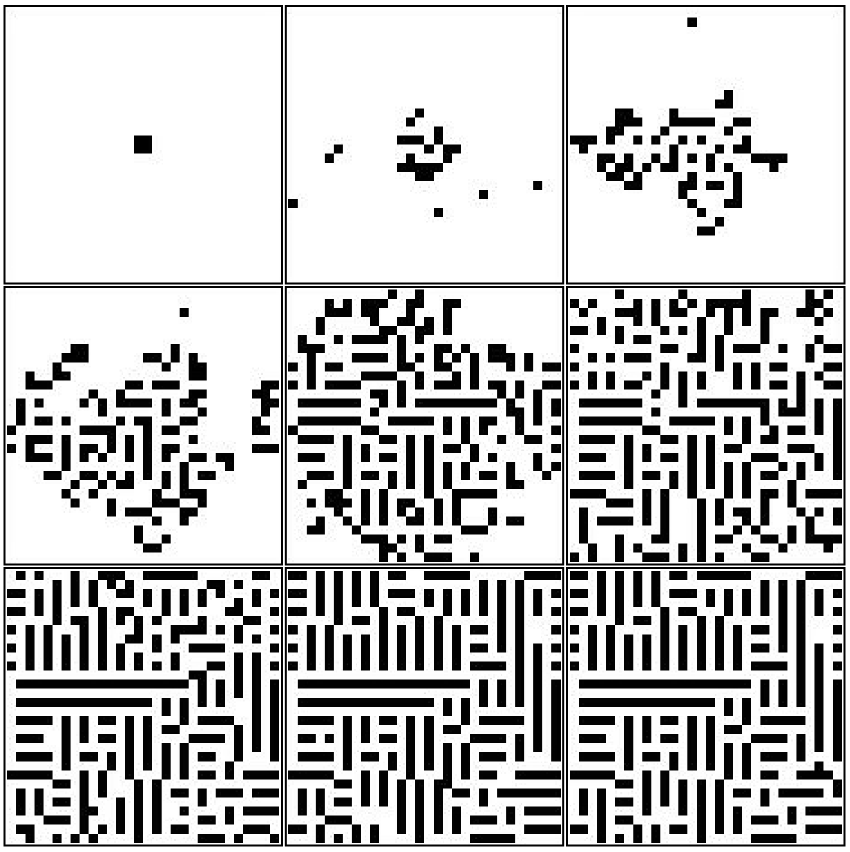

Figure 4.34: The evolution of the dissipative CA whereby each cell has a probability of $p_d = 0.001$ to be perturbed to be alive. Large scale patterns evolve that are seen to persist but are not completely static. Interestingly, these patterns arise even without any black cells in the initial conditions due to the perturbations.

Chapter 5

Applications

The scientist does not study nature because it is useful; he studies it because he delights in it, and he delights in it because it is beautiful. If nature were not beautiful, it would not be worth knowing, and if nature were not worth knowing, life would not be worth living. Of course I do not here speak of that beauty that strikes the senses, the beauty of qualities and appearances; not that I undervalue such beauty, far from it, but it has nothing to do with science; I mean that profounder beauty which comes from the harmonious order of the parts, and which a pure intelligence can grasp.

Henri Poincaré

... *It becomes plausible that many, perhaps all, of the processes upon which life is based are algorithmically describable and that, therefore, life itself is achievable by machines.*

Christopher Langton

Cellular automata have applications to many diverse branches of science, such as biology, chemistry, physics and astronomy. In the models that follow, we are able to accurately reproduce many physical phenomena when we attempt to emulate the underlying mechanisms in the setting of a cellular automaton. And this approach has some virtues. According to Ermentrout & Edelstein-Keshet [1993]: "CA models are fast and fairly easy to implement. Furthermore, the visual feedback they provide is striking and often resembles the pattens experimentally observed. These two aspects of CA modeling are its biggest advantages over more traditional approaches. CA are thus an excellent way of formalizing a theory of purported mechanism into computational terms. This is an important first step in the understanding of any physical process."

In ancient China, patterns appearing naturally were referred to as *li*, and were thought to represent an underlying order in the world. Some of the ones described in the sequel can be found in the charming little book by David Wade [2003]. One of the first attempts to mathematically recreate forms found in Nature using simple rules, was demonstrated by Alan Turing in a seminal work in 1952. Turing's inhomogeneous patterns were formed by the changing spatial concentrations of two chemical reactants in a solution and were described by a set of 'reaction-diffusion' equations. These equations in two-dimensions describe how the two reactants having concentrations u and v respectively change with time:

$$\begin{aligned}\frac{\partial u}{\partial t} &= f(u,v) + d\Delta u\\ \frac{\partial v}{\partial t} &= g(u,v) + d'\Delta v,\end{aligned}$$

where f and g are the reaction terms, and the diffusion terms are represented by the Laplacian operator $\Delta = \frac{\partial^2}{\partial x^2} + \frac{\partial^2}{\partial y^2}$ times (diffusion) constants d, d'. This sort of interplay lies at the heart of various CA models such as the first three models in the sequel.

5.1 Excitable Media

This term refers to a group of models that are characterized by a transition of a cell's state following a basic pattern: a quiescent state transits to an excited state, then to a refractory state before returning again to the quiescent state from which the cell can become excited again, and so forth. These models all tend to exhibit waves of various forms.

5.1.1 Neural Activity

Our first example is a cellular automaton model for generating waves, say to heuristically model a network of neuron excitation and recovery, and is due to Greenberg and Hastings [1978]. We have already seen a special case of this model in Silverman's Brian's Brain. Either the von Neumann or Moore neighborhood (as in Brian's Brain) is considered. Each cell (or neuron) in a rectangular lattice has a 'quiescent' state'$= 0$, 'excited states' $= 1, 2, ...e$ and 'refractory states' $= e+1$, $e+2$, ..., $e+r$. Note that in Brian's Brain, there was one excited (= 'firing') state and one refractory state. The G-H rules are as follows:

• a cell in state k, for $1 \leq k \leq e+r-1$, at the next time step becomes state $k+1$;

• a cell in the last refractory state $e+r$ at the next time step becomes state 0;

• a cell in the quiescent state 0:

– at the next time step becomes the excited state 1 if one or more of its neighbors is in an excited state;

– if none of its neighbors is in an excited state, then at the next time step its state remains 0.

Interpreting the quiescent state as ‘susceptible’, the excited states as ‘infectious’ and the refractory states as ‘immune’, Birgitt Schönfisch [1995] has developed a similar epidemiological model whereby a susceptible individual becomes infectious with a certain probability that depends on how many neighbors are infectious, rather than simply if one or more neighbors is infectious. Deterministic examples are presented in Figures 5.1 and 5.2.

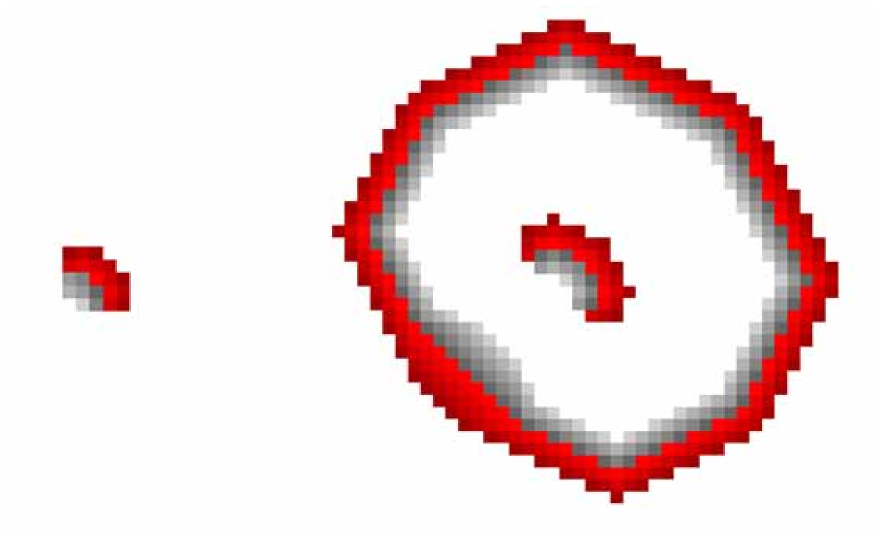

Figure 5.1: In this Greenberg-Hasting model using the von Neumann neighborhood, there are 5 excited stages (red) and 5 refractory stages (gray) with the transition at each stage from darkest to lightest. White is the rested state. At least 3 excited neighbors are required for a cell in the rested state to become excited. The figure shows the initial configuration (left) and after 36 iterations (right). Waves are generated in the center of the figure and grow and move outwards. Courtesy Birgitt Schönfisch, University of Tübingen.

The first two conditions of the Greenberg-Hastings model can be considered as the ‘reaction’ phase and the third condition is the ‘diffusion’ phase. Simplified versions can have one excitatory state and/or one refractory state. In the simplest version we have: ‘quiescent’ = 0, ‘firing’ = 1, ‘refractory’ = 2, so that we can formulate the Greenberg-Hastings reaction(**R**)-diffusion (**D**) process as:

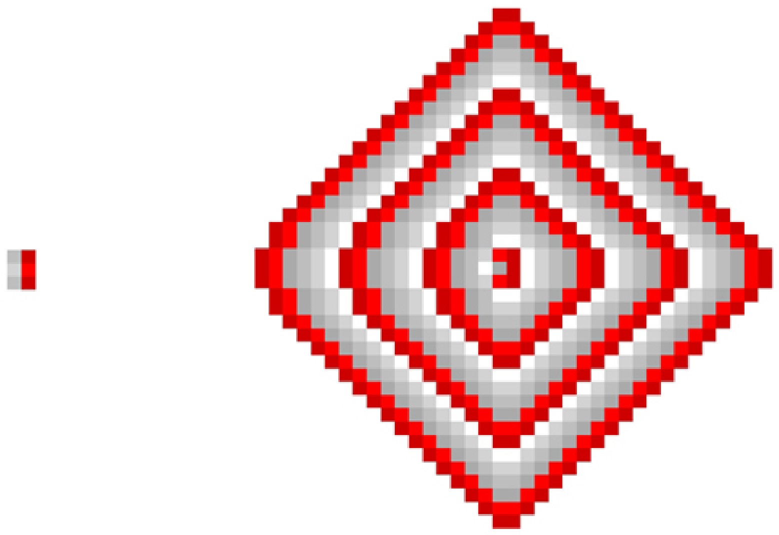

Figure 5.2: In this Greenberg-Hasting model using the von Neumann neighborhood, there are 2 excited stages (red) and 3 refractory stages (gray). As above the transition at each stage is from darkest to lightest. White is the rested state. At least 2 excited neighbors are required for a cell in the rested state to become excited. The figure shows the initial configuration (left) and after 19 iterations (right). Waves are generated in the center of the figure and grow and move outwards. Courtesy Birgitt Schönfisch, University of Tübingen.

$$c_{i,j}(t+1) = \mathbf{R}[c_{i,j}(t)] + \mathbf{D}[c_{i-1,j}(t), c_{i+1,j}(t), c_{i,j-1}(t), c_{i,j+1}(t)],$$

where

$$\mathbf{R} = \begin{cases} 2 & \text{if } c_{i,j}(t) = 1 \\ 0 & \text{otherwise} \end{cases} \qquad \mathbf{D} = \begin{cases} k & \text{if } c_{i,j}(t) = 0 \\ 0 & \text{otherwise} \end{cases}$$

and $k = 1$ if at least one of the von Neumann neighbors is firing and $k = 0$ otherwise.

As one would expect, varying the parameters leads to different wave forms propagating outwards (Figure 5.2).

A interesting reversible G-H model can constructed by using Fredkin's idea of subtracting the state of the central cell at the previous time step (Tamayo & Hartman [1989]):

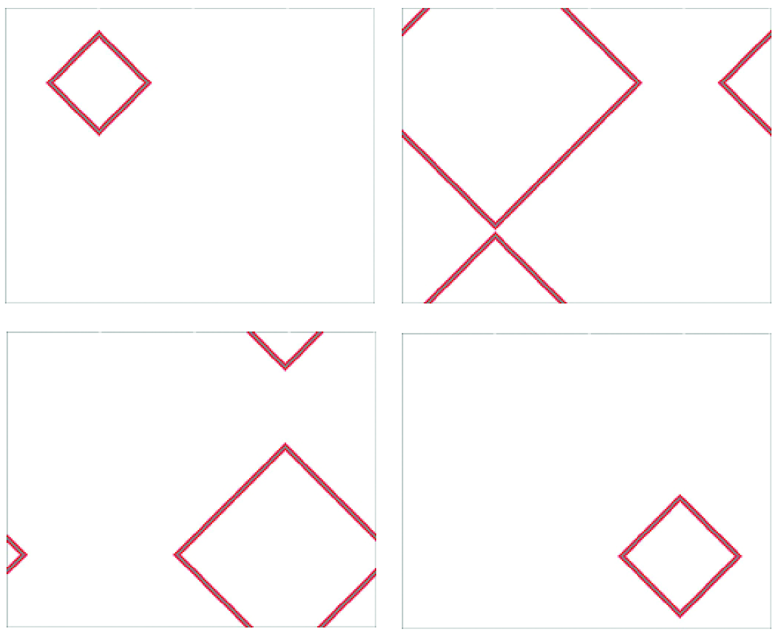

Figure 5.3: This is the regular regime at time steps 20, 80, 120, 150 (l to r respectively). The initial conditions are: cell (50,40) is firing and all others are quiescent. The array is 160 x 160 with periodic boundary conditions.

$$c_{i,j}(t+1) = \mathbf{R}[c_{i,j}(t)] + \mathbf{D}[c_{i-1,j}(t), c_{i+1,j}(t), c_{i,j-1}(t), c_{i,j+1}(t)] - c_{i,j}(t-1),$$

where the sum is taken mod 3 and the reaction-diffusion parts are the same as in the preceding. Here the initial conditions are quite significant as they are preserved in the subsequent dynamics. The authors have identified three basic regimes that the system eventually falls into:

Regular regime (Figure 5.3). Here regular wavefronts move about in an unperturbed environment.

Random regime (Figure 5.4). Regularity gradually breaks down and gives way to randomness lacking any structure.

Turbulent regime (Figure 5.5). Ring-like structures emerge and form around source and sink regions that gradually become diffused.

5.1.2 Cyclic Space

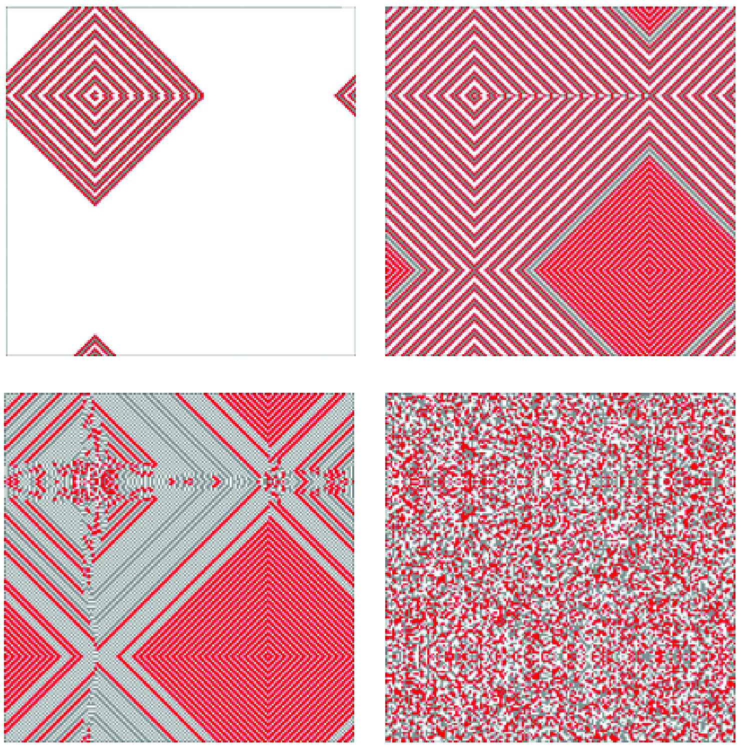

Figure 5.4: This is the random regime at time steps 50, 500, 1400, 2000 (l to r respectively). The initial conditions are: cell (40,40) is firing, (41,40) is refractory, and all others are quiescent.

Another interesting wave generating model similar to the preceding one was created by David Griffeath of the University of Wisconsin and dubbed the Cyclic Space cellular automaton by A.K. Dewdney in his *Scientific American* column of August 1989. Again we employ a rectangular grid with each cell taking state values $0, 1, 2, \ldots$ up to a maximum value of m and we can use either the 4-cell von Neumann or the 8-cell Moore neighborhood. The array is then initialized with all cells taking on a random value from 0 to m. The rules for the automaton are:

• if a cell in state k, for $0 \leq k < m$, has any neighbor with state value $k + 1$, then at the next time step the cell takes on the value $k + 1$;

• if a cell has the maximum state value m and if any neighbor has the state value 0, then the cell at the next time step takes on the value 0;

• the cell state remains unchanged if there are no neighboring cells meeting the required conditions.

Note the similarities with the Greenberg-Hastings model. The second

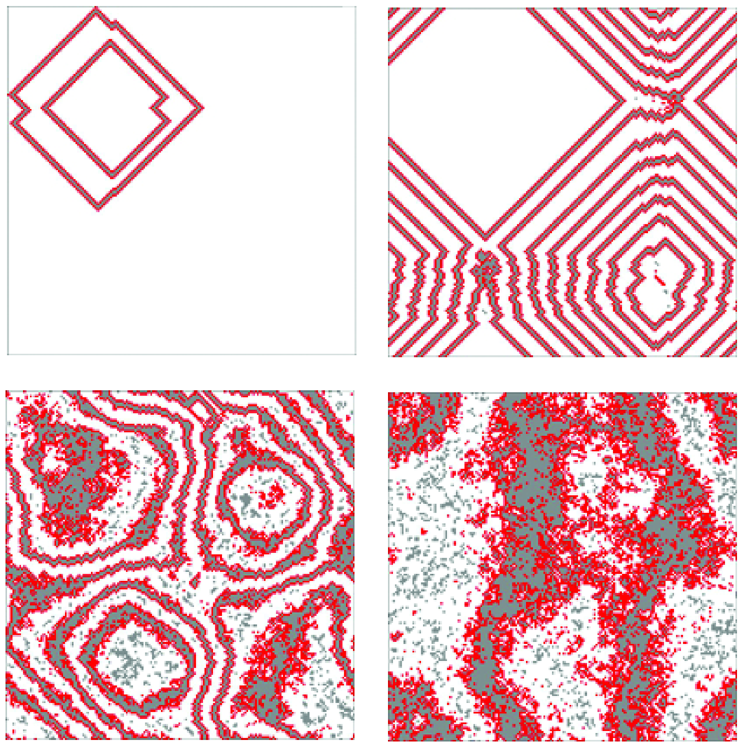

Figure 5.5: This is the turbulent regime at time steps 40, 700, 1400, 2000 (l to r respectively). The initial conditions are: cells (40,40), (49,46), (41,53) are firing, and all others are quiescent. Wavefronts first interact (top right) and then form around source and sink regions (bottom left) that finally become diffused.

condition here is like the neuron cell state changing from the rested to excited state. However, a point of difference is that in the neuron model a cell (in the excited and refractory states) updates its state value independent of the state of its neighbors, whereas in the cyclic space model the update depends on at least one neighbor being in the next higher state. We can also think of a cell in state k having a neighbor in state $k + 1$ as being 'eaten' by the latter.

According to Griffeath, there are four phases that the automaton goes through: debris, droplet, defect, and demon that are illustrated in the Figure 5.6. Starting from an initially random configuration, which soon looks like debris, we find that droplets of solid color begin to emerge and grow by eating neighbors. Then certain non-intersecting loops of cells can form 'defects' that initiate the next phase of spiral formation. A defect occurs when each of the cell states of the loop differs by $+1, -1$, or 0 from the next cell in

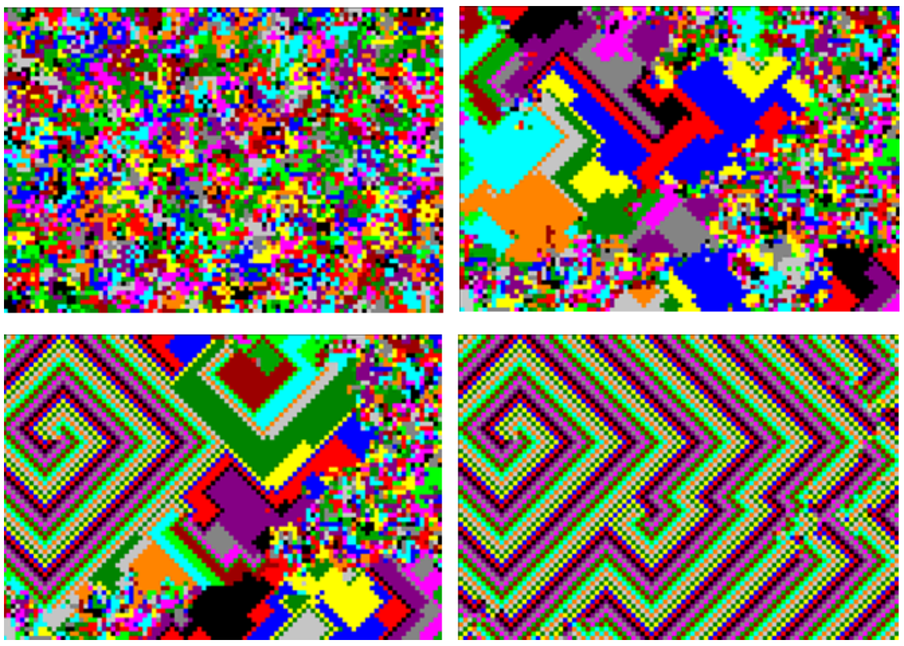

Figure 5.6: The time evolution from a random initial state to the formation of waves of the cyclic space automaton. The frames (left to right) represent the debris, droplet, defect and demon phases respectively.

the loop (bearing in mind that highest and lowest states differ by 1) and furthermore when all of these flux changes are added consecutively, the sum is nonzero. The newly formed spirals grow larger with some being absorbed by others leading to the final stage of demons that are spiral configurations that continue to cycle in their own confined region and occupy the entire space (Figure 5.6).

The first three phases are what are called 'metastable' in so far as they persist for many generations. The reason for this persistence is because it is not very likely that a cell will change its state value. In fact, using a von Neumann neighborhood and n state values, the probability p that the central cell will change its value is given by 1 minus the probability that none of its four neighbors is one integer value higher, i.e.

$$p = 1 - \left(\frac{n-1}{n}\right)^4,$$

since the probability that a single neighbor is not one integer value higher is $(n-1)/n$. For $n = 14$, we find that $p = 0.256$, or about one chance in four. And this is the case when all the neighbors can have random values. If all the neighbors have the same value as the central cell, then of course the cell remains constant until the situation in the neighborhood changes. The preceding formula also says that the higher the number of states, the longer the phases persist.

5.1.3 The Hodgepodge Machine

Certain types of complex chemical reactions oscillate displaying features of waves and spirals. One such reaction is the combination of carbon monoxide (CO) with oxygen to form carbon dioxide (CO_2) catalyzed by tiny palladium crystallites. Because of the multitude of the latter a cellular automata model was suggested by Martin Gerhardt and Heike Schuster [1989] of the University of Bielefeld, whereby each cell represents a catalytic unit.

For each cell, there are $n+1$ states given by $0, 1, 2, ...n$. According to Gerhardt and Schuster, a cell in state 0 is 'healthy', a cell in state n is 'ill', and all states in between $1, 2, ...n-1$ are 'infected'. Infection represents the level of oxygen saturation of each catalytic unit and increases until a maximum saturation level is reached (ill). There are three rules governing the transition to the next state that reflect the chemistry of the reaction:

• If $c(t) = 0$, (cell is *healthy* – no oxygen), then it will become infected if a suitable number of neighboring cells are infected:

$$c(t+1) = \left[\frac{N_{ftd}}{k_1} + \frac{N_{ill}}{k_2}\right],$$

where N_{ftd} is the number of infected cells in a neighborhood (either von Neumann 5-cell or Moore 9-cell), N_{ill} is the number of ill cells in a similar neighborhood, and k_1, k_2 are constants representing minimal levels for the cell to become infected. That is to say, if the expression in the brackets is less than 1 because N_{ftd} and N_{ill} are not sufficiently large enough, then $c(t+1)$ remains 0 and thus healthy. Here the square brackets means to round down to the nearest integer.

• If $1 < c(t) < n$, (cell is *infected*), then the degree of infection increases at the next time step to:

$$c(t+1) = g + \left[\frac{\Sigma}{N_{ftd}}\right],$$

where g is a (constant positive integer) 'infection rate' and Σ is the sum of the infected state values of the cell neighborhood. If the value computed on the right-hand side of the expression exceeds n, then the value for $c(t+1)$ is taken to be just n. Here we see that the infection state of a cell increases by the fixed amount g plus a local average of infection.

• Finally, if $c(t) = n$, (cell is *ill*), then $c(t+1) = 0$, i.e. ill cells become healthy due to a phase transition of the catalytic units.

To run the colorfully named hodgepodge machine, one must first specify the number of cell states n, the constants k_1, k_2, and the infection rate g. A typical example has values $n = 100$, $k_1 = 2$, $k_2 = 3$, and $g = 20$. One starts with a random initial configuration and after awhile the system has the appearance of Figure 5.7.

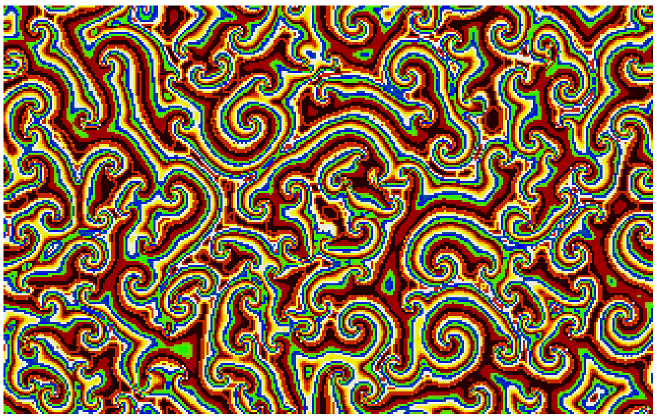

Figure 5.7: The spiral waves generated by the hodgepodge machine cellular automaton.

This pattern appears to emulate the actual wave pattern depicted in the well-known Belousov-Zhabotinskii reaction: the oxidation of malonic acid by potassium bromate with iron or cerium as a catalyst (Figure 5.8). (See also the subsequent works of Gerhardt, Schuster & Tyson [1990 a,b,c]). The chemical waves of this reaction are normally described in terms of partial differential equations in the form of reaction-diffusion equations – one popular model is known as the 'Oregonator' whose name betrays its origins. Another application is to the chemical waves and spiral patterns seen in the slime mold formation (Chapter 5).

Various investigators have developed other excitable cellular automata models that have for example, multiple-armed spirals (Madore & Freeman [1983]) or 3-dimensional twisted scrolls (Winfree *et al.*, [1985]).

5.2 Schelling Segregation Model

Since human interactions can and often do function on a local level, cellular automata have also found various applications in the social sciences. The earliest known work seems to have been James Sakoda's 'The checkerboard model of social interaction' [1971], although the model had its origins in Sakoda's unpublished 1949 dissertation which takes us back to the very origins of the Ulam/von Neumann cellular automata theory itself. A now

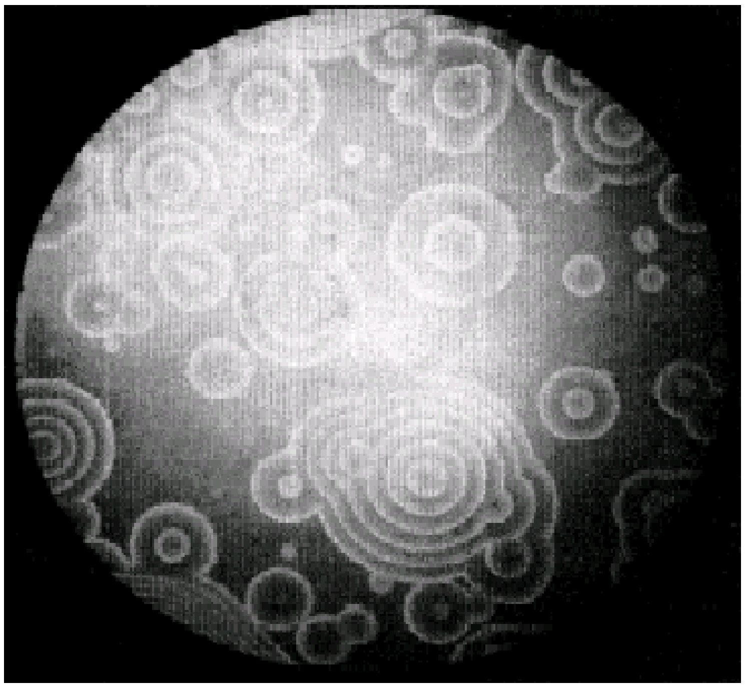

Figure 5.8: Wave patterns seen on the surface in the Belousov-Zhabotinskii reaction.

classical model due to Harvard economist Thomas Schelling in 1971 has to do with the formation of segregated neighborhoods. He believed that people had a certain tolerance level for different ethnic groups and felt comfortable with where they lived as long as a certain proportion of individuals of their own kind lived in their neighborhood. In general, when the neighborhood fell below this proportion, then the individual would move to another neighborhood more to their liking. Schelling used two types of coins representing two different ethnic groups on graph paper which he distributed over some of the grid sites (leaving some blank regions) and which obeyed the simple contentment criterion:

• If the proportion of neighbors in an 8-cell Moore neighborhood that are of the same kind (state) as the central cell becomes lower than some threshold x, then the central cell moves to a 'nearby' site in which the neighborhood has a proportion of neighbors of the same kind that is at least x.

Schelling was interested in finding out what values of the threshold x produced segregated neighborhoods and it was quite surprising to find that even with quite low values for x, initially integrated neighborhoods resulted in high levels of segregation. Of course in reality, not all people living in a neighborhood would have the same contentment threshold and many would not care who the neighbors were as long as they were quiet. Moreover, as Schelling pointed out, there are other mainly economic factors that have a segregating effect. So the model is mainly of heuristic value but does indicate an emergent feature that is rather unexpected. However, it is pleasing to note that Schelling was a joint winner of the 2005 Nobel Prize in Economics in part for this work.

To implement the Schelling model, by 'nearby' we take Moore neighborhoods of ever increasing radius until a suitable neighborhood is found or until all sites have been tried. The updating of cell sites is done asynchronously by choosing a cell site at random and if it is occupied, then applying the above contentment criterion. This is done until the system reaches an equilibrium state. Schelling found that 25% to 30% of vacant space was the most desirable in the initial random configuration of equal numbers of black and white cells. On average it is found that even a low contentment threshold of 30% leads to 70% of same cell state neighbors.

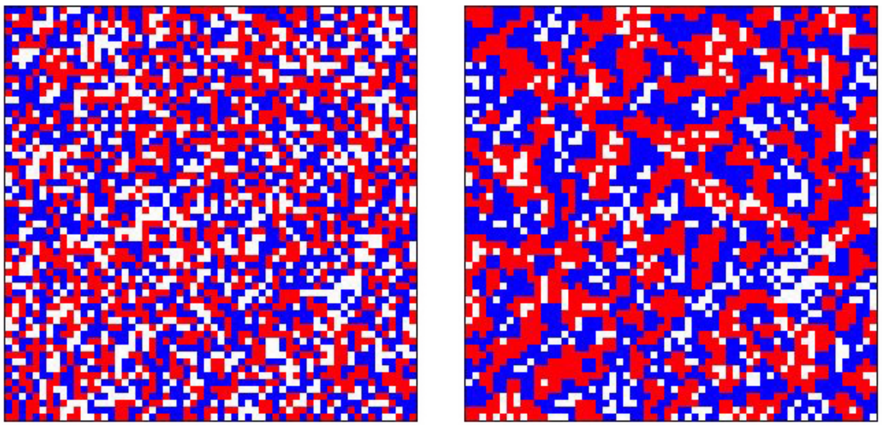

Figure 5.9: The left-hand side is an initial random distribution of occupied cell sites (25% white vacant space) and the right-hand side represents the segregated equilibrium state of the red and blue cells reached after applying the contentment requirement that 37.5% of the neighbors should be of the same kind.

It is worth noting that neither Sakoda nor Schelling used the term 'cellular automaton' at any point in their work. Interestingly, there is now even a *Journal of Artificial Societies and Social Simulation,* no doubt a direct descendent of the pioneering works of Sakoda and Schelling. A *Mathematica* based toolkit for the CA modelling of social interactions can be found in the book by Gaylord & D'Andra [1998] and the Schelling model is also discussed in Gilbert & Troitzsch [1999].

5.3 Prisoner's Dilemma

The Prisoner's Dilemma is a classic model of the dynamics of cooperation and non-cooperation. In order to play a single round of the Prisoner's Dilemma, two players, A and B, have but two options and must decide whether on not they will cooperate (C) or defect (D). The classical payoffs to each player are indicated by the following table:

		B	
		Cooperate (C)	Defect (D)
A	Cooperate (C)	3\3	0\5
	Defect (D)	5\0	1\1

Thus if both players decide to cooperate they are rewarded with 3 points each, whereas if both players defect, they obtain only 1 point each. What is known as the 'sucker's payoff' is when player A defects and receives 5 points but player B cooperates and ends up with 0 points.

What does all this have to do with prisoners? It is based on the scenario of two people (A and B) being arrested for committing some crime (and incidently was featured in the David Bowie movie, "The Labyrinth"). Both A and B are interrogated separately by the police who do have some evidence against them. We will use the value of $5-p$, where p is the number of points obtained by one of the apprehended to calculate their prison terms. So, if they both deny their guilt (that is, they cooperate with each other), they get relatively light 2 year sentences since they were each rewarded with 3 points. However, if they both confess to the crime (i.e. defect), then they each get relatively severe 4 year sentences reflected in their mutually low reward of 1 point. In the sucker's payoff, one player makes a deal with the police admiting guilt (defects) while the other one still denies it (cooperates) with the latter getting the harshest prison sentence of 5 years (since their reward was 0) and the former getting none (with reward 5).

If you are one of the players, what should your response be? Clearly, no matter what the other player does, you should defect. If they happen to cooperate, then you've scored a massive 5 points to their nil and they are a sucker for it. Even if they have defected too, you would still score something (1 point) whereas if you had cooperated you'd end up with nil yourself. Of course your partner also faces the same situation and should choose defection as well.

Viewed collectively, it is certainly true that if you both cooperate then the rewards (3 points each) are greater than if you both defect (1 point each), but from an individual's perspective, there is the temptation of even greater rewards from defection if only the other cooperates, leaving them with nothing. Thus the potential personal gain from defection outweighs the potential collective gain from cooperation.

It becomes more interesting however, if the game is played over and over in what is known as the Iterated Prisoner's Dilemma (dating back to M.M. Flood [1952]). The object for each player is to accrue the largest points total which now requires that some overall strategy be adopted. According to logician Patrick Grim, "It is no simplification to say that our strongest and simplest models of the evolution of biological and sociological cooperation – and in that respect our strongest and simplest models of important aspects of ourselves as biological and social organisms – are written in terms of the Iterated Prisoner's Dilemma."

One simple strategy would be to always cooperate, but this approach is easily taken advantage of. And always defecting can lead to low total scores. Political scientist Robert Axelrod of the University of Michigan conducted a round-robin tournament between strategies submitted by colleagues (see the famous paper by Axelrod and evolutionary biologist W.D. Hamilton [1981] in *Science*). Each game between competing strategies consisted of 200 moves, yielding possible scores from 0 to 1000, so that a 'good performance' score was judged to be 600 points (complete mutual cooperation) and a 'poor performance' score would be 200 points (complete mutual defection). In the first round of the tournament, the overall winner with an average of 504 points per game, submitted by game theorist Anatol Rapoport, was called Tit-for-Tat. In this simplest of strategies, a player cooperates on the first move and then does exactly what the other player did on the previous move. While never actually attaining a higher score in any particular game, this strategy can lead to many rounds of cooperation between opponents with its commensurate rewards, whereas the more defecting strategies do poorly. While Axelrod has shown that there is no best strategy over all competing environments, he has shown that Tit-for-Tat is very robust over a range of environments. In fact, Tit-for-Tat has many strengths. "What accounts for Tit-for-Tat's robust success is its combination of being nice [not being the first to defect], retaliatory, forgiving, and clear. Its niceness prevents it from getting into unnecessary trouble. Its retaliation discourages the other side from persisting whenever defection is tried. Its forgiveness helps restore mutual cooperation. And its clarity makes it intelligible to the other player, thereby eliciting long-term cooperation" (*The Evolution of Co-operation* [1984]).

On the other hand, it was pointed out by Axelrod that at least three other strategies would have won the first round over Tit-for-Tat. One of them was the example strategy he sent to prospective contestants, called Tit-for-Two-Tats but remarkably no one submitted it! This strategy defects only when the opponent has defected on the *two* previous moves and is thus more forgiving than Tit-for-Tat. In a second round of the tournement conducted by Axelrod, with a much larger pool of competitors, Tit-for-Tat won again in spite of everyone knowing the results of the first round. Tit-for-Two-Tats was submitted this time but did quite poorly as some competing strategies were able to capitalize on its tolerance of a single defection. According to Axelrod, "The moral of the story is that the precise level of forgiveness that is optimal depends upon the environment."

Axelrod [1987] also performed computer experiments in order to evolve genetic algorithm strategies to play the Iterated Prisoner's Dilemma. The opposition was eight human developed strategies and it was found that most of the evolved GAs had similar traits to Tit-for-Tat and some of them performed even better *in that particular environment.*

A spatial component can be added to the game so that it is played on a square grid against multiple partners. One can take those partners to be the cells of a von Neumann or Moore neighborhood with the central cell playing off against each one (employing periodic boundary conditions). In one adapation, each player will employ either the strategy of simply cooperating or defecting. At each time step, every square plays one round of the Prisoner's Dilemma against its four or eight neighbors and the score for each cell is then totaled. Each cell at the next time step will then adopt the strategy of the most successful cell in its own neighborhood. Clearly a cooperator surrounded completely by defectors will get swallowed up and at the next time step become a defector. The outcome over time very much depends on the payoff values and often a stable equilibrium is reached. A rigorous treatment of the evolution of cooperation in the spatial prisoner's dilemma setting was made by Schweitzer, Beher, and Műhlenbein [2002] utilizing a von Neumann neighborhood, and asynchronous as well as synchronous interactions with long term memory have been considered by O. Kirchkamp [2000].

There is another way to depict the payoff values. Let R be the (Reward) payoff for mutual cooperation, T the (Temptation) payoff for defecting in the hope your opponent cooperates, S the (Sucker) payoff for cooperating when your opponent has defected and P the (Punishment) payoff for mutual defection.

		B	
		Cooperate (C)	Defect (D)
A	Cooperate (C)	R\R	S\T
	Defect (D)	T\S	P\P

In the classical Prisoner's Dilemma, $\{R; S; T; P\} = \{3; 0; 5; 1\}$, or more generally it can be assumed that $T > R > P > S$ and $R > (S + T)/2$. This latter condition insures that the reward for mutual cooperation should still be greater than that earned if players in turn exploited each other.

Nowak and May [1992] used the nonstandard payoff values $\{R; S; T; P\} = \{1; 0; b > 1; 0\}$, (note that $S = P$ so that this is not strictly a Prisoner's Dilemma) which permitted a measure of control over the outcome by adjusting the temptation parameter b. In this scenario, in a square block

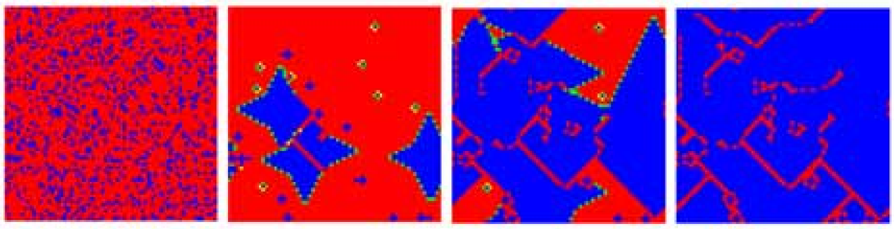

Figure 5.10: The evolution of cooperation (blue) starting with a random array of 80% defectors (red) using a von Neumann neighborhood. The payoffs are: $\{R; S; T; P\} = \{3; 0; 3.5; 0.5\}$. Implementation by Christoph Hauert.

of four cooperators surrounded by a sea of defectors, the cooperators will score a total of 4 points (if we also include cells playing against themselves), whereas any nearby defectors are only exposed to two cooperators, resulting in their scoring $2b$ points. Thus if b is less than 2, clusters of cooperators can hold their own against hordes of defectors (Figure 5.11).

Starting with a single defector cell, a mosaic of regions of defection and cooperation can evolve that allows them to coexist indefinitely in an ever changing state of flux (Figure 5.12).

Another approach to the spatial iterated prisoner's dilemma is to allow for various strategies to compete against each other. Initially, a particular strategy can be randomly assigned to each cell of the array. Each cell then competes for a fixed number of rounds with each of its eight neighbors using the standard payoffs. At the end of each session, a cell will adopt the strategy of its most successful neighbor in terms of highest total score. If two or more neighbors have the highest score, then the central cell will retain its present strategy. In Figure 5.13 we have depicted just such an event with five competing strategies: Always Cooperate, Tit-for-Tat, Random, Pavlov, and Always Defect.

The Random strategy simply cooperates with a certain probability, and defects the rest of the time. It came last place in Axelrod's first round. The other new strategy, Pavlov, begins by cooperating and then will change its response whenever the opposition defects, the philosophy being, 'if winning – continue, if not – try something else.' With time, Tit-for-Tat is seen to predominate.

5.4 Biological Models & Artificial Life

Cellular automata models have proven very useful in biology for as Ermentrout and Edelstein-Keshet put it, in biology, "unlike physics, there are few 'laws' such as the Navier-Stokes equations or Newton's laws". So one has

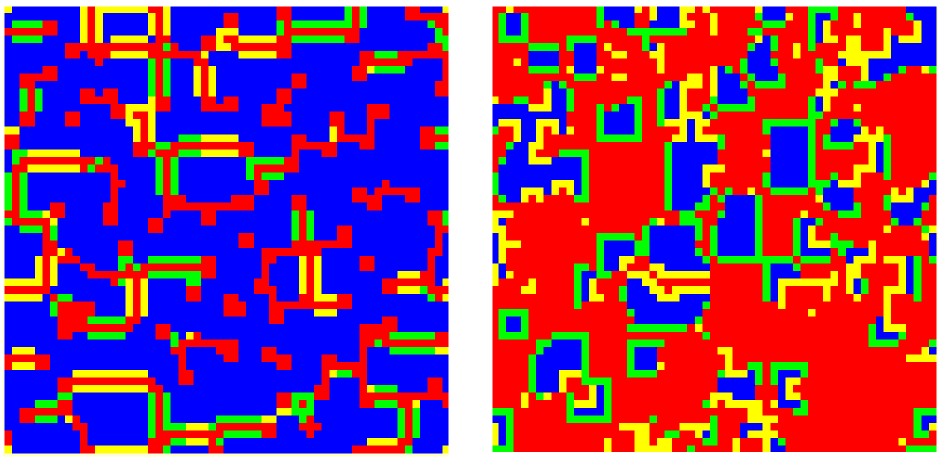

Figure 5.11: Using the Nowak and May payoffs with $b = 1.6$ (left) and $b = 1.85$ (right), with an initial distribution of 10% defectors distributed randomly. Here the central cell also plays against itself using a 9-cell neighborhood. Color code is: blue = cooperator, green = new cooperator, red = defector, yellow = new defector. Periodic boundary conditions are used. Cooperation is seen to decrease with increasing values of the temptation parameter b. Implementation by Serge Helfrich.

to create models of systems by extracting the most salient features of the interactions of various components over time and describing these in some suitable framework, be it differential equations or cellular automata. A very early model for filamentous cell growth using local interactions between cells to update their state in discrete time was proposed by A. Lindenmayer already back in 1968. Detailed and useful CA models have arisen in the work of say Kaplan *et al.,* [1988] on the dynamics of cardiac conduction which was studied using an excitable CA model in a spatially inhomogeneous medium, or in Pytte *et al.* [1991] who deduced an elegant model of a region of the hippocampus (a structure in the floor of the brain) with up to 10,000 neurons which gives qualitative and quantitative data that otherwise would require the numerical solution of about 250,000 coupled differential equations. CA models have been made of the immune system (De Boer & Hogeweg [1992] and Celada & Seiden [1992]), tumor growth (Moreira & Deutsch [2002], and genetic disorders (Moore and Hahn [2000] and [2001] among numerous others. An informative discussion of cellular automata models in biological modeling can be found in the survey paper by Ermentrout and Edelstein-Keshet [1993] and in the text by Deutsch & Dormann [2004].

Biological CA models can also be considered as a form of *artifical life*, which is according to Chrisopher Langton, one of the subject's founders,

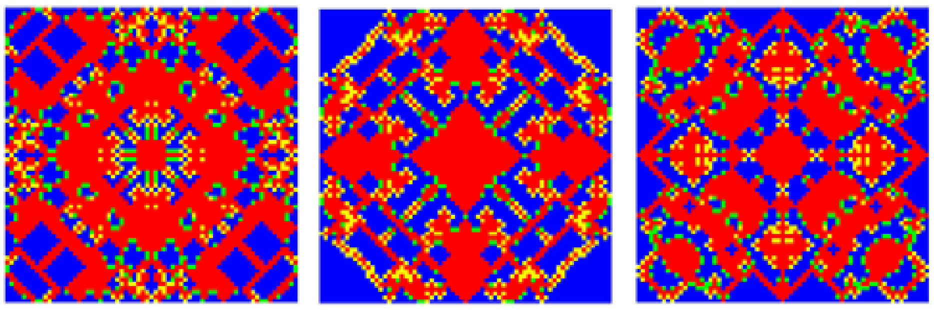

Figure 5.12: Employing a von Neumann neighborhood, these are three images in the time-evolution of of the spatial prisoner's dilemma with a value of $b = 1.4$ and an initial sole defector set in a sea of cooperators. Periodic boundary conditions are used. The color code is: blue = cooperator, green = new cooperator, red = defector, yellow = new defector. Implementation by Christoph Hauert.

"devoted to understanding life by attempting to abstract the fundamental dynamical principles underlying biological phenomena, and recreating these dynamics in other physical media, such as computers, making them accessible to new kinds of experimental manipulation and testing." So much work now goes on in this subject that it has its own journal: *Journal of Artificial Life.* Of course the field of *AL* goes beyond the scope of cellular automata, as for example in the *Blind Watchmaker* program of Richard Dawkins [1989] that generates a whole menagerie of two-dimensional artificial organisms called 'biomorphs' that are found to emerge under suitable biology-inspired conditions, or the highly addictive *Creatures* program created by Steve Grand that utilizes a combination of genetic based algorithms and artificial neural networks. As well, there is the *Terrarium* web-based ecosystem game in which players create their own creatures that have specifically programmed attributes and which then compete for survival against the creatures developed by others.

Further biological/artificial life models are also considered in the next chapter on Complexity.

5.4.1 Genetic Algorithms

One of the remarkable things about biological organisms is that they have evolved to solve very complex tasks – the swimming skill of a shark, the flying skill of a bat, the 3-dimensional vision of the human eye. All of these have evolved through a gradual process of natural selection, so it is tempting to apply this wonderful mechanism of Nature to the computational

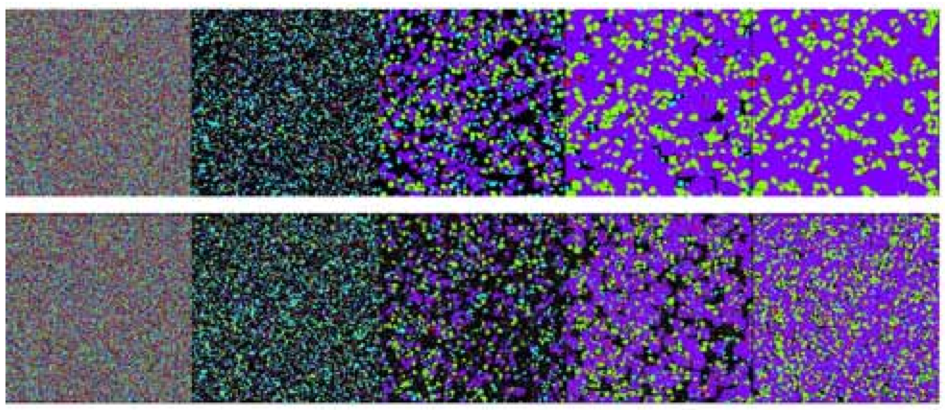

Figure 5.13: The evolution of the spatial iterated prisoner's dilemma with five competing strategies with the standard payoffs from an initial random configuration. Each cell's strategy plays off five times against its eight neighbors and then adopts the strategy of its most successful neighbor. Color code: Always Cooperate = red, Tit-for-Tat = purple, Random, cooperating with a probability of 0.5 = cyan, Pavlov = green, and Always Defect = black. The predominance of Tit-for-Tat over time is evident, with the Random strategy hardly noticable. The second row has a certain level of 'noise' introduced, that is, a cell will make a random move in a single round thus increasing the dynamics of the evolution. Images are taken at the initial state, after 2, 5, 10, and 50 iterations. The code is from G.W. Flake (*The Computational Beauty of Nature* [1998]).

solution of problems. This was first discussed in the 1950s (Box [1957]) and subsequently explored by others, with the modern theory of what are now known as *genetic algorithms* (*GAs*) being developed by John Holland with his students and colleagues at the University of Michigan in a series of works in the 1960s and 70s (see [1966, 1988, 1992]). See also the monograph by Mitchell [1996] for an excellent introduction to this fascinating subject. The wide ranging list of applications of GAs includes population genetics, immunology, ecology, economics, machine and robot learning, and automatic programming.

So how do we artificially mimic natural selection in the form of a genetic algorithm? For a given task to be solved, we begin with a random population of algorithms that act as first approximations to solving the problem. These are encoded in some way, typically as strings of binary digits. After each algorithm has been run, they are all evaluated by a 'fitness test', that is to say, as to how close they come to actually solving the problem. The algorithms are then selected to breed according to their fitness level in order to form a new population of algorithms which are again subjected to the

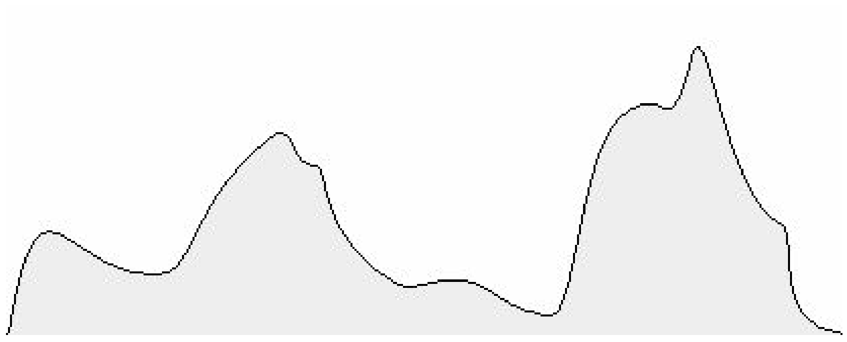

Figure 5.14: Graphical representation of a fitness landscape illustrating the peaks towards which the most fit solutions of a GA migrate and the valleys in which the least fit lie. Note that there can be peaks of varying heights.

fitness test and so on. After several 'generations', one expects to have created a number of highly fit algorithms for the given task.

To visualize all this, the fitness function acting on the space of all possible solutions generates a graph of peaks and valleys called the 'fitness landscape'. The most fit solutions are near the peaks and the least fit lie in the valleys and typically an initial population will climb one of the peaks (a local maximum) as it evolves and becomes more fit (Figure 5.16).

There are three basic genetic operations that can be performed on the algorithms:

- exact reproduction whereby multiple copies of an algorithm are taken (*cloning* or *reproduction*);
- swapping some part of their genetic encoding with another algorithm (called *crossover* or *recombination*);
- random *mutation* of some part of their genetic encoding.

As an illustration of how these operations come into play, we present a genetic algorithm that was created by Auckland University student Michael Brough. Starting from an array in an initial random configuration of black (= 1) and white (= 0) cells, our aim is to turn the whole array into a checkerboard pattern. (Note that this is not completely possible since initial conditions having all cells in the same state will remain so, but this is of no consequence). A 9-cell Moore neighborhood will be used along with periodic boundary conditions. Since each cell can be in either one of two states, there are $2^9 = 512$ different neighborhood-states. Any particular transition function will tell us the state value of the central cell (either 0 or 1) at the next time step for each of the 512 neighborhood-states and so can be represented by a binary string 512 digits long, such as 1001101...110. This is analogous to representing the Rule 150 as the rule-string: 10010110, only now our strings are somewhat longer. In keeping with a biological milieu, the rule-strings are thought of as 'chromosomes' and the bits in the rule-strings are 'genes'. For our example, a hundred or so chromosomes are chosen at random to get things underway.

First of all, each chromosome is given a fitness test in the form of how well it converts an array of random black and white cells into an approximation of a checkerboard. This test is repeated on a few random initial configurations to give a fair evaluation of each chromosome's performance. Choosing the fitness function must be done with considerable care since one that is a bit flawed will not deliver the end result. In our particular example, points are awarded to a chromosome for producing patches of cells in a checkerboard pattern (after 100 time steps) according to the scheme:

For each cell (x, y):

• subtract 3 points if cell $(x + 1, y)$ or $(x, y + 1)$ is in the same state as (x, y);

• otherwise, add 8 points if cell $(x+1, y+1)$ is in the same state as (x, y) and subtract 5 points if it is not, and likewise add 8 points if cell $(x+1, y-1)$ is in the same state as cell (x, y) and subtract 5 points if it is not.

Next, all chromosomes are ranked from highest to lowest according to their fitness score. Each chromosome is then copied (*cloned*) a certain number of times that depends on its level fitness compared to the average fitness score for all the chromosomes. In this way, those chromosomes that are below average are weeded out ('survival of the fittest'). Of course, there are other schemes that can be implemented here that pass on all chromosomes to the next phase, but the idea is to weight the chromosomes in some fashion towards the most fit.

The remaining chromosomes are allowed to 'breed' with each other, that is, exchange some of their genetic material (0s and 1s). In our example, pairs of chromosomes are chosen at random from the initial population and these now become 'parents'. Typically, in other scenarios, designated blocks of digits are exchanged between parents (*crossover*), but in this instance adjacent digits have no particular relation to one another. So what has been done instead is that a new 'baby' string is created by selecting one of the state values at each of the 512 digit positions randomly from either one of the parents. This new baby string is then added to the population of chromosomes. This procedure resulting in new offspring is a digital version of actual sexual reproduction.

Finally, a few bits in each chromosome are adulterated (flipping 1 to 0 or 0 to 1) by random *mutation* – one or two bits worked best. There needs to be some mutation in order to introduce new genetic material, but if there is too much then the positive qualities found at each generation can be lost.

The resulting new set of chromosomes are now given the fitness test again and the above procedure repeated until the desired task is achieved or not. The proof is in the evolution (Figure 5.15).

With the above genetic algorithm, it was found that it was successful

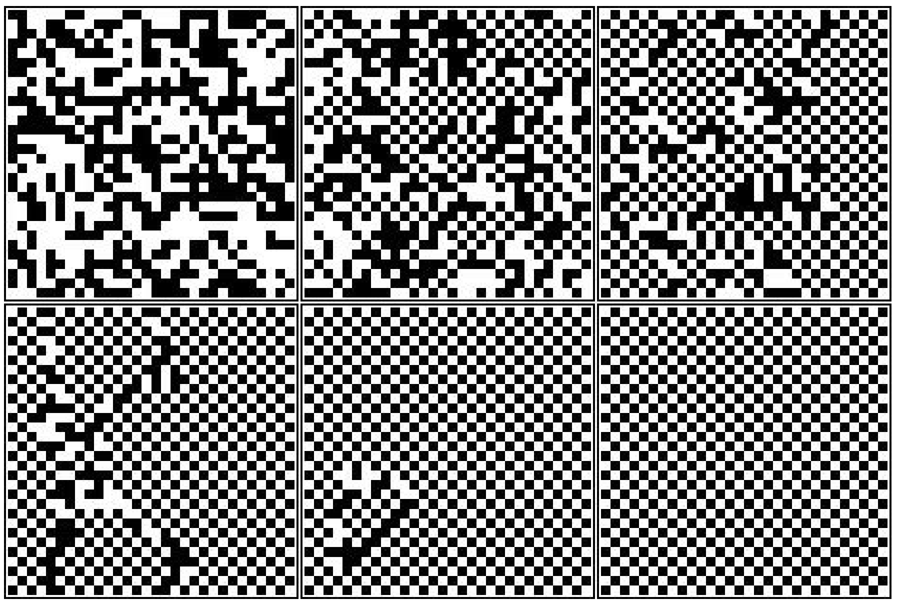

Figure 5.15: The evolution of the checkerboard pattern produced by the GA described in the text at 0 (random configuration), 10, 30, 50, 80, and 100 time steps.

most of the time and almost worked the rest of the time (producing patterns that were mostly correct but having minor flaws in them). Note that the graph of the fitness (Figure 5.16) shows a gradual increase (although at the beginning sometimes there are decreases between generations demonstrating a random tendency at first), then a rapid jump, followed by further gradual increases until the maximum possible fitness score is attained. The GA with this maximum fitness score may not be successful on all possible initial configurations, but has done so on all the ones given to it. At this stage one could start making the fitness function more stringent.

Thus we have employed the essence of natural selection to solve a problem in pattern formation. Further examples in *AL* are discussed in Chapter 5 and for more on GAs, see Mitchell & Forrest [1994].

Genetic algorithms fall under the purview of *complex adaptive systems*, that is, self-organizing systems of autonomous agents that over time exhibit some form of adaptive behavior. A beehive, a slime mold or ant colony are among the many complex adaptive systems found in Nature (see Chapter 6) and this notion has even found its way into the world of business and commerce. A very readable account of this whole circle of ideas can be found in the book by Nobel Prize winner Murray Gell-Mann [1994].

Neurons have evolved to produce complex adaptive behavior in humans and animals and it is to these that we now turn our attention.

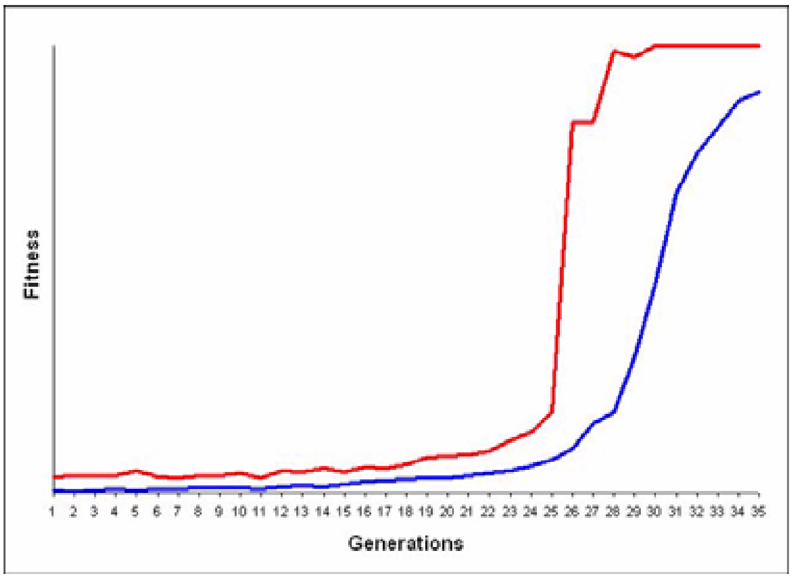

Figure 5.16: The fitness graph for the GA described in the text comparing the maximum fitness level at each generation to the average.

5.4.2 McCulloch-Pits Neural Model

This a simple neural model whereby the state of the *ith* neuron at the next time step is given by:

$$c_i(t+1) = H\left(\sum_j w_{ij}c_j(t) - \theta_i\right),$$

where H is the Heaviside step-function, w_{ij} are weight values given to the coupling strength between (pre-synaptic) neuron j and (post-synaptic) neuron i, with $c_i(t)$ taking on the values 0 and 1 and θ_i a threshold value for the *ith* neuron. Thus if the weighted sum of of all incoming signals to a neuron achieves a threshold value, the neuron fires, taking state value 1. If the threshold is not reached, the state value of the neuron is 0. A prior example was the cellular automaton Vote, in which the weights w_{ij} all had the value 1 and the threshold was $\theta = 5$. The seminal, rather difficult paper by McCulloch-Pitts [1943] containing this model spawned a large amount of research into neural networks that continues to the present. A version of this model has been used by Young [1984] to study a wide range of animal coat markings and indeed, the Vote patterns themselves look very much like coat markings. Further work in the area was carried out by Rosenblatt

[1958] on *perceptrons* that are capable of a limited form of learning and these were also investigated more fully by Minsky and Papert in their now classic text, *Perceptrons: An Essay in Computational Geometry.* A neural network model capable of learning having different dynamics was developed by Hopfield [1982] (see the excellent exposition in Ilachinski [2002]).

The McCulloch-Pitts model uses an 'all-or nothing' threshold simulation of neuron firing with fixed weight factors which is not actually the case for real neurons, but useful nonetheless for many simulation purposes. For example, these features allow one to simulate the basic logic gates that we have seen in Chapter 1. Actually, we'll make a slight modification to the Heaviside function and write

$$c_i(t+1) = sgn\left(\sum_j w_{ij}c_j(t) - \theta\right)$$

where *sgn* is the *sign* function that takes the values

$$sgn(x) = \begin{cases} 1 \text{ if } x \geq 0 \\ -1 \text{ if } x < 0 \end{cases}$$

and $c_i(t)$ takes on the values $+1$ and -1. With this change, we can implement the three logic gates, AND, OR, and NOT in the McCulloch-Pitts model. What is more, McCulloch-Pitts demonstrated that a synchronous neural network composed of neurons of this type can emulate a universal Turing machine and hence is capable of universal computation.

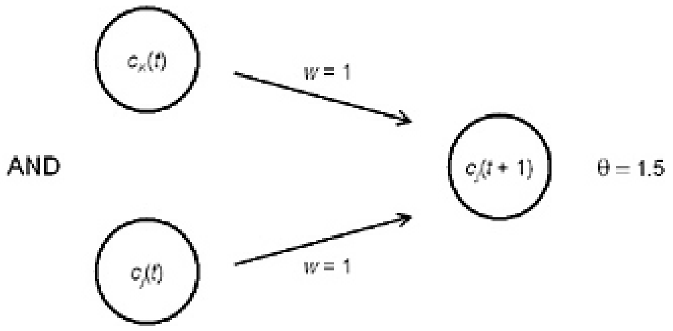

Figure 5.17:

Above is a schematic diagram of a McCulloch-Pitts AND gate. The sum of the two weighted inputs exceeds the threshold only when they are both $+1$, giving an output of $+1$, and -1 otherwise.

If one or both of the inputs is $+1$ in the OR gate, then the output is also $+1$. Otherwise the output is -1.

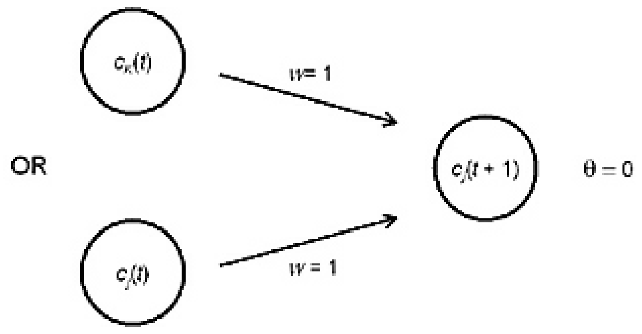

Figure 5.18:

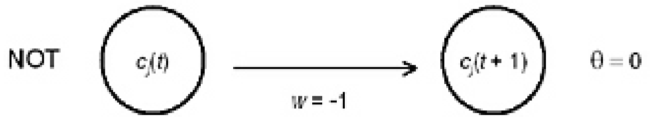

Figure 5.19:

The input of $+1$ or -1 is reversed by the NOT gate.

This suggests, at least to some people, that the brain is nothing more than a highly sophisticated digital computer and that consciousness is an 'emergent' property of complex neural activity. There is also the complementary notion that a digital computer can in principle perform all the functions of the human brain and itself achieve consciousness. These have been highly contentious scientific and philosophical issues. Roger Penrose argues against this position throughout much of his book *The Emperor's New Mind* [1989]:

"Is it not 'obvious' that mere computation cannot evoke pleasure or pain; that it cannot perceive poetry or the beauty of an evening sky or the magic of sounds; that it cannot hope or love or despair; that it cannot have a genuine autonomous purpose?...

"Consciousness seems to me to be such an important phenomenon that I simply cannot believe that it is something just 'accidentally' conjured up by a complicated computation. It is the phenomenon whereby the universe's very existence is made known...

"Yet beneath all this technicality is the feeling that it is indeed 'obvious' that the *conscious* mind cannot work like a computer, even though much of what is actually involved in mental activity might do so."

The reference to consciousness not being 'accidentally' conjured up refers of course to the phenomenon of emergence. Rather, Penrose believes that consciousness is that result of quantum effects that arise within microtubules inside the neurons themselves and has written another book expounding on this theory (Penrose [1994]). One the other hand, people like computer scientist Marvin Minsky take a completely opposite view:

"We humans do not possess much consciousness. That is, we have very little natural ability to sense what happens within and outside ourselves...

"In short, much of what is commonly attributed to consciousness is mythical – and this may in part be what has led people to think that the problem of consciousness is so very hard. My view is quite the opposite: that some machines are already potentially more conscious than are people, and that further enhancements would be relatively easy to make."

Minsky provides a thought experiment in his book *Society of Mind* [1988] in which you are to imagine that all the neurons in your brain have been replaced by computer chips that perform exactly the same functions and are connected in the same fashion to other chips as the neurons. "There isn't any reason to doubt that the substitute machine would think and feel the same kinds of thoughts and feelings that you do – since it embodies all the same processes and memories. Indeed, it would surely be disposed to declare, with all your own intensity, that it is you."

CA researcher Norman Packard holds a similar view. In a conversation with Roger Lewin in his book *Complexity*, we have the following dialogue:

"The simple evolutionary models of the sort I'm working with will eventually develop behavior rich enough that I'll see some kind of consciousness emerge."

"You're saying that your computer model, a form of artificial life, will develop consciousness?"

"I'm saying that the level of information processing in the system will evolve toward what we could call consciousness, that the organisms will reach a point where they will do information processing on their own, and become aware."

"Artificial life, becoming aware of itself?"

"Yes."

The debate over whether the brain (mind) is just a computer capable of consciousness or not will likely continue for some time to come. There are others, such as Colin McGinn of Rutgers University who hold that an understanding of consciousness is beyond the scope of human senses in the same way that humans are unable to see in the infrared. Let's let Penrose have the last word, "Let's be honest. No one can really say what consciousness is."

If one is not at all concerned with the lofty notion of consciousness, there is the system called BrainWorks by Michael Travers [1989] that uses simple neurons such as those in the preceding to construct the nervous system of simple animals. Neural networks have also been combined with a cell structure in a hybrid called *cellular neural networks* (Chua & Yang [1988]).

On a more abstract level, we have the notion of a random Boolean network.

5.4.3 Random Boolean Networks

Rather than implement cellular automata in the usual array format, it is possible to consider a network whereby each cell becomes a node that is connected to various other nodes. The nodes can be considered in various states and these are updated at each time step by a local rule in accordance with the other nodes to which an individual node is connected. Because the network is finite in extent, the output tends to be similar to cellular automata of finite size, that is periodic.

However, it is possible to enhance the dynamics of a finite network of nodes by allowing each node to operate under its own rule picked at random, which means that we are no longer in the realm of a classical cellular automaton. Taking two allowable states for each node, 0 and 1 (off and on), for a system in which each node has K inputs, there are 2^K different combinations of states and hence 2^{2^K} possible Boolean rules that can be formed. For example, if each node is connected to $K = 2$ other nodes and thus receives two inputs, there are $2^{2^2} = 16$ possible Boolean functions to choose from for each node. We list them as the following with O representing the output of the node receiving the given inputs I_1, I_2:

I_1	I_2	O
0	0	0
0	1	0
1	0	0
1	1	0

I_1	I_2	O
0	0	0
0	1	0
1	0	0
1	1	1

I_1	I_2	O
0	0	0
0	1	0
1	0	1
1	1	0

I_1	I_2	O
0	0	0
0	1	1
1	0	0
1	1	0

I_1	I_2	O
0	0	1
0	1	0
1	0	0
1	1	0

I_1	I_2	O
0	0	0
0	1	0
1	0	1
1	1	1

I_1	I_2	O
0	0	0
0	1	1
1	0	0
1	1	1

I_1	I_2	O
0	0	1
0	1	0
1	0	0
1	1	1

I_1	I_2	O
0	0	1
0	1	0
1	0	1
1	1	0

I_1	I_2	O
0	0	1
0	1	1
1	0	0
1	1	0

I_1	I_2	O
0	0	0
0	1	1
1	0	1
1	1	0

I_1	I_2	O
0	0	1
0	1	1
1	0	1
1	1	0

I_1	I_2	O
0	0	1
0	1	1
1	0	0
1	1	1

I_1	I_2	O
0	0	1
0	1	0
1	0	1
1	1	1

I_1	I_2	O
0	0	0
0	1	1
1	0	1
1	1	1

I_1	I_2	O
0	0	1
0	1	1
1	0	1
1	1	1

Some of these are previously encountered logic functions – the AND function is the second rule listed, the OR function is second to last rule and the EXCLUSIVE OR function is the eleventh rule.

Research on random Boolean networks was initiated by Stuart A. Kauffman and is discussed in his 1993 book, *The Origins of Order – Self-Organization and Selection in Evolution* in order to study the emergence of order in biological systems such as genes. With two possible states of 0 and 1 for each node, if there are N nodes, then the number of possible states for the network as a whole to be in is 2^N and represents the size of the *state space*. It is helpful in this regard when thinking about the response of a network to consider the nodes as lightbulbs that are off when in state 0 and on when in state 1. No matter what the initial state of the network, it will eventually find itself in a state it has already reached and thus will repeat its behavior in a repeating *state cycle* much like an attractor of a dynamical system. The maximum possible length of a state cycle is of course the size of the state space itself, that is, 2^N. But even for a modest sized network of say $N = 200$ nodes, the state space is so large ($2^{200} \approx 10^{60}$) as to be effectively infinite in extent.

Kauffman spent years experimenting with Boolean networks, "...counting the number of attractors, the lengths of attractors, the stability of attractors to perturbations and mutations, and so forth. Throwing the dice again, we can randomly wire another network with the same general characteristics and study its behavior. Sample by sample, we build up a portrait of a family of Boolean nets, and then we change the values of N and K and build up another portrait." It was found in the simplest case when $K = 1$ where each node is only connected to one other, that the network exhibited very short state cycles, often of length one. The latter is analogous to the fixed point attractor of a dynamical system.

At the extreme of network behavior, when $K = N$, which means that every node receives input from all others including itself, it was found that the length of the state cycles was on average about $\sqrt{2^N}$ which is still virtually infinite even for $N = 200$. This means that one can wait for an eternity to observe the state cycle repeat itself in real time! Nevertheless, there are a number of different state cycles, on average that number will be N/e, where e is the exponential number 2.71828... In $K = N$ networks, if a single node is perturbed by having its state flipped, then the network's future evolution is also completely altered thus exhibiting extreme sensitivity to initial conditions. These networks can be considered chaotic except for their modest number of state cycles. Similarly chaotic behavior was found in networks with $K \geq 3$.

Very orderly Boolean networks where found when $K = 2$. On average state cycles have length about $\sqrt{N}$ which is also about equal to the average number of different cycles. Thus, even in a very large network with $N = 100,000$ having the staggering number of $2^{100,000}$ possible states to roam around in, the network "quickly and meekly settles down and cycles amoung the square root of 100,000 states, a mere 317... Here is, forgive me, stunning order... Order for free". (Kauffman [1995]). If the network is perturbed slightly it will return to the same state cycle, exhibiting a kind of homeostasis. Kauffman contends that the cell types of an organism as determined by the available genes are in some sense equivalent to the state cycles of a Boolean network with the nodes representing the genes. The numbers seem to agree reasonably well. For example, the human genome has approximately 100,000 genes yet these produce only 254 cell types. In other organisms it is found that the number of cell types is close to the square root of the number of genes which is the relationship Kauffman found between the number of nodes of a Boolean network and its state cycles (Figure 5.20).

The output for the $K = 2$ network in Figure 5.20 at the next time step is given by:

1	2	3	$t \to t+1$	1	2	3
0	0	0		0	0	0
0	0	1		1	0	0
0	1	0		1	0	0
0	1	1		1	0	0
1	0	0		0	0	0
1	0	1		1	1	0
1	1	0		1	0	1
1	1	1		1	1	1

which is the transition table for the 8 possible inputs for each of the three nodes at time t and $t+1$ respectively. Node 1 is an OR gate, and nodes 2 and 3 act as AND gates. From this we can observe a state cycle 2: 101 À 110 as well as other state cycles.

It was found by Bernard Derrida and Gerard Weisbuch [1986] that it is possible to vary a control parameter called P measuring the internal ho-

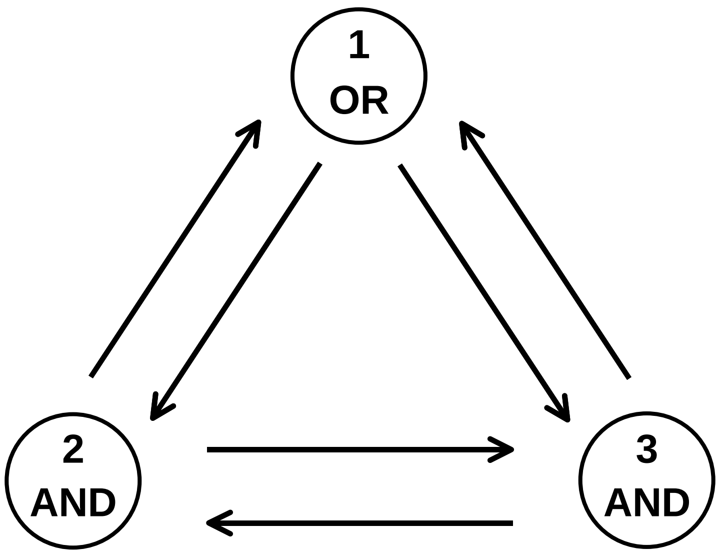

Figure 5.20: A schematic diagram of a $K = 2$ Boolean network.

mogeneity of the set of Boolean functions. It is analogous to the Langton λ parameter, allowing one to move from ordered networks to chaotic ones. There is also some critical value of P, which is just at the boundary between the two – the edge of chaos. Regarding biological systems, Kauffman contends, "The reason complex systems exist on, or in the ordered regime near, the edge of chaos is because evolution takes them there".

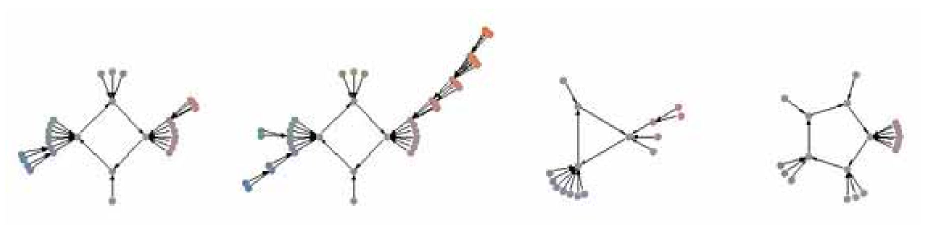

Figure 5.21: A schematic diagram showing some state cycles and their basins of attraction for $K = 2$, $N = 8$. Different colors represent different network states.

5.4.4 Predator-Prey

For many years, biologists have studied predator-prey models, in which a predator inhabits the same environment as its prey and the fluctuating populations of both are investigated subject to a variety of conditions. A set of differential equations known as the Lotke-Volterra equations have been traditionally used to describe predator-prey models based on continuous inputs. Their solution encapsulates the cyclic waxing and waning of the predator and prey populations. Since predator-prey populations are actually discrete in nature, we shall explore the popular cellular automaton model proposed by A.K. Dewdney in his *Scientific American* article [1984, 1988] known as WATOR.

Dewdney imagines a water (i.e. WATOR) world inhabited by sharks and fish where the fish are the prey, the sharks the predators, and both are allowed to reproduce. This scenario leads to five parameters which can be varied by the experimenter:

N_f = initial number of fish

N_s = initial number of sharks

B_f = number of generations before a fish can breed

B_s = number of generations before a shark can breed

S = number of generations since its last fish meal before a shark starves to death.

The fish and sharks live out their lives within the framework of a two-dimensional cellular array where of course time is discrete. Let us give the water, cell state = 0, fish, cell state = 1, and sharks, cell state = 2. We use periodic boundary conditions so that the fish and sharks are actually swimming around on the surface of a torus. The various rules of engagement governing our aquatic inhabitants at each time step are:

(i) Fish swim at random to an adjacent cell in either a N,E,S,W direction provided one of these cells is unoccupied. If all adjacent cells are occupied, the fish remains where it is.

(ii) Sharks are also able to move in a N,E,S,W direction. If some of these adjacent sites are occupied by fish, it chooses one at random, moves to that site and eats the fish which now departs this imaginary WATOR-World. If no fish occupy adjacent cell sites, the shark swims to one of them at random as a fish does, avoiding other sharks.

(iii) When a stipulated number of generations have elapsed (B_f, resp. B_s), fish and sharks are allowed to breed one of their own kind. A ready-to-breed fish or shark that can swim to an adjacent cell deposits one of its offspring in the cell it is just leaving and both the offspring and adult have their biological clocks set to zero for breeding purposes. If there is no free adjacent cell for a fish, then it can neither swim nor breed. However, a shark with adjacent cells occupied by fish can still breed by choosing to eat one of the fish at random and depositing its offspring in the cell it just left. Neither fish nor sharks need need to mate for the purposes of reproduction.

(iv) Sharks will starve to death and depart WATOR-World if they have not eaten any fish after S generations. After a meal of fish however, the life clock for the shark starts at zero again.

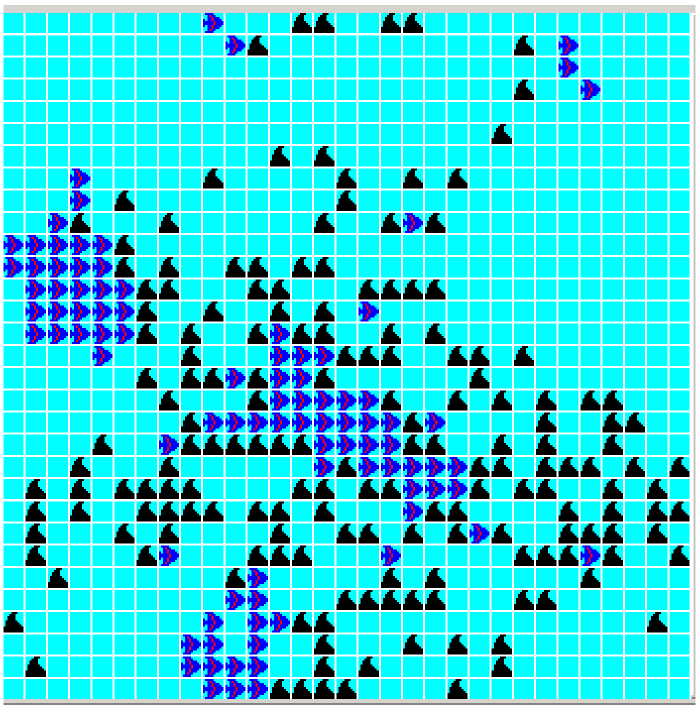

Figure 5.22: The WATOR-World of fish (dark blue), sharks (black) and water (pale blue). There is an initial random mixing of 200 fish and 5 sharks. The image is taken at the 297th time step where the fish population is now 93 and the shark population has risen to 177. Breeding ages for fish and sharks is 2 and 10 generations respectively and the starvation time for sharks has been set at 3. The geometry of the local population mix can affect the dynamics. Image generated by the Wa-Tor predator-prey program of Kovach Computing Services.

The fish and sharks are initially distributed at random in the lattice with the vacant cells being water. In general, with a small number of sharks, the fish population increases significantly, resulting in an increase of sharks which produces a drop in the fish population which in turn leads to starvation and death of sharks. The remaining fish population can again increase and so on (Figure 5.23).

However, this cyclic behavior of both fish and shark populations all depends on the spatial geometry of the two populations and the fine tuning of the five parameter values. With too many fish or too many sharks, the model soon becomes overwhelmed with one of them.

This model is not a cellular automaton in the strict sense as it has asynchronous updating. Indeed, if a fish is surrounded with four empty cells in its von Neumann neighborhood, then the fate of these cells is indeterminate

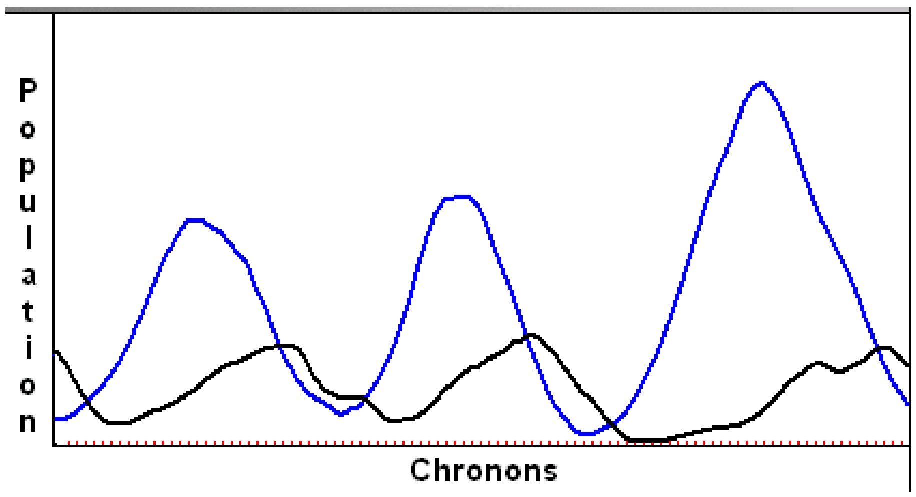

Figure 5.23: The ebb and flow of the fish (blue) and shark (black) populations from the above simulation demonstrating how the predator population follows the trend of the prey population but out of phase with it. Time steps are referred to as 'chronons', a term used by A.K. Dewdney in his *Scientific American* article. Image generated by the Wa-Tor predator-prey program of Kovach Computing Services.

until the next time step when the fish chooses one at random and the fish cell and the chosen empty cell effectively exchange states.

Of course there are many variants of WATOR. Among others, if a fish or a shark cannot breed because of lack of available space, it would have to wait until the next multiple of its breed time rather than breeding at the next possible time step. This introduces a 'stress factor'. One can also allow fish and sharks to swim in eight directions of the Moore neighborhood, instead of the von Neumann neighborhood employed here. Or the model can be made completely deterministic, dispensing with the random aspects altogether. In an earlier predator-prey model, Auslander *et al.* [1978] found that in one scenario, the prey population exhibited chaotic behavior. It was even suggested that this could be a mechanism to prevent the predator from 'tracking' the prey. On the topic of fish, an interesting probabilistic fish migration model is presented in Schönfisch & Kinder [2002].

The predator-prey model employs autonomous agents and is referred to as an IBM (individual based model).

5.4.5 Bacteria growth

Here we are interested in studying the spread of a bacteria colony (through cell division) in the presence of diffusable nutrient with overcrowding playing an important role. The model is due to Ermentrout and Edelstein-Keshet [1993] and uses an 8-cell Moore neighborhood. Since the word 'cell' can now have two different meanings in the present context, let us stipulate that 'cell' means a bacteria cell occupying a 'site' (having state value 1) of a two-dimensional lattice.

The amount of nutrient in every site at the next time step is deduced from the amount at the current time step, $n(t)$, plus a weighted average of nutrient in the eight neighboring sites minus the amount consumed, according to the formula:

$$n(t+1) = (1-\delta)n(t) + \delta \cdot average - eaten$$

where

$$average = \frac{4(N+S+E+W) + (NE+SE+SW+NW)}{20}$$

δ is a diffusion parameter, and

$$eaten = \begin{cases} a_1 & \text{if a new cell is formed (food for growth)} \\ a_2 & \text{if a cell already exists (food for sustenance)} \\ 0 & \text{otherwise.} \end{cases}$$

Now it is necessary to take the effects of crowding into account by considering the number of surrounding sites that are occupied. This will be a function $k(t)$ for each site that takes small values for small and large numbers of occupied neighboring sites, with a suitable maximum somewhere in between. Cell growth occurs every m time steps in an unoccupied site (in state 0) with probability 1/2 if for that particular site

$$k(t) \cdot n(t) > \theta$$

for some threshold value θ. The above formula means that when an unoccupied site is crowded by a lot of neighbors so that $k(t)$ is small, then a large amount of the nutrient $n(t)$ is required before cell growth can occur. A 'new' cell remains as such until the next m time steps. Notice that making a_1 significantly larger than a_2 has the effect of inhibiting growth adjacent to a site where a new cell has formed as opposed to having an old cell at that site (Figure 5.24).

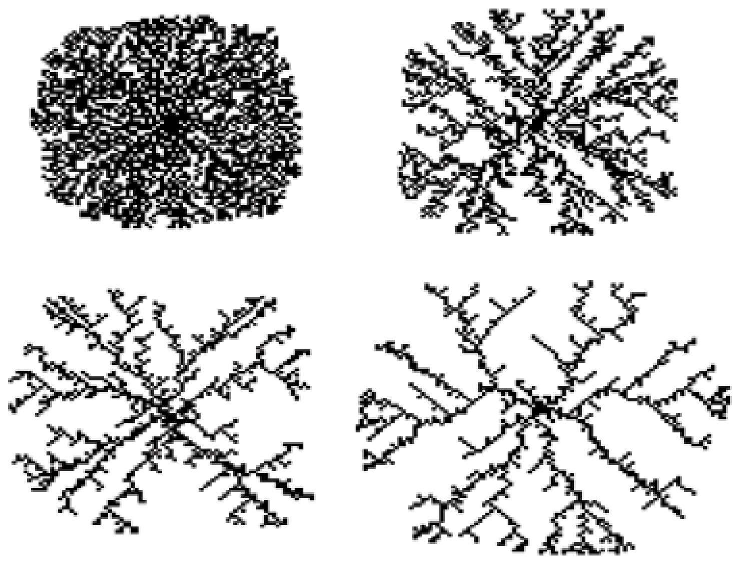
Figure 5.24: A bacteria colony and the forms it takes with increasing values of the threshold θ. Note the fractal-like appearance that develops.

This model is related to the solidification model of Packard [1986] in which higher temperature results in fewer cells experiencing the phase transition from liquid to solid. This is analogous to lower nutrient levels and lowered rates of cell growth in the bacteria model. Other features, such as inhibition and crowding, are also found in the Packard model. Perhaps the simplest solidification model based on inhibition and crowding is the one of snow crystal formation that follows.

5.5 Physical Models

Cellular automata have been used to model many of the dynamic features of the physical world. In this section we will discuss just a few of the more notable applications.

5.5.1 Diffusion

The dispersion of heat or of one chemical substance into another due to the random movement of molecules has classically been modelled by the diffusion equation, which in one-dimension is given by

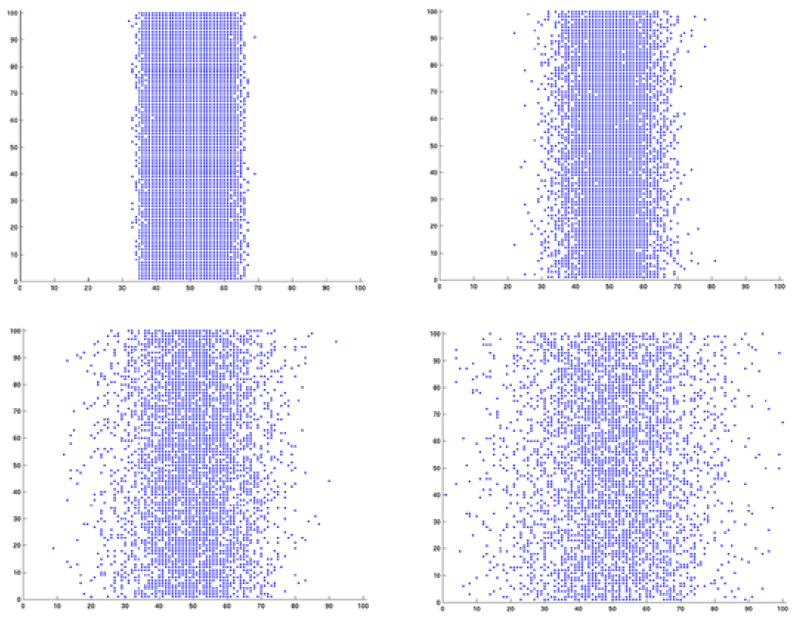

Figure 5.25: The diffusion of a solid substance after 100, 1000, 5000, and 10,000 steps.

$$\frac{\partial u}{\partial t} = c\frac{\partial^2 u}{\partial x^2},$$

where $u = (x, t)$ is the amount of heat or concentration of the dispersing substance at distance x and time t, and c is just a constant that depends on the medium. One shortcoming of the solution is that at any given distance from the source, there is to be expected some quantity of the substance, at any given time. So for example, if you throw a lump of sugar into a swimming pool, the diffusion equation solution of this event always predicts a small quantity of sugar far from the site of the initial lump even a short time after it enters the water.

By contrast we can produce a cellular automaton model that is much closer to what one expects as in Figure 5.25.

The automaton employed here is quite simple and tends to mimic the actual diffusion of a substance like sugar in water in which particles of sugar swap places with parcels of water. In our example, we are taking 100 rows with the solid substance such as sugar, represented by the vertical strip of cells in blue which can diffuse into the surrounding medium of water represented by white cells. Taking one row at a time, we choose a cell at random and swap its contents (i.e. state) with the adjacent cell to its left.

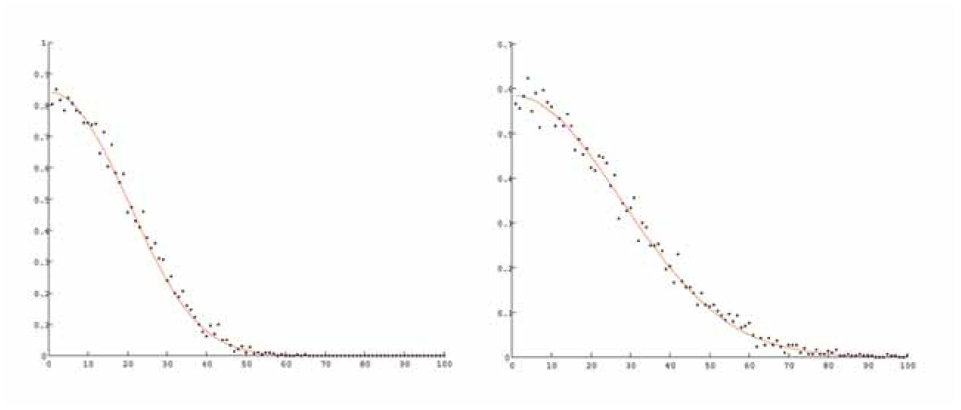

Figure 5.26: The density values (vertical axis) for $u(x,t)$ for $t = 100$ (10,000 iterations) and $t = 300$ (30,000 iterations) respectively plotted with the theoretical values of u given by the solution to the diffusion equation. The diffusion of the material into the surrounding medium is evident. Only the right-half of the bar is considered.

We then proceed to do this for each of the 100 rows and count this as the first time step. Then we start again with the first row, choosing a cell at random and swapping its contents with the adjacent cell to the right, again carrying out this procedure for each of the rows. This is the second time step. We continue in this fashion so that at each odd time step (1,3,5,...) we swap the contents of a random cell in each of the rows with the adjacent cell to the left, and at even time steps (2,4,6,...) we swap with the cell to the right. If two cells have the same contents, then their swapping will result in no change to either.

Quantitative data can even be extracted from the cellular automaton model by choosing a particular vertical column, i.e. a distance x from the source, and adding up the number of occupied cells n. Then the average, $n/100$ (since there are 100 cells vertically), is a density value for $u(x,t)$, for the given time t, representing say, the amount of sugar present at the given distance and time.

Another interesting example of the process of diffusion can be found in the formation of a particular type of meteorite. In certain asteroids, there has been a process of differentiation, as has happened with the Earth, in which a heating event causes the nickle-iron content to sink to a central core with the silicate material forming an outer mantle. At the core/mantle boundary the two components are immiscible when in a fluid state, but certain events like an impact with another asteroid can cause the two materials to diffuse into one another. Sometimes solidification due to cooling then takes place before the two components of silicate and metal can sepa-

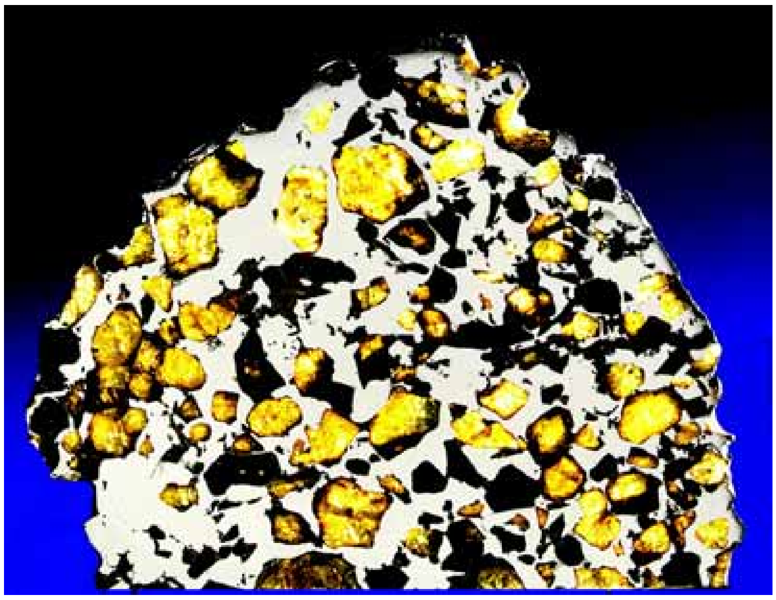

Figure 5.27: A slice of the gorgeous Marjalahti pallasite, a witnessed fall in 1902. The yellow crystals are the mineral olivine and the slice is sufficiently thin that light passes through them. Photo about 3/4 actual size. Courtesy Darryl Pitt/The Macovich Collection.

rate again. If the asteroid then suffers another major impact exposing the core/mantle boundary material and this is acted upon by certain astrophysical forces that send it onto a collision course with the Earth, and enough of it survives the atmospheric burnup to reach the ground, then we have the very rare, but certainly the most beautiful of meteorites – a *pallasite* (Figure 5.27).

To simulate the formation of a pallasite, we have taken a hexagonal array. As in the preceding example, taking one row at a time, we pick a random cell and swap its state with the cell to the left, but in this case we alternate between 'upper left' and 'lower left' at each time step. The time evolution is represented in Figure 5.28, with the olivine layer (left) overlaying a nickel-iron core (right) of a differentiated asteroid.

5.5.2 Snow Crystals

Snow crystals form when water vapor condenses on some seed, usually a speck of dust. When water freezes, molecules of water ice arrange themselves in a hexagonal lattice, the result being that ice crystals take the form of a hexagonal tablet or prism. At certain temperatures the sides grow much more rapidly than the top and bottom surfaces and the crystal spreads out

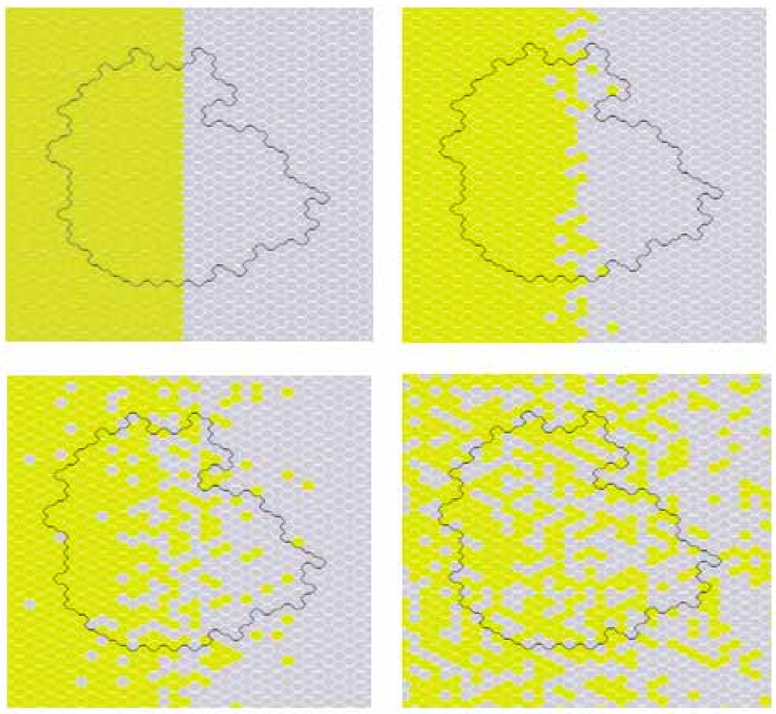

Figure 5.28: A two-dimensional simulation of the formation of a pallasite meteorite. This results from the diffusion of silicate and nickel-iron at the core boundary of a differentiated asteroid and subsequent solidification at the final stage. There is still a sequence of astrophysical events that have to happen before this material can be recovered on Earth. The CA images represent 0, 100, 1000, and 10,000 time steps.

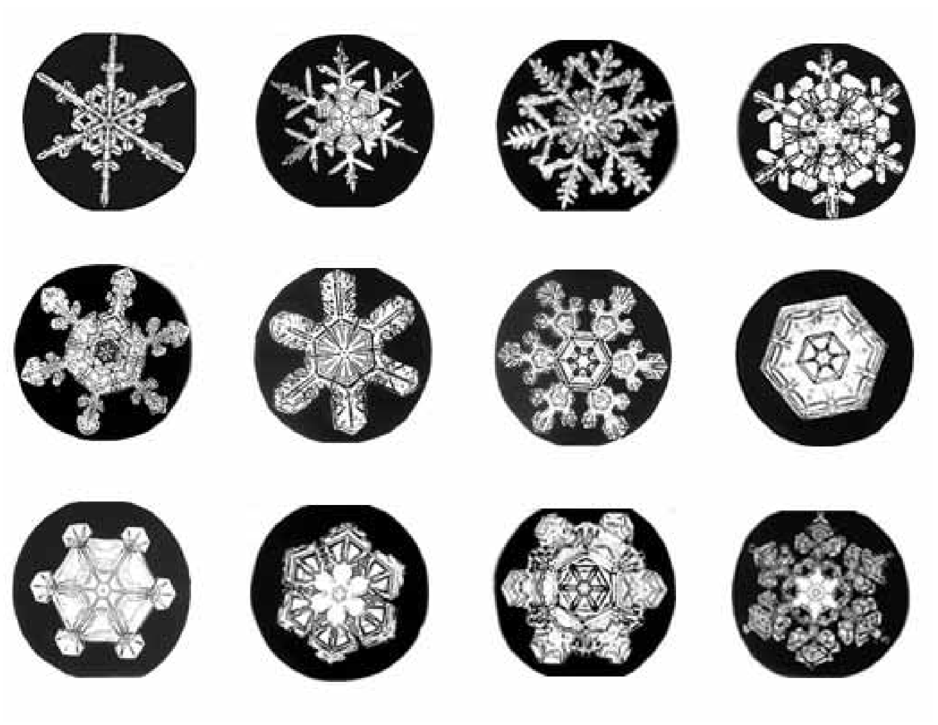

Figure 5.29: Some of the exquisite forms of actual snow crystals. Photographs taken by Wilson Bentley. Courtesy The Jericho Historical Society, Jericho, VT.

into a planar figure. Since the snow crystal experiences the same ambient conditions across its entire face, it grows with a six-fold symmetry. However, the crystal growth is strongly influenced by the temperature and as the snow crystal is blown about it experiences different temperatures which lead to different morphological features. Thus the physics of how water molecules are added to the growing crystal structure can be very complex. By the way, snowflakes are actually assemblages of snow crystals that are loosely bound together.

One of the pioneers of snowflake photography was Wilson Bentley(1865-1931) a Vermont farmer who turned to snow crystal photography taking more than 5,000 images in his lifetime (see Figure 5.29). His book, *Snow Crystals* published in 1931 has been re-released by Dover [1962] and is still in print.

Norman Packard [1986] has shown that a simple automaton model can reproduce many of the snow crystal patterns quite effectively. When a water molecule is added to the crystal structure, a small amount of heat is released at the site which acts as an inhibiting factor for more water molecules to

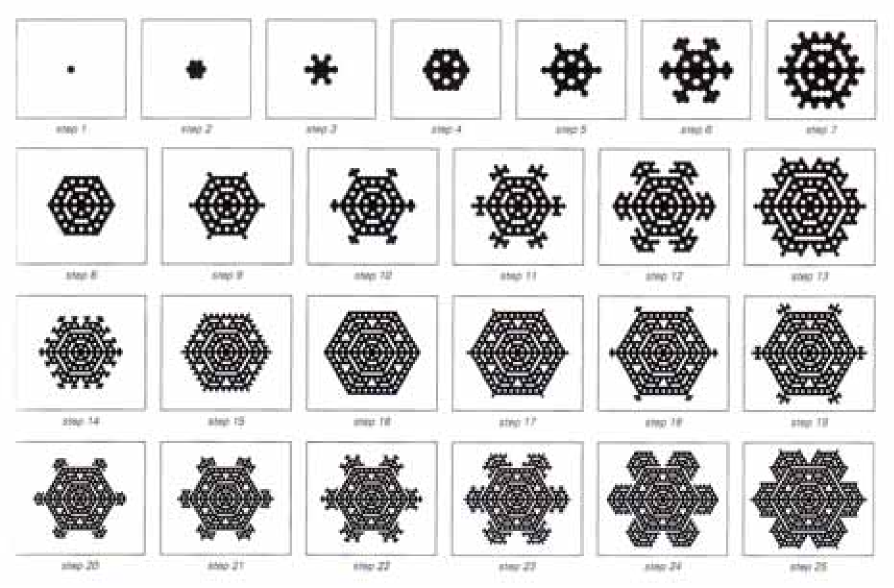

Figure 5.30: The evolution of the Packard model of snow crystal formation starting with a seed of a single black cell on a hexagonal lattice. A close correlation with actual snow crystals is observed. From Wolfram [2002], p. 371.

attach at the same site. So the Packard automaton model states that:

• a cell site becomes black (representing the presence of solid material) if it has exactly one black neighbor;

• a cell remains white (representing the absence of solid material) if it has more than one black neighbor.

Starting with a single black cell (the seed) on a hexagonal lattice, we obtain a sequence of cellular automata snow crystals (Figure 5.30):

Very clear similarities can be seen between the actual snow crystals above and the cellular automata ones. One can also note an evolution that alternates from a branched structure to the tablet form and back again.

A more sophisticated model capable of capturing snow crystals forms has been presented by Clifford Reiter [2004]. This model also employs a hexagonal grid and states of cells are allowed to take on real number values as opposed to simply integer values. Such models with states allowed to take real values are referred to as *continuous automata.* In this instance the values are a measure of the amount of water at a particular cell site and if that value is ≥ 1 then the water is taken to be ice. The cellular array is divided into two distnct classes that are updated differently:

• Receptive (**R**): cells that are ice (value ≥ 1) or have an immediate neighbor that is ice;

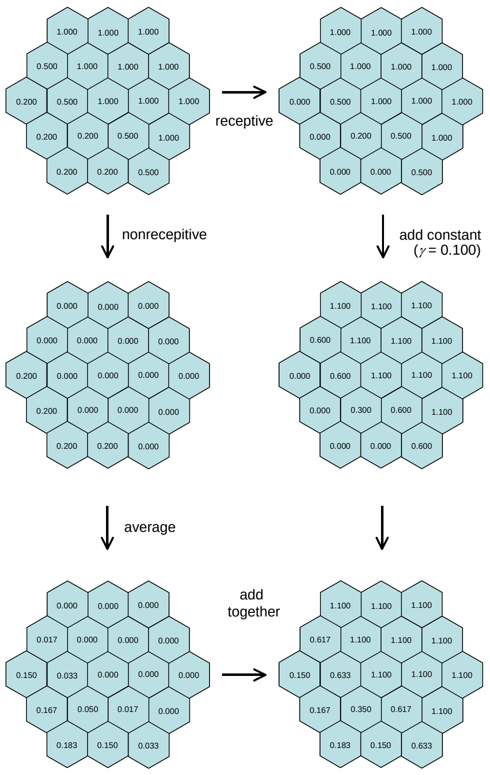

Figure 5.31: The updating of the hexagonal array of Receptive and Unreceptive cell sites as described in the text. Adapted from Reiter [2004].

• Unreceptive (**UR**): all other cells.

The **R** sites are updated at the next time step by just adding a constant parameter γ, the idea here being that water may be supplied from outside the plane of growth and stored.

The **UR** cell sites are not yet ice and so are governed by the diffusion of water vapor. If $u = u(P, t)$ represents the amount of water vapor at position P and time t, then the diffusion equation describing the vapor flow is:

$$\frac{\partial u}{\partial t} = a\Delta u,$$

where $\Delta u = \frac{\partial^2 u}{\partial x^2} + \frac{\partial^2 u}{\partial y^2}$ is the Laplace operator applied to u. On a hexagonal array, this can be expressed in a discrete form as

$$u(P, t+1) \approx \frac{u(P,t)}{2} + \frac{\sum_{N \in nn(P)} u(N,t)}{12},$$

where $nn(P)$ represents the set of nearest neighbors of P, and we have taken $a = 1/8$ as the canonical case

The updating is a two-stage process. Firstly, the array is split into Receptive and Unreceptive groupings. The Receptive group consists of all the **R** cell sites but also has 0 as a *place holder* at any **UR** cell sites. The Unreceptive group consists of all the **UR** cell sites with 0 as a *place value* for the purposes of averaging at any of the **R** cell sites. See Figure 5.31.

As mentioned above, all the **UR** cell sites in the Receptive group have the constant γ added to their value with 0 placeholding the **UR** sites. All the sites in the Unreceptive group are updated according to the averaging given by the preceding equation, even the sites having value 0. Finally, the corresponding cell values of the Receptive and Unreceptive groups are added together and this gives the state of the array at the next time step.

There is one other parameter that we are free to set and that is the background level given by the constant β. By a suitable choice of the two parameters γ and β, the model is able to generate a large variety of snow crystal forms. Of course we could also vary the parameter α but Reiter has found that in general the qualitive behavior of snow crystal growth is not affected by the choice of α. In Figure 5.32 we start from a single seed of value one with all other cells having background value β.

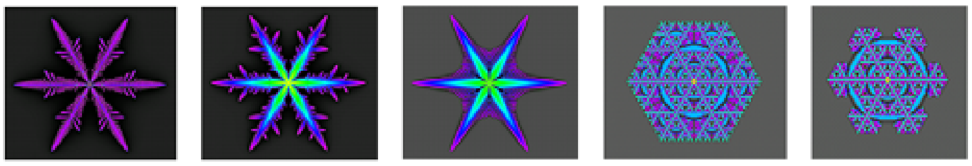

Figure 5.32: Images have parameter values $\beta = 0.35$, $\gamma = 0$; $\beta = 0.4$, $\gamma = 0.001$; $\beta = 0.8$, $\gamma = 0.002$; $\beta = 0.95$, $\gamma = 0$; $\beta = 0.95$, $\gamma = 0$, respectively. The last two have the same parameter values and represent different time steps. The first three types are stellar dendrites and the last two are plate forms. Courtesy Clifford Reiter.

The morphological changes with varying β and γ can be seen in Figure 5.33 (from Reiter [2004]).

A fascinating account of snow crystals formation and morphology can be found in the book by Kenneth Libbrecht/Patricia Rasmussen [2003].

5.5.3 Lattice Gases

Our first model for the simulation of fluid flow is due to Hardy, de Passis, and Pomeau [1973], and accordingly is known as the HPP model. It is a

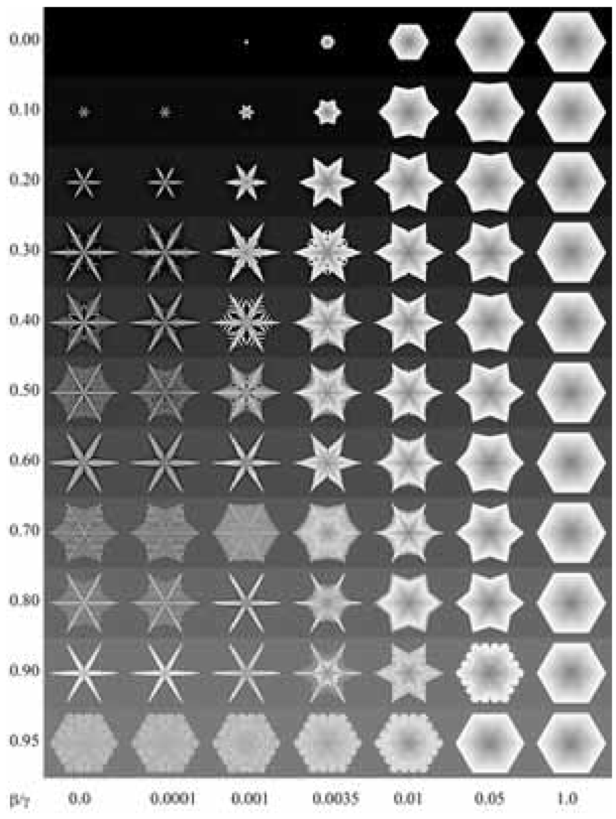

Figure 5.33: The morphological changes of the snow crystals in the Reiter model as a function of the background parameter β and the additive constant γ. From Reiter [2004].

two-dimensional model of fluid particle interactions, where time is discrete, particles are all identical and travel at unit speed. The lattice is rectangular and particles are deemed to be at the nodes of the lattice and can travel only in the four directions of the lattice itself. One's first impression is that this is not really a cellular automaton, but as we shall see it turns out that it is equivalent to the partitioning cellular automata of Margolus. Lattice gas models also appear in biology models (cf. Ermentrout & Edelstein-Keshet [1993]) since the particles can also represent cells or organisms.

At each time step, each particle travels from one node to the next nearest node as indicated by its velocity vector (which is just an arrow indicating the direction of flight along one of the lattice lines). An exclusion principle forbids any two identical particles to occupy the same node at the same time, but up to four particles can be at the same node. The rules for interaction between particles at the same node is the following:

- Particles arriving at a node from opposite directions (head-on col-

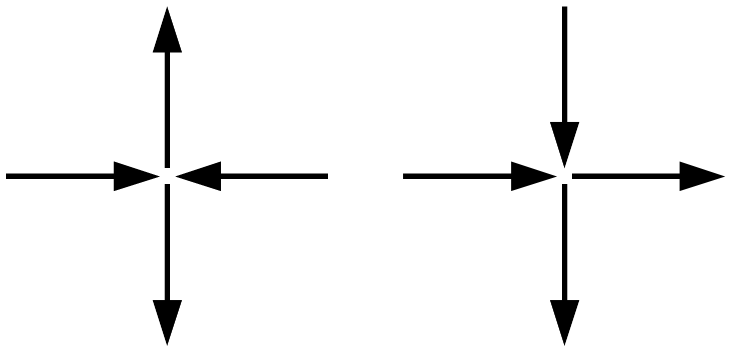

Figure 5.34: Particle interactions in the HPP model. Head-on collisions result in particles exiting at right angles (left) and any other type of collision results in the particles continuing on their original course.

lisions) give rise to two particles traveling at right angles to the original direction of flight (Figure 5.34 left);

• In all other particle collisions (say at right angles or between more than two particles) the particles simply continue on the path indicated by their velocity vector (Figure 5.34 right).

So that the above collisions rules make sense when thinking about collisions say between billiard balls, it is important to note that individual particles cannot be distinguished after a collision takes place. There are actually 16 possible interactions at a node which we may describe in the following table, where we have indicated the directions of flight by N (north), W (west), S (south), E (east) with a '1' denoting the presence of a particle, and a '0' the absence of one:

I	n				O	u	t				I	n				O	u	t	
N	W	S	E		N	W	S	E			N	W	S	E		N	W	S	E
0	0	0	0		0	0	0	0			1	0	0	0		1	0	0	0
0	0	0	1		0	0	0	1			1	0	0	1		1	0	0	1
0	0	1	0		0	0	1	0			1	0	1	0	*	0	1	0	1
0	0	1	1		0	0	1	1			1	0	1	1		1	0	1	1
0	1	0	0		0	1	0	0			1	1	0	0		1	1	0	0
0	1	0	1	*	1	0	1	0			1	1	0	1		1	1	0	1
0	1	1	0		0	1	1	0			1	1	1	0		1	1	1	0
0	1	1	1		0	1	1	1			1	1	1	1		1	1	1	1

Only the two head-on collision events indicated by (*) produce any change in direction for the incoming particles. Observe that the number of

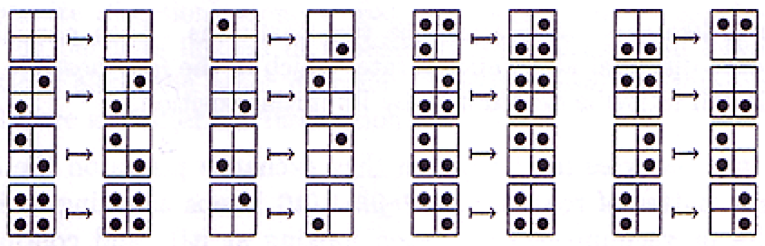

Figure 5.35: SWAP-ON-DIAG: In every 2x2 block of the current partition, swap the contents of each cell with that of the cell diagonally opposite to it in the block.

incoming particles (which are identical in mass and velocity) always equals the number of the outgoing particles so that energy and momentum (mass x velocity vector) is conserved by collisions. The HPP model captures many of the macroscopic properties of fluid dynamics. However, one pecularity of this model is that the horizontal component of momentum is conserved along all horizontal lines of the lattice, and the vertical component of momentum is conserved along all vertical lines. As this does not actually happen in the real physical sense, it leads to discrepancies.

However, let us see how the HPP model follows from the Margolus neighborhood notion. Following Toffoli and Margolus [1987], let us adopt just the simple rule that the authors call SWAP-ON-DIAG (see Figure 5.35).

By considering say, a particle in the bottom left-hand corner of a dark 2x2 block, it will according to the SWAP-ON-DIAG rule go diagonally to the top right-hand corner of the block. Next it will be considered in a light block, again at the bottom left-hand corner, and the rule will move it further diagonally to the top right as in Figure 5.36 (left). Particles at other positions will also move diagonally.

At this stage we have produced particle motion but not any collisions and particles heading directly towards one another will just by-pass one another, traveling merrily on their way as in Figure 5.36(right).

In order to account for the collision rule of the HPP model we need only make one slight emendation to the SWAP-ON-DIAG rule. Namely, where there are two particles are at opposite ends of a diagonal in a block (and no other particles in the block!), we ROTATE the two particles 90^o to the other diagonal. Thus we simply need to amend the 2nd and 3rd rules of SWAP-ON-DIAG as in Figure 5.37 and maintain all the others as they were.

By way of illustration, in Figure 5.38 we have the movement of two particles moving freely through space (left) and colliding head-on (right).

Thus all the dynamics of the HPP lattice gas model have been repro-

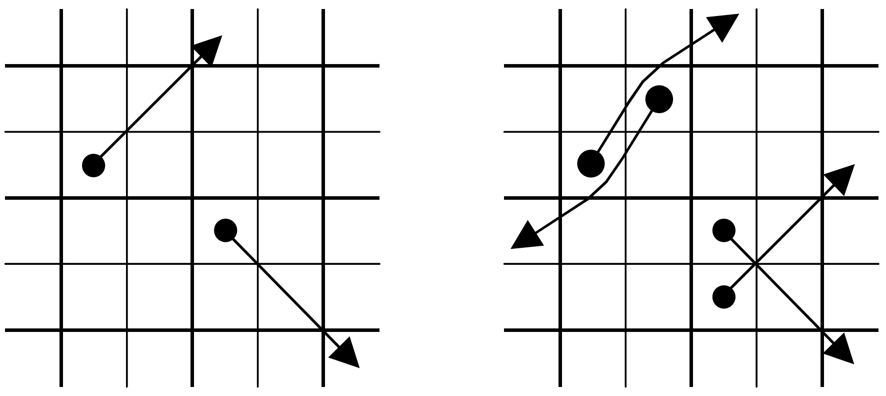

Figure 5.36: Particle movement following the SWAP-ON-DIAG rule. Movement is always diagonally across the lattice. Particles that encounter one another, either head-on or side-on move as if 'through' one another.

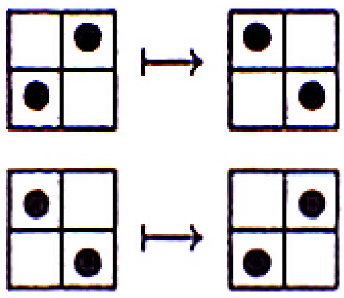

Figure 5.37:

duced using the Margolus neighborhood and the preceding modification of the SWAP-ON-DIAG rule.

A model employing the same general principles but which provides a much better fit with real fluids is due to Frisch, Hasslacher, and Pomeau [1986], and known as the FHP model. It uses a hexagonal lattice (again in two dimensions) so that particles can travel along six different directions. A sample of particle interactions is given in Figure 5.39. Both mass and momentum are again conserved at each vertex.

The virtue of the FHP model is that in the macroscopic case taking a sufficiently large number of particles, the classical two-dimensional Navier-Stokes equations are satisfied. The Navier-Stokes equations are the fundamental partial differential equations governing the fluid flow of liquids and gases. For some additional technical discussion regarding the behavior of the viscosity of the model, see the references of Frisch [1987] and [1990]. Various

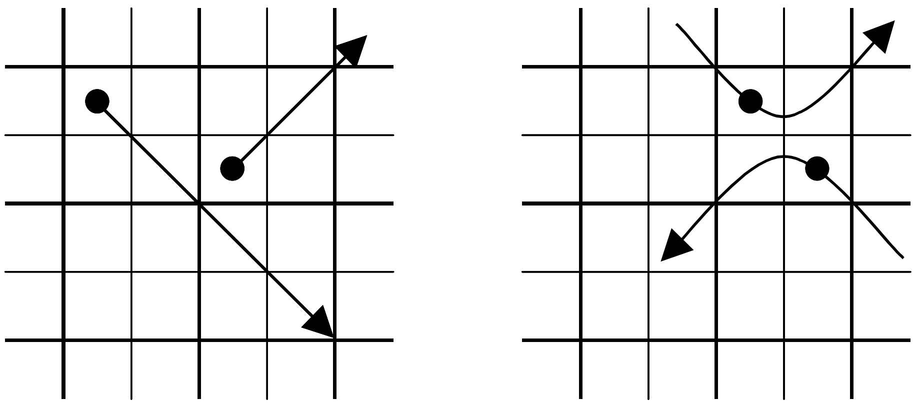
Figure 5.38: Particle movement with the modified SWAP-ON-DIAG rule showing free movement in space and a head-on collision.

other lattice gas models have been devised including one for 3-dimensional hydrodynamics (Henon [1987]).

5.5.4 Ising Spin Models

The Ising spin model originally arose out of a study of ferromagnetic materials. A lattice model of spins was proposed by Wilhelm Lenz in 1920 and investigated by his student Ernst Ising. The resulting model considers a lattice of sites at which is placed a 'spin' which takes on either the value $+1$ or -1. Equivalently, one can think of the $+1$ spin as an arrow [$\uparrow$] representing 'spin up' and the -1 spin as an arrow [$\downarrow$] representing 'spin down'. The lattice we consider in the sequel consists of squares, but triangular or hexagonal lattices have also been employed in two dimensions, although the lattice can be in any dimension. The Ising system also serves to model a large class of thermodynamic systems that experience phase transitions.

The spins lie at the vertices of the lattice which results in an interaction energy (or 'bond energy') between each site's spin and those of its von Neumann nearest neighbor sites. The energy contributed by these interactions is $+1$ whenever the sites have *opposite* spins and -1 whenever the sites have the *same* spin, in a sense like opposite poles of a magnet attract each other and like poles repel. This is illustrated in the example below.

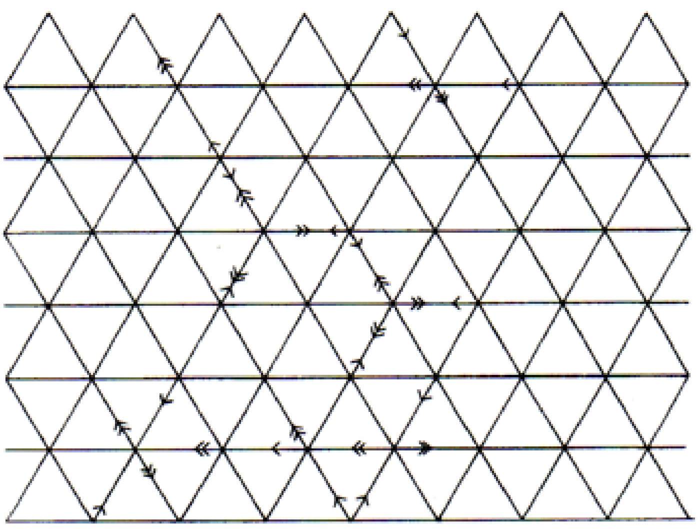

Figure 5.39: Various particle interactions in the FHP model. Particles at time t are given by a single arrow, and those at time $t+1$ are given by double arrows. Head-on two body collisions have two possible outcomes with equal *a priori* weights (bottom left and bottom right). Other particle interactions not depicted are unaffected by collisions. Redrawn from Frisch, Hasslacher, and Pomeau [1986].

[↓]	-1	[↓]	$+1$	[↑]	$+1$	[↓]
$+1$		$+1$		$+1$		$+1$
[↑]	-1	[↑]	$+1$	[↓]	$+1$	[↑]
-1		-1		-1		-1
[↑]	-1	[↑]	$+1$	[↓]	$+1$	[↑]
-1		$+1$		-1		$+1$
[↑]	$+1$	[↓]	-1	[↓]	-1	[↓]

Here the spins up [↑] and spins down [↓] each have four bond energies with their nearest neighbors in the NESW directions which are $+1$ when the spins are opposite and -1 when the spins are the same.

In order to compute the total energy of the system, one adds up all the nearest neighbor energies for the lattice. If we denote by s_i $(= \pm 1)$ the value of the spin at site i, then the bond energy between the nearest neighbor pair s_i and s_j is given by the negative of their product: $-s_i\, s_j$. Taking the sum over all of these nearest neighbor pair interactions gives the total magnetic energy of the system

$$\mathcal{E} = \frac{1}{2}\sum_{i,j} -s_i\, s_j = -\frac{1}{2}\sum_{i,j} s_i\, s_j.$$

Periodic boundary conditions are taken to achieve the closest approximation to an infinite lattice. In order that the total energy value does not depend on the size of the system, we will normalize it by dividing by the total number of spins N and denote: $E = \mathcal{E}/N$. In the extreme cases when *all* the spins are either up $(+1)$ or down (-1), we find that $E = -2$ since there are four bond energy sums for each of the N spin sites with each having a value of -1 and the factor of $1/2$ compensates for the fact that we have counted each bond energy twice, giving $E = -2N/N = -2$. In the other extreme case when all the spins alternate consecutively between up $(+1)$ and down (-1) over the entire lattice, then there are $4N$ bond energy sums each having the value $+1$ so that $E = 2$. Thus the total energy has the bounds: $-2 \leq E \leq 2$.

The magnetization of the system is given by the sum of all the values s_i and normalized again by dividing by the number of spins N, giving

$$M = \frac{1}{N}\sum_i s_i. \tag{5.1}$$

This means that if all the spins were up $(+1)$ then $M = +1$ and if all the spins are down then $M = -1$ so that the magnetization lies in the range: $-1 \leq M \leq 1$. The formulation for magnetization in Equation 5.1 also represents M as the fraction of the up spins minus the fraction of the down spins and hence $M = 0$ when exactly half of the spins are up and half are down.

Let us just take note of what we have created here. For an array that is 10x10 so that $N = 100$, the total number of different lattice configurations equals $2^{100} \approx 10^{30}$, a rather large number indeed. The set of all these configurations is called the *phase space*. This is the universe we get to roam around in to explore the dynamics of magnetization. Taking the extreme case again when all the spins are either all up $(+1)$ or all down (-1), we found that $E = -2$ and either $M = 1$ or $M = -1$, respectively. Even when a large proportion of the spins are either all up or all down, the energy E will be low and close to its minimum. Furthermore, from the model we can glean the fact that whenever exactly half the spins are either up and half are down, then $M = 0$ as mentioned above. Moreover, there are many different possible configurations with half the spins up and half the spins down (essentially where there is a random ordering of the spins) and each one has a possibly different total energy. We can conclude that for a large number of values of E, we will have $M = 0$. This includes the case when the spins alternate consecutively up and down and the energy has the maximum

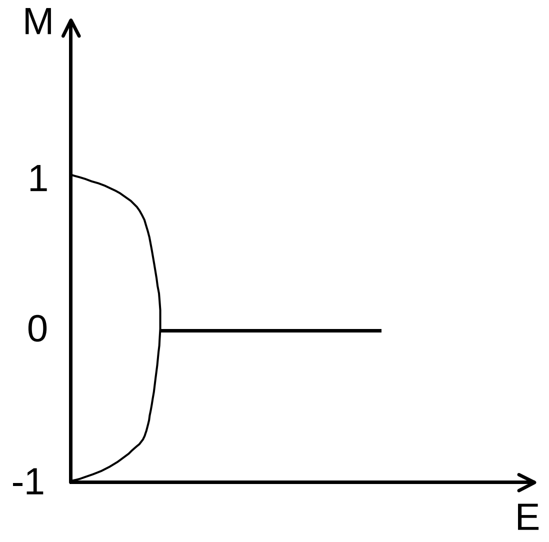

Figure 5.40: In the Ising spin model, large numbers of configurations (essentially half the spins up, half down) have magnetization values close to zero. This includes the highest energy state $E = 2$ in which the spins alternate between up and down over the entire array. When the spins are oriented mostly up $(+1)$ or mostly down (-1) then the magnetization M takes values close to $+1$ or -1 respectively and correspond to the lowest energy levels E. The graph represents the idealized situation for an infinite array of spins.

value $E = 2$. It turns out that the (ideal) situtation looks like Figure 5.40 when we graph the magnetization vs. energy for different configurations.

In a physical context, it is observed that the magnetization of a magnetic material is influenced by its temperature. That is, at high temperature, there is essentially no magnetization, and as the temperature is lowered below some critical (*Curie*) temperature, T_c, regions of magnetization are spontaneously generated. The high temperature scenario corresponds to a high internal energy and a random ordering of the spins (essentially half the spins up, half down), so that M is effectively 0, whereas in the lower temperature case, spins tend to orient in a particular direction over regions wherein M is either positive or negative. This spontaneous generation of magnetism is called a *phase transition* and represents a kink in the behavior of M at T_c (i.e. a discontinuity in the rate of change of M) as can be seen in the graph.

In 1944, it was demonstrated by Lars Onsager that in the two-dimensional case there is a mathematical description of the phase transition in the Ising spin model. This model has become the the natural way in which to study phase transitions in general, such as occurs during freezing, melting, or superconductivity.

In order to explore the dynamical behavior of the Ising model since there is no time parameter in the model itself, the system is made to evolve according to some algorithm that will 'flip' the spins in some fashion. We discuss an elementary formulation that preserves the total energy E that is based on the so-called Q2R rule of Vishniac and developed in Toffoli & Margolus [1987]. The algorithm is: *we flip all and only spins that have two nearest neighbors with spins* $+1$ *and two with spins* -1, so that the sum of the four bond energies associated with each such spin remains unchanged. However, one must be a bit careful how the flipping of spins is carried out. In the figure below, the two central (down) spins can both flip according to our rule,

$$\begin{array}{cccccc} & \cdots & [\uparrow] & [\uparrow] & \cdots & \\ \cdots & [\uparrow] & [\downarrow] & [\downarrow] & [\downarrow] & \cdots \\ & \cdots & [\downarrow] & [\uparrow] & \cdots & \end{array}$$

but if they did both flip simultaneously and their neighbors remained unchanged, yielding

$$\begin{array}{cccccc} & \cdots & [\uparrow] & [\uparrow] & \cdots & \\ \cdots & [\uparrow] & [\uparrow] & [\uparrow] & [\downarrow] & \cdots \\ & \cdots & [\downarrow] & [\uparrow] & \cdots & \end{array}$$

then each of their bond energies will have changed from 0 to -2 with a resulting change in the total energy. To avoid this we place the spin sites on a black/white checkerboard grid and we apply the flip rule by alternating between the black and white sites. This circumvents the aforementioned difficulty and results in a reversible cellular automaton. This procedure can still be construed as simultaneous updating of all cells by introducing a spatial parameter that alternates at each time step between the values 1 on the black cells, 0 on the white cells, to 0 on the black cells and 1 on the white cells. Each cell with the parameter value 1 will have the flip rule applied and if the cell value is 0 then the cell state is to remain unchanged.

More specifically, the total energy is computed for any initial configuration by first taking the total bond energies for all the black cells of the lattice, allowing all spins on black cells to flip that are energy preserving, and then computing the energies of the spins on all white cells and flipping all of those spins that are energy preserving. The total energy is computed by taking one-half the sum of the energies of the spins on black and white cells respectively.

For a typical simulation, with proportions of spins up (and down) whose energy levels are greater than the critical value, the system evolves to a

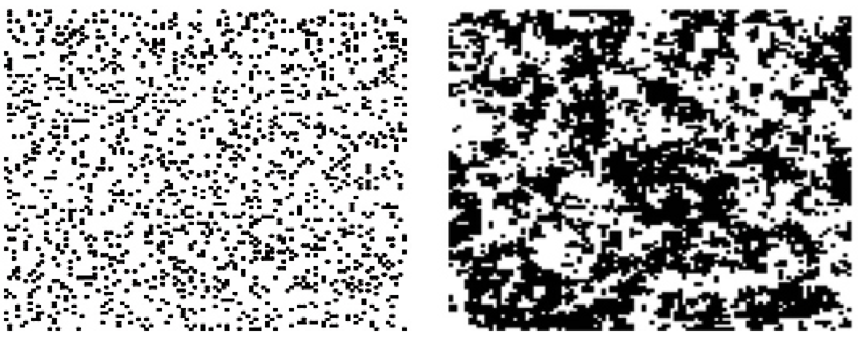

Figure 5.41: An Ising spin simulation with an initial configuration of 15% spins up (black) and after 1000 iterations. This shows the system evolving to the equilibrium state of 50% up spins and 50% down spins with a magnetization of zero.

more or less stable configuration of half the spins up and half the spins down whose magnetization is zero as in Figure 5.41.

Generally, there is a small degree of fluctuation of the magnetization over subsequent iterations that preserve energy because the system is finite.

Moreover, if we also plot values of energy) vs. magnetization for the equilibrium configuration after the system has settled down, and do this over a wide energy range, we find a relationship close to the idealized one (Figure 5.42). Just below the critical value, the equilibrium magnetization can fluctuate rapidly between the higher and lower states but the overall result looks much like the ideal graph.

Another more sophisticated cellular automata model of Ising spin dynamics has been developed by Creutz [1986] but the algorithm also conserves constant total energy and updates cell spins in a checkerboard fashion. Of course there are many other types of models that have been explored and we have only given the briefest introduction to the subject here.

5.5.5 Steady-State Heat Flow

By allowing the cells of our lattice to have any values whatsoever, we can obtain quantitative information on a whole host of problems in physics. One such is the determination of the steady-state temperature (i.e. not changing with time) of the interior of a homogeneous body when only the surface temperature is known. The temperature at each point of the interior is governed by a famous partial differential equation known as the Laplace equation:

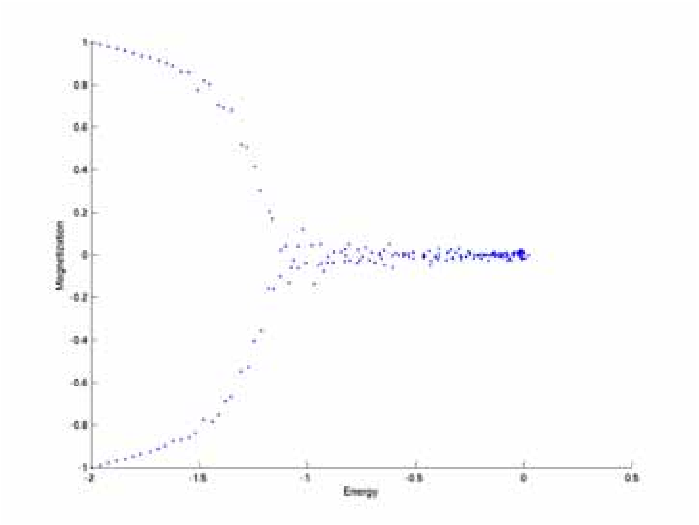

Figure 5.42: In this depiction of *magnetization* vs. *energy*, we have considered on a checkerboard lattice a range of random initial sites with the proportion of up spins ranging from 0% to 100% respectively. The spins that are energy preserving on black and white cells are flipped until the magnetization stabilizes and that value is then plotted for the given energy value. Note that the graph is very close to the ideal depicted above.

$$\frac{\partial^2 u}{\partial x^2} + \frac{\partial^2 u}{\partial y^2} + \frac{\partial^2 u}{\partial z^2} = 0,$$

where $u(x, y, z)$ denotes the temperature at each point (x, y, z). This equation is also satisfied by electrostatic and gravitational potentials and is thus one of the fundamental equations governing how the world works.

Let us consider a solid sphere of some homogeneous material and suppose that the surface of the sphere is held at a specified temperature which may vary continuously from point to point on the surface. The interior will in time reach an equilibrium steady-state temperature which we now seek to determine. The salient feature about this situation is that the temperature at the center of the sphere should be exactly the *average* of all the values on the surface of the sphere. This is so because each point on the surface is equidistant from the center and thus influences the temperature there exactly to the same degree (no pun intended); see Figure 5.43.

Mother Nature knows this and makes this obvious choice for the temperature at the center. This feature of the steady-state temperature (or electrostatic and gravitational potentials for that matter) is called the *mean value property.* The same property holds if we consider a thin circular disk and put a suitable temperature distribution on its circumference. The steady-state temperature at the center of the disk will be the average of the temperature values on the circumference. For this important property of the mean value to hold, the boundary temperature distribution should essentially be continuous but it can have a finite number of jumps or 'discontinuities'. These are actually of no consequence and Mother Nature can deal with these as well. We will employ such a boundary temperature with a few discontinuities in the example below.

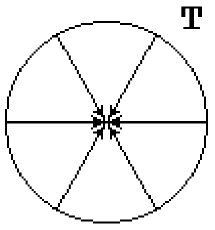

Figure 5.43: A circular region with a continuous temperature distribution T on the boundary. Since every point on the boundary is equidistant from the center, the (steady-state) temperature at the center will be the average of all the values of T.

Suppose that we wish to measure the temperature inside a rectangular region that is twice as long as it is wide and for the sake of simplicity, say this is just a two-dimensional figure. Let us put a temperature distribution of 100^o F on one long side and maintain 0^o F on the three other sides as in the Figure 5.44.

Let us try to find the steady-state temperature at the *center* of the rectangle. We fill up the rectangular region with a lattice of square cells and can cheat a trifle here by putting in 101 square cells along the long sides of the rectangle and 51 square cells along the shorter sides, thus giving us a cell that surrounds the point in the center. The ratio of length to width is not exactly 2-to-1, but certainly near enough. The cells bordering one long side take the fixed boundary value of 100^o F and the cells along the other sides take the fixed value 0^o F as in Figure 5.44.

All we need now is the transition rule which will follow naturally from the mean value property. Taking a Moore neighborhood for each cell, the eight neighbors around the central cell will be a sufficient approximation to a circular neighborhood.

By the mean value property, each central cell should be the average of its neighbors and so this is how each central cell will be updated at the next

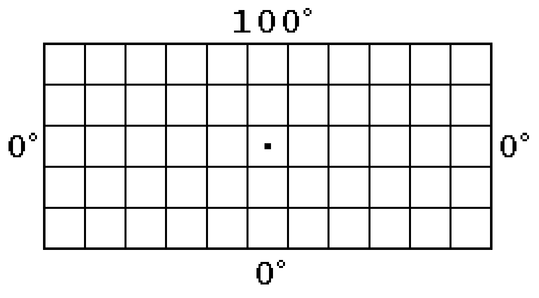

Figure 5.44: The rectangular region with length twice as long as it is wide and having a temperature distribution as indicated on its boundary. How warm will it be at the center of the figure?

time step. However, the cells at the corners of the Moore neighborhood, namely, a, c, f, h do not have the same influence as the cells b, d, e, g that are directly facing the central one and we take their value to be one-half that of the former ones. A little algebra gives us the formula for the transition rule:

$$T = \frac{b+d+e+g}{6} + \frac{a+c+f+h}{12},$$

where T is the temperature at the next time step of the central cell, and a, b, c, d, e, f, g represent the values of the neighboring cells at the current time step. We can check this is correct by putting a temperature of 1 in each of the eight neighborhood cells. Then the value at the center will then be $T = \frac{1+1+1+1}{6} + \frac{1+1+1+1}{12} = 1$, the desired 'average' value.

Running the cellular automaton we find that the value of the central cell converges to $T = 44.5120^o$ F, where all cell values have been rounded off to 4 decimal places in each calculation. Thus we have actually used in the entire procedure, a finite number cell values (= states), but we did not *a priori* specify each of them, and so the number of cell states must be considered potentially infinite. While we have not actually found the temperature at the central point of our region, but rather a value for the whole of the central cell, this is consistent with what can actually be measured in practice.

There is another rather interesting way in which to determine the value of the temperature at the center of our rectangle. In 1941, the Japanese mathematician Shizuo Kakutani discovered that for a problem such as this one, the temperature at any interior point p of the rectangle was equal to the probability (times 100) of a 'random walk' that started at p first hitting the side having the 100^o F temperature, i.e. the top side.

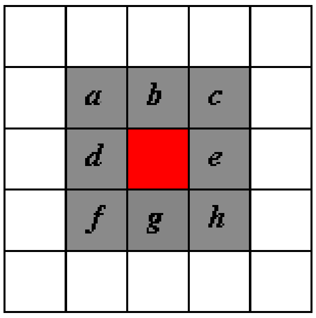

Figure 5.45: The eight neighbors taken in the mean-value temperature calculation of the central cell.

Firstly, what is a random walk? Basically, it is a path consisting of very small steps such that each step is taken in a random direction, like the path a drunkard would take after a few too many (Figure 5.46).

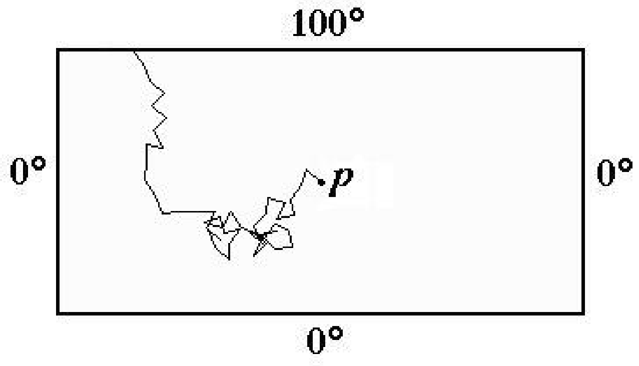

Figure 5.46: Random walk simulation inside a rectangle in order to determine the temperature at the starting point at the center.

So, if we start a particle at the center of the rectangle and take a sequence of small steps each time in a random direction, eventually we will hit one of the sides (it is a mathematical fact that we will not wander around the interior of the rectangle forever). If we first hit the side with the 100^o F, we stop the particle and keep a tally of this and repeat the random walk of the particle from the center again and again after each time we hit a side. The number of hits on the 100^o F side divided by the total number of random walks taken gives us the desired probability of hitting the 100^o

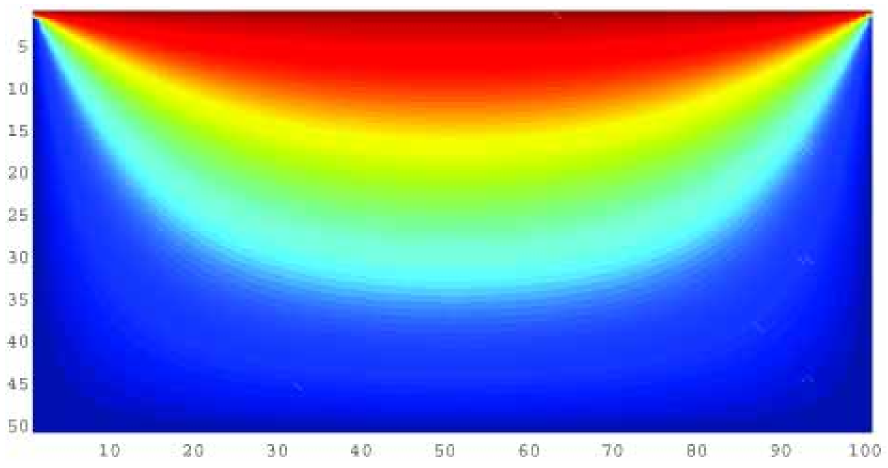

Figure 5.47: Here we have color coded the steady-state temperature values of our cellular automata simulation from red (hot) to blue (cold). See text for details.

F side first. This little algorithm is easily implemented on a computer and the simulation was run a total of ten times taking 2,000 random walks each time, with the average of these ten values at the center of the rectangle being: $T = 44.3500^o$ F, which is in very good agreement with our method using cellular automata. Of course each time we ran the random walk simulation we obtained a slightly different value because each individual random walk does indeed have a random outcome, which will not be the case in the cellular automaton approach.

Another more analytical mathematical technique available to solve this problem called the *method of separation of variables.* Without going into the technical mathematical details, the answer it gives for the temperature $u(x, y)$ at any interior point (x, y) is in the form of an infinite series,

$$u(x,y) = \frac{400}{\pi} \sum_{n=1}^{\infty} \frac{\sinh((2n-1)\pi y/a)}{(2n-1)\sinh((2n-1)\pi b/a)} \sin((2n-1)\pi x/a),$$

where a is the length of the rectangle and b is the height of the rectangle.

If we put in the coordinates of the center of the rectangle, namely (50.5,100.5), with $a = 201$, $b = 101$, and take a suitably large but finite number of terms of the series in order to calculate the sum (so even in the analytic case, we are forced to make a finite approximation), we find that $u(50.5, 100.5) = 44.4258^o$ F. This value is the most accurate, but the others are in excellent agreement with it. The value obtained by using cellular automata could have been improved further by taking the cell size even smaller, since the temperature we obtained is that for the entire central cell and we are really interested in the value at the central point. Of course this is just an illustration of what can be done using the cellular automata technique when other methods are not so accessible.

5.5.6 The Discrete Universe of Edward Fredkin

Your theory is crazy, but it's not crazy enough to be true.
Physicist Werner Heisenberg to Wolfgang Pauli

Many entities in the physical world are indeed discrete. Even though a table appears like a solid object, we know that it is made up of atoms which themselves are composed of discrete subatomic particles. Light is another entity that made up of discrete photons, and even the angular momentum of particles is known to be discrete.

It is now thought by many scientists that the fabric of space time is also discrete rather than smooth and continuous. Although this at first seems highly contradictory to experience, much of Quantum Mechanics, which is the physics of the subatomic world, has no counterparts in everyday experience. In Quantum Mechanics, the smallest components of space-time are the Planck length $\lambda_p = \sqrt{hG/c^3} \approx 10^{-33}$ cm (where h is Planck's constant, G is the universal gravitational constant, and c is the velocity of light) and Planck time $t_p \approx 10^{-43}$. The two are related in that t_p is the time it takes for a photon of light to travel a distance of λ_p, so that, $t_p = \lambda_p/c$ These are the smallest measurements of length/time that have any meaning in physics as we know it. So it is quite possible that at these scales, the physical world looks granular rather than continuous and that it evolves in a step-like process, much like the still frames in a movie film. Some work on a discrete quantum mechanics has been initiated by Succi [2002].

Computer scientist Edward Fredkin [1990, 1993], has proposed the notion of Finite Nature which is "the assumption that, at some scale, space and time are discrete and that the number of possible states of every finite volume of space-time is finite." Let us explore this idea further and see what are some of its consequences. Interestingly, Stephen Wolfram does not propose a cellular automata model of discrete space-time, but rather a different model based on a causal network of nodes (Wolfram [2002], Chapter 9) in which space-time and its contents are made up of the same ingredients.

You can see that we are now talking about a Cellular Automaton here and the scale of the Fredkin cells is somewhere between the Planck length and the Fermi distance of 10^{-13} cm, which is about the size of a proton or neutron. In fact, the exact scale is not so important for many of the consequences of the theory. Each cell has the usual 3-dimensional space coordinates x, y, z, as well as a time coordinate t in an absolute fixed reference lattice of cells.

One important consequence of the assumption that all entities in Nature are discrete is that each Fredkin cell contains only a *finite* amount of information and thus can be coded as a finite string of integers representing a particular state. Then in order for the discrete universe to evolve with (discrete) time, it must be acted upon by a *fundamental informational process* that takes the present state of the cells, and probably their past state as well, in order to determine their future, in other words, a second order system. In the resulting model of physics that Fredkin calls Digital Mechanics, the convention is adopted that a particle contains such information as its momentum, energy, spin, and rest mass in digital form.

A feature such as rectilinear motion of a particle would be achieved by the sequential updating of the particle's position with respect to the reference lattice. Such a preferred reference coordinate system is indeed essential for the description of motion in an informational based system. But Fredkin states that these coordinates are most likely implicit and contained in the bits that represents a particle's other properties, rather than explicit in the fabric of the entire universe.

Of course, there is no experimental evidence to support the existence of such a universal reference frame (although according to Fredkin, the Cosmic Background Radiation is one such example) and the famous Michelson-Morley experiment explicitly failed to detect the Earth's movement through any such reference frame. However, the existence of such an absolute reference frame does not contradict any of the laws of physics nor the Theory of Relativity.

Support for a notion of this kind comes from the Nobel Prize winning physicist, Richard Feynman (The Character of Physical Law, *Messinger Lectures*, Cornell University, 1964):

"It has always bothered me that, according to the laws as we understand them today, it takes a computing machine an infinite number of logical operations to figure out what goes on in no matter how tiny a region of space, and no matter how tiny a region of time. How can all that be going on in that tiny space? Why should it take an infinite amount of logic to figure out what one tiny piece of space/time is going to do? So I have often made the hypothesis that ultimately physics will not require a mathematical statement, that in the end the machinery will be revealed, and *the laws will turn out to be simple, like the chequer board with all its apparent complexities.*" (italics added).

The fundamental process beating at the heart of Digital Mechanics, Fredkin views as one capable of universal computation, and the reason is that the laws of physics have allowed us to build computers that are capable of universal computation and hence the fundamental process should be capable of this as well. Moreover, the fundamental process is a reversible cellular automaton (because the laws of physics are) and so the universe is run by a reversible, universal cellular automaton, or RUCA. As Fredkin claims, "What cannot be programmed cannot be physics".

Reversibility implies a conservation law of Fredkin's: Information (in Finite Nature) is conserved. We have encountered this aspect of reversible cellular automata before and seen that reversibility allows one to retrieve the initial conditions no matter how complex the subsequent evolution has been (see Section 3.7). Information is lost in a non-reversible system when two distinct configurations have the same successor so that it is not possible to choose which predecessor to return to. (Another of Fredkin's interesting achievements [1982] was the creation with Tommaso Toffoli of a billiard ball computer that allowed complete reversibility of computation, which is not normally a feature of even ordinary computers).

One essential feature of Quantum Mechanics, is randomness. Yet the randomness generated by a computer is deterministic and will be the same each time it is generated. But here we can invoke Wolfram's notion of computational irreducibility in that there is no way to predict the outcome of some computations and the only way to know the future is to compute it. This notion is embodied in the Fredkin statement, "In general, physics is computing the future as fast as it can."

Concepts such as Conservation of Energy and Momentum for particles that interact, are, in the Fredkin world, consequence of the sharing of the information that the particles possess about their energy and momentum. Since the energy and momentum information cannot be lost, it is just reshuffled among the particles and hence conserved.

So far so good, and many scientists might agree that in some sense the universe acts *as if it were* a cellular automaton. However, in Fredkin's view, it *is* a cellular automaton. This means that there is some computer (the engine) that runs the fundamental processes that run physics and that this engine exists outside our universe.

Now the theory of Fredkin is beginning to sound a bit crazy, but could it be crazy enough to be true?

Chapter 6

Complexity

Order vast, order ordained, order for free.
Stuart Kauffman

The physicist's problem is the problem of ultimate origins and ultimate natural laws. The biologist's problem is the problem of complexity.

Richard Dawkins

We have seen that with cellular automata one can sometimes achieve self-organization whereby a higher-level order is created from the local interaction of autonomous agents obeying simple rules. This type of behavior of a system of interacting units that engender some self-organizing global order that is not present at the lower level is part of the notion of *complexity.* The self-organization is an *emergent* property in that it emerges spontaneously from simple local interactions with the result that in some sense the whole is greater than the sum if its parts. This is contrary to the conventionally held reductionist view in science that the whole can be understood only through a thorough understanding of each of its parts. Who would have expected that the power of a desktop computer lay hidden in the transition function for elementary Rule 110? Could one ever have anticipated the vast diversity of Lifeforms that arose in the Game of Life or their complex interactions that produced new Lifeforms simply from knowing the rules of the game? Or the completely ordered structure that arose from the mists of the seemingly random conditions of Rule 94R in Figure 3.17? None of this order was imposed by recipe or design (which is another way to achieve complex structure such as in the blueprints for a building), but was rather an invisibly preordained consequence of the rules of local interaction, or as Kauffman says, "order for free". It is the 'ghost in the machine' if you will.

Moreover, according to Camazine *et al.*, "Complex systems... may show diverse responses that are often sensitively dependent on both the initial state of the system and nonlinear interactions among its components. Since these nonlinear interactions involve amplification or cooperativity, complex behaviors may emerge even though the system components may be similar and follow simple rules. Complexity in a system does not require complicated components or numerous complicated rules of interaction." This has been in evidence throughout all our investigations thusfar.

Self-organization can be either *intrinsic* as in the cellular automata examples examined thusfar, or it can be *extrinsic* and come about by some external stimulus, such as in the self-aggregation of the slime mold discussed in the sequel.

One problem that needs to be faced in dealing with complexity is how to define and measure it. Many people have an intuitive understanding of the concept, and would agree for example, that the human brain is more complex than that of a rat, but there is no formally accepted definition. In fact, it means somewhat different things in different fields. Ilachinski in his book on cellular automata [2002] discusses eight measures of complexity from varying perspectives under the headings: algorithmic complexity, computational complexity, graph complexity, hierarchical complexity, Shannon's information, logical depth, simplicial complexity, and thermodynamic depth. All of them are of some value in the appropriate context but all have some drawbacks as well. In computer science, complexity is related to the theoretical limits of computation itself. In biology, Dawkins [2004] gives the example (borrowing ideas from information theory) of comparing the complexity of a lobster to a millipede by writing a book describing a lobster and writing another one "down to the same level of detail" as the millipede. The lobster book is longer and so the lobster is a more complex organism. But Shannon information obeys an additive property, so this cannot be the whole story of complexity because we should not be able to generate more complex systems by simply adjoining multiple copies of simpler ones. Indeed, "The millipede book would consist of one chapter describing a typical segment, followed by the phrase, 'Repeat N times', where N is the number of segments." (Dawkins [2004]). Actually, the whole notion of biological complexity very much exercises the minds of evolutionary biologists like Dawkins and others, because highly complex systems like the human brain have already evolved over millions of years from simpler forms and are not just theoretical constructs. Indeed, Stuart Kauffman goes so far as to say that the complexity found in Nature is not only the result of natural selection but the result of self-organization as well.

Likewise, the notion of emergence is somewhat ill-defined. "None of us has a solid grasp of emergence, far less a full definition" (John Holland in *Complexity* by Roger Lewin). So in the sequel, we will content ourselves by illustrating the concepts of complexity and emergence with a number of examples. Of course, we have already seen many such examples of both concepts throughout the text. Popular accounts of the subject of emergence and complexity from a variety of perspectives can be found in Johnson [2002] and Lewin [1999].

6.1 Sea Shell Patterns

Probably most people have picked up a sea shell at one time or another and marveled at its pattern of pigmentation. There are many varieties of such patterns, each with its own beauty and challenge to the scientist as to understanding its formation. It is not known why these patterns are formed as much of the life of the mollusc is spent buried in mud and so they do not seem to be related to adaptation to their environment. The pigmentation is secreted by individual cells along the growing edge of the mollusc and it is thought that the cells are activated and inhibited by a kind of central nervous system.

As we have mentioned in Chapter 5, it was Alan Turing who first worked on the problem of mathematically replicating patters found in Nature using reaction-diffusion equations. Some years later, a computer simulation model for a pigmentation pattern on the seashell belonging to the genus *Conus* was first proposed by C.H. Waddington and Russell Cowe in 1969. Then in 1973, G.T. Herman and W.H. Liu, using their Cellular Linear Iterative Array Simulator (CELIA), obtained good results of mollusc pigmentation patterns employing one-dimensional cellular automata. Wolfram (see [2002]) uses even simpler one-dimensional cellular automata to depict similar sea shell patterns. A very successful simulation of sea shell pigmentation patterns over a wide range of pattern types was demonstrated by Hans Meinhardt in his attractive text, *The Algorithmic Beauty of Sea Shells* [1995]. Meinhardt presented numerous sophisticated reaction-diffusion models (based on work with M. Klinger) and was able to replicate details of a large variety of shell pigmentation patterns. The entire topic of the use of cellular automata modeling of biological patterns can be found in the text by Deutsch & Dormann [2005].

Ermentrout, Campbell, & Oster [1986] proposed a neural activation-inhibition model which can be presented in the basic CA form:

$$x_{n+1}^{j} = H\left(A_n^j - I_n^j - \theta\right),$$

where x_n^j represents the state (either 0 or 1) of the jth cell position in the nth row and A_n^j is the activation component, I_n^j is the inhibition component, θ the threshold, and H is the Heaviside step-function. The activation and inhibition are suitably defined in terms of weighting factors involving long range interactions. Another approach by Vincent [1986] used a totalistic cellular automaton model that did not seem to have much justification in a biophysical sense.

The cellular automata model we discuss below is due to Ingo Kusch and Mario Markus [1996] that developed out of an earlier CA model for stationary Turing patterns and spiral waves by Schepers and Markus [1992]. It is a probabalistic activation-inhibition model that uses the traditional 1-dimensional array and also a circular array to permit radian growth found in some molluscs, although only the former is considered here. There are only two states for a cell $c(t)$ at time step t: 0 (resting – no pigment) and 1 (activated – pigment). Whether a cell becomes activated or deactivated at the next time step depends on the amount of chemical inhibitor present at each cell site, $I(t)$. Denote by N the number of activated cells in a neighborhood of radius r about the central cell c. Two intermediate cell states are required for both $c(t)$ and $I(t)$ in order to compute their respective values at the next time step, namely

$$x(t) \to x_1 \to x_2 \to x(t+1) \qquad \text{for } x = c, I.$$

The rules of the automaton are:
(i) **Decay of inhibitor**
If $I(t) \geq 1$, then $I_1 = I(t) - 1$, otherwise $I_1 = 0$.
(ii) **Activator production due to random fluctuations**
If $c(t) = 0$, then $c_1 = 1$ with probability p, otherwise $c_1 = c(t)$.
(iii) **Production of inhibitor due to activator**
If $c_1 = 1$, then $I_2 = I_1 + w_1$, otherwise $I_2 = I_1$.

(iv) **Activator production from diffusion of activator**
If $c_1 = 0$ and $N > \{m_0 + m_1 I_2\}$, then $c_2 = 1$, otherwise $c_2 = c_1$.

(v) **Diffusion of inhibitor**
$I(t+1) = \{\langle I_2 \rangle\}$.
(vi) **Suppression of activator due to inhibitor**
If $I(t+1) \geq w_2$, then $c(t+1) = 0$, otherwise $c(t+1) = c_2$.

Here the notation $\langle\rangle$ means take the average over a neighborhood of radius R, and $\{\}$ means take the nearest integer. The authors found that at times another rule was needed which replaced rule (i):

(i*) **Decay of inhibitor**
If $I(t) \geq 1$, then $I_1 = \{(1-d)I(t)\}$, otherwise $I_1 = 0$.

There are eight free parameters that the experimenter has to play with: r, R, w_1, w_2, m_0, m_1, p, and d. Here R denotes the typical length for the spread of the inhibitor whose average is determined in rule (v). Also, w_1 is the amount of inhibitor produced in each activated cell per time step (rule

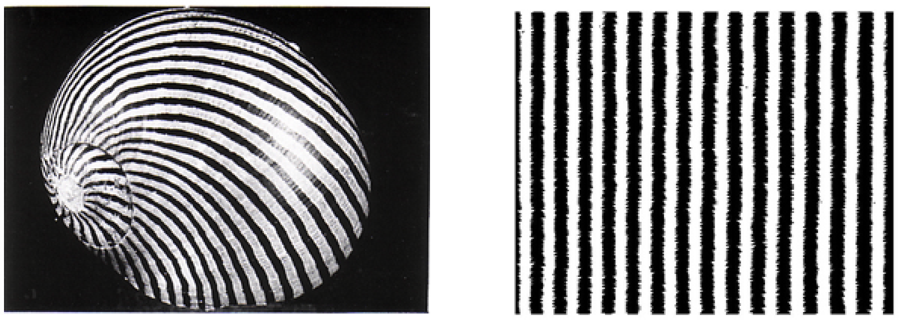

Figure 6.1: Left: *Neritina ziczac* (Philippines). Right: $r = 1$, $R = 17$, $w_1 = 1$, $w_2 = 1$, $m_0 = m_1 = 0$, $p = 2 \times 10^{-3}$. Left image courtesy Kusch & Markus.

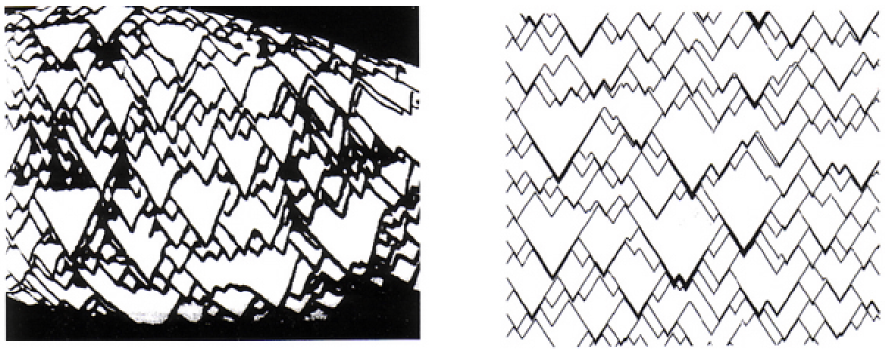

Figure 6.2: Left: *Olivia porphyria* (Panama). Right: $r = 2$, $R = 0$, $w_1 = 10$, $w_2 = 48$, $m_0 = m_1 = 0$, $p = 2 \times 10^{-3}$. The activation is propagated from cell to cell via 'traveling waves' that annihilate upon contact with another. Images courtesy K&M.

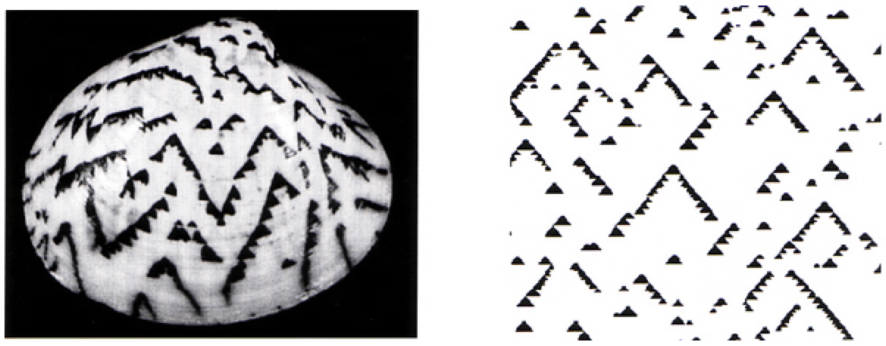

Figure 6.3: Left: *Lioconcha castrensis* (Philippines). Right: $r = 1$, $R = 16$, $w_1 = 8$, $w_2 = 6$, $m_0 = m_1 = 0$, $p = 2 \times 10^{-3}$. Considered to be of Class IV although this is not so apparent as in some other patterns. Images courtesy K & M.

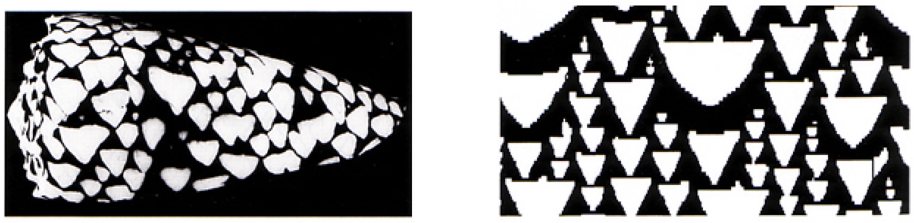

Figure 6.4: Left: *Conus marmoreus* (Philippines). Right: $r = 4$, $R = 9$, $w_1 = 2$, $w_2 = 19$, $m_0 = 0$, $m_1 = 0.2$, $p = 0$. Images courtesy K & M.

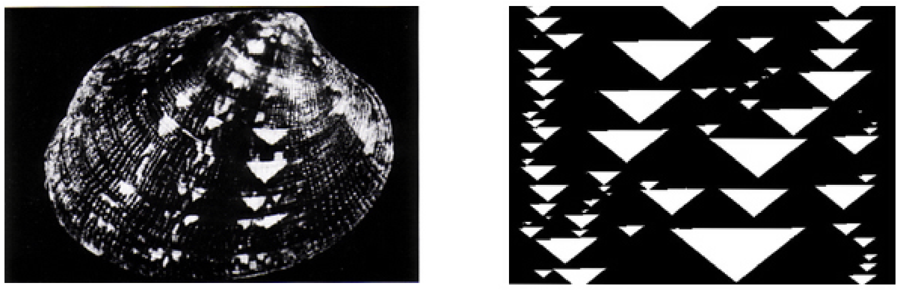

Figure 6.5: Left: *Chione grisea*. Right: $r = 1$, $R = 23$, $w_1 = 4$, $w_2 = 71$, $m_0 = m_1 = 0$, $p = 0$, $d = 0.05$ (rule i*). Left image courtesy K & M.

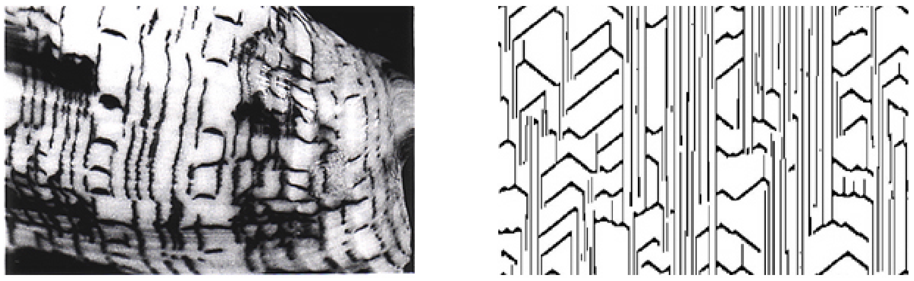

Figure 6.6: Left: *Voluta hebraea.* Right: $r = 1$, $R = 2$, $w_1 = 5$, $w_2 = 10$, $m_0 = 0$, $m_1 = 0.3$, $p = 2 \times 10^{-3}$. Stationary lines (where the inhibitor is high) and traveling waves (where the inhibitor is low) are the two competing forms. Considered to be of Class IV. Images courtesy K & M.

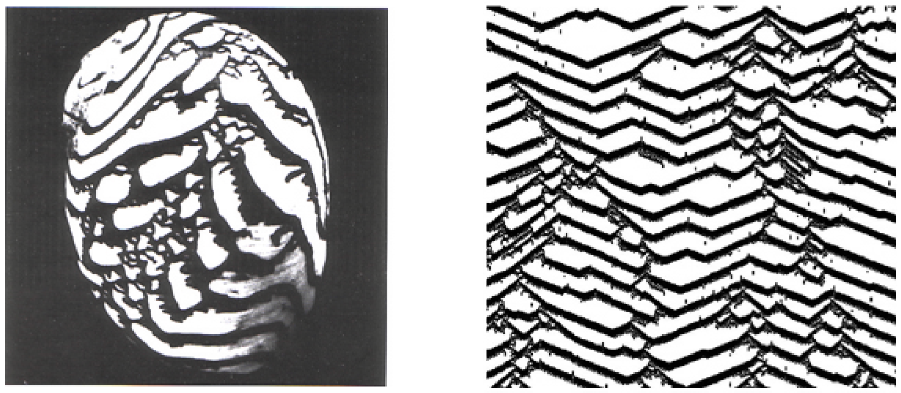

Figure 6.7: Left: *Neritina pupa* (Antilles). Right: $r = 2$, $R = 0$, $w_1 = 6$, $w_2 = 35$, $m_0 = 0$, $m_1 = 0.05$, $p = 2 \times 10^{-3}$, $d = 0.1$ (rule i*). Considered to be of Class IV. Left image courtesy K & M.

(iii)) and w_2 is a threshold that once it is surpassed, inactivates the cell at the next time step (rule (vi). The radius r is the typical length over which the activation is propagated and m_0 is the threshold for activating a cell whenever there is no inhibitor (i.e. when $I_2 = 0$ in rule (iv)), and m_1 is another activation threshold value dependent on the inhibitor value (I_2). The variable d is the fraction of the inhibitor $I(t)$ that is lost at each time step, so that rule (i*) means that the inhibitor decays exponentially, as opposed to the linear decay of the inhibitor in rule (i). Lastly, p is the probability that an inactivated cell becomes activated by random fluctuations (rule (ii)). The automaton starts with initial conditions $I(0) = 0$ for each cell site with the activated and non-activated cells distributed randomly.

Above are some samples of various species of mollusc and their cellular automaton counterparts together with the parameters used in each case.

One very noteworthy feature of this model is that the pigmentation patterns generated by it include the Wolfram classes 2,3, and 4. In Figure 6.1 we see an example of Class II behavior, and in Figures 6.2, 6.4 and 6.5, Class III dynamics is evident. In Figures 6.6 and 6.7 we see evidence of Class IV phenomena, and Kusch and Markus have even devised a quantitative measurement which is used to discriminate between the four classes to support their assertions. Accordingly, Figure 6.3 is also given Class IV status although this is not obvious visually. The authors claim these examples, "would be the first experimental evidence for class IV processes in nature."

It is interesting to compare the CA approach of Kusch and Markus with the reaction-diffusion models of Meinhardt. As it turns out, some shell patterns are modeled equally well in both approaches, some are more effectively simulated using the CA approach (those involving traveling waves and Class IV patterns), while it is conceded that the Meinhardt-Klinger partial differential equations have managed to reproduce some patterns that the CA's could not. At least not yet.

6.2 Autonomous agents

The notion of an autonomous agent has taken on a life quite independent of cellular automata theory and is a major subject of research, such as in the study of complex adaptive systems. Often the differences between cellular automata and agent based models (or individual based models – IBMs) are purely semantic. Over the years, numerous definitions of an autonomous agent have been proposed (see Franklin & Graesser [1996]) but a general one might be: *a computational system in a dynamic environment that senses this environment and acts autonomously within it.* Of course, an individual cell of a cellular automaton falls into this category but some autonomous agent models are more general in nature than a cellular automaton. A notable example is the popular interactive computer simulation, *The Sims*, that allows the user to interact with a host of human-like autonomous agents. Autonomous agents have also been used to model political conflicts (Ian Lustick's *Virtual Pakistan*, and *Middle East Polity*) as well as military ones (the Pentagon's *OneSAF*). Of course, all of these are just models, based on the rules built into them, so that the output is virtual and not necessarily real. On the other hand, Lustick has successfully tested *Virtual Pakistan* against real field data like, "What proportion of Pushtuns who live in cities are also part of the commercial elite?", even though this sort of data was not part of the program itself (*Popular Science*, March, 2004).

In this regard, a particularly useful software development is *Swarm* created by Christopher Langton and developed at the Santa Fe Institute in New Mexico. It provides the environment in which autonomous agents can be employed to model a whole host of collective behavior and has been used by scientists to study among other things, rain forest ecosystems and nuclear fission chain reactions.

Swarm is intended to be a useful tool for researchers in a variety of disciplines. The basic architecture of *Swarm* is the simulation of collections of concurrently interacting agents: with this architecture, we can implement a large variety of agent based models. For an excellent presentation of how self-organization pertains to swarms and its many applications to problems of optimization, see the monograph by Bonabeau, Dorigo, and Theraulaz [1999].

6.2.1 Honey Bees

One creature that does indeed swarm is the honey bee, a subject of much fascination. "The challenge here is to understand how a colony-level (global) structure emerges from the activities of many individuals, each working more or less independently. In the building of these large biological superstructures, it is difficult to imagine that any individual in the group possesses a detailed blueprint or plan for the structure it is building. The structures are orders of magnitude larger than a single individual and their construction may span many individual lifetimes. It seems far more likely that each worker has only a local spatial and temporal perspective of the structure to which it contributes. Nonetheless, the overall construction proceedes in an orderly manner, as if some omniscient architect were carefully overseeing and guiding the process." [Camazine *et al.* 2003]. The authors then proceed to demonstrate how a characteristic pattern develops on the honeycomb due to a self-organizing process of the bees.

But let us look into the actual construction of the honeycomb. First of all, each cell of the honeycomb is hexagonal in shape, which itself appears to be a self-organizing phenomenon. "There is a theory, originally propounded by Buffon and now revived, which assumes that the bees have not the least intention of constructing hexagons with a pyramidal base, but that their desire is merely to contrive round cells in the wax; only, that as their neighbours, and those at work on the opposite sides of the comb, are digging at the same moment and with the same intentions, the points where the cells meet must of necessity become hexagonal." (Maeterlinck [1901]).

Each cell of the honeycomb is about 12 mm long and the worker bees deposit royal jelly into them onto which the egg is laid. The honeycomb is double sided with the cells from each side meeting in the middle. But the base of each cell is not just flat across the bottom because a little depression or well is required to keep in the royal jelly in place as well as the egg. The bees create this depression in the form of a 3-sided pyramid. The pyramidal bases for each cell from one side of the honeycomb are interleaved with the pyramidal bases coming from the other side of the honeycomb so that it all fits snugly together.

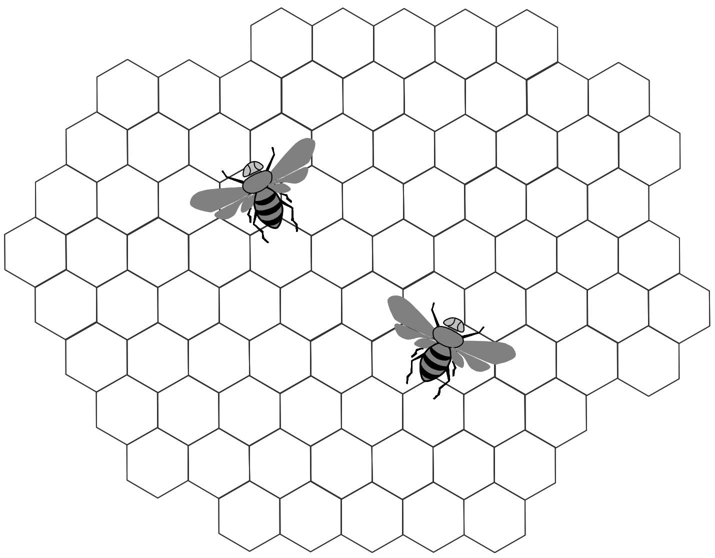

Figure 6.8: The honeycomb consists of a double-sided hexagonal array of cells wih a pyramidal base at the bottom end of each cell.

But something even more profound happens in the construction of the honecomb. The question one can ask is, "At what angles should the three planes of the pyramid meet, if one wished to minimize the amount of labor and material that goes into their construction?" This turns out to be a rather non-trivial mathematical question requiring a knowledge of Calculus:

"... it has been demonstrated that, by making the bottoms of the cells to consist of three planes meeting in a point, there is a saving of material and labour in no way inconsiderable. The bees, as if acquainted with these principles of solid geometry, follow them most accurately. It is a curious mathematical problem at what precise angle the three planes which compose the bottom of a cell ought to meet, in order to make the greatest possible saving, or the least expense of material and labour. This is one of the problems which belong to the higher parts of mathematics. It has been accordingly been resolved by the ingenious Maclaurin, by a fluctionary calculation, which is to be found in the Transactions of the Royal Society of London [1743]. He has determined precisely the angle required [70° 32′, 109° 28′], and he found, by the most exact mensuration the subject would admit, that it is the very angle in which the three planes at the bottom of the cell of a honeycomb do actually meet."(Maeterlinck [1901]).

Maeterlinck then attempts to come to terms with the notion of complexity well before the concept was ever enunciated, "I myself do not believe that the bees indulge in these abstruse calculations; but, on the other hand, it seems equally impossible to me that such astounding results can be due to chance alone, or to the mere force of circumstance."

6.2.2 Slime Molds

Another model based on Turing's morphogenesis work was formulated by Evelyn Keller and Lee Segel [1970] to describe the unusual behavior of the species of slime mold, *Dictyostelium discoideum.* It consists of thousands of independent-living amoebae that feed off bacteria on the forest floor and normally live and move freely from one another. During periods of adverse conditions such as food scarcity, up to 100,000 cells aggregrate into a single organism (the 'slug' stage) that moves about in search of food. At a later stage, the slug transforms itself into a 'fruiting body' comprised of a globule of spores sitting atop a slender stalk. Under suitable conditions the spores are released and germinate to begin the life-cycle anew. How this oscillation between single organism - multiple organisms is achieved has been the subject of intense scientific investigation. Prior to Keller and Segal's work, the prevailing theory due to B.M. Shafer of Harvard was that so-called "pacemaker" cells of the slime mold would release a chemical signal, known as cyclic AMP, which would trigger other cells to do the same and so on throughout the dispersed community of cells. The cyclic AMP was a signal to re-form the aggregate. The only difficulty with this theory, since the release of cyclic AMP was well documented, was that all slime mold cells were much like any other and no "pacemakers" could be found.

According to the Keller-Segel version of the theory, the individual amoebae begin to aggregrate on their own when some cells (which could be thought of as 'pacemakers') perceive adverse environmental conditions and begin releasing cyclic AMP. This triggers a chain-reaction of the other amoebae in the colony to release the chemical and in response they would gravitate towards regions of highest concentrations of cyclic AMP in a process known as *chemotaxis* This leads to the formation of small clusters which become

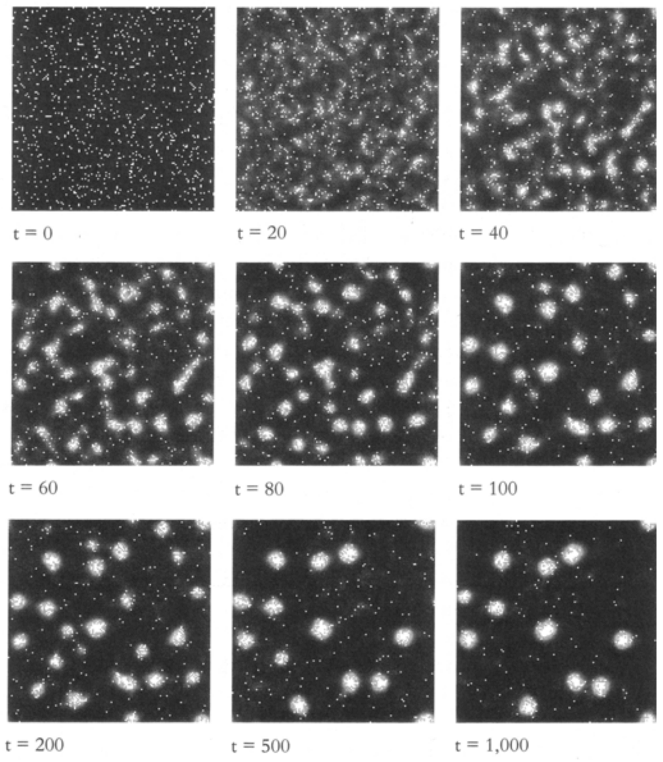

Figure 6.9: The slime mold simulation of Mitchel Resnick starting with 1,000 cells at various time steps. It is thought that eventually one aggregate will form. Courtesy Mitchel Resnick, *Turtles, Termites, and Traffic Jams.*

larger with the final result being the aggregrate slime mold organism. *D. discoideum* illustrates how in Nature a self-organizing system can be formed from the simple interaction of autonomous agents. A comprehensive discussion of various models of slime mold aggregation can be found in the paper by Alan Garfinkel [1987]. A computer simulation that captures some of the salient features of slime mold aggregration has been developed by Mitchel Resnick of MIT and is discussed in his book, *Turtles, Termites, and Traffic Jams* [1994]; see Figure 6.9.

Rather interestingly, the cyclic AMP released by the amoebae washes through the colony in waves and spirals that can be described by the Hodgepodge Machine (Section 5.1.3)! However, this particular feature does not appear to be essential to the aggregration process as was demonstrated by Prigogine and Stengers [1984] although Camazine *et al.* [2001] point out that it may serve some adaptive purpose in the case of the slime mold.

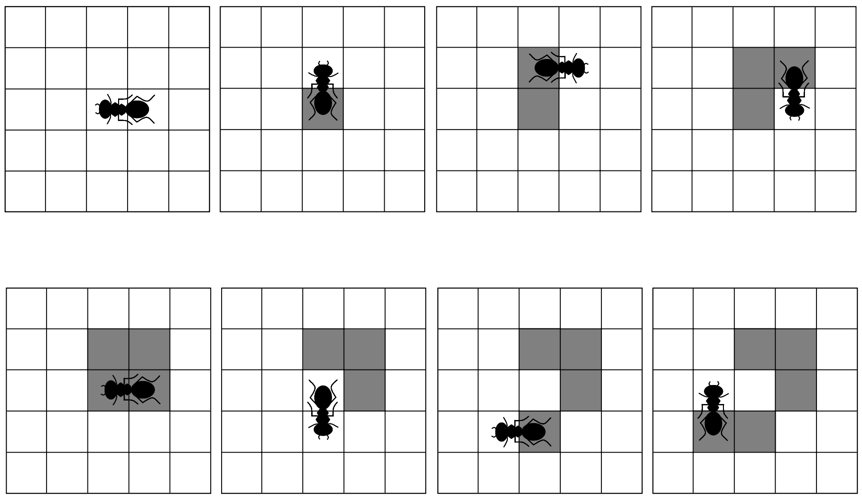
Figure 6.10: The first eight steps taken by Langton's ant.

6.2.3 Langton's Ants

In Christopher Langton's 1986 study of artificial life, one of the things he considered was the activities of ants because they can exhibit complex behavior arising from very simple interactions with their environment. To this end he created *virtual ants* or *vants* that play out their lives in a cellular array. These were independently discovered by Greg Turk, although in the more general setting of Turing machines moving on a two-dimensional grid (see A.K. Dewdney's *Scientific American* article [1989] who christened them of 'tur-mites'). Let us start with an initial configuration of all white cells (state 0), although a random initial condition of white and black cells (state 1) is also possible. Consider a solitary vant on a central white cell that is facing in an E-W (or N-S) direction. The ant behaves in the following manner:

• It changes any white cell it is on to black, then turns 90° to the right and moves one cell forward;

• It changes any black cell it is on to white, then turns 90° to the left and moves one cell forward.

Thus a vant operates as a virtual Turing machine on a two-dimensional tape and as such is not a true cellular automaton in that all cells are not updated simultaneously by a local rule.

It can be seen in the figures above that the ant quickly starts to run into cells that have already been visited, and for the first 500 or so steps creates somewhat symmetrical patterns with 180° rotational symmetry, returning periodically to the central square. It then begins to move in a very random fashion for thousands of steps. The long term evolution of the vant however,

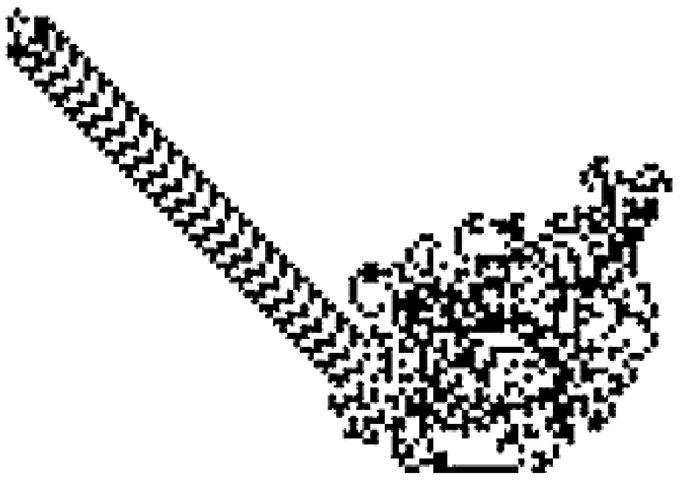

Figure 6.11: Langton's ant after 11,000 steps with the infinite highway well under construction. This same structure was independently discovered by Greg Turk and appears in *Scientific American*, September 1989, p. 126.

is quite unexpected.

Eventually, after more than 10,000 time steps have elapsed, a diagonal "highway" is constructed by the ant that consists of a sequence of 104 steps that then shifts one cell horizontally and vertically (Figure 6.11) and then repeats this process endlessly.

Although it has so far not been proven that the ant will always build a diagonal highway, empirical evidence suggests that this is indeed the case even if the initial grid contains a finite number of black squares!

Various generalizations of the vant have been considered. The simplest is to change the rectangular array to some other shape such as a hexagonal grid (see http://www.dim.uchile.cl/~agajardo/langton/general.html).See Figure 6.12.

Another way to generalize the virtual ant is to allow each of the cells of the array to exist in n states instead of just two, say states (or colors): $0, 1, ...n-1$. If the ant lands on a cell in state k, it changes it to state $k+1$ $(\text{mod}\, n)$, so that each state value is increased by one and state $n-1$ changes to state 0. The direction the ant is to turn is governed by a fixed *rulestring* of n symbols consisting of **0**'s and **1**'s. If the ant lands on a cell that is in state k, one then checks the $(k+1)st$ symbol of the rule-string and if it is **1** the ant turns right 90° and moves one cell forward and if it is **0**, the ant

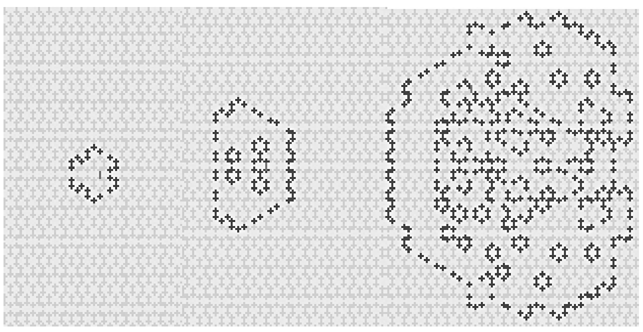

Figure 6.12: The Langton ant on a hexagonal array showing bilateral symmetry in an enlarging pattern. Time steps are at 72, 810, and 15,600.

turns left 90° and moves one cell forward. The rulestring also serves to give an identification number in base 2 so that the ant with rulestring **1001** is called ant 9. Langton's original ant is ant 2 since its rulestring is **10**.

Generalized ants were considered by Greg Turk as remarked above and independently by Leonid Bunimovich and S.E. Troubetzkoy [1994]. Although there are not many definite results that have been proven about generalized ants or even Langton's original ant for that matter, we do have the following beautiful theorem:

Bunimovich-Troubetzkoy Theorem. *The time evolution of the generalized ant is unbounded if the rulestring contains at least one* 0 *and one* 1.

That is to say, that the complete trajectory of the ant is not contained within the bounds of any finite array of cells, no matter how large. The argument goes like this. Let us suppose that we are dealing with the Langton ant (rulestring **10**), although the proof (given in Bunimovich-Troubetzkoy [1992]) also applies to the general case. Note first that the cell pattern the ant has created together with its current position and heading uniquely determine the ant's future, and the same is true for its past because the rule governing its behavior is completely reversible. Now if we assume to the contrary that the trajectory of the ant is actually bounded, it follows that at some stage, the ant will repeat the same pattern sequence, position and heading because these are only finite in number. By reversibility, the ant's past must be a repetition of this pattern and clearly, so must the ant's future behavior. In other words, the ant exhibits periodic behavior visiting the same collection of cells infinitely often and nothing more.

Because the ant always turns 90° to the left or right after it enters a cell, if it enters horizontally it leaves vertically and if it enters vertically it leaves horizontally. Thus, (depending on the ant's starting orientation), all the cells can be labelled either h (entered horizontally) or v (entered vertically) with contiguous cells taking the opposite designation in a checkerboard fashion. Now there will be one cell which we call M that is as far to the right and top of the array as is possible. Thus any cells to the top or right of M are not visited by the ant. If M happens to be an h cell, it must have been visited horizontally from the left. It must turn $90°$ to the right implying that M must have been a white cell which the ant turns to black. On the next cycle of the ant, since M is now black and entered horizontally from the left, the ant must turn $90°$ to the left and exit vertically out the top of M. But no cells above M are visited, resulting in a contradiction. If M is a v cell, a similar contradiction arises. Thus it must be the case that the trajectory of the ant is unbounded, proving the theorem.

Some trajectories of the generalized ant are trivial, such as the one with rulestring **11** which simply goes around and around a 2 x 2 square. Other trivial rulestrings are **111**, **1111** etc. Rulestring **01** is just the mirror image of the Langton ant. For ants with rulestring of length $n > 2$, take cell state 0 to be white and cell state $n - 1$ to be black, using shades of gray for the intermediate cell states with all cells initially in state 0. In what follows are some results of computer simulations by James Propp.

Ant 4 (**100**) creates various symmetrical patterns with bilateral symmetry (6.13), but then resorts to random behavior without any evidence of settling down to some regular structure as was the case with ant 2.

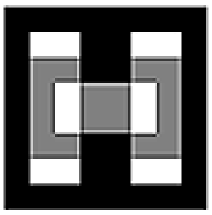

Figure 6.13: The bilateral symmetry exhibited by ant 4 at step 236 of its evolution.

Ant 5 (**101**) is similar to ant 2, but does not seem to create a highway. However, ant 6 (**110**) does create a "highway" after 150 steps, but this time the structure is composed of a sequence consisting of only 18 steps, or "period" 18 (Figure 6.14) unlike the period 104 highway of the Langton ant 2.

Ant 8 (**1000**) does not build highways nor any do other regular patterns emerge. Ants 9 (**1001**) and 12 (**1100**) create ever larger patterns that are

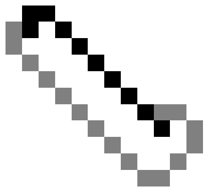

Figure 6.14: The highway exhibited by ant 6 consisting of a sequence of period 18.

exactly bilaterally symmetric the moment the ant returns to the initial cell, a phenomenon already noted by Greg Turk (Figure 6.15). Moreover, Bernd Rummler has proved that ant 12 will continue forever to build increasingly large bilaterally symmetric structures.

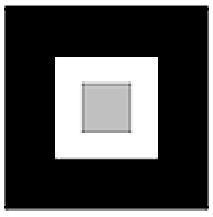

Figure 6.15: A bilaterally symmetric pattern exhibited by ant 12 at step 392 of its evolution.

Ant 10 (**1010**) has the same behavior as ant 2 (**10**) only with a 4-color trail instead of one with two colors. This is due to the general principle that if a rulestring is built up of repetitions of a shorter rulestring, then the behavior of the former will be that of the latter.

Ant 13 (**1101**) wanders around in a random fashion for about 250,000 steps, but then builds a highway having period 388. Ant 14 (**1110**) is rather interesting in that it possesses some features of ants 2 and 6. It creates a highway, but the period is 52, i.e. half that of ant 2, and the appearance is like that of ant 6. Experimental evidence of Olivier Beuret and Marco Tomassini suggests that whenever the triple **110** is preceded by **1**'s, as in **1110**, **11110**, etc. then that particular ant will also build a highway.

Employing 5-bit rulestrings, unlike ants 9 and 12, there were no ants that exhibited increasing bilateral symmetric structures. However, James Propp found one new feature in ant 27 (**11011**), namely, an increasing spiral pattern. With rulestrings of length 6, Propp found that ants 33, 39, 48, 51, 57 and 60 each exhibited bilateral symmetry, all of whose numbers are divisible by 3, but why this is so remains a mystery.

One interesting aspect of all of this is the fact that even though we know the explicit rule by which an ant's behavior is governed, the emergence of a highway after 10,000 steps for ant 2 or 250,000 steps for ant 13 is totally unexpected. Nothing in their prior behavior gives any hint that the long term future of these ants is periodic highway building, nor is there any hint in the simplistic rulestring. It is quite possible that the question of whether certain ants, such as ant 4 say, ever produces a highway is undecidable and hence their long term behavior can only be ascertained by living it.

6.2.4 Multi-ant systems

Empirical investigations of systems containing two three and four ants have been considered by my student Malcolm Walsh, using software provided by the website (in Spanish): http://cipres.cec.uchile.cl/˜anmoreir/ap/multi.html

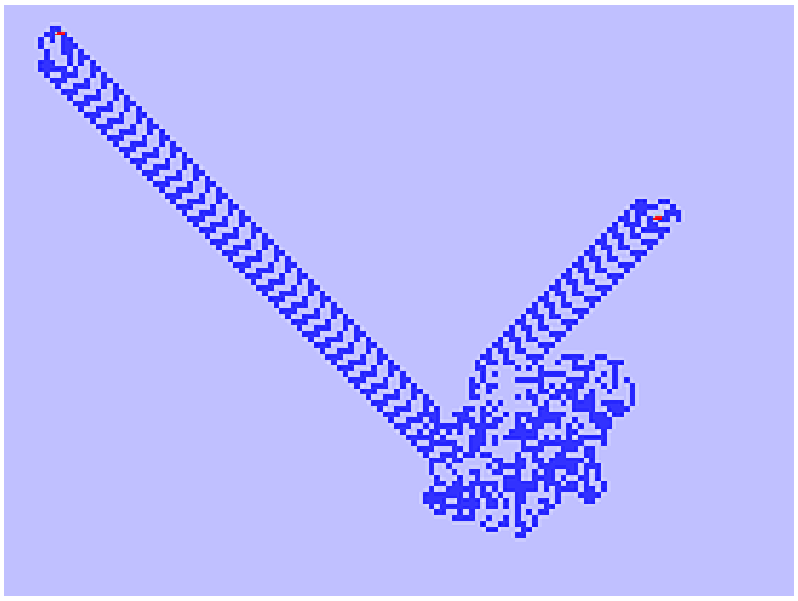

Figure 6.16: The production of individual orthogonal highways by two ants in ∼1700 steps and ∼3800 steps respectively. The ants were initially 16 cells apart horizontally with one facing north, the other south.

Interactions between two ants can have varying consequences. In dealing with multi-ant systems, there is always the possibility that at any particular time step two (or more) ants will meet up at the same square. In this instance, a right-of-way rule must be agreed upon and by numbering the ants 1,2 ... we agree that 1 preceeds 2, 2 preceeds 3 and so forth. In our first experiment with two ants 16 cells apart with one ant facing north and the other south, we find that they construct individual orthogonal highways. This is not exceptional in itself, except that the first highway appears at ∼1700 steps and the other at ∼3800 steps, whereas it takes more than 10,000 steps for a single ant to produce a highway. Whether or not two ants will always produce a highway or highways is completely unknown as in the single ant case.

Of course with two ants there is always the possibility that they will undo each other's work and return to their initial positions. This phenomenon indeed ocurrs as in the following experiment where the ants are initially displaced 16 cells apart horizontally and 1 cell vertically and facing north and south respectively. This results in periodic behavior (Figure 6.17).

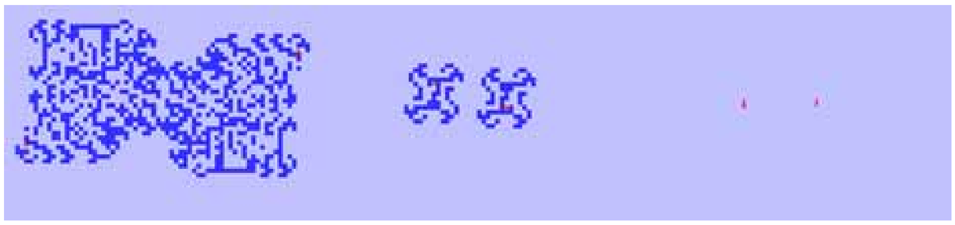

Figure 6.17: The interaction of two ants leading to the mutual destruction of all their work and their return to the initial positions and orientations, resulting in periodic behavior.

A fascinating interaction in the following experiment had the two ants forming a highway relatively quickly by one of them in ∼1700 steps. Then at ∼2500 steps, the other ant ascends the highway in order to 'attack' it, initiating the mutual destruction of all trails resulting in the ants returning to their initial positions after 5611 steps! On the surface, this certainly appears like 'intelligent' behavior, but we know that the ants are both just following the simple, dare we say 'dumb', rule set down by Langton.

In the preceding, the ants' orientations at the final stage are rotated by 180^o. Continuing to let the ants run on, they interact once more but ultimately again undo each other's work, this time returning to their original positions and orientations. This results in a periodic 2-cycle of frenzied activity. Significantly, this experiment demonstrates that: *A system of two ants can result in their behavior being entirely bounded,* in contrast to the necessarily unbounded behavior of one ant established in the Bunimovich-

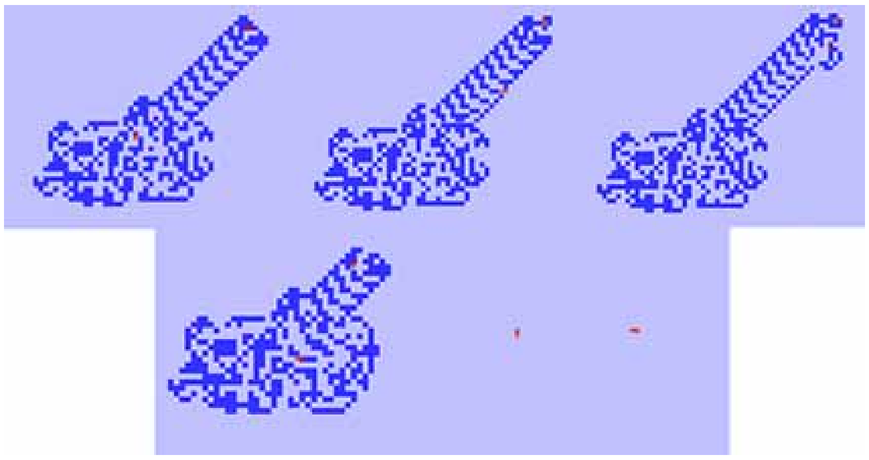

Figure 6.18: This sequence shows the construction of a highway by one of the ants (top left); the scaling of the highway by the second ant (top middle); the beginning of the destruction of the highway (top right) initiated by the second ant; the destruction of the highway by both ants (bottom left); the complete annihilation of all work by both ants and return to their initial positions but with orientations rotated by 180^o (bottom right). The original positions had one ant facing south and the other facing it from the east separated by 22 cells horizontally.

Troubetzkoy Theorem. After running this experiment and discovering this bounded behavior we found that this phenomenon has also been noted in the book by Chopard and Droz [1998]. Of course, as we have seen above, there are two-ant systems that exhibit unbounded behavior as well. Similarly, four-ant and eight-ant systems have been found that exhibit analogous 2-cycle bounded behavior for all time.

In a further two ant scenario, if ant1 and ant2 are separated by 10 cells horizontally and 11 cells vertically, with ant2 northwest of ant1 and facing east, while ant1 is facing north, then the ants begin to make a *cooperative* highway after around 500 steps which seems to be a heretofore unobserved phenomenon. This cooperative highway extends itself slightly faster then the normal Langton highway and has a period of 102 compared to the Langton highway which has a period of 104. It seems that the creation of this cooperative highway is the fastest way for an ant to travel, that is, if an ant has somewhere to go, it saves time to work in pairs.

Another interaction that can occur is that one ant building a highway will meet the highway of another ant. One scenario is that the ants cease their highway construction and revert to more disorderly behavior. On the other hand, it is possible for the ant hitting the highway of the other to actually proceed out the other side of the first ant's highway as in Figure

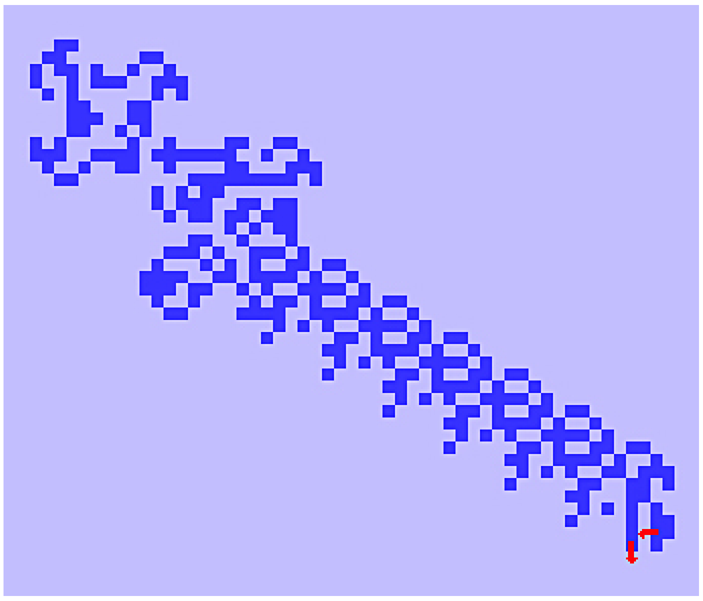

Figure 6.19: The cooperative highway made by two ants having period 102 and a form of rapid transit for each ant.

6.20 below.

In three-ant systems, experiments have shown that multiple highway systems can be built and unbuilt, however it seems to be the case that these systems are again unbounded as for a single ant. Once again, the 102 step cooperative highway structure can be created by two of the ants with suitable initial conditions. Around step 5000 ant3 will begin creating its own Langton highway in nearly the opposite direction, never to interact with the other two ants again (Figure 6.21).

Four-ant systems display similar characteristics to two-ant systems with most leading to four unbounded highways, and as mentioned above, along with eight-ant systems some have been shown to remain bounded. This occurs if the ants are symmetrically placed so that they will pair off with the result that the highway constructed by one of the pair will eventually be undone by the other.

6.2.5 Traveling Salesman Problem

Virtual ants have found a very real application in finding a solution to the famous 'traveling salesman problem'. An early instance of it was presented at a mathematical colloquium in Vienna by the mathematician Karl Menger in 1930 as 'Das botenproblem' ('messenger problem').

A number of cities are spread out across a two-dimensional map and

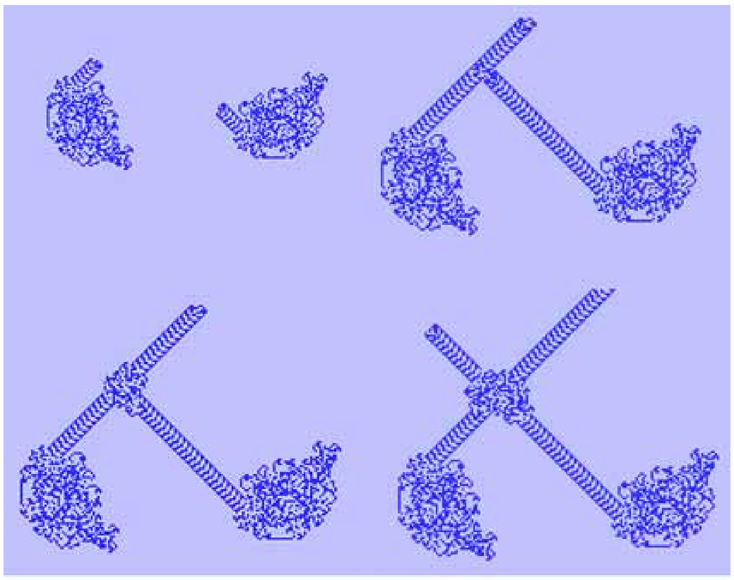

Figure 6.20: In a 2-ant system we can have intersection of two highways and the continued construction of both, one out the other side of the other. Here the initial positions were 93 cells apart horizontally with one facing south and the other to the west of it facing west.

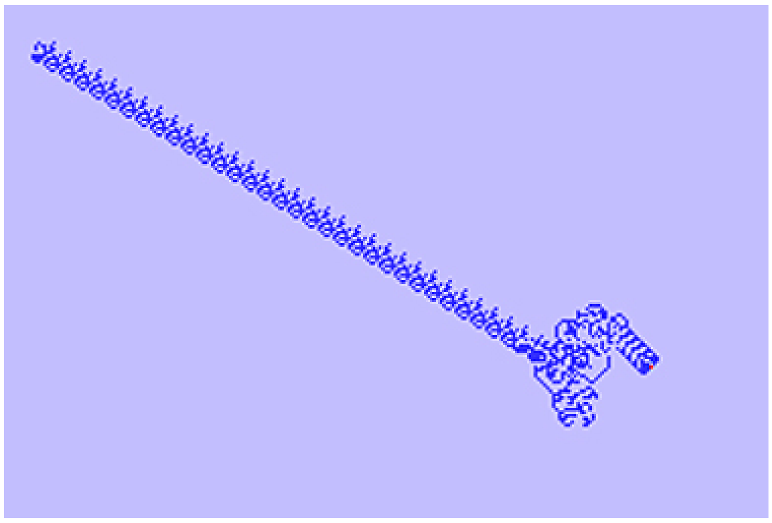

Figure 6.21: The 3-ant system after 500 steps that shows the construction of the period 102 cooperative highway by two of the ants (left) and the third ant starting to make its own Langton highway (right).

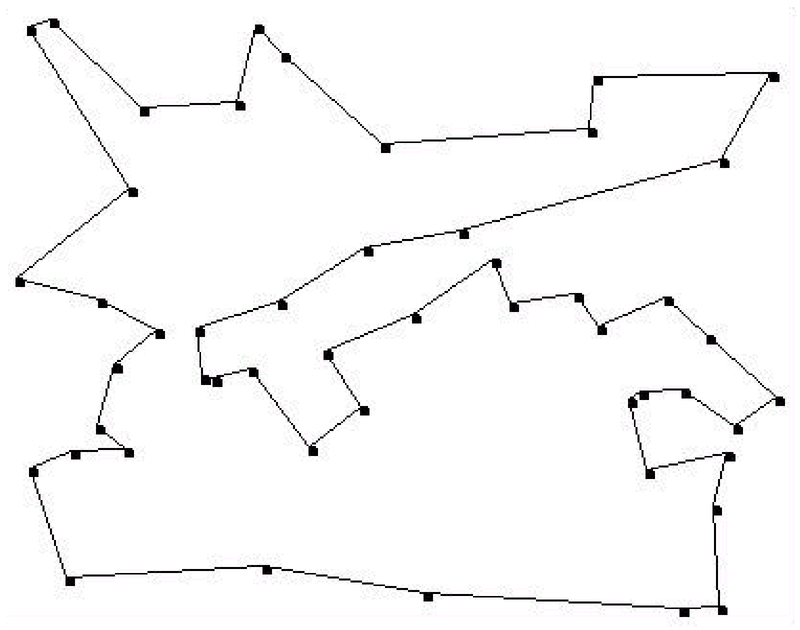

Figure 6.22: A 50 city optimal route solution to the traveling salesman problem by Tomáš Kojetinský.

a traveling salesman is required to find the shortest route that visits each of the cities once and returns to the original site. Of course the salesman knows the distance between each pair of cities. The difficulty arises from the fact that for n given cities, there are $n!$ possible routes. However, we need only consider half this number as every route can be traversed in reverse order which is essentially the same route, and since we can start in any given city, the number of different routes is further reduced by a factor of n. This still leaves $(n-1)!//2$ different routes to choose from. So for example, with only 15 cities there are over 43 billion different possible routes. There is simply no mathematical algorithm that can find the shortest route in all cases, and this is the sort of problem computer scientists call *NP complete.* The traveling salesman problem has many practical applications, not only involving traveling between cities but to telecommunication networks and even to the machine punching of holes into circuit boards.

There are various schemes to find optimal routes, or at least near optimal ones, and one recent one due to Marco Dorigo and Luca Gambardella [1997] involves virtual ants. Their work was inspired by the behavior of *real* ants.

The interesting thing about real ants is that they are capable of finding the shortest route from their nest to a food source without using any visual cues from their environment. Even if an obstacle is put in their path, the ants will soon find the next shortest path to the food source. They manage to do this because each ant lays a chemical pheromone trail whenever it is carrying food. Coupled to this is the ants' preference to follow a trail that is richer in pheromones over one that is not (see Ermentrout & Edelstein-Keshet [1993] for a simple model of this behavior). Since an ant who has taken a shorter route to a food source will return with it somewhat sooner than an ant who travels to a more distant source, the former ant's trail becomes reinforced by other ants and accumulates more pheromone per unit of time than longer routes. Soon the latter die out and all ants will follow the shortest one.

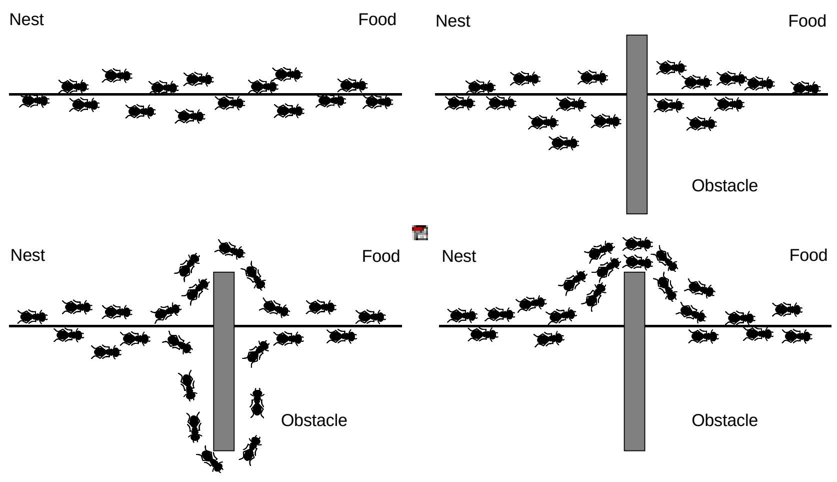

Figure 6.23: Ants following a pheromone trail will soon discover the shortest route to a food supply even if an obstacle is put in their way as the shorter route will accumulate more pheromone. Redrawn from Dorigo and Gambardella [1997].

Dorigo and Gambardella realized that the ants finding the shortest route was an emergent phenomenon that could be put to use in finding optimal routes in the traveling salesman problem. In the electronic version, the cities are connected by pathways and an army of virtual ants is allowed to travel along them leaving a virtual 'pheromone' trail as they go from city to city. The ants are given the propensity to prefer trails with a lot of pheromone along pathways that connect nearby cities. Once all the ants have completed their tour of duty, the ant with the shortest route has its route further enhanced with pheromone so that the shorter the route, the more enhancement it receives. This process is then repeated many times even allowing for the evaporation of pheromone at a steady rate as happens in real ant colonies (although the rate adopted by the researchers was much higher). The resulting *ant colony system* (ACS) can achieve near-optimal to optimal solutions to the traveling salesman problem and is as good or better than other competing systems having already been applied to telecommunications networks. Ant colony behavior is providing impetus to other fields such as robotics, data sorting, and office design.

Chapter 7

Appendix

Wolfram's 256 elementary cellular automata, all starting with one black cell.

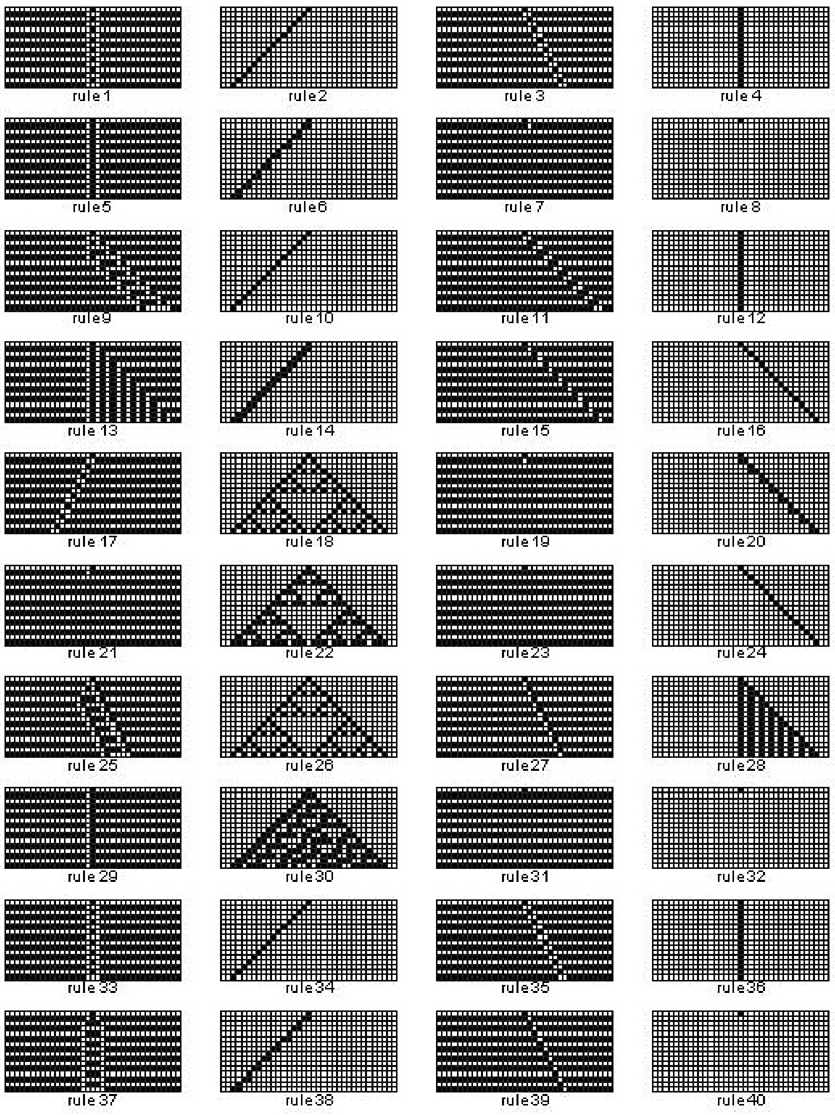
rule 1
rule2
rule 3
rule 4
rule5
rule6
rule 7
rule 8
rule9
rule 10
rule 11
rule 12
rule 13
rule 14
rule 15
rule 16
rule 17
rule 18
rule 19
rule 20
rule 21
rule 22
rule 23
rule 24
rule 25
rule 26
rule 27
rule 28
rule 29
rule 30
rule 31
rule 32
rule 33
rule 34
rule 35
rule 36
rule 37
rule 38
rule 39
rule 40

Figure 7.1:

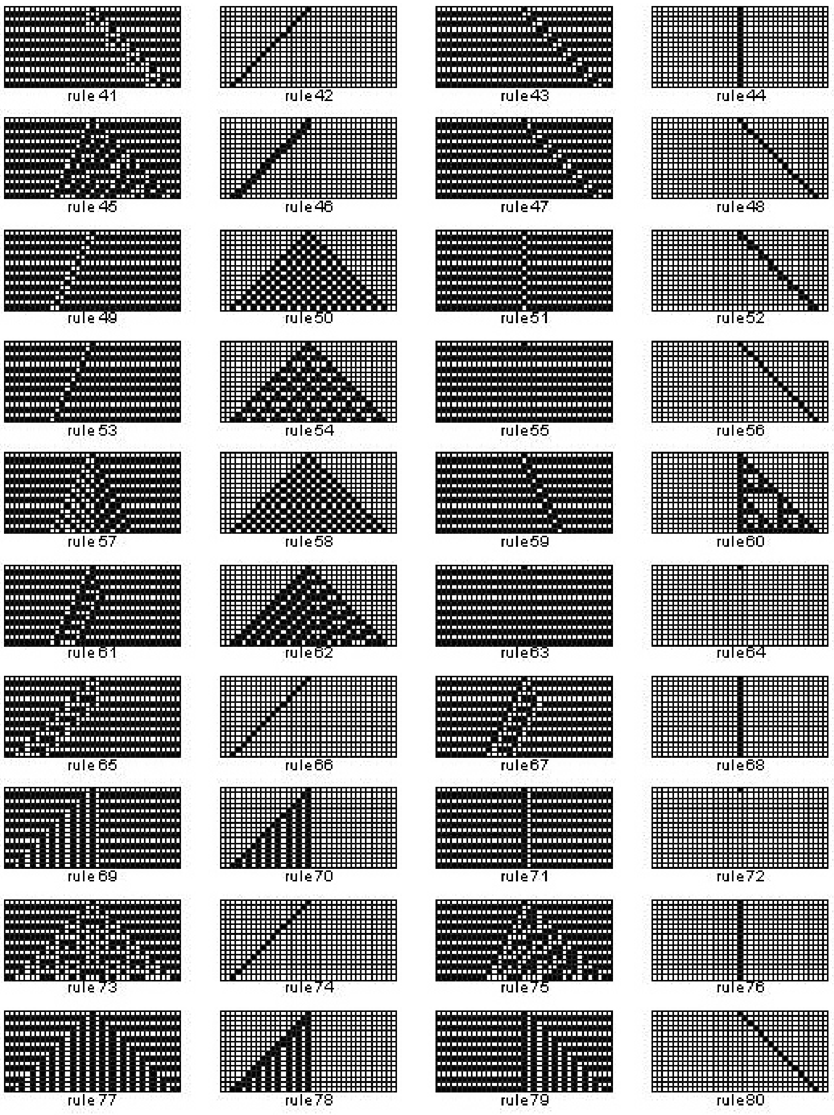

rule 41
rule 42
rule 43
rule 44
rule 45
rule 46
rule 47
rule 48
rule 49
rule 50
rule 51
rule 52
rule 53
rule 54
rule 55
rule 56
rule 57
rule 58
rule 59
rule 60
rule 61
rule 62
rule 63
rule 64
rule 65
rule 66
rule 67
rule 68
rule 69
rule 70
rule 71
rule 72
rule 73
rule 74
rule 75
rule 76
rule 77
rule 78
rule 79
rule 80

Figure 7.2:

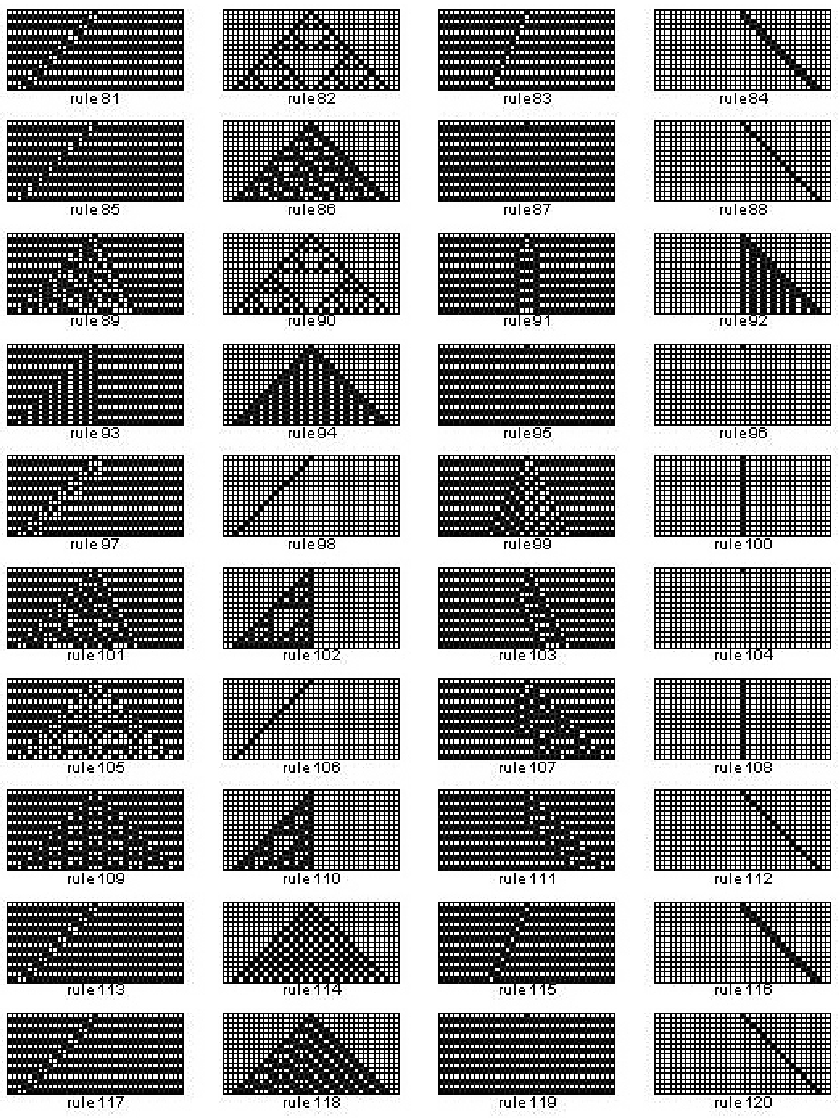
rule 81
rule 82
rule 83
rule 84
rule 85
rule 86
rule 87
rule 88
rule 89
rule 90
rule 91
rule 92
rule 93
rule 94
rule 95
rule 96
rule 97
rule 98
rule 99
rule 100
rule 101
rule 102
rule 103
rule 104
rule 105
rule 106
rule 107
rule 108
rule 109
rule 110
rule 111
rule 112
rule 113
rule 114
rule 115
rule 116
rule 117
rule 118
rule 119
rule 120

Figure 7.3:

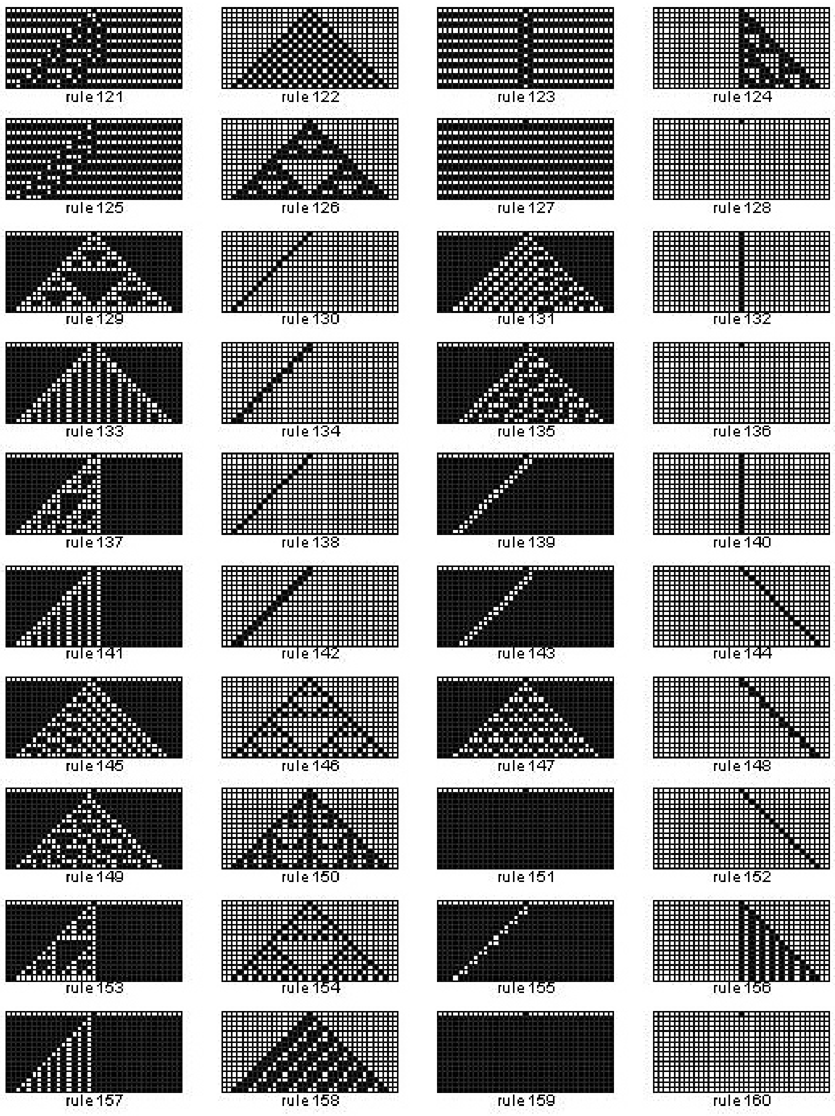
rule 121
rule 122
rule 123
rule 124
rule 125
rule 126
rule 127
rule 128
rule 129
rule 130
rule 131
rule 132
rule 133
rule 134
rule 135
rule 136
rule 137
rule 138
rule 139
rule 140
rule 141
rule 142
rule 143
rule 144
rule 145
rule 146
rule 147
rule 148
rule 149
rule 150
rule 151
rule 152
rule 153
rule 154
rule 155
rule 156
rule 157
rule 158
rule 159
rule 160

Figure 7.4:

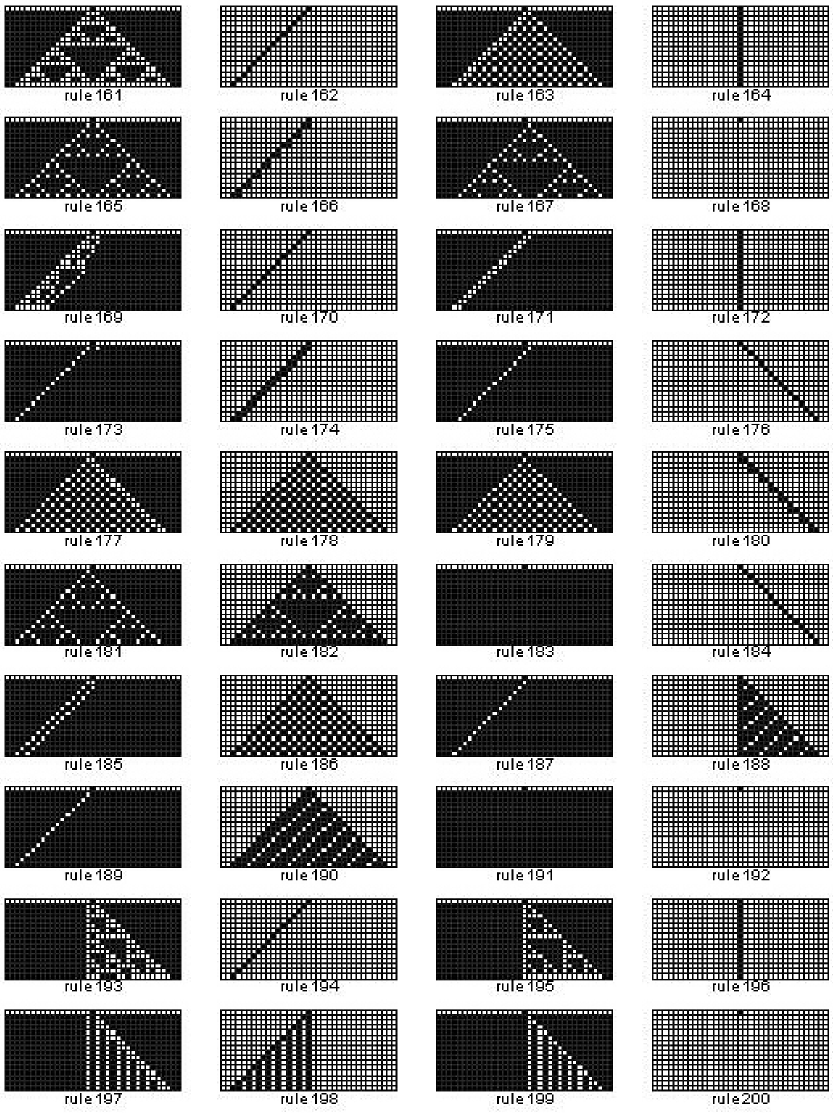
rule 161
rule 162
rule 163
rule 164
rule 165
rule 166
rule 167
rule 168
rule 169
rule 170
rule 171
rule 172
rule 173
rule 174
rule 175
rule 176
rule 177
rule 178
rule 179
rule 180
rule 181
rule 182
rule 183
rule 184
rule 185
rule 186
rule 187
rule 188
rule 189
rule 190
rule 191
rule 192
rule 193
rule 194
rule 195
rule 196
rule 197
rule 198
rule 199
rule 200

Figure 7.5:

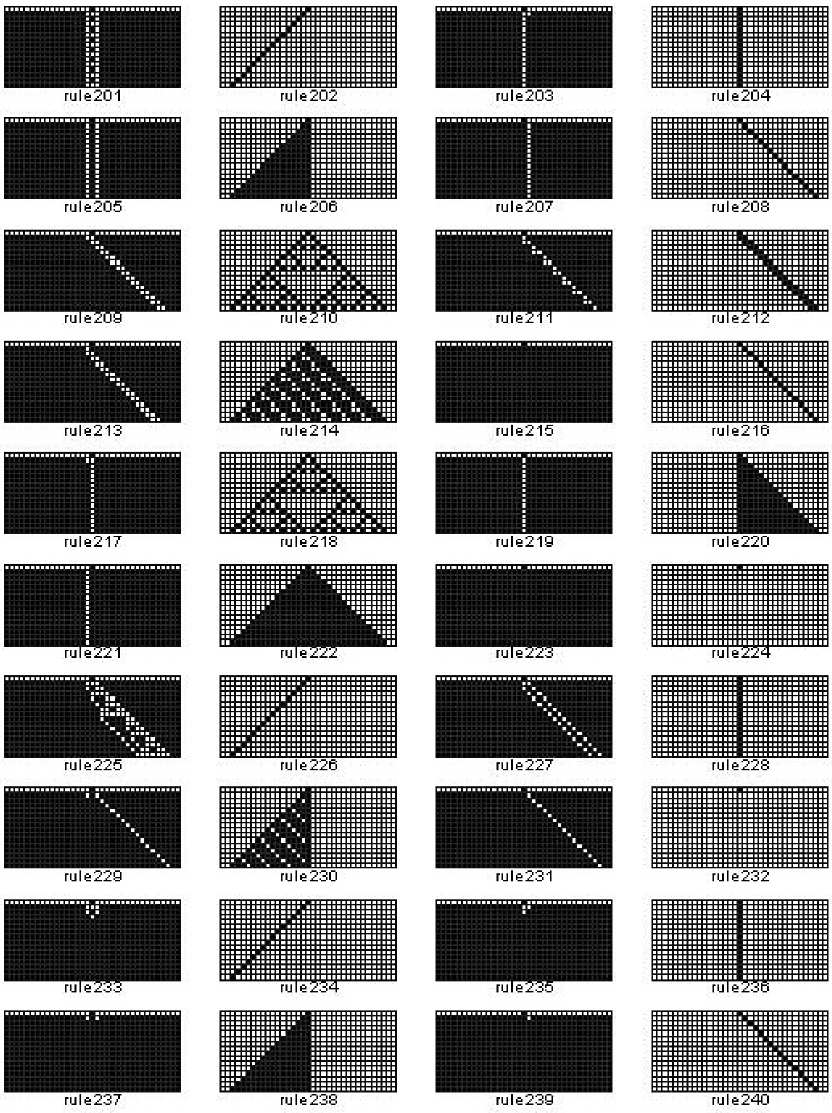
rule201
rule202
rule203
rule204
rule205
rule206
rule207
rule208
rule209
rule210
rule211
rule212
rule213
rule214
rule215
rule216
rule217
rule218
rule219
rule220
rule221
rule222
rule223
rule224
rule225
rule226
rule227
rule228
rule229
rule230
rule231
rule232
rule233
rule234
rule235
rule236
rule237
rule238
rule239
rule240

Figure 7.6:

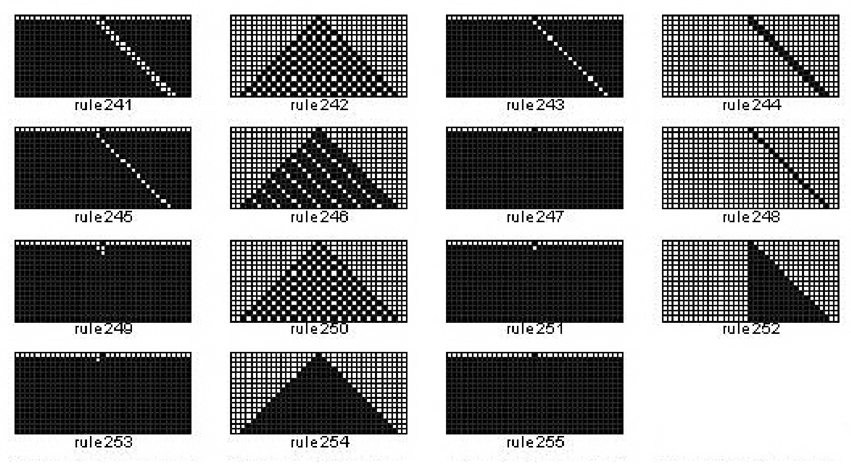
rule241
rule242
rule243
rule244
rule245
rule246
rule247
rule248
rule249
rule250
rule251
rule252
rule253
rule254
rule255

Figure 7.7:

Chapter 8

Bibliography

Adamatsky, A., *Identification of Cellular Automata*, Taylor & Francis Ltd., 1994.

Adami, C., *Introduction to Artificial Life*, Springer-Verlag New York Inc., 1998.

Amoroso, S. & Patt, Y.N., Decision procedures for surjectivity and injectivity of parallel maps for tessellations structures, *J. Comp. Sys. Sci.* **6** (1972), 448-464.

Auslander, D., Guckenheimer, J. & Oster, G., Random evolutionary stable strategies, *Theor. Pop. Biol.* **13** (1978), 276-293.

Axelrod, R. *The Evolution of Co-operation*, Basic Books, 1984.

—, The evolution of strategies in the iterated Prisoner's Dilemma, in L.D. Davis ed. *Genetic Algorithms and Simulated Annealing*, Research Notes in Artificial Intelligence, Los Altos, CA, 1987.

Axelrod, R. & Hamilton, W.D., The Evolution of Cooperation, *Science*, **211** (1981), 1390-1396.

Balzer, R., An 8-state minimal time solution to the firing squad synchronization problem, *Inform and Control* **10** (1967), 22-42.

Bennett, C.H. Brassard, C., & Ekert, A., Quantum cryptography, *Scientific American*, **269** (1992), 26-33.

Bentley, W. A., *Snow Crystals*, Dover, 1962.

Berlekamp, F.R., Conway, J.H. & Guy, R.K., *Winning Ways for your Mathematics Plays*, Vol. 2, Academic Press, 1982.

Bersini, H. & Detour, V., Asynchrony induces stability in cellular automata based models. In R. A. Brooks and P. Maes, eds, *Artificial Life IV*, 382-387, Cambridge, MA, The MIT Press, 1994.

Bonabeau, E., Dorigo,M., Theraulaz, G., *Swarm Intelligence: From Natural to Artificial Systems*, Santa Fe Institute Studies in the Science of Complexity, Oxford University Press, 1999.

Bricmont, J., Science of chaos or chaos of science, in P. R. Gross, N. Levitt, and M. W. Lewis, eds., *Flight from Science and Reason.* John Hopkins University Press, 1997.

Bunimovich, L. & Troubetzkoy, S., Recurrence properties of Lorentz lattice gas cellular automata, *J. Stat. Phys.* **67** (1992), 289-302.

Burks, A.W., Ed., *Essays on Cellular Automata*, University of Illinois Press,1970.

Buckingham, D.J., Some facts of life, *Byte* **3** (1978), 54.

Camazine, S., Deneubourg, J-L., Franks, N., Sneyd, J., Theraulaz, G., Bonabeau, E., *Self-Organization in Biological Systems*, Princeton University Press, 2001.

Capcarrere, M.S., Sipper, M. & Tomassini, M., Two-state, $r = 1$ cellular automaton that classifies density, *Phys. Rev. Lett.* **77** (1996), 4969-4971.

Celada, F. & Seiden, P.E., A computer model of cellular interactions in the immune system, *Immunol. Today*, **13** (1992), 56-62.

Chaudhuri, P.P., Chowdhury, D.R., Nandi, S., & Chattopadhyay, S., *Additive Cellular Automata: Theory and Applications Vol.1*, Wiley 1997.

Chua, L.O. & Yang, L., Cellular neural networks: Theory, *IEEE Trans. on Circuits and Systems*, **35** (1988), 1257-1272.

—, Cellular neural networks: Applications, *IEEE Trans. on Circuits and Systems*, **35** (1988), 1273-1290.

Chopard, B. & Droz, M., *Cellular Automata Modelling of Physical Systems*, Cambridge University Press, 1998.

Codd, E.F., *Cellular Automata*, Academic Press, New York, 1968.

Creutz, M., Deterministic Ising dynamics, *Ann. Phys. 167* (1986), 62-72.

Dawkins, R., The 'information challenge', essay in *A Devil's Chaplain*, Phoenix, 2004.

—, The evolution of evolvability, in *Artificial Life I,* C.G. Langton ed., Addison-Wesley, 1989, 201-220.

De Boer, R.J. & Hogeweg, P., Growth and recruitment in the immune network, in *Theoretical and Experimental Insights into Immunology*, A.F. Perelson & G. Weisbuch, eds. **66**, Springer-Verlag, New York, 1992.

Denbigh, K.G. & Denbigh, J.S., *Entropy in Relation to Incomplete Knowledge*, Cambridge University Press, 1985.

Derrida, B., & Weisbuch, G., Evolution of overlaps between configurations in random Boolean networks, *J. Physique* **47** (1986), 1297-1303.

Deutch, A. & Dormann, S., *Cellular Automaton Modeling of Biological Pattern Formation*, Birkhäuser Boston Inc., 2004.

Dewdney, A.K., Sharks and fish wage an ecological war on the toroidal planet Wa-Tor, *Scientific American*, December (1984), 14-22.

—, The hodgepodge machine makes waves, *Scientific American*, August (1998), 86-89.

—, *The Armchair Universe*, W.H. Freeman, NY, 1988.

—, A cellular universe of debris, droplets, defects and demons, *Scientific American,* August (1989), 88-91.

—, Two-dimensional Turing machines and tur-mites make tracks on a plane, *Scientific American*, September (1989), 124-127.

Devaney, R.L., *Introduction to Chaotic Dynamical Systems*, 2nd ed. Addison-Wesley, 1989.

Dorigo, M. & Gambardella, L.M., Ant colonies for the traveling salesman problem, *Biosystems* **43** (1997), 73-81.

Elaydi, S.N., *Discrete Chaos*, Chapman & Hall/CRC, 2000.

Ermentrout, G.B., Campbell, J. and Oster, A., A model for shell patterns based on neural activity, *The Veliger* **28** (1986), 369-388.

Ermentrout, G.B. & Edelstein-Keshet, *Cellular automata approaches to biological modeling*, J. Theor. Biol. **160** (1993), 97-133.

Farmer, J.D., Dimension, fractal measures, and chaotic dynamics, in *Evolution of Order and Chaos in Physics*, Chemistry and Biology, Ed. H. Haken, Springer-Verlag, 1982, 229-246.

Flake, G.W., *The Computational Beauty of Nature*, MIT Press, 1998.

Flood, M.M., Some experimental games. Technical Report RM-789-1. The Rand Corporation, Santa Monica, CA 1952.

Franklin, S. & Graesser, A., *Proceedings of the Third International Workshop on Agent Theories, Architectures, and Languages*, Springer-Verlag, 1996.

Fredkin, E., Digital Mechanics: an informational process based on reversible universal cellular automata, *Physica D* **45** (1990), 254-270.

—, A new cosmogony, in *Proceedings of the Workshop on Physics and Computation*, Oct. 2-4, 1992, IEEE Comp. Soc. Press (1993), 116-121.

Fredkin, E., & Toffoli, T., Conservative logic, *Internat. J. Theor. Phys.* **21** (1982), 219-253.

Frisch, U., Hasslacher, B. & Pomeau, Y., Lattice-gas automata for the Navier-Stokes equation, *Phys. Rev. Lett.*, **56** (1986), 1505-1508.

Frisch U., d'Humieres D., Hasslacher B., Lallemand P., Pomeau Y., Rivet J.P., Lattice gas hydrodynamics in two and three dimensions, *Complex Systems* **1** (1987), 648-707. Reprinted in *Lattice Gas Methods for Partial Differential Equations*, G.D.Doolen, U.Frisch, B.Hasslacher, S.Orszag and S.Wolfram eds., pp.77-135, Addison-Wesley 1990.

Gale, D., The industrious ant, *The Math. Intelligencer,* **15** no.2 (1993), 54-55.

—, Further travels with my ant, *The Math. Intelligencer*, **17** no.3 (1995), 48-56.

Gardner, M., *Wheels, Life and Other Mathematical Amusements*, W.H. Freeman & Co., 1983.

Gaylord, R. & Nishidate, K., *Modeling Nature - Cellular Automata Simulations with Mathematica*, Springer-Verlag New York, 1996.

Gaylord, R. & D'Andra, L., Simulating Society: *A Mathematica Toolkit for Modelling Socioeconomic Behavior*, Springer-Verlag, New York, 1998.

Gaylord, R. & Wellin, P.R., *Computer Simulations with Mathematica: Explorations in Complex Physical and Biological Systems*, TELOS/Springer-Verlag, 1994.

Gell-Mann, M., *The Quark and the Jaguar – Adventures in the Simple and Complex,* W.H. Freeman & Co., 1994.

Gerhardt, M. & Schuster, H., A cellular automaton describing the formation of spatially ordered structures in chemical systems, *Physica D* **36** (1989), 209-221.

Gilbert, N. & Troitzsch, K.G., *Simulation for the Social Scientist,* Open University Press, 1999.

Goles, E. & Martínez, S., *Neural and Automata Networks.* Mathematics and its Applications **58** Kluwer, 1990.

Goles, E. & Martínez, S. Eds. *Cellular Automata and Complex Systems*, Kluwer, 1999.

Grand, S., *Creation: Life and How to Make It* , Harvard University Press, 2001.

Greenberg, J.M. & Hastings, S.P., Spatial patterns for discrete models of diffusion in excitable media, *SIAM J. Appl. Math.* **34** (1978), 515-523.

Griffeath, D. & Moore, C., *New Constructions in Cellular Automata*, Oxford University Press, 2003.

R K Guy, John Horton Conway, in Albers and G L Alexanderson (eds.), *Mathematical People : Profiles and Interviews* Cambridge, MA, 1985, 43-50.

Hardy, J., de Pazzis, O. & Pomeau, Y., Molecular dynamics of a classical lattice gas: Transport properties and time correlation functions, *Phys. Rev. A* **13** (1976) 1949-1960.

Hedlund, G.A., Endomorphisms and automorphisms of the shift dynamical system, *Math. Systems Theory* **3** (1969), 320-375.

Hegselmann, R. & Flache, A., Understanding complex social dynamics: A plea for cellular automata based modelling, *J. Artificial Societies and Social Simulation*, 1 (1998), http://www.soc.surrey.ac.uk/JASSS/1/3/1.html.

Hénon, M., Isometric collision rules for the four-dimensional FCHC lattice gas, *Complex Systems* **1** (1987), 475-494.

Herman, G.T. & Liu, W.H., The daughter of Celia, the French flag, and the firing squad, *Simulation* **21** (1973), 33-41.

Holland, J.H., Universal spaces: A basis for studies in adapation, *Automata Theory,* Academic Press (1966), 218-230.

—, The dynamics of searches directed by genetic algorithms, in *Evolution, Learning and Cognition*, Y.C. Lee ed., World Scientific (1988), 111-128.

—, *Adaption in Natural and Artificial Systems: An Introductory Analysis with Application to Biology, Control and Artificial Intelligence*, 2nd ed. MIT Press, 1992.

— *Emergence: From Chaos to Order*, Helix, 1998.

Hopfield, J.J., Neural networks and physical systems with emergent collective computational abilities, *Proc. Nat. Acad. Sci. U.S.A.* **79** (1982), 2554-2558.

Ilachinski, A., *Cellular Automata: A Discrete Universe*, World Scientific Publ. Co., 2nd, ed. 2002.

id Quantique, Random numbers generation using quantum physics, White Paper, 2004, www.idquantique.com

Ingerson, T.E. and Buvel, R.L., Structure in asynchronous cellular automata. *Physica D*, **10 (**1984**),** 59-68.

Johnson, S., *Emergence: the connected lives of ants, brains, cities and software*, Penguin, 2002.

Kaplan, D.T., Smith, J.M., Saxberg, B.E.H. & Cohen, R.J., Nonlinear dynamics in cardiac conduction, *Math. Bioscience* **90** (1988), 19-48.

Kari, J., Reversibility of 2D cellular automata is undecidable, *Physica D* **45** (1990), 379-385.

Kauffman, S.A., *The Origins of Order: Self-Organization and Selection in Evolution*, Oxford University Press, 1993.

—, *At Home in the Universe: the search for laws of self-organization and complexity*, Oxford University Press, 1995.

Keller, E.F. & Segel, L., Initiation of slime mold aggregation viewed as an instability, *J. Theor. Biol.* **26** (1970), 399-415.

Krugman, Paul, *The Self-Organizing Economy,* Blackman, New York, 1996.

Kirchkamp, O., Spatial evolution of automata in the prisoners' dilemma, *J. Economic Behavior & Organization*, **43** (2000), 239-262.

Knuth, D., *Seminumerical Algorithms*, Addison-Wesley, 1981.

Kusch, I. & Markus, M., Mollusc shell pigmentation: Cellular automaton simulations and evidence for undecidability, *J. Theor. Biol.* **178** (1996), 333-340.

Land, M. & Belew R.K., No perfect two-state cellular automaton for density classification exists, *Phys. Rev. Lett.* **74** (1995), 5148-5150.

Langton, C., Self-reproduction in cellular automata, *Physica D* **10** (1984), 135-144.

— Studying artificial life with cellular automata, *Physica D* **22** (1986), 120-149.

— Computation at the edge of chaos: Phase transitions and emergent computation, *Physica D* **42** (1990), 12-37.

Lewin, R., *Complexity – Life at the Edge of Chaos*, The University of Chicago Press, 1999.

Libbrecht, K. & Rasmussen, P., *The Snowflake: Winter's Secret Beauty*, Voyageur Press, 2003.

Lind, D., Applications of ergodic theory and sofic systems to cellular automata, *Physica D* **10** (1984) 36-44.

Lindenmayer, A., Mathematical models for cellular interactions in development, *J. Theor. Biol.* **18** (1968), 280-315.

Lumer, E.D. & Nicolis, G., Synchronous versus asynchronous dynamics in spatially distributed systems, *Physica D* **71** (1994), 440-452.

Madore, B.F. & Freedman, W.L., Computer simulations of the Belousov-Zhabotinsky reaction, *Science*, **222** (1983), 615-616.

Maeterlinck, M., *The Life of the Bee*, translated by Alfred Sutro, George Allen & Unwin Ltd., 1901.

Mandelbrot, B., *The Fractal Geometry of Nature*, W.H. Freeman & Co., 1982.

Martin, O., Odlyzko, A. & Wolfram, S., Algebraic properties of cellular automata, *Comm. Math. Phys.* **93** (1984), 219-258.

Mazoyer, J., A six-state minimal time solution to the firing squad synchronization problem, *Theoretical Computer Science*, **50** (1987),183-238.

McCulloch, W.S. & Pitts, W., A logical calculus of the idea immanent in nervous activity, *Bull. Math. Biophys.* **5** (1943), 115-133.

McIntosh, H.V., Wolfram's class iv automata and a good life, *Physica D* **45** (1990), 105-121.

Meihnardt, H., *The Algorithmic Beauty of Sea Shells*, Springer-Verlag, Heidelberg, 1995.

Minsky, M., *Computations: Finite and Infinite Machines*, Prentice Hall, 1967.

—, *Society of Mind*, Simon & Schuster, 1988.

Minsky, M. & Papert, S., *Perceptrons: An Essay in Computational Geometry*, MIT Press, 1969.

Mitchell, M., *An Introduction to Genetic Algorithms*, MIT Press, 1996.

Mitchell, M., Hraber, P.T. & Crutchfield, J.P., Revisiting the edge of chaos: Evolving cellular automata to perform calculations, *Complex Systems* **7** (1993), 89-130.

Mitchell, M. & Forrest, S., Genetic algorithms and artificial life, *Artificial Life* **1** (1994), 267-290.

Moore, E.F., Machine models of self-reproduction, *Proc. Symposia Appl. Math. Amer. Math. Soc.* **14** (1962), 17-33, reprinted in, *Essays on Cellular Automata*, A. W. Burks ed., University of Illinois, 1970.

—, Sequential Machines: *Selected Papers*, Addison-Wesley, 1964.

Moore, J.H. & Hahn, L.W., A cellular automata-based pattern recognition approach for identifying gene-gene and gene-environment interactions, *Amer. J. Human Genetics* **67** (2000), 52.

—, Multilocus pattern recognition using cellular automata and parallel genetic algorithms, *Proc. of the Genetic and Evolutionary Computation Conference* (GECCO - 2001), 1452.

Moreira, J. & Deutsch, A., Cellular automaton models of tumor development: A critical review, *Advances in Complex Systems* **5** (2002), 247-269.

Morita, K. & Imai, K., A simple self-reproducing cellular automaton with shape-encoding mechanism, *Artificial Life V*: Proceedings of the Fifth International Workshop on the Simulation and Synthesis of Living Systems, C. G. Langton and K. Shimohara, eds., pp.489-496, 1997, MIT Press.

Mukherjee, M., Ganguly, N. & Chaudhuri, P.P., Cellular automata based authentication, in *Cellular Automata*: *5th International Conference on Cellular Automata for Research and Industry*, S. Bandini, B. Chopard & M. Tomassini eds., Springer-Verlag 2002, 259-269.

Myhill, John, The converse of Moore's Garden-of-Eden theorem, in *Essays on Cellular Automata*, edited by Arthur W. Burks, Univ. of Illinois Press, Urbana, 1970.

Nicolis, G. & Prigogine, I., *Exploring Complexity: An Introduction*, W.H. Freeman, 1989.

Nowak, M.A. & May, R.M., Evolutionary games and spatial chaos, *Nature* **359** (1992), 826-829.

Nowak, M.A., May, R.M, & Sigmund, K., The arithmetics of mutual help, *Scientific American*, June (1995), 76-81.

Oppenheimer, P., The artificial menagerie, in *Artificial Life I*, C.G. Langton ed., Addison-Wesley, 1988, 251-274.

Packard, N.H., Lattice models for solidification and aggregation, in *Theory and Applications of Cellular Automata*, S. Wolfram ed., World Scientific Publ. 1986, 305-310.

—, Adaptation toward the edge of chaos. In *Dynamic Patterns in Complex Systems*, J.A.S. Kelso, A.J. Mandell & M.F. Schlesinger, eds. (1988), World Scientific, 293-301.

Packard, N.H. & Wolfram, S., Two-dimensional cellular automata, *J. Stat. Phys.* 38 (1985), 901-946.

Penrose, R., The Emperor's New Mind: Concerning Computers, Minds, and the Laws of Physics, Oxford University Press, 1989.

Poundstone, W., *The Recursive Universe*, Oxford University Press, 1985.

—, *The Prisoner's Dilemma*, Doubleday, New York, 1992.

Preston Jr., K. & Duff, M. J.B., *Modern Cellular Automata: Theory and Applications*, Plenum Press, 1984.

Prigogine, I. & Nicolis, G., *Exploring Complexity*, New York, W.H. Freeman, 1989.

Prigogine, I. & Stengers, I., *Order Out of Chaos*, Bantam Books, 1984.

Propp, J., Further ant-ics, *The Math. Intelligencer*, **16** no.1 (1994), 37-42.

Pytte, E., Grinstein, G. & Traub, R.D., Cellular automaton models of the CA3 region of the hippocampus, *Network* **2** (1991), 149-167.

Reggia, J.A., Armentrout, S.L., Chou, H.-H. & Peng, Y., Simple systems that exhibit self-directed replication, *Science* **259** (1993), 1282-1287.

Reiter, C.A., A local cellular model for snow crystal growth, *Chaos, Solitons & Fractals*, **23**(4) (2004), 1111-1119.

Resnick, M., *Turtles, Termites, and Traffic Jams*, The MIT Press, 1994.

Richardson, L.F., The problem of contiguity: an appendix to Statistics of deadly quarrels. *General Systems Yearbook* **6** (1961), 139-187.

Roli, A. & Zambonelli, F., Emergence of macro spatial structures in dissipative cellular automata, in *Cellular Automata*: *5th International Conference on Cellular Automata for Research and Industry*, S. Bandini, B. Chopard & M. Tomassini eds., Springer-Verlag 2002, 44-55.

Russ, J. C., *Fractal Surfaces*, Plenum Press, 1994.

Sakoda, J.M., The checkerboard model of social interaction, *J. Math. Sociology* (1971), 119-132.

Sandefur, J.T., *Discrete Dynamical Systems: Theory and Applications*, Oxford University Press, 1990.

Schelling, T.C., Dynamic Models of Segregation. *J. of Math. Sociology* **1** (1971), 143-186.

Schepers, H. & Markus, M., Two types of performance of an isotropic cellular automaton: stationary (Turing) patterns and spiral waves, *Physica A* **188** (1992), 337-343.

Schönfisch B., *Propagation of fronts in cellular automata*, *Physica D* **80** (1995), 433-450.

Schönfisch B. & de Roos, A., Synchronous and asynchronous updating in cellular automata, *BioSystems* **51** (1999), 123-143.

Schönfisch B. & Kinder, M., A fish migration model, in *Cellular Automata*, Bandini, Chopard, Tomassini eds. (2002), 210-219.

Schrandt, Robert G. & Ulam, S.M., On recursively defined geometrical objects and patterns of growth, *Los Alamos Report 3762*, August, 1967. Also reprinted in: S.M. Ulam, *Analogies Between Analogies: The Mathematical Reports of S.M. Ulam and His Los Alamos Collaborators*, University of California Press, 1990.

Schulman, L.S. & Seiden, P.E., Percolation and galaxies, *Science* **233** (1986), 425-431.

Schweitzer, F., Behera, L. & Mühlenbein, H., *Evolution of cooperation in a spatial prisoner's dilemma*, Advances in Complex Systems, **5** (2002) 269-299.

C. E. Shannon, A mathematical theory of communication, *Bell System Technical Journal* **27**, pp. 379-423 and 623-656, July and October, 1948.

Singh, S., *The Code Book*, Fourth Estate Ltd. 1999.

Sipper, M., Non-uniform cellular automata: Evolution in rule space and formation of complex structures, *Artificial Life IV*, R.A. Brooks and P. Maes, editors, Cambridge MA, The MIT Press,1994.

—, Studying artificial life using simple, general cellular automata, *Artificial Life* **2** (1995), 1-35.

—, Fifty years of research on self-replication: An overview, *Artificial Life* **4** (1998), 237-257.

Smith, A.R., Simple, nontrivial self-reproducing machines, in *Artificial Life II*, C.G. Langton, C.Taylor, JD. Farmer, and S. Rasmussen, eds, Addison-Wesley, 1991, 709-725.

Stauffer, A. & Sipper, M., An interactive self-replicator implemented in hardware, *Artificial Life* **8** (2002), 175-183.

Stewart, I., The ultimate in anty-particles, *Scientific American*, July (1994), 104-107

Tamayo, P. and Hartman, H., Cellular automata, reaction-diffusion systems and the origin of life, in *Artificial Life I,* C.G. Langton ed., Addison-Wesley, 1989, 105-124.

Toffoli, T. & Margolus, N., *Cellular Automata Machines - A New Environment for Modeling*, The MIT Press, 1987.

—, Invertible cellular automata: A review, *Physica D* **45** (1990), 229-253.

Tomassini, M. & Venzi, M., Artifically evolved asychronous cellular automata for the density task, in *Cellular Automata*: *5th International Conference on Cellular Automata for Research and Industry*, S. Bandini, B. Chopard & M. Tomassini eds., Springer-Verlag 2002, 44-55.

Turing, A., On computable numbers, with an application to the Entscheidungsproblem, *Proc. London Math. Soc.* Ser.2 **42** (1936), 230-265.

—, *The chemical basis for morphogenesis*, Phil. Trans. Roy. Soc. **237** (1952), 37-72.

Ulam, Stanislaw, Random processes and transformations, *Proc. Int. Cong. Math.* 1950.

Analogies Between Analogies, University of Berkeley Press, 1990.

Vincent, J.F.V., Cellular automata: a model for the formation of colour patterns in molluscs, *J. Moll. Stud.* **52**, 97-105.

Vichniac, G., Simulating physics with cellular automata, *Physica D* **10** (1984), 96-116.

Von Neumann, *Papers of John von Neumann on Computing and Computer Theory*, The MIT Press, 1987.

— *Theory of Self-reproducing Automata*, edited and completed by Arthur W. Burks, University of Illinois Press, 1966.

Waddington, C.H. and Cowe, R.J., Computer simulations of a molluscan pigmentation pattern, *J. Theor. Biol.* **25** (1969), 219-225.

Wade, D., *Li – Dynamic Form in Nature*, Walker & Co., 2003.

Waksman, A., An optimum solution to the firing squad synchronization problem, *Inform. and Control* **8** (1966), 66-78.

Waldrop, M.M., *Complexity, the Emerging Science at the Edge of Order and Chaos*, Simon & Schuster, 1992.

Williams, G.P., *Chaos Theory Tamed*, Joseph Henry Press, 1997.

Wolfram, S., Universality and complexity in cellular automata, *Physica D* **10** (1984), 1-35.

—, *Theory and Applications of Cellular Automata*, World Scientific, 1986.

—, Random sequence generation by cellular automata, *Advances in Applied Math.* **7** (1986), 123-169.

— *A New Kind of Science*, Wolfram Media Inc. 2002.

Yates, Eugene. F., Editor, *Self-Organizing Systems*, Plenum Press, 1987.

Zuse, K., *Rechnender Raum* (Vieweg. Braunschweig, 1969): translated as *Calculating Space*, Tech. Transl. AZT-70-164-GEMIT, MIT Project MAC, 1970.

Zykov V., Mytilinaios E., Adams B., Lipson H., Self-reproducing machines, *Nature* **435** (2005), 163-164.